

MONOLITH ABSORBANTS AS A CAPTURE STEP FOR VIRUS-LIKE PARTICLES

CLAIRE SUZANNE BURDEN

Advanced Centre for Biochemical Engineering,

Department of Biochemical Engineering,

University College London,

Torrington Place,

London.

WC1E 7JE

Submitted to UCL for the degree of Doctor of Engineering
(EngD) in Biochemical Engineering and Bioprocess Leadership

September 2012

I, Claire Burden, confirm that the work presented in this thesis is my own. Where information has been derived from other sources, I confirm that this has been indicated in the thesis.

Signed.....Date.....

ABSTRACT

Monoliths are an alternative stationary phase format to conventional particle based media for large biomolecules. Conventional resins suffer from limited capacities and flow rates when used for viruses, virus-like particles (VLP) and other nanoplex materials. Monoliths provide an open pore structure to improve pressure drops and mass transport via convective flow. The challenging capture of a VLP from clarified yeast homogenate was used to develop a new monolith separation which found hydrophobic interaction based separation using a hydroxyl derivatised monolith had the best performance. The monolith was then compared to a known beaded resin method, where the dynamic binding capacity increased three-fold for the monolith with 90% recovery of the VLP.

Confocal microscopy was used to visualise lipid contaminants, deriving from the homogenised yeast. The lipid formed a layer on top of the column, even after column regeneration, resulting in increasing pressure drops over a number of cycles. Removal of 70% of the lipid pre-column by Amberlite/XAD-4 beads significantly reduced the fouling process. Applying a reduced lipid feed versus an untreated feed further increased the dynamic binding capacity of the monolith from 0.11 mg/mL column to 0.25mg/mL column.

Control of chromatographic conditions can impact the product concentration during elution. Critical parameters which influenced the concentration of measurable VLP eluted included column contact time, salt concentration in mobile phase, and inclusion of lipid. The parameters were co-dependant with a crude lipid feed loaded at low salt and extra wash time of 40 minutes causing the largest decrease of 40%. Reducing the time of contact between the column and the VLP helped reduce such adverse effects. Increasing the flow rate in the column had no effect on the elution profile with crude or reduced lipid feeds. This informs process development strategies for the future use of monoliths in vaccine bioprocessing.

ACKNOWLEDGEMENTS

It has been a long and amazing five years since I arrived back at UCL. First of all I would like to thank my supervisor Dan Bracewell, for his guidance and help. Thanks must also go to my sponsor company BIA Separations, my industrial supervisors Aleš Podgornik and Aleš Strancar for their support and the welcome when I came to stay for a few weeks. A huge amount of thanks are due to Gaik Sui Kee and Jing Jin for welcoming me to the VLP group. Your input and guidance was invaluable.

A massive thank you must go to my parents for all their support and for putting up with me going back to university once again, after they thought I'd finished. Also thank you to my brother for my very cute nephew Thomas, hopefully one day I can make him an engineer too.

Over the four years I had the privilege of sharing a department with some brilliant people. Big thanks to The Colonnades and The Vineyard offices, particularly for the tea and the cake, and to everyone else in Biochemical Engineering. Thanks for the laughs, ULU beers and anyone who has helped me along the way. I mustn't forget the friends who have had to put up with me reminding them about my student discount, including Abena, Miriam, Lindsey, Vicky, the 7P ladies and the rest from Sheffield, and everyone in New Zealand.

Anyone I've not mentioned I'm sorry and thank you.

TABLE OF CONTENTS

ABSTRACT	3
ACKNOWLEDGEMENTS	4
TABLE OF CONTENTS	5
LIST OF FIGURES	11
LIST OF TABLES	19
LIST OF SYMBOLS AND ABBREVIATIONS	20
1 INTRODUCTION	23
1.1 RELAVANCE OF PROJECT	23
1.2 AIMS OF PROJECT	25
1.2.1 Development of a monolithic VLP separation.....	25
1.2.2 Interactions of impurities with hydrophobic monoliths	25
1.2.3 Interactions and loss of product on hydrophobic monoliths	26
1.3 ORGANISATION OF THESIS	27
1.4 VIRUS-LIKE PARTICLES (VLP) AND VACCINES	29
1.4.1 Traditional vaccines	29
1.4.2 VLP vaccines	30
1.4.3 Hepatitis B virus (HBV)	31
1.4.4 Hepatitis B surface antigen (HBsAg).....	32
1.4.4.1 Production.....	32
1.4.4.2 Structure.....	33
1.4.5 Vaccine.....	38
1.5 PURIFICATION OF NANOPLEX MOLECULES.....	39
1.5.1 Non-adsorption purification methods - Precipitation.....	40
1.5.2 Non-adsorption purification methods - Ultracentrifugation	42
1.5.3 Adsorption purification methods – Porous beads	45

1.5.4	Adsorption purification methods – Monoliths	49
1.5.5	Adsorption purification methods – Membranes.....	56
1.5.6	Cryogels	58
1.6	CHARACTERISTICS OF PROCESS CHROMATOGRAPHY PERFORMANCE	62
1.6.1	Fouling of chromatographic resins.....	62
1.6.2	Cleaning-in-place (CIP)	65
1.6.3	Confocal microscopy	66
1.6.4	Dynamic Light Scattering	68
1.6.5	Zeta potential.....	70
1.7	HYDROPHOBIC INTERACTION CHROMATOGRAPHY	72
1.7.1	Theory	72
1.7.2	HIC columns	76
1.7.3	Column resins	77
1.7.4	Column ligands	77
1.7.5	Optimising a HIC step.....	79
1.7.5.1	Salt	79
1.7.5.2	Temperature	80
1.7.5.3	pH.....	80
1.7.5.4	Additives	80
1.7.6	Protein unfolding on HIC columns	81
1.8	CIM MONOLITHS	85
1.8.1	Principles.....	85
1.8.2	Applications	88
1.8.3	Scale up	89
2	METHODS AND MATERIALS	93
2.1	MATERIALS	93

2.1.1	Chemicals.....	93
2.1.2	2.1.2 HBsAg Cell line	93
2.2	FERMENTATION OF SACCHAROMYCES CEREVISIAE.....	93
2.2.1	Media.....	93
2.2.2	Evaluation of yeast extract.....	94
2.2.3	Fermentation protocol	94
2.2.4	Fermentation harvest.....	95
2.3	PRIMARY RECOVERY OF VLP.....	96
2.3.1	Reduced lipid feed.....	96
2.4	CONVENTIONAL CHROMATOGRAPHY	97
2.5	MONOLITHIC ABSORBENTS.....	98
2.5.1	CIM [®] disks and tubes	98
2.5.2	CIMac [™] OH columns	99
2.6	CONFOCAL LASER SCANNING MICROSCOPY (CLSM).....	100
2.7	LIPID REMOVAL METHODS.....	100
2.8	TRANSMISSION ELECTRON MICROSCOPY (TEM)	101
2.9	ATOMIC FORCE MICROSCOPY (AFM).....	101
2.10	ZETA POTENTIAL MEASUREMENTS.....	102
2.11	ANALYTICAL TECHNIQUES.....	102
2.11.1	Optical density measurements.....	102
2.11.2	Dry cell weight analysis	102
2.11.3	Glucose and galactose measurements	103
2.11.4	Enzyme Linked Immunosorbent Assay (ELISA) for HBsAg.....	103
2.11.5	Total protein assay using Bicinchonic acid assay (BCA)	105
2.11.6	Total protein assay using Coomassie Blue reagent (Bradford).....	105
2.11.7	Lipid quantification by HPLC.....	105
2.11.8	Dynamic light scattering (DLS).....	106

2.11.9	SDS-PAGE.....	106
2.11.10	Size Exclusion Chromatography (SEC).....	107
3	DEVELOPMENT OF A PURIFICATION PROCESS FOR VIRUS-LIKE PARTICLE ON A MONOLITHIC ADSORBENT	108
3.1	INTRODUCTION.....	108
3.2	MATERIALS AND METHODS	111
3.3	RESULTS AND DISCUSSION	112
3.3.1	Fermentation of <i>Saccharomyces cerevisiae</i>	112
3.3.1.1	75L fermentations	112
3.3.1.2	20L fermentations	113
3.3.2	Change of yeast extract and effect on VLP production	114
3.3.3	Primary Purification	117
3.3.3.1	Effect of detergent in primary purification.....	117
3.3.4	Selection of monolith chemistry for VLP separation.....	119
3.3.5	Determination of salt concentration in mobile phase.....	122
3.3.6	Dynamic binding capacity of CIM 1mL OH columns.....	125
3.3.7	Comparison of monoliths and conventional resin chromatography ..	126
3.3.8	Comparison of standard and large pore CIM 1mL monoliths	127
3.3.9	Topography of HBsAg particle.....	128
3.3.10	Analysis of VLP using dynamic light scattering.....	129
3.3.11	Analysis of VLP using Zeta potential	130
3.3.12	Analysis of VLP using Size Exclusion Chromatography	133
3.3.13	Analysis of VLP using Bradford or BCA assays – comparison of methods	136
3.4	CONCLUSIONS	138
4	PRE-TREATMENT OF A VLP-YEAST HOMOGENATE AND THE EFFECT ON THE CHROMATOGRAPHIC STEP	139
4.1	INTRODUCTION.....	139

4.2	MATERIALS AND METHODS	141
4.3	RESULTS AND DISCUSSION	142
4.3.1	Effect of lipid fouling on monoliths.....	142
4.3.2	Visualisation of lipid fouling on monoliths	143
4.3.3	Lipid removal methods	144
4.3.3.1	Ammonium sulphate precipitation.....	145
4.3.3.2	Lipid removal absorbent (LRA)	146
4.3.3.3	Delipid filters	146
4.3.3.4	XAD-4/Amberlite	147
4.3.3.5	Integration of lipid removal method	148
4.3.4	Effect of reduced lipid feed on the dynamic binding capacity in monoliths.....	149
4.3.5	Effect of reduced lipid feed on dynamic binding capacity in Butyl-S - a comparison.	151
4.3.6	Effect of lipid removal on the life span of the monolith column.....	151
4.3.7	Sample purity after monolithic process from SDS-PAGE.....	152
4.4	CONCLUSION	155
5	INVESTIGATION OF THE BEHAVIOUR OF A VLP ON MONOLITHS	156
5.1	INTRODUCTION.....	156
5.2	MATERIALS AND METHODS	158
5.3	RESULTS AND DISCUSSION	159
5.3.1	Gradient and step elutions on the monolith.....	159
5.3.2	The effect of wash time on the elution profile	161
5.3.3	Influence of binding strength on the elution profile.....	164
5.3.4	Influence of lipids on the elution profile.....	166
5.3.5	Reduction of residence time on the column.....	168
5.3.6	Use of a monolith column as an advanced analytical method	169

5.3.7	Use of monolith analytical method to investigate the influence of residence time on monoliths	173
5.3.8	Comparison of analytical monolith method to the ELISA and Bradford assays	176
5.4	CONCLUSION	178
6	PROJECT CONCLUSIONS AND FUTURE WORK	180
6.1	REVIEW OF PROJECT OBJECTIVES	180
6.1.1	Development of a monolithic VLP separation.....	180
6.1.2	Interactions of impurities with hydrophobic monoliths.....	181
6.1.3	Interactions and loss of product on hydrophobic monoliths	182
6.2	FUTURE WORK	184
6.2.1	Controlling and understanding the adsorptive environment	184
6.2.2	Adjustment of VLP feed material	185
7	VALIDATION AND PROCESS ECONOMICS OF A CHROMATOGRAPHY UNIT OPERATION.....	187
7.1	PROCESS VALIDATION.....	187
7.2	POST-APPROVAL CHANGES TO A COMMERCIAL MANUFACTURING PROCESS	189
7.3	PROCESS ECONOMICS	193
8	REFERENCES.....	195
9	APPENDIX	234
9.1	SECTION 3	234
9.2	SECTION 4	237

LIST OF FIGURES

<i>Figure 1-1 A schematic diagram of the virus-like particle HBsAg from yeast. Each VLP is around 22nm in size and 3.5mDa. It is made of approximately 75% protein (S-protein) and 25% lipid. The core of the VLP contains free host lipids.</i>	34
<i>Figure 1-2 A model for the biogenesis of HBsAg particles. Particle formation occurs in several steps. Step 1: Synthesis of p24s in the ER membrane; Step 2: within 40 minutes all of this material has become protease resistant, which may represent simply a conformational change or aggregation in the membrane or both. Over the next 3 hours, the bulk of this material is transferred to the ER lumen (Steps 3& 4). (Simon et al., 1988)</i>	34
<i>Figure 1-3 Secondary structure model of the HBV S protein. The major antigenic region is originally translocated into the ER lumen and it is only after assembly and secretion that it is exposed on the surface of the S protein (Mangold and Streeck, 1993, Mangold et al., 1995).</i>	36
<i>Figure 1-4 Example schematic of a production process for a VLP vaccine. Only the upstream, recovery and purification steps are details on the process flow diagram.</i>	40
<i>Figure 1-5 Predicted buoyant position of hydrated constituents in CsCl gradients.</i>	44
<i>Figure 1-6 Schematic of examples of solid phases that are available or custom made for nanoplex purification (Zhang et al., 2001)</i>	46
<i>Figure 1-7 Diagram of pore structure in a perfusive particle (Afeyan et al., 1990).</i>	47
<i>Figure 1-8 Schematic of a Pall “gel-in-a-shell” bead. (From Pall Corporation website www.pall.com)</i>	48
<i>Figure 1-9 Mechanism of polymer monolith formation.</i>	51
<i>Figure 1-10 Scanning electron microscopy picture of a monolithic GMA-EDMA-based disk (Tennikova and Freitag, 2000)</i>	52
<i>Figure 1-11 The mass transfer characteristics of common chromatographic media. Areas of diffusion are indicated by small channels within the support matrix. The difference between bead-based columns and monoliths can be clearly seen (Gagnon, 2006).</i>	53

<i>Figure 1-12 Membrane absorbers commercially available A) Millipore ChromaSorb; B) Pall Mustang Q; C) Sartorius Stedim Sartobind.</i>	58
<i>Figure 1-13 Schematic of formation of cryogels (Plieva et al., 2004).....</i>	59
<i>Figure 1-14 Mechanical squeezing of the cryogel matrix for the recovery of bound cells. Affinity-bound cells on cryogel matrix were removed by compressing the cryogel column up to 50% of its original length by using an external piston that squeezes out the liquid that contains cells. In the next step, the buffer was added to re-swell the affinity cryogel matrix and then the column was flushed with fresh cold buffer.....</i>	60
<i>Figure 1-15 Fouling of 6 Sepharose FF beads (GE Healthcare, Sweden) by lipids in a yeast homogenate feed after 10 cycles, including CIP, as visualised by electron microscopy (Courtesy of Jing Jin, UCL).</i>	64
<i>Figure 1-16 Confocal study of the rate of adsorption of Cy5.5-labelled BSA to fresh Q Sepharose FF. The BSA and resin were mixed for different times before being analysed (as indicated below pictures). (Siu et al., 2006b)</i>	67
<i>Figure 1-17 Confocal laser scanning microscopy image of Sepharose Butyl-S 6 FF beads after repeated loading cycles with a crude yeast feed. Neutral lipids in the feed were labelled green by BODIPY 493/503 dye (Jin et al., 2010).</i>	68
<i>Figure 1-18 The colloidal model for net electronegative particle. (Malvern Instruments, UK. www.malvern.com)</i>	71
<i>Figure 1-19 Schematic diagram showing hydrophobic interaction between proteins in solution (A) and between proteins and a hydrophobic ligand on HIC absorbent (B). As detailed in McCue (2009).</i>	75
<i>Figure 1-20 Hofmeister series of cations and anions.</i>	76
<i>Figure 1-21 Ligands substituted on HIC media. Reproduced from Hydrophobic Interaction and Reverse Phase Chromatography handbook available from GE Healthcare.</i>	78
<i>Figure 1-22 The four state model. N = native protein and U = unfolded protein. S indicates the form in the stationary phase. Reproduced from (Xiao et al., 2007b).</i>	82
<i>Figure 1-23 Different format of CIM monolith columns available from BIA Separations. (A) Analytical columns, 0.1ml; (B) Disks, 0,34ml (C) Radial monolith, 1ml. The yellow plastic ring around the disk indicates that the</i>	

column chemistry is C4 HIC. The white ring on the analytical column indicates the column chemistry is OH HIC.....	86
Figure 1-24(A) CIM monolith disk (0.34ml) and disk housing available from BIA separation. (B) A complete disk housing.....	87
Figure 1-25 (A) Shape of CIM monoliths at 80ml, 800ml and 8L; (B) Shape of 1ml CIM monolith.	90
Figure 1-26 Schematics of the flow of the mobile phase and the sample through CIM disk (a) and CIM tube (b).....	91
Figure 2-1 Flow sheet of primary purification and pre-chromatography preparation steps. Material can then follow two different routes; route one is for crude material and is filtered before the column, route two is for a reduced lipid feed where a lipid removal method is applied before filtration.	97
Figure 2-2 Schematic illustrating the elution steps of CIMac monolith method for VLP analysis.	100
Figure 2-3 Example of a calibration curve used for ELISA analysis of VLP samples post experiment.	104
Figure 3-1 Example fermentation data for the production of the VLP in the 75L fermenter.	113
Figure 3-2 Example fermentation data for VLP production in the 20L fermenter..	114
Figure 3-3 Fermentation data for OD and glucose in the 450L fermenter.	115
Figure 3-4 Comparison of OD and glucose consumption in shake flasks with either Sigma-Aldrich (●) or BD Difco media (○) (n=3).	116
Figure 3-5 Comparison of VLP production by yeast extract supplier. The negative and positive control samples were purchased as part of the ELISA kit.....	116
Figure 3-6 Comparison of VLP recovery between different detergents and heat (no detergent). The recovery was compared at 2 and 4 hours, at 20°C and 50°C. The XAD-4 was carried out at 20°C for all samples.	118
Figure 3-7 DLS results from extraction steps using Triton X-100 at 20°C to 50°C.	119
Figure 3-8 Chromatograms obtained during screening for a suitable monolith column ligand with post-hydrophobic interaction chromatography material. Material was loaded on to C4 and OH column at 0.6M (NH ₄) ₂ SO ₄ and 0.3M (NH ₄) ₂ SO ₄ to adjust binding affinities within in the column. Absorbance profiles at 280nm are shown with peaks marked out for (L) Loading Zone;	

(E) Elution Zone and (R) Regeneration. Graphs correspond to (A) High ligand density (HLD) C4 1mL monolith columns, (B) Low ligand density (LLD) C4 disks, (C) 50% C4 and 50% OH 1mL monolith columns, (D) OH 1mL monolith columns. Columns A/B/D are commercially available. Column C was a gift from BIA Separations.	121
Figure 3-9 Chromatograms of monolith runs with mobile phase of 0.6M to 1.2M ammonium sulphate. The first peak corresponds to binding, the second to elution and third to the regeneration step.	123
Figure 3-10 Breakthrough curves for VLP binding to an OH monolith at 0.6M to 1.2M ammonium sulphate.	124
Figure 3-11 Comparison of VLP and protein levels in elution samples over increasing salt levels in the mobile phase buffer.	124
Figure 3-12 Breakthrough curve for crude feed at 1.0M ammonium sulphate on an OH monolith. (n=3). 10% breakthrough is indicated by the dotted line. (Please see Section 9 Figure 9-1 for raw VLP data)	125
Figure 3-13 Breakthrough curves using 25mL of crude feed material over 3 consecutive run on a new column. The amount of VLP was monitored using ELISA. (Please see Section 9 Figure 9-2 for raw VLP data).....	126
Figure 3-14 Comparison of dynamic binding capacity of butyl-S Sepharose 6 FF 1mL HiTrap column (▲) and a monolith OH 1mL column (●). 10% breakthrough is indicated by the dotted line. The columns were loaded with untreated homogenised yeast and the VLP breakthrough was monitored using ELISA. (n= 2 for butyl-S column and n=3 for OH monolith. Error bars are 1 S.D.) (Please see Section 9 Figure 9-3 for raw VLP data).....	127
Figure 3-15 Breakthrough curve of VLP on a large pore OH monolith, analysed by ELISA. (n=3). (Please see Section 9 Figure 9-4 for raw VLP data).	128
Figure 3-16 Pictures of HBsAg from elution samples after hydrophobic interaction chromatography using an OH monolith. The black bar is equal to 100nm on both pictures. A) Transmission electron microscope (TEM). Samples were negatively stained with 2% uranyl acetate on carbon grid. B) Atomic force microscopy picture (AFM). Samples were adhered to a silanised glass slide. AFM was in tapping mode.	129
Figure 3-17 An example DLS size graph on a post-chromatography sample. Size distribution is by volume (n=3).	130

<i>Figure 3-18 Graph showing zeta potential results for five measurements on a VLP sample. The sample was diluted x15 with 10mM Sodium phosphate, pH 7.</i>	131
<i>Figure 3-19 Zeta potential results for purified VLP samples over a range of salt concentrations. The samples were diluted with 20mM sodium phosphate pH 7.0 to 7% v/v (n=3).</i>	132
<i>Figure 3-20 Titration graphs showing the zeta potential over a range of pH values from pH 4 to 9. The samples were diluted to 7% v/v (n=3).</i>	132
<i>Figure 3-21 Calibration curve for proteins and LDL using PBS as the mobile phase. LDL = low density lipoprotein; tg = thyroglobulin (669 KDa); apo = apoferritin (443 KDa); BA = β-amylase (200 KDa); ADH = ADH (150 KDa); alb = albumin (66 KDa); ca = carbonic anhydrase (29 KDa).</i>	134
<i>Figure 3-22 Graphs comparing absorbance at 280nm for the size exclusion chromatography and VLP ELISA results from collected samples. (A) 20°C; (B) 30°C.</i>	135
<i>Figure 3-23 Comparison between Bradford Assay and BCA Assay for three elution samples. The box below indicates which sample each column corresponds to. Each sample was analysed in triplicate.</i>	137
<i>Figure 4-1 Pressure increases over 10 consecutive runs during loading. The column is a 1mL OH monolith column run with a crude feed at 1.0M ammonium sulphate.</i>	142
<i>Figure 4-2 Confocal microscopy showing the fouling of lipids in a C4 disk monolith. The lipids were fluorescently labelled with BODIPY 493/503 dye (Invitrogen, Paisley, UK). (1) The column was challenged with the labelled crude VLP material; (2) the column was cut into sections and placed under the confocal microscope; (3i) the lipids form a layer on top of the column, causing an increase in pressure and reducing the recovery; (3ii) the lipids move throughout the column too, affecting the VLP recovery.</i>	144
<i>Figure 4-3 Amount of VLP and lipid remaining in samples after ammonium sulphate precipitation from 0-35% w/v.</i>	145
<i>Figure 4-4 Amount of VLP and lipid remaining in the feed after the addition of LRA from 0 – 80 mg/mL.</i>	146
<i>Figure 4-5 Lipid and VLP remaining in the pooled filtrate after filtration through Zeta Plus delipid filters at 6.5/20/65 mL/min.</i>	147

<i>Figure 4-6 Lipid and VLP remaining in the crude feed after the addition of XAD-4 to the material and subsequent filtration.</i>	<i>148</i>
<i>Figure 4-7 Analysis of the VLP:Lipid ratios for each of the lipid removal methods to determine the ideal method of use.....</i>	<i>149</i>
<i>Figure 4-8 Comparison of the dynamic binding capacity of the 1mL OH monolith when a crude feed (▲) and a reduced lipid feed (●) are applied to the column. 10% breakthrough is indicated by the dotted line.(See Section 9 Figure 9-5 for raw VLP data)</i>	<i>150</i>
<i>Figure 4-9 Comparison of the dynamic binding capacity on a Butyl-S resin column when a crude feed (solid line ▲) and reduced lipid feed (dotted line ●) are applied to the column.(See section 9 Figure 9-6 for raw VLP data)</i>	<i>151</i>
<i>Figure 4-10 Comparison of the pressure increase over consecutive runs in a monolith column when a crude feed (●) or reduced lipid feed (○) is applied.</i>	<i>152</i>
<i>Figure 4-11 SDS-PAGE of material from a 1ml OH monolith separation process. The feed, flow through (breakthrough) and elution material were collected and concentrated down to approximately 1mg/ml before loading. Material from an equivalent run with crude material on a butyl-S resin column has been added for comparison.</i>	<i>154</i>
<i>Figure 5-1 Gradient elutions on a OH 1mL column using crude material. (A) 0.6M (B) 1.2M. Only graph B contains any VLP as nothing was seen on the ELISA assay for graph A.</i>	<i>160</i>
<i>Figure 5-2 Chromatographic profile for runs on a 1mL OH monolith column with crude homogenate material bound at 1.0M ammonium sulphate. The wash step was increased from 0 to 40 minutes (25CV to 145 CV). (A) Full profile for absorbance at 280nm. L=loading, E = elution, R=regeneration; (B) Elution and regeneration peaks at absorbance 280nm for no wash step (0 min) and 40 minutes.</i>	<i>162</i>
<i>Figure 5-3 ELISA results from elutions with crude material with binding buffer with 1.0M ammonium sulphate. Samples were collected after a wash time from 0 (no additional wash time) to 40 minutes. (n=3).....</i>	<i>163</i>
<i>Figure 5-4 ELISA results for VLP on the effect of wash time on the VLP elution profile on a 1mL Butyl-S HiTrap column, using a crude homogenate VLP</i>	

<i>feed, binding at 0.6M ammonium sulphate . Increased wash time was from 0 minutes to 40 minute.) (n=3). L=loading, E=elution, R= regeneration.</i>	164
<i>Figure 5-5 The effect of residence time with a crude yeast homogenate VLP feed, at 0.6M ammonium sulphate on a 1mL monolith column . (A) ELISA results (n=3); (B) Elution and regeneration peaks.</i>	166
<i>Figure 5-6 Residence time on OH monolith with reduced lipid yeast homogenate VLP feed material at loading salt concentration of 1.0M (A) and 0.6M (B) ammonium sulphate. (ELISA results n=3).</i>	167
<i>Figure 5-7 Comparison of the amount of VLP in the elution peak from a 1mL monolith, using 1M ammonium sulphate in the binding buffer, with crude (●) and reduced lipid (▲) material. The column was run from 1ml/min to 12ml/min.....</i>	169
<i>Figure 5-8 Dynamic light scattering graphs of material eluted during a two step process on a OH 1mL column, using 1M ammonium sulphate in the binding buffer. Step 1 is at 60% B (A) and step 2 at 100% B (B). The peaks correspond to 13nm for step 1 and 210nm for step 2. (n=3).</i>	170
<i>Figure 5-9 Final analytical method on the CIMac using a two-step process at 80% and 100% steps. The binding buffer was 0.8M ammonium sulphate and 100 µl was loaded. The absorbance profile at 280nm shows the majority of material was eluted in the first step at 80%.</i>	172
<i>Figure 5-10 Initial runs on 0.1M CIMac at 0.8M ammonium sulphate, loading 100µL using triplicate samples showed a shift in peak sizes over successive runs, with or without cleaning between each sample run. As the size of peak 1 decreased peak 2 increased indicating that the binding affinity within the column was changing over runs, probably due to fouling.</i>	173
<i>Figure 5-11 Graphs showing the absorbance trace seen at 280nm and comparisons with samples collected and tested for protein and VLP. (A) Crude sample 0 minutes; (B) Reduced lipid sample 0 minutes</i>	174
<i>Figure 5-12 Results from CIMac column for elution samples after a wash time of 0 (standard elution profile) to 40 minute with crude (●) and reduced lipid (▼) feed material. (A) 1.0M binding buffer; (B) 0.6M binding buffer.</i>	175
<i>Figure 5-13 Comparisons for each residence time condition (salt level and lipid content) between all three assays (CIMac, ELISA and protein). (A) 1.0M Crude feed; (B) 1.0M Reduced lipid feed; (C) 0.6M Crude feed; (D) 0.6M</i>	

<i>Reduced lipid feed. Protein was unavailable for 0.6M as the level was below assay limits.</i>	<i>177</i>
<i>Figure 9-1 Breakthrough curve for crude feed at 1.0M ammonium sulphate on an OH monolith. (n=3). (Raw data for Figure 3-12).....</i>	<i>234</i>
<i>Figure 9-2 Breakthrough curves using 25mL of crude feed material over 3 consecutive run on a new column. The amount of VLP was monitored using ELISA. (Raw date for Figure 3-13).....</i>	<i>235</i>
<i>Figure 9-3 Comparison of dynamic binding capacity of butyl-S Sepharose 6 FF 1mL HiTrap column (▲) and a monolith OH 1mL column (●). 10% breakthrough is indicated by the dotted line. The columns were loaded with untreated homogenised yeast and the VLP breakthrough was monitored using ELISA. (n= 2 for butyl-S column and n=3 for OH monolith. Error bars are 1 S.D.) (Raw data for Figure 3-14).....</i>	<i>235</i>
<i>Figure 9-4 Breakthrough curve of VLP on a large pore OH monolith, analysed by ELISA. (n=3). (Raw date for Figure 3-15)</i>	<i>236</i>
<i>Figure 9-5 Comparison of the dynamic binding capacity of the 1mL OH monolith when a crude feed (▲) and a reduced lipid feed (●) are applied to the column. 10% breakthrough is indicated by the dotted line. (Raw data for Figure 4-8).....</i>	<i>237</i>
<i>Figure 9-6 Comparison of the dynamic binding capacity on a Butyl-S resin column when a crude feed (solid line ▲) and reduced lipid feed (dotted line ●) are applied to the column. (Raw data for Figure 4-9)</i>	<i>237</i>

LIST OF TABLES

<i>Table 1.5-1 Gradient materials used in density gradient ultracentrifugation.</i>	<i>43</i>
<i>Table 1.5-2 Details on commercial membranes available for membrane chromatography.</i>	<i>57</i>
<i>Table 1.7-1 Non-polar amino acids which contribute to the hydrophobicity of proteins.</i>	<i>73</i>
<i>Table 1.8-1 The range of ligand chemistries for CIM Monoliths available from BIA separations. List from www.biaseparations.com.</i>	<i>87</i>
<i>Table 1.8-2 Scale up options for monolithic columns.</i>	<i>90</i>
<i>Table 3-1 The recovery levels of VLP from each of the five columns tested at the two salt levels of 0.6M and 0.3M ammonium sulphate.</i>	<i>122</i>
<i>Table 3-2 Standards used to calibrate the SEC column.</i>	<i>133</i>
<i>Table 5-1 Pressure drop seen over flow rates with 1ml OH monolith column at 1M ammonium sulphate.</i>	<i>168</i>
<i>Table 7.2-1 Table of validation documents needed for post-approval changes switching from resin columns to a monolith.</i>	<i>192</i>

LIST OF SYMBOLS AND ABBREVIATIONS

Symbols

°C	Degrees Celsius
C	Concentration (mg/mL) at value x
C ₀	Concentration (mg/mL) at value 0
C4	Butyl ligand
cm	Centimetres
CV	Column volumes
g	Grams
h	Hours
kDa	Kilo daltons
kg	Kilograms
L	Litres
M	Molar concentration
M Da	Million Daltons
mg	Milligrams
ml	Millilitres
mm	Millimetres
mM	Millimolar
n	Number of samples averaged
nm	Nanometres
OH	Hydroxyl

pI	Isoelectric point
s	Seconds
µg	Micrograms
µL	Microlitres

Abbreviations

ADH	Alcohol dehydrogenase
Au	Arbitrary unit (absorbance)
AFM	Atomic force microscopy
BCA	Bicinchonic acid (Protein Assay)
BSA	Bovine Serum Albumin
CIM	Convective Interaction Monolith
CHAPS (detergent)	3-[(3-cholamidopropyl)dimethylammonio]-1-propanesulfonate
CSLM	Confocal Scanning Laser Microscopy
Cys	Cysteine
DBC	Dynamic binding capacity
DNA	Deoxyribonucleic acid
DCW	Dry cell weight
DLS	Dynamic light scattering
ELISA	Enzyme linked immunosorbent assay
ELSD	Evaporative light scattering detection
ER	Endoplasmic reticulum

HBsAg	Hepatitis B surface antigen
HBV	Hepatitis B virus
HCP	Host cell proteins
HIC	Hydrophobic interaction chromatography
HPLC	High pressure liquid chromatography
HPV	Human papilloma virus
IEX	Ion exchange chromatography
IPA	Isopropanol alcohol
LDL	Low density lipoprotein
MWCO	Molecular weight cut off
OD	Optical density
PEG	Polyethylene glycol
RQ	Respiratory quotient
s.d	Standard deviation
SDS-PAGE	Sodium dodecyl sulphate polyacrylamide gel electrophoresis
TEM	Transmission electron microscopy
TFA	Trifluoroacetic acid
v/v	Concentration of substance by volume (%)
VLP	Virus-like particle
w/v	Weight of substance by volume (%)

1 INTRODUCTION

1.1 RELAVANCE OF PROJECT

Vaccines represent the one of the greatest contributions to disease prevention in both humans and animals. Per year vaccines prevent in excess of 3 million deaths and have a positive economic impact in excess of a billion dollars per year (Ulmer et al., 2006). Often vaccines involve the use of attenuated or inactivated live viruses. There is a potential to produce disease in healthy individuals after vaccination and this must be minimised to the lowest possible probability (Noad and Roy, 2003).

Virus-like particles (VLPs) represent a new range of vaccines, producing immune responses via a highly effective and safe macromolecule which mimics the overall structure of the virus. VLPs contain no genetic material and so cannot cause disease. Current commercially available vaccines produced from VLPs include Hepatitis B (HBV) and Human Papilloma Virus (HPV). There are a number of vaccines in development including for Influenza, Human Parvovirus and Norwalk viral infections (Roldao et al., 2010).

Advances and improvements in expression systems, better cell lines, optimising media and more efficient bioreactors have resulted in higher yields at concentrations most process technology cannot deal with (Langer, 2011). Often downstream processing steps can form bottlenecks in the process, increasing processing times and reducing batch numbers per year. Chromatography is commonly one of those steps which may form a bottleneck. Often a process may contain two or three chromatography steps which are used in purification, as capture steps, polishing steps or for viral removal.

Chromatography media was originally developed for small protein molecules, which are a number of factors smaller than large macromolecules. The use of resins with large macromolecules has resulted in yields significantly less than those with small proteins (Jungbauer, 2005). Alternative chromatography media such as a monolith adsorption system have favourable physical properties giving greatly enhanced capacity for large (<1,000 kDa) macromolecules, when compared

to bead based pack beds. Wide pores allow the application of faster flow rates, reducing processing times. Monoliths have previously been used for commercial scale plasmid DNA processing (Urthaler et al., 2005). Currently research on monoliths has focused on how they may help with the technical challenges faced in viral vaccine production, not only for downstream processing steps, but also as an analytical method.

Large macromolecular assemblies, such as VLP, have complex interactions with surfaces and other molecules. These characteristics can give rise to difficulties in controlling adsorption based purification with conditions leading to the formation of aggregates or loss of yield. Understanding the phenomena involved can help develop optimal strategies to help determine the ideal chromatographic conditions.

1.2 AIMS OF PROJECT

The aim of this project is look at the purification of a macromolecule using a novel chromatography matrix, known as a monolith. Focus will be on how the monolith performs with a yeast derived VLP. The project is in collaboration with BIA Separations, Slovenia, who have developed the monoliths into a commercially available product. A range of current and novel analytical techniques will be used to achieve a number of objectives:

1.2.1 Development of a monolithic VLP separation

Currently there is a conventional chromatography process, used to purify the HBsAg VLP, based on a hydrophobic interaction column with ligands of weak hydrophobicity. Using HBsAg VLP produced recombinantly from a *Saccharomyces cerevisiae* yeast strain, by a batch fermentation process, a HIC purification process will be developed. Once a suitable monolith column has been identified the process will be modified to ensure that the loading and elution conditions are ideal. The two processes will be compared on capacity, yield, purity and throughput.

1.2.2 Interactions of impurities with hydrophobic monoliths

Lipid fouling in chromatography has a detrimental effect on the purification process and lifetime of the column. Conventional resins show irreversible fouling over time, from contaminants such as lipids and proteins, inside the pores, reducing capacity and yield (Jin et al., 2010, Siu et al., 2006a). Due to the difference in the pore structure for monoliths it is unknown where and how the fouling would occur. From the results of the study an effective strategy for lipid removal will be developed and integrated into the full purification process. The feeds with or without lipid will be compared to determine the effect on the chromatography process from the inclusion of lipids.

1.2.3 Interactions and loss of product on hydrophobic monoliths

A variety of binding and elution conditions will be studied to determine what effects this may or may not have on the VLP. The conditions of chromatography may result in reversible or irreversible changes in the structure of the molecule. This can result in the formation of aggregates, loss of product viability or significant yield losses. Hydrophobic interaction is known to cause unfolding of proteins upon adsorption on the chromatographic media (Xiao et al., 2007b). The conditions of the chromatographic process will be varied to provide insights into any structural changes which may occur.

1.3 ORGANISATION OF THESIS

The first chapter introduces the project, including the relevance and aims behind choosing to look monoliths as an adsorption media and a macromolecule like VLP. A literature review and background behind a number of the themes and areas studied in the project are presented. These include VLP, chromatography techniques, monoliths, BIA-specific CIM monoliths, and methods to analyse chromatographic performance.

The second chapter covers the details on the experimental methods that were used during the project. Details are given on the volume and concentration of materials, equipment setup and experimental conditions.

The third chapter reports on the development of the monolithic chromatography process using a range of hydrophobic ligands and monolithic formats. A comparison with the conventional resin column is presented. The standard monolith is compared to a large pore column to determine the effect of pore size on the process. A number of analytical methods are tested for their suitability in analysis of the VLP and VLP purification process.

The fourth chapter highlights the effect of the presence of lipid in the feed material. Four lipid removal methods are presented, with the selection of one method which can then be used before the chromatography step to produce a lipid-reduced feed material. The dynamic binding capacity of the monolith with the reduced lipid feed is compared to the full lipid feed.

The fifth chapter focus on the effects of the chromatographic process on the VLP yield and structure. The effect of time on the structure of the VLP and subsequent elution yield was studied. The use of a small monolith, from BIA separations, was used to gain some understanding of the processes that may be occurring.

The sixth chapter summarises the findings and conclusions from the project areas. A number of areas for future work are discussed.

The seventh chapter talks about validation of a chromatography process and the validation issues which arise when a chromatography process is changed. The economics of using a new chromatography matrix, such as the monolith, is discussed.

The final chapter includes an inventory of all references accessed and used throughout the project.

1.4 VIRUS-LIKE PARTICLES (VLP) AND VACCINES

1.4.1 Traditional vaccines

Numerous vaccines have been developed against both bacterial and viral diseases. The purpose of a vaccine is to elicit an immune response, giving long-term protection from the particular disease. Vaccines can be made using:

- Killed (Inactivated) microorganisms
- Living microorganisms
- Weakened (attenuated) microorganisms
- Inactivated bacterial toxins (toxoid)
- Purified cellular subunits
- Recombinant vectors
- DNA

Inactivated vaccines are composed of viruses which have lost their infectivity through the use of various agents, such as formaldehyde and UV irradiation, which damage the DNA (Levy et al., 1994). They differ from attenuated vaccines, which use virus strains that are “mild” or lack virulence either in nature or through forced mutations (Levy et al., 1994). Whole cells do not have to be used in a vaccine, as shown by the use of capsular polysaccharides in the *Streptococcus pneumonia* vaccine, and small peptides (e.g. 15 to 20 amino acids) which are synthesised in the lab.

The use of recombinant vectors involves placing genes from the pathogen encoding the major antigens, for example the adenovirus, into non virulent viruses and bacteria. The antigen is then replicated in the host and expresses as the product of the pathogen, which will elicit an immune response when it leaves the cell or is displayed on the cell surface (Willey et al., 2008). DNA vaccines are similar, by generating foreign proteins in the cell which the host immune system then responds too (Willey et al., 2008).

1.4.2 VLP vaccines

Although the types of vaccines stated in section 1.4.1 have proved to work effectively they do have disadvantages. Inactivated pathogens are very stable, with no tendency to become active again, although multiple boosters are normally needed (Willey et al., 2008). Issues may arise if minuscule portions of virus particle survive chemical treatment and produce disease. Attenuated vaccines do not require multiple boosters, but there is the possibility of reversal to a more virulent form which may cause full blown illness in the immune compromised (Willey et al., 2008). The same disadvantage can be seen with the use of a recombinant vector vaccine.

Vaccines using virus-like particles (VLPs) offer an alternative solution. Structural proteins of many viruses can form VLPs following recombinant DNA expression in a variety of culture systems (Grgacic and Anderson, 2006). The VLPs mimic the overall structure of the virus particles, without the requirement of containing infectious genetic material (Noad and Roy, 2003). VLPs stimulate the efficient cellular and humoral immune responses for both viral and non-viral disease (Noad and Roy, 2003) often proving more immunogenic than subunit or recombinant protein immunogens (Grgacic and Anderson, 2006).

Production of VLPs can happen in mammalian or insect (Pattenden et al., 2005) or yeast expression systems (Liu et al., 2009, Fu et al., 1996b) and even plants (Guan et al., 2010). Formation of the VLPs is either by self-assembly or chemical modification following the production of separate subunits (Pattenden et al., 2005).

VLPs have also shown that they can be used as carrier molecules for the delivery of epitopes (Noad and Roy, 2003). A high immune response comes about from the repetitive high density display of the epitopes (Grgacic and Anderson, 2006). The display of non-infectious subunits of pathogens is achieved via the use of linkers, an example is the development of an allergy vaccine using bacterial pili (Lechner et al., 2002).

Currently there are two commercially available VLP vaccines, one against the hepatitis B virus (HBV), and one against various types of the human papilloma virus (HPV). The HBV vaccine has been available since 1982, but it took a long period of time before the next VLP vaccine for HPV came to market in 2006 (Merck

& Co) and 2007 (GSK) (Inglis et al., 2006, Harper, 2009). The HPV vaccine is composed of a number of VLPs from a range of HPV strains to protect against cervical cancer and genital warts (Harper, 2009). Work is being carried out on other VLP vaccines, with potentials including HIV (Doan et al., 2005) and influenza (Galarza et al., 2005, Mahmood et al., 2008, Bright et al., 2008).

The technical challenges of producing viral vaccines (whether VLP or viruses themselves) is not only limited to finding suitable antigens but encompasses all aspects, from the expression systems and process train, to the process analytics and the regulatory considerations. Buckland (2005) provides an overview of the development of some viral vaccines, in particular focusing on Merck's HPV vaccine.

To produce a VLP vaccine at a manufacturing scale which would satisfy the anticipated market demand, the process development in scaling up from the lab is crucial. For example development and use of a suitable expression system is important to prevent the issue of low productivity levels, and produce correctly formed VLP (Vicente et al., 2011b), as well as DSP steps which work with the complex nature of the VLPs but can be used at large scale.

The development of advanced analytical methods must occur alongside vaccine development to ensure that vaccine characterisation, potency and safety are possible. But this can prove problematic due to the complex nature of VLPs, and result in numerous methods being applied to ensure the correct data is achieved. It is important that these issues are addressed early to prevent analytical limitations. Ultimately the combination of a suitable purification process and good analytical techniques ensure that the resultant vaccine is safe for either human or animal use. This is particularly important as vaccines are injected into healthy humans, or are used in animals which enter the food chain. In terms of purity it is up to the manufacturer to remove as much as possible all contaminants/extraneous matter from the final bulk product (CBER regulations).

1.4.3 Hepatitis B virus (HBV)

Hepatitis B is a highly infectious disease, with about 2 billion people infected worldwide (WHO information sheet No. 204) and about 350 million people with a

chronic infection. Approximately 1 million deaths occur annually (Wright, 2006). Around 15-40% of infected patients will develop cirrhosis, liver failure or hepatocellular carcinoma (HCC) making it the 10th leading cause of death worldwide (Lavanchy, 2004).

Individuals may also be carriers of the virus acting as reservoirs of infection. Often these are those in infancy or childhood, and the immunodeficient (Peterson, 1987). In the Middle and Far East, and Sub-Saharan Africa, they can account for around 10-30% of the population (O'Grady, 2002). Transmission is through contact with infected body fluids, such as blood, saliva, and semen. HBV is 50-100 times more infectious than HIV (WHO information sheet No. 204).

1.4.4 Hepatitis B surface antigen (HBsAg)

1.4.4.1 Production

The isolation of the gene for HBsAg from the genome of the Dane particle enabled the development of recombinant organisms producing HBsAg (Valenzuela et al., 1979). The initial use of bacterial systems failed (Valenzuela et al., 1982) but yeast, such as *S.cerevisiae* and *P.pastoris*, and mammalian systems, such as CHO cells, produced mature particles (Valenzuela et al., 1982, Wampler et al., 1985, Miyanochara et al., 1983, Fu et al., 1996a, Petre et al., 1987, Carty et al., 1989, Belew et al., 1991, Diminsky et al., 1997, Burns et al., 1992). Comparison of the recombinant HBsAg to human plasma derived HBsAg shows that the recombinant HBsAg was similar in size and composition (Valenzuela et al., 1982, Wampler et al., 1985, Miyanochara et al., 1983, Yamaguchi et al., 1998).

Production of the HBsAg particle has also been proven in plant expression systems (Smith et al., 2002, Richter et al., 2000) which would enable oral delivery of the vaccine instead of the traditional needle/syringe method. The use of plants would also reduce the cost of the bulk antigen, although higher doses are needed because of the gut environment (Smith et al., 2002).

1.4.4.2 Structure

During HBV infection hepatocytes produce and secrete HBsAg to excess. They were identified in the late 1960s and were originally called Australia Antigen. This was because they were first identification in the sera of an Australian aborigine (Bayer et al., 1968, Almeida and Waterson, 1969). Identification of infected individuals is due to the presence of these particles and not the infectious virus, called the Dane particle, which is present in much lower quantities (Dane et al., 1970).

HBsAg is a lipoprotein, approximately 20nm and 3.5MDa in size. It is composed of approximately 25-40% lipids and 75-60% proteins, (as seen in *Figure 1-1*) (Gavilanes et al., 1982, Diminsky et al., 1997, Greiner et al., 2010). The HBsAg particle mimics the structure of the outer coat of the HBV Dane particle. In the HBV Dane particle there are three different types of protein making within this outer coat. These are synthesized by 3 overlapping envelope genes within one single open reading frame (Yamada et al., 2001). The proteins are the S (small) protein at 226 amino acids, M (medium) which is the S protein plus 55 amino acids, and the large (L) protein which is the M protein plus 108 or 119 amino acids (Yamada et al., 2001). It is synthesised in the endoplasmic reticulum and subsequently buds out, *Figure 1-2* (Huovila et al., 1992, Simon et al., 1988, Eble et al., 1986). The rate limiting step in the export process is the budding of the lipoproteins particle from the membrane (Huovila et al., 1992).

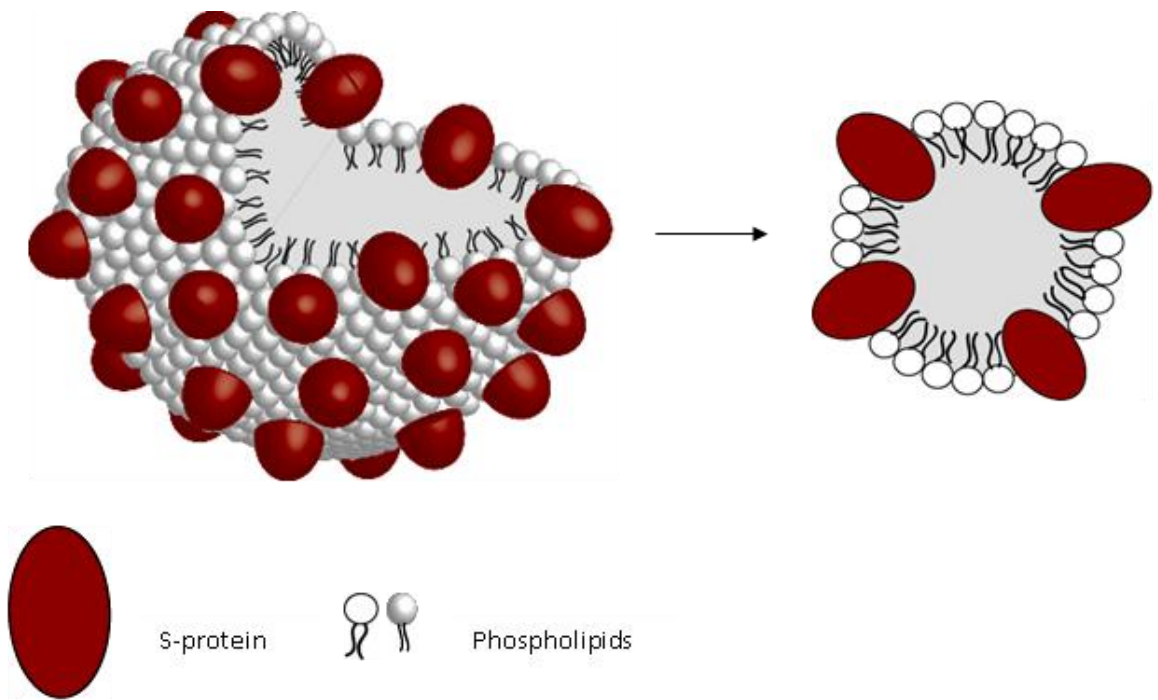


Figure 1-1 A schematic diagram of the virus-like particle HBsAg from yeast. Each VLP is around 22nm in size and 3.5mDa. It is made of approximately 75% protein (S-protein) and 25% lipid. The core of the VLP contains free host lipids.

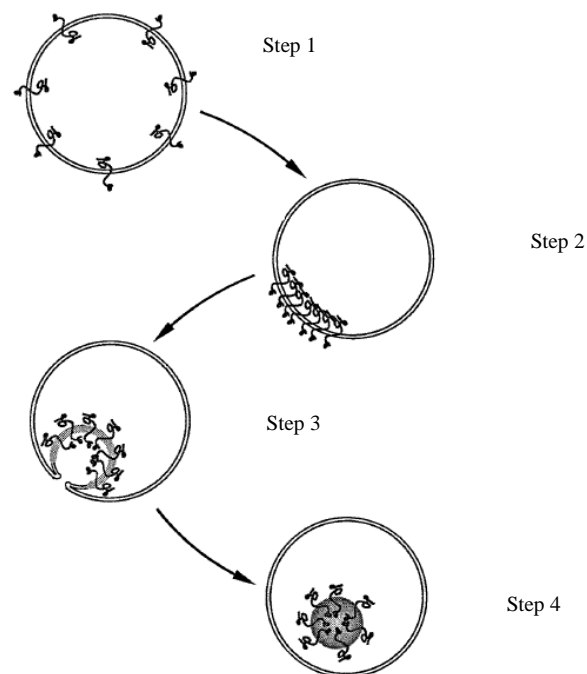


Figure 1-2 A model for the biogenesis of HBsAg particles. Particle formation occurs in several steps. Step 1: Synthesis of p24s in the ER membrane; Step 2: within 40 minutes all of this material has become protease resistant, which may represent

simply a conformational change or aggregation in the membrane or both. Over the next 3 hours, the bulk of this material is transferred to the ER lumen (Steps 3 & 4). (Simon et al., 1988)

If HBsAg is made in yeast only the S protein is in the VLP lipid membrane (Honorati and Facchini, 1998, Sonveaux et al., 1994, Gilbert et al., 2005), whereas CHO cells can produce HBsAg with all 3 proteins (Diminsky et al., 1997). The M protein has been shown to be dispensable and not required to form complete particles, whereas the L protein has been shown to be a key requirement in helping with budding of the Dane particles (Bruss and Ganem, 1991b). In yeast this budding is absent. The L protein contains the pre-S1 domain (Diminsky et al., 1997), which is needed for infectivity of the HBV (Blanchet and Sureau, 2007). Yeast HBsAg contains only the S protein with about 70 per particle (Greiner et al., 2010). The S protein is a 24-kD protein (also called p24s) which can be also be in a glycosylated form of 27-kD (gp27s) (Simon et al., 1988, Hemling et al., 1988, Petre et al., 1987), although glycosylation does not appear important for immunogenicity (Peterson, 1987). In HBsAg from human plasma samples around 25% of the proteins are glycosylated (Petre et al., 1987). Glycosylation can occur in CHO HBsAg, but is not seen in those produced in yeast (Diminsky et al., 1997).

The S protein is exceedingly hydrophobic and has an abundance of hydrophobic amino acids, such as proline and tryptophan (Hemling et al., 1988). There are 3 main hydrophobic regions, including one named the 'a' determinant. The 'a' determinant is a highly conformational section between amino acids 100 to 160 (Coleman, 2006, Chiou et al., 1997). Mutations of various amino acids in the S protein can have an effect on antigenic regions which may affect antibody recognition (Bruce and Murray, 1995, Chiou et al., 1997, Hemling et al., 1988, Bruss and Ganem, 1991a, Sonveaux et al., 1994, Coleman, 2006). There are also a number of cysteine molecules which appear to be important in structural formation and secretion with the S protein (Mangold et al., 1995). The major cysteines are in position Cys-107, Cys-138, Cys-149 and either Cys-137 or Cys-139, as indicated in *Figure 1-3* (Mangold et al., 1995, Bruce and Murray, 1995).

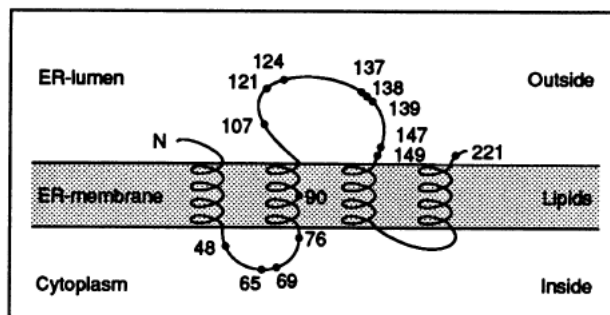


Figure 1-3 Secondary structure model of the HBV S protein. The major antigenic region is originally translocated into the ER lumen and it is only after assembly and secretion that it is exposed on the surface of the S protein (Mangold and Streeck, 1993, Mangold et al., 1995).

Cysteines play a major part in the formation of the disulphide bonds within the S protein (Mangold et al., 1995, Mangold and Streeck, 1993, Wampler et al., 1985, Coleman, 2006). The conformation and stability of the tertiary structure in the S protein is mainly driven by the formation of these disulphide bonds (Bundy and Swartz, 2011). These disulphide bonds likely do not form until it buds into the ER (Bundy and Swartz, 2011). Zhao et al showed that additional disulphide bond formation can be formed using KSCN and heat to produce a more mature particle, with high regularity and uniformity and an increase in antigenicity (Zhao et al., 2006). Wampler et al saw a similar effect when using thiocyanate (Wampler et al., 1985).

The 'a' determinant is of particular significance as research shows that any genetic variability in this region also causes different serotypes to appear. There are four different epitopes and four overlapping epitopes in the region (Seddigh-Tonekaboni et al., 2000). The 4 major serotypes for HBsAg are *adw*, *adr*, *ayw* and *ayr* (Norder et al., 1992). The 'a' determinant region is important for antibody recognition. Any change in the region may reduce the ability of any tests which use antibodies, such as ELISA tests, to recognise the HBsAg (Seddigh-Tonekaboni et al., 2000, Chiou et al., 1997, Coleman, 2006).

The lipid layer of the HBsAg is composed of lipids common to the species of production. Therefore the lipid composition is different when HBsAg is produced in human or yeast or CHO cells. Common to all species though is the high percentage of phospholipids present in the membrane, with levels around 67-90% in yeast (Sonveaux et al., 1995, Jin et al., 2010), 90% in transformed cell lines (Satoh et al., 2000), and 70% in humans (Gavilanes et al., 1982). Studies on the lipid layer suggest that it is not a traditional bilayer as is normally seen in enveloped viruses but is either a single layer or a discontinuous bilayer (Greiner et al., 2010, Satoh et al., 2000, Gilbert et al., 2005, Sonveaux et al., 1995) (as seen in *Figure 1-1*). This layer then surrounds a hydrophobic core containing the lipid triglyceride/neutral lipids (Greiner et al., 2010, Diminsky et al., 1997). The lipid layer has a tight association with the S protein, restricting its movement (Satoh et al., 2000, Greiner et al., 2010) and also helping to maintain the native conformation (Gavilanes et al., 1990).

Removing around 70% of the lipids in the bilayer can cause a big decrease in the antigenic activity of HBsAg in Guinea pigs (Gavilanes et al., 1990) but a partial delipidation of the particle has been shown to increase the efficacy of vaccination by preserving the particle structure and keeping it in solution (Desombere et al., 2006). Approximately 5% of vaccine recipients and chronic sufferers are non-responsive to the current vaccines. Delipidation of the HBsAg makes it 100 to 200 times more T-cell antigenic than normal, and has been shown to cause immune responses in both non-responders and chronic sufferers. It is possible that the delipidation exposes the 4 hydrophobic regions in the membrane better, but at the expense of reduced B-cell antigenicity (Desombere et al., 2006).

The aggregation of HBsAg is poorly understood as limited research has been conducted into its characterisation. Understanding the mechanism behind aggregation can ultimately help reduce the degree of aggregation formation in a final vaccine preparation, especially when the effect on efficacy, and immunogenicity, from aggregates is unknown. Guidelines from the ICH recommend that the percentage of aggregates is minimised and the levels evaluated against known criteria values (ICH guideline Q6B). Research by Tleugabulova et al. (1999) using size exclusion chromatography with HBsAg showed that peak broadening in chromatography samples was due to a degree of aggregation of the particles. As the extent of protein degradation with the HBsAg particle increased the particles were

retained longer on the column, suggesting modifications in the charge or hydrophobicity of the particle. Earlier work suggested that particle adhesion may be responsible for aggregation, with the aggregates containing a few active sites on its surface available to accommodate other HBsAg particles. When saturation of these sites is reached it can be seen that aggregation ceases (Tleugabulova et al., 1998).

Diminsky et al. (2000) investigated HBsAg aggregation as a result of storage conditions to determine the stability of the final bulk vaccine. They found that an increase in temperature was a major factor in promoting aggregation. The lipid components had a greater stability than the proteins components, seeing that changes in the conformation of the HBsAg S protein resulted in a loss of antigenic activity. Reduction in the helical content of HBsAg S proteins from 49% at 23°C to 26% at 60°C abolished the antigenic activity. Li et al. (2007) investigated aggregation during ultrafiltration. They also saw a change in the percentage content of α -helix (48%-34%) and γ -turns (29%-38%) between the standard HBsAg and aggregated particles. Their results also showed a change in the lipid structure of the particle.

Aggregation studies on proteins have shown that there is often a structural transition between the aggregation-prone protein formation and the standard protein formation. This is characterised by an increase in β -sheets. It is recognised as a key step in the misfolding of proteins and spontaneous aggregation (McAllister et al., 2005). Aggregation can be visualised by electron microscopy. But as Tleugabulova points out this is difficult in HBsAg as both aggregates and non-aggregated forms are composed of spherical particles which are indistinguishable by electron microscopy and as such the aggregation pattern is masked (Tleugabulova et al., 1999).

1.4.5 Vaccine

The vaccine against Hepatitis B has been available since 1982. Vaccination is 95% effective in preventing the development of chronic infection (Lavanchy, 2004). Development of a recombinant vaccine greatly reduced the price per dose, from around \$100 plus per vaccination when human plasma was used in the late 70's/early 80's (Peterson, 1987) to an price per dose of approximately \$10-\$30 now (CDC website, US government).

1.5 PURIFICATION OF NANOPLEX MOLECULES

The collection of unit operations which form the production process for a biopharmaceutical drug, therapy or vaccine can be broken down into upstream, recovery, purification and formulation. See *Figure 1-4* for an example production process flow diagram for the production of a VLP. Ultimately the unit operations produce a final product which meets regulatory specifications, and is deemed safe for use by humans or animals.

Upstream will normally consist of a number of fermentation steps, producing the product either from a natural, or recombinant cell line. Once harvested from the fermentation vessel the media is then sent through recovery steps, such as centrifugation or filtration. Unit operations such as these will separate out the cells in the media, which will either be disposed of, or retained if there are intracellular products. Homogenisation may be used to release the intracellular product. Purification steps will involve removing all contaminants, such as DNA, host proteins or endotoxins; buffer exchange; or preparation of the molecule into its final form, such as refolding. Various purification steps include chromatography, precipitation, ultrafiltration, diafiltration and ultracentrifugation. The following steps of formulation ensure that the molecule is in the correct buffer and may be with or without adjuvants.

Purification steps are therefore some of the most important in the whole process. They can also be some of the most expensive as well! For example in chromatography Protein A resins can be thousands of pounds for just one litre, taking up a significant proportion of the cost of goods. Chromatography is one of the most common purification steps, and downstream process can often feature 2, 3 or 4 columns. The first capture chromatography step is of high importance and can have a major influence over the post unit operations, as well as the upstream steps before. Selection of the purification steps are important and are dependent on the molecule. A description of some of the main purification steps, both adsorptive (i.e. chromatography based) or non-adsorptive methods, which are used in biopharmaceutical production follows.

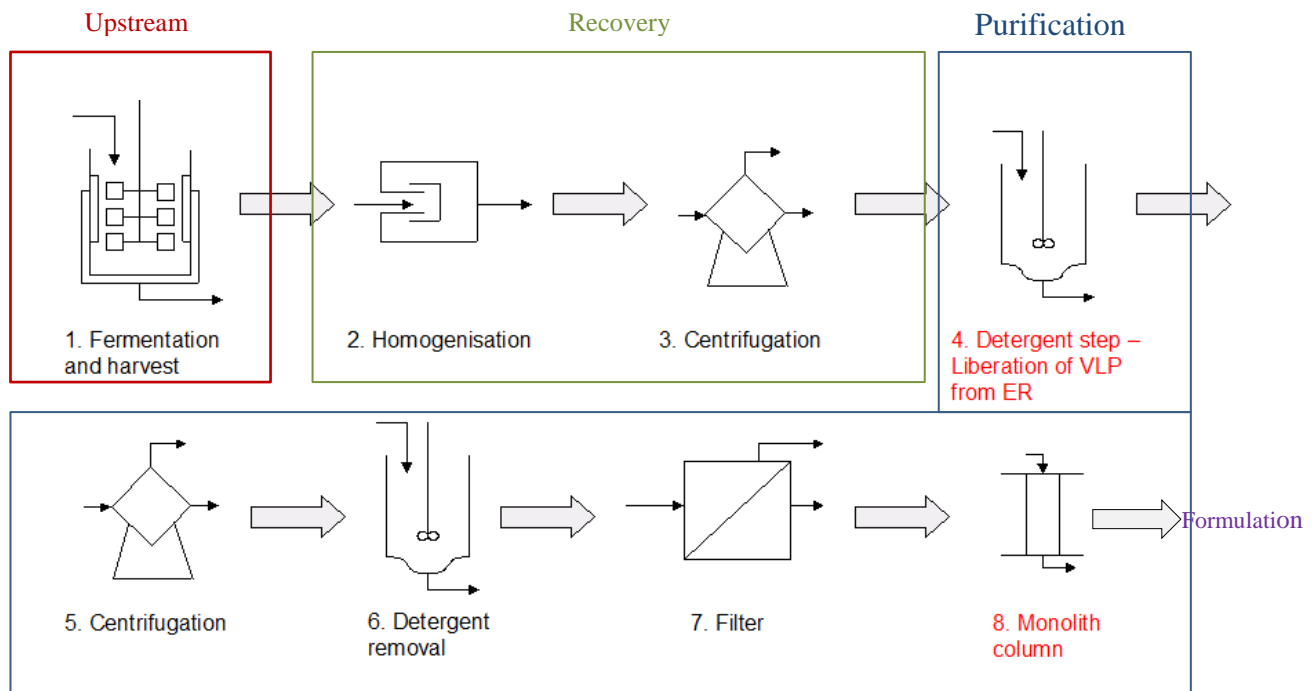


Figure 1-4 Example schematic of a production process for a VLP vaccine. Only the upstream, recovery and purification steps are details on the process flow diagram.

1.5.1 Non-adsorption purification methods - Precipitation

Precipitation is a cheap and effective method for protein purification. The idea behind precipitation is to take a substance, or molecule, which is soluble and make it insoluble. This can be done by changing a chemical or physical parameter in its environment (Hilbrig and Freitag, 2003). With proteins the solubility can be reduced by a single or a variety of techniques:

1. Adding salt to a high concentration – called “salting out”
2. Adjusting the pH to the isoelectric point
3. Reducing the dielectric constant of the medium to enhance electrostatic interactions
4. Adding non-ionic polymers to reduce the amount of water available for protein solution
5. Adding polyelectrolytes to cause flocculation
6. Adding polyvalent metal ions (Bailey and Ollis, 1986).

The principles of protein precipitation have been applied to macromolecules for conventional viral vaccines and plasmids DNA (Lyddiatt and O'Sullivan, 1998).

Plasmid DNA has emerged as an important macromolecule in the development of gene therapy, as a method of delivering the target genes to the target cell, or as a new vaccine material. For use it must be in the supercoiled or covalently closed circular (ccc) form, with the regulatory bodies stating that it must make up 90% or more of the total plasmid DNA within a product (Urthaler et al., 2005). The open forms must be minimised, as these are less transfective than the supercoiled form in gene therapy (Lander et al., 2002).

Various agents have been used to precipitate plasmid DNA including PEG (polyethylene glycol), $MgCl_2$, $LiCl_2$, PEI, CTAB (cetyltrimethylammonium), SDS, spermine, spermidine, sodium acetate, PEG and salt, ammonium sulphate, 2-propanol and affinity ligands (Lander et al., 2002, Ferreira et al., 2000, Shamlou, 2003, Hilbrig and Freitag, 2003, Freitas et al., 2006). Use of precipitation for nucleic acids by salts is a known technique in molecular biology, but requires well balanced conditions to avoid significant product loss (Voss, 2008). CTAB has proved to be highly selective approach for initial recovery in clarified lysate and scale up should be easy (Lander et al., 2002), although it may be hard to have fine control over the reaction at the large scale (Shamlou, 2003).

The use of precipitation for viral products is limited but PEG (polyethylene glycol) has proved successful in the purification of a formalin-inactivated hepatitis A vaccine, VAQTA (Merck), to concentrate the virus. But the process is sensitive to small changes in the growth and harvest conditions (Josefsberg and Buckland, 2012). Effect on the molecules is important in selection of the precipitating agent, for example the precipitation of contaminating proteins in the purification of HPV 16 proteins by ammonium sulphate also increases the extent of disulphide bonding, increasing the stability of the VLPs (Kim et al., 2012).

Affinity precipitation was developed in the 1970s as an alternative to affinity chromatography. There are two types of affinity precipitation, primary and secondary. Primary affinity precipitation involves the interaction between a multivalent enzyme and a bifunctional ligand. Secondary affinity precipitation uses affinity and stimulus-responsiveness combined in an agent called the affinity microligand (AML). The AML is a polymeric substance with one or several ligands

which precipitates reversibly because it is pH-sensitive, thermosensitive or oligomeric.

The pellet formed from the precipitation reaction can be collected either through centrifugation or ultrafiltration and then resuspension (Freitas et al., 2006, Shamlou, 2003, Lander et al., 2002). Care has to be taken when centrifuging and resuspending the pellet as the solid-liquid separation involved can cause shear-induced damage, which would reduce the yield of product collected (Levy et al., 2000). Although precipitation is a cheap and simple technique to use it is still limited in its use for a commercial manufacturing process, namely as it is very difficult to scale up successfully.

1.5.2 Non-adsorption purification methods - Ultracentrifugation

Ultracentrifugation has widely been used in the biotechnology industry as a downstream processing method since the first ultracentrifuges were developed for analytical use in the 1920's in Sweden. It differs from the traditional method of centrifugation due to the very high rotational speeds that are used during operation. Ultracentrifuges can run up to and exceed forces of 100,000g (Wheelwright, 1991).

There are two types of ultracentrifugation, differential pelleting or density-gradient centrifugation (Pinheiro and Cabral, 1992). Differential centrifugation involves components of diverse size, shape and densities being forced to move to the bottom of the centrifuge bottle at different rates. Density gradient centrifugation relies on the formation of a gradient along the depth of the cell, separating components by density and viscosity (Pinheiro and Cabral, 1992). The use of density gradient centrifugation is most common.

Density gradient centrifugation can be used to concentrate as well as purify a target product. It can be run in a batch or continuous mode (Desai and Merino, 2000). Three basic strategies are available for the operation of density gradient ultracentrifugation: 1) to pellet the target protein to the rotor wall; 2) sediment onto a dense liquid; or 3) banding in a gradient. Pelleting is only for robust particles, sedimentation involves minimal losses and banding enables removal of impurities but requires lengthy development and optimisation (Desai and Merino, 2000).

Separation can be based on size or density differentials and is known by the following names (Desai and Merino, 2000, Pinheiro and Cabral, 1992):

- Rate-zonal centrifugation – separation by size. The density gradient inside the tube never exceeds the density values of the settling particles.
- Isopycnic centrifugation – separation based on relative densities. The maximum density inside the tube is higher than the components.

A gradient inside the ultracentrifuge is achieved by the addition of a gradient material. The choice is dependent on the density and stability of the molecule in question being separated. Feed enters the bottom and the particles, move into the gradient with the less dense supernatant removed from the top. The choice of material must produce a smooth gradient from one edge to another (Wheelwright, 1991). An example of how this may look is illustrated by the separation of lipopolysaccharides in a CsCl (caesium chloride) gradient, *Figure 1-5* (Hamel et al., 1990). A gradient can be defined as preformed or self-forming dependant on the type of gradient material used (Wheelwright, 1991).

Type of gradient	Definition	Examples
Preformed	Gradient is set before sample is applied	Sugars, i.e. sucrose Polysaccharides, i.e. ficoll
Self-forming	Gradient is generated as the sample and fluid are spun together	Colloid silica, i.e. percoll Metal salts, i.e. caesium chloride

Table 1.5-1 Gradient materials used in density gradient ultracentrifugation.

CsCl is frequently used as a gradient material and can achieve a high density (up to 1.9 g/cm³) but can denature certain proteins. Sucrose is more widely use as it is a cheaper gradient material and covers sufficient density range for most operations (up to 1.3 g/cm³), but can also damage proteins (Desai and Merino, 2000).

Ultracentrifugation has traditionally been used to purify vaccines, for example influenza, hepatitis B and rabies (Desai and Merino, 2000, Perez and Paolazzi, 1997). It has also been used in the development of new viral vaccines, including Lentiviral vector production (Lesch et al., 2011) and VLP-based vaccines (Vicente et al., 2011b, Herbst-Kralovetz et al., 2010, Wolf and Reichl, 2011, Rolland et al., 2001, Bellier et al., 2006, Crawford et al., 1994). Historically ultracentrifugation has been used to purify plasmid DNA by a CsCl and ethidium bromide (EtBr) density gradient (Prather et al., 2003, Singer and Muller, 2007). The CsCl creates the gradient, followed by the addition of the EtBr to visualise the nucleic acids (Singer and Muller, 2007).

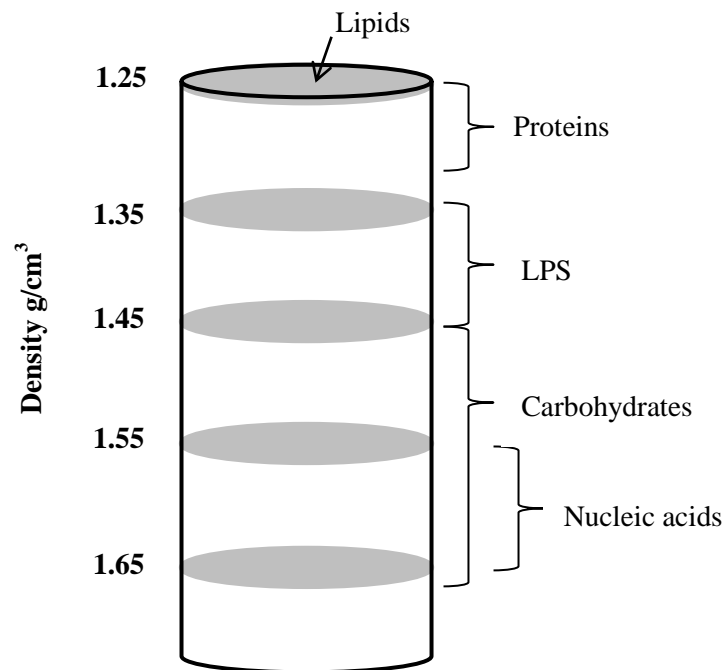


Figure 1-5 Predicted buoyant position of hydrated constituents in CsCl gradients.

The use of ultracentrifugation as a purification step is limited as it does not scale up well. The method is tedious, labour intensive, and can have low recovery yields, with several impurities (Peixoto et al., 2007, Vicente et al., 2011b). The method developed for plasmid DNA purification is particularly difficult to scale up as it is difficult to control but also because the solvents are toxic and carcinogenic, resulting in personnel safety issues and hazardous waste considerations (Prather et al., 2003, Singer and Muller, 2007). Ultracentrifugation has largely been replaced by chromatographic methods, due to significant advances with medias and ligands

(Desai and Merino, 2000). Chromatographically purified material may be of a better quality and purity when compared (Rolland et al., 2001, Singer and Muller, 2007).

1.5.3 Adsorption purification methods – Porous beads

Conventional resin based chromatographic columns were developed for the purification of proteins and other small molecules. Eight different column chemistries are now available for use within analytical and commercial processes, such as ion-exchange (IEX), hydrophobic interaction (HIC) size exclusion (SEC), affinity (AFC), normal phase (NPC) and reverse phase chromatography (RPC) (Jungbauer, 2005).

In conventional chromatography convective flow governs the transport of product in the extra-particle void of the packed adsorbent and diffusion governs the transport within the channels of each particle (Lyddiatt, 2002). Media for protein chromatography has a pore size of around 30nm (Jungbauer, 2005) but nanoparticles often have a particle diameter of around 20-300nm which makes them unable to enter into pores (Lyddiatt, 2002). This results in the majority of the binding only occurring on the edge of the beads, with a limited fraction using the void volume of the resin. This results in a decrease in the binding capacity compared to use of the resin with proteins, for example Q-sepharose decreases from 120mg/ml gel with proteins to 40µg/ml gel with plasmid DNA (Prazeres et al., 1998). Capacity of a column can drop as much as 30 or 50 fold with macromolecules (Lyddiatt and O'Sullivan, 1998, Trilisky and Lenhoff, 2007). The rate of diffusion into these pores also has an effect as it is slower for larger molecules and therefore becomes a rate limiting step. A high binding capacity can be achieved by increasing the surface area, for example with a highly porous material, or reducing the size of the particles, see *Figure 1-6*. Reducing the size of the particles dramatically increases the flow resistance, but can result in an increase in back pressure (Palsson et al., 1999).

To combat the issues surrounding the lack of diffusion for macromolecules chromatographic matrices have been designed with larger particles, around 50-300µm, and pores which are around 30-400nm (Lyddiatt and O'Sullivan, 1998). Other chromatographic matrices that have been developed for use with macromolecules are hydroxyapatite (Jungbauer, 2005, Cook, 2003), controlled pore

glass (Barton, 1977, Schuster et al., 2001), perfusion particles (Afeyan et al., 1990) and traditional resins with altered beads structure, including Q-Sepharose RTM-XL (Blanche et al., 2000, Blanche et al., 2003), superpose 6 (Pharmacia Biotech), Sephacryl S1000 (Ferreira et al., 2000), and Sepharose 6 fast flow (Shamlou, 2003, Belew et al., 1991). Non-porous resins, such as cellulose sulphate (Lyddiatt and O'Sullivan, 1998) have also been developed for use with macromolecules and have particles which are around 20-500µm in size (Shamlou, 2003).

Even if resins do have an increased pore structure they may still exhibit a low capacity when the purification of the macromolecule is compared to use with a protein (Prazeres et al., 1998). The enlarged pore structure may be a disadvantage as the volumetric capacity is reduced and the physical strength is compromised (Lyddiatt, 2002).

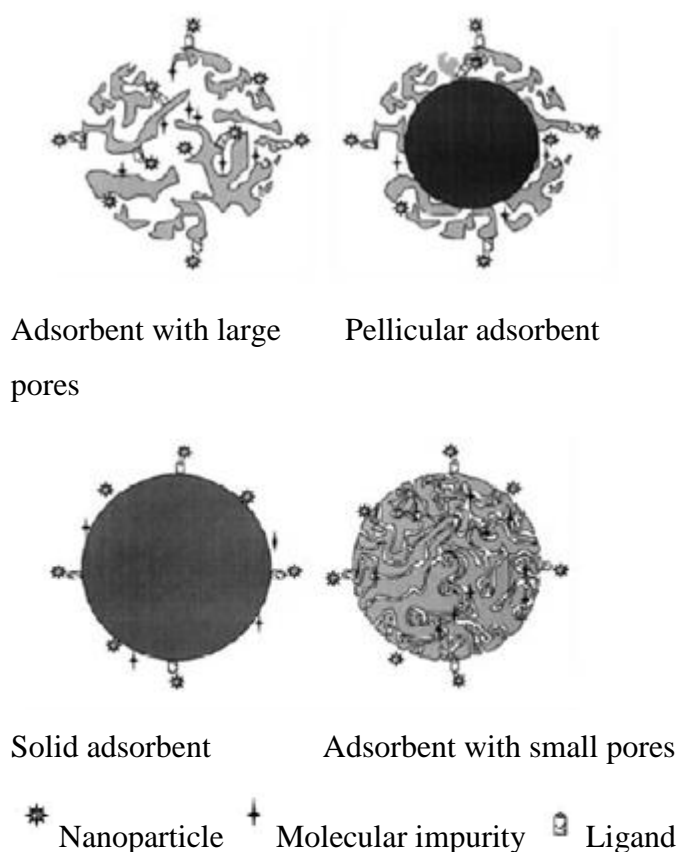


Figure 1-6 Schematic of examples of solid phases that are available or custom made for nanoplex purification (Zhang et al., 2001).

Perfusion particles look like traditional bead particles but have additional perfusion pores within their structure, see *Figure 1-7*. The pores of perfusion particles are in excess of $5000\text{\AA}/0.5\mu\text{m}$. The result of this is to trigger convective flow as the mobile phase moves through the particle, dramatically reducing resistance to the stagnant mobile phase mass transfer rate and increasing column efficiency. Extent of the flow-through is governed by the ratio of pore size to particle size (Afeyan et al., 1990). To increase the surface area, and therefore increase capacity of the column, particles also have some small diameter pores. These are very shallow and as such there is limited effect from diffusion (Afeyan et al., 1990).

Perfusion particles display low backpressures and improved hydrodynamic characteristics (Persson et al., 2004). A perfusion particle column with POROS 50 HS resin (PerSeptive Biosystems) was used to purify a VLP solution because its large pores would be accessible to the VLP. The recovery of VLP was between 25 and 45% and showed a significant drop at this step (Cook et al., 1999). Issues with perfusion particles can involve entrapment of macromolecules due to the convective flow. This can result in a reduction in elution concentration but can be reversed by using a very low flow rate (Trilisky and Lenhoff, 2007).

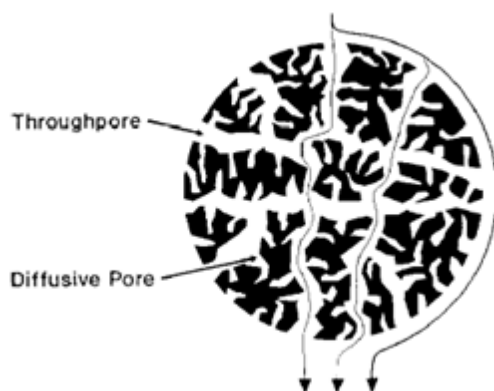


Figure 1-7 Diagram of pore structure in a perfusive particle (Afeyan et al., 1990).

Another type of absorbent that has been reported for use with plasmid DNA is a pellicular absorbent. These beads have a solid core around an agarose pellicle

estimated to be less than 5µm deep. It has been shown to have a modest capacity of less than 1mg nanoparticle/mL absorbent (Lyddiatt, 2002).

Both Pall and GE Healthcare have developed a core bead resin. Pall have named this technology “gel-in-a-shell” (Cheng et al., 2010). These beads are made by mixing hydrophilic cores with a solution containing hydrophilic gel forming component at a temperature above its gelling point, followed by blending with a hydrophobic fluid and subsequent cooling to solidify the gel coating, see *Figure 1-8* (Wang et al., 2007, Johnson et al., 1990). The Capto Core resin from GE Healthcare is used for flow through applications, as the inactive shell excludes large molecules (cut off ~MW 700 000) from entering through the pores of the shell (GE Healthcare Life Sciences Data file 28-9983-07 AA). GE showed that they could be used for the reduction of HCP in influenza virus hemagglutinin (HA) purification. Wang et al. (2007) showed that it could be used for antibody purification. When compared to other anion-exchange resins for the purification of DNA Palls Ceramic HyperD resin exhibited the highest capacity over specialist resins (Eon-Duval and Burke, 2004).

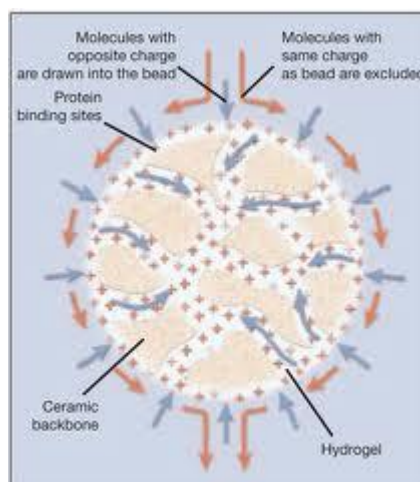


Figure 1-8 Schematic of a Pall “gel-in-a-shell” bead. (From Pall Corporation website www.pall.com)

1.5.4 Adsorption purification methods – Monoliths

The initial research behind the development of monoliths was carried out in 1950s and beyond (Kun and Kunin, 1968, Sederel and Dejong, 1973, Hansen and Sievers, 1974). It was not until the end of 1980's/beginning of 1990's that the current monolithic forms first emerged. There were a few groups, looking at different monolith technologies, such as those led by Hjertén in Uppsala, Sweden, Svec and Fréchet in Prague and at Berkeley and Nakanishi and Soga at Kyoto University (Hjerten et al., 1992, Hjerten et al., 1989, Liao et al., 1991, Svec and Frechet, 1992, Svec and Frechet, 1995c, Svec and Frechet, 1996, Tennikova and Svec, 1993, Tennikova et al., 1990, Tennikova et al., 1991, Nakanishi and Soga, 1991). The original name for monolith chromatography was High-performance membrane chromatography (HPMC), as the columns were produced as disks (Tennikova and Svec, 1993, Tennikov et al., 1998). Svec and Tennikova have written a detailed history of monolith material development, detailing the early attempts and recent developments (Svec and Tennikova, 2003).

The advantages of using monoliths include (Tennikova et al., 1991):

1. A monolith is synthesized directly in the final size in a mould. Classic chromatography supports prepared by suspension processes have to be size classified.
2. In fabrication of beads many are produced which are not the correct size, causing waste. A monolith prepared efficiently will be the correct shape.
3. The holder is simple and the monolith easily positioned. Packing of a column requires substantial experience of packing procedures.
4. A monolith can easily be used in a single-use or disposable form.
5. For analytical use flowrates are at least one order magnitude lower than those in traditional analytical columns, making the use of a highly efficient pump unnecessary.
6. Scale up is easily achievable by enlarging the monolith or stacking them. Scale up in packed columns has specific problems associated with packing, radial gradients and requires heavy duty equipment.

Monolith columns can be produced by a variety of methods (Svec, 2010, Svec et al., 2003):

- Free radical polymerisation - including thermally initiated polymerisation, photoinitiated polymerisation, radiation polymerisation;
- Polymerised high internal phase emulsions;
- Cryogels;
- Living polymerisations;
- Polycondensation;
- Soluble polymers.

As this thesis is concerned with the use of a column produced by thermally initiated free radical polymerisation only this techniques will be described in detail. The review from Svec (2010) as well as the monolith reference book (Svec et al., 2003) should be consulted for all other techniques.

Polymerisation can occur either as a suspension in a solution or in a mould, with the mould made monolith having a smaller surface area(Svec and Frechet, 1995a). The polymerisation mixture for a monolith needs to contain both a crosslinking monomer and an inert diluent, the porogen. Porogens can be solvating or non-solvating solvents, soluble polymers or a mixture (Svec and Frechet, 2003). It is the porogen that forms the pores (Svec, 2010). The steps in the mechanism of formation are as detailed in *Figure I-9* (Svec and Frechet, 2003), and will result in a monolithic structure that looks like a number of beads joined together (*Figure I-10*).

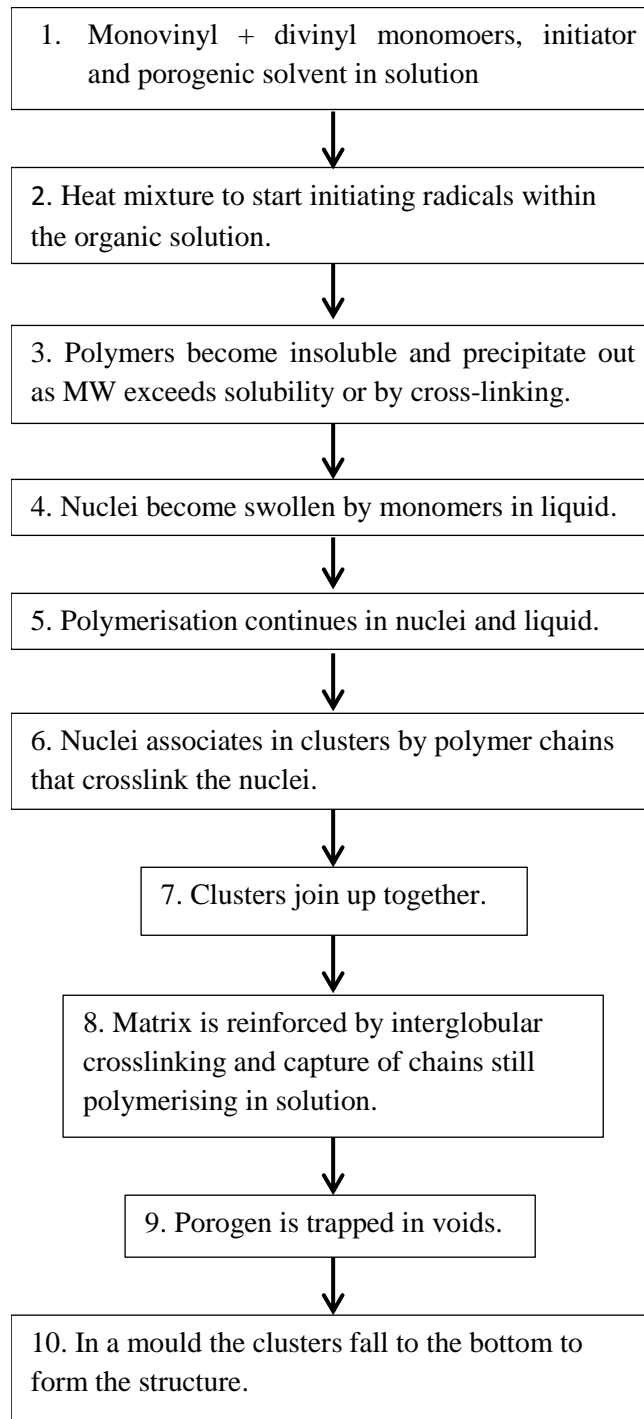


Figure 1-9 Mechanism of polymer monolith formation.

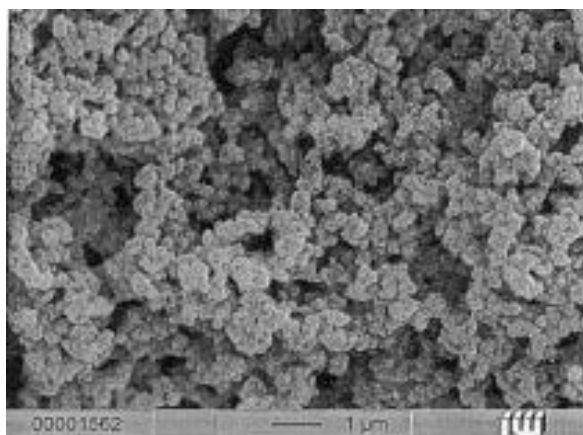


Figure 1-10 Scanning electron microscopy picture of a monolithic GMA-EDMA-based disk (Tennikova and Freitag, 2000)

Control of the porous properties and ultimately the pore size distribution and surface area, is through alteration of the variables polymerisation temperature, composition of porogenic solvent and percentage of cross-linking monomer (Viklund et al., 1996). Temperature is the most convenient and easiest variable to adjust for control of the pore size distribution. As the polymerisation temperature is increased the size of the pores decreases (Viklund et al., 1996, Svec and Frechet, 1995a). This can be explained in terms of nucleation rates and the number of nuclei that are formed. Higher temperatures result in a larger number of free radicals and in turn a larger number of nuclei and globules (Svec and Frechet, 1995d). The surface area is also decreased (Svec, 2010). The polymerisation reaction is exothermic and it is this reason that the production of large monoliths becomes an issue. The heat generated by the reaction, further fuels the polymerisation in the solution, changing the pore structure at different monolith sizes (Danquah and Forde, 2007, Mihelic et al., 2001). One method is to heat up the porogen to initiate decomposition and continuously add this to the polymerisation mixture, controlling the rate of heat generation (Danquah and Forde, 2008).

Varying the type of porogen or the percentage of crosslinking monomer is a less simple way of controlling the pore size distribution. A porogen which causes an earlier onset of phase separation will result in larger pores (Svec, 2010, Viklund et al., 1996). Changing the ratio of monomers to divinyl monomers will not only

induce the formation of a different porous structure but also materials with different compositions (Svec, 2010). Increasing the percentage of divinyl monomers will result in more crosslinked polymers and smaller nuclei. These smaller nuclei result in smaller pore sizes but a larger surface area (Svec, 2010).

Monoliths have proved advantageous for macromolecules due to higher binding capacities, and the ability to run at faster flow rates, in comparison to conventional resin beads. These two characteristics are a direct result of the structural properties of the monolith. As already mentioned the ligands on conventional resin beads are both on the outside of the beads and in small channels/pores into the centre. A molecule small enough to enter the pores of the resin will do so by diffusion. The speed of diffusion is greatly reduced in large macromolecules; hence the amount of lateral movement along the pore is reduced over the run time compared to smaller molecules, such as proteins.

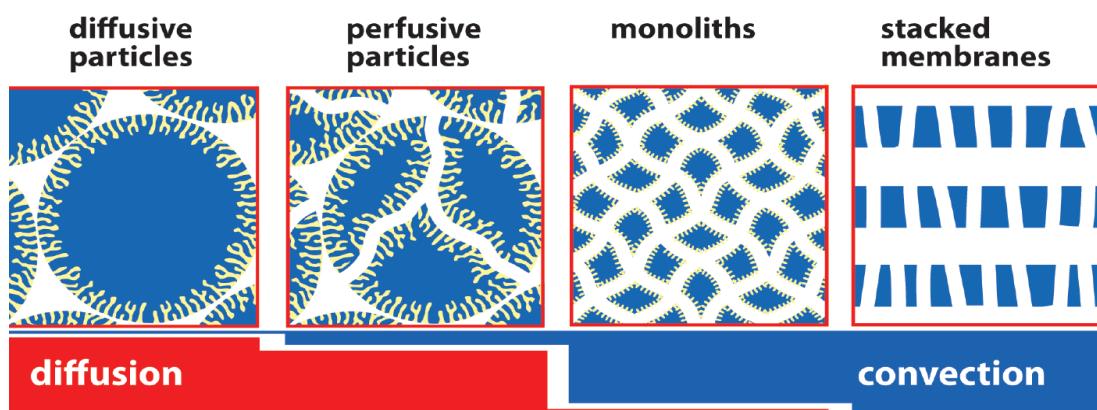


Figure 1-11 The mass transfer characteristics of common chromatographic media. Areas of diffusion are indicated by small channels within the support matrix. The difference between bead-based columns and monoliths can be clearly seen (Gagnon, 2006).

The better performance of monoliths compared to conventional columns is usually explained by enhanced mass transport. Mass transport of a molecule to the ligand is by convection, not by concentration gradients, with flow used to accelerate the mass transfer rate (see *Figure 1-11*) (Svec and Frechet, 1999). The large wide

flow-through pores of a monolith are connected in such a way that the diffusional path is extremely short (Josic et al., 2001). There has been some research on modelling the monolith pore network and flow paths (Meyers and Liapis, 1999, Koku et al., 2011). The size of the pores is important to consider; small pores may exhibit size exclusion as flow is restricted, but too large and molecules cannot reach the wall prior to elution so the number of absorption/desorption steps decrease (Tennikov et al., 1998). The breakthrough curve is substantially steeper when a sufficiently high intraparticle convective flow is assumed (Josic et al., 2001).

Another advantage of the wide pore structure is the ability of the monolith column to run at high flow rates without any effect to the breakthrough curve or elution profile (Etzel and Riordan, 2009, Josic et al., 2001, Jungbauer and Hahn, 2008, Hahn and Jungbauer, 2000, Svec and Frechet, 1992, Martin et al., 2005). The back pressure increases linearly with the increase in flow rate (Persson et al., 2004), but remains lower when compared to a conventional resin column at equivalent flow rates (Jungbauer and Hahn, 2008).

A monolith is only useful if it has the correct surface chemistry. There are three ways to prepare a column with a particular chemistry, 1) preparation from functional monomers; 2) modification of reactive monoliths and 3) grafting (Svec and Frechet, 2003). Almost any monomer can be used to prepare a monolith in a mould, allowing a variety of surface chemistries that can be obtained directly. Chemical modification can be used when a monomer precursor is not available. Reactions are easily performed using monoliths prepared from monomers with reactive groups. Grafting involves filling the pores of a monolith prepared from polymerisation mixtures with a high percentage of crosslinking monomer (presumably with a large number of unreacted vinyl functionalities) with a secondary polymerisation mixture, consisting of a solution of functional polymer and a free radical initiator. A second polymerisation takes place inside the pores (Svec and Frechet, 2003).

Columns can be prepared from a variety of materials, including methacrylate based polymers (Svec and Frechet, 1995b), styrene divinylbenzene (Kun and Kunin, 1968, Sederel and Dejong, 1973) or silica (Motokawa et al., 2002, Siouffi, 2006, Pous-Torres et al., 2010). Guiochon (2007) provides a thorough review of the many

types of monolithic columns that have been produced. The CIM monoliths from BIA separation are a type of polymer column and are made from glycidyl-methacrylate (GMA) and ethylene-diamethacrylate (EDMA) to form poly(glycidyl methacrylate-*co*-ethylene diamethacrylate) polymer columns (Podgornik et al., 2000), using cyclohexanol and dodecanol as inert porogenic (Mihelic et al., 2001). Other polymers used for columns include piperazine diacrylamide (PDA) plus methacrylamide (Hjerten et al., 1993a, Hjerten et al., 1993b), poly(acrylamide-*co*-butyl methacrylate-*co*-N, N'-methylenebisacrylamide) (Xie et al., 1997b) and poly(acrylamide-*co*-methylene bisacrylamide) (Xie et al., 1997a). The choice of the polymeric materials can influence the chemistry of a column. By altering the monovinyl and divinyl monomers it has been shown that it is possible to produce a hydrophobic columns (using butyl methacrylate) (Xie et al., 1997b, Zeng et al., 1996) or hydrophilic (using methethylenebisacrylamide) columns (Xie et al., 1997a).

There are only a small number of commercially available monolith chromatography columns including (Jungbauer and Hahn, 2004):

- CIM – BIA separations
- UNO – Bio-rad
- Proswift – Dionex (Thermo Scientific)
- Chromolith – Merck Millipore

The Chromolith columns are an example of a silica monolith, first available in 2000. Commercially available silica monolith columns have a bimodal pore structure composed of macropores and mesopores of 2 μ m and 13nm (Chambers et al., 2007, Unger et al., 2008). Silica monoliths are prepared by a sol-gel method using tetramethoxysilane (TMOS), tetraethoxysilane or n-alkyltrialkoxysilanes (Unger et al., 2008) and methyltrimethoxysilane (Motokawa et al., 2002). However, its uses are limited as silica dissolves at pH >8, resulting in packing instability, poor reproducibility, poor efficiencies, poor peak shapes and high back pressure (Chambers et al., 2007). It also is liable to shrink after being prepared (Chambers et al., 2007).

Monoliths can be used in the separation of a number of different macromolecules. A detail list of the uses for a CIM monolith can be seen in section

0. Other reviews and books provide details on the use of monoliths in plasmid DNA separation, protein separation, enzymatic conversion, virus purification or removal, antibody purification, or to mimic virus-cell interactions (Jungbauer and Hahn, 2008, Svec et al., 2003, Josic and Buchacher, 2001, Josic et al., 2001, Jungbauer and Hahn, 2004, Mallik and Hage, 2006, Etzel and Riordan, 2009, Danquah and Forde, 2008, Danquah and Forde, 2007, Zochling et al., 2004, Kalashnikova et al., 2008).

1.5.5 Adsorption purification methods – Membranes

Similar to monoliths is membrane chromatography, also known as membrane absorbers. Like monoliths they have large interconnected pores, where transport of macromolecules to ligands is by convective flow, reducing any mass transfer resistance (such as that associated with diffusion of macromolecules into pores). Membranes also have lower pressure drops than packed beds, as the flow path is shorter (Han et al., 2005, Yang et al., 2002, van Reis and Zydney, 2007) and flow independent resolution (Teeters et al., 2003, Reif and Freitag, 1993). The functional groups are attached to these pores (Han et al., 2005). Common chemistries for membranes include anion or cation ion exchange, hydrophobic interaction and protein A.

Comparison with an equivalent resin shows that the membrane absorber has a higher binding capacity, such as in the case of the Sartobind Q membrane compared to Q sepharose for MAbs (Haber et al., 2004, Zhou and Tressel, 2006, Lutkemeyer et al., 1993). With plasmid DNA a membrane has been shown to have an increase in capacity which was two times greater than a “superporous” particle and five times greater than equivalent 15 μ m particles (Teeters et al., 2003). Buffer usage can be 95% less than for the same process in a conventional chromatography column (Zhou and Tressel, 2006).

Although the membrane may prove to have a higher binding capacity its use in any commercial product has been limited by the high price of the absorbers (Zhou and Tressel, 2006, Knudsen et al., 2001). Zhou and Tressel (2006) compared a Q columns with an absorber and found that the absorber was more cost effective when run in the flow-through method, due to reduced process development costs, no initial equipment investment and minimal validation needed.

Commercial membrane absorbers are based on macroporous support from established membrane formation process technology, with chemical modifications, see *Table 1.5-2*. (Wang et al., 2008). There are 3 types of commercial available membranes, see *Figure 1-12* (details from supplier websites). All of these membrane absorbers are available in a variety of sizes, from small process development batches to manufacturing. They are provided ready to use, in plastic housing, which makes them suitable in a single use facility.

Supplier	Membrane name	Chemistry	Membrane	Pore size/ Membrane thickness
Millipore	ChromaSorb	Primary amine	Ultra high molecular weight polyethylene (UPE)	0.5µm 0.0125cm
Pall	Mustang Q/S/E	IEX	Hydrophilic polyethersulfone (PES)	0.8µm 0.01375cm
Sartorius Stedim	Sartobind Q	IEX, HIC	Polypropylene/polyester	3-5µm 0.0275cm

Table 1.5-2 Details on commercial membranes available for membrane chromatography.





Figure 1-12 Membrane absorbers commercially available A) Millipore ChromaSorb; B) Pall Mustang Q; C) Sartorius Stedim Sartobind.

Membranes can be used in bind and elute, and flow through chromatographic modes. Examples of bind and elute processes include large proteins (Yang et al., 2002), viruses (Han et al., 2005), plasmids (Tseng et al., 2004, Haber et al., 2004, Teeters et al., 2003) and monoclonal antibodies (Zhou and Tressel, 2006, Lutkemeyer et al., 1993, Vicente et al., 2011a, Knudsen et al., 2001). The use of membranes in the flow-through mode can be to remove host cell proteins in monoclonal antibody processes as a polishing step (Knudsen et al., 2001, Zhou and Tressel, 2006).

Scale up of membrane absorbers requires increasing the surface area within the membrane holder. This can be done by adding in layers by stacking membranes in the holder, increasing the surface area. Knudsen et al. (2001) showed that scaling up of membranes for MAb purification, by adding layers, resulted in a linear increase in the breakthrough capacity. The column diameter is another method of scale up that is possible (Teeters et al., 2002).

1.5.6 Cryogels

Cryogels are another type of supermacroporous separation media, very similar to monoliths. They are also composed of a single stationary phase produced through a polymerisation reaction. The main difference between monoliths and cryogels is related to the method of production. Cryogels are formed at very low temperatures (cryogel from the Greek word κρυος (kryos) meaning frost or ice)

(Plieva et al., 2004). The gels that form are sponge like, with large interconnecting pores.

The formation of the porous structure of cryogels relies on the phase separation during freezing, with one phase being frozen crystals of water and another a non-frozen liquid microphase (Svec, 2010). The unfrozen part contains a high concentration of non-frozen components from the original solution (cryoconcentration) dissolved in the unfrozen solvent, where chemical reactions occur although the sample appears to be a solid block (Lozinsky et al., 2001). The high concentration of components accelerates the chemical reactions which take place. Cryogels can be formed at significantly lower concentrations of polymers and cross-linking agents than gels at room temperatures (Lozinsky et al., 2001).

Figure 1-13 illustrates the steps on the formation of cryogels. After completion the system is brought to ambient temperature causing water within pores to thaw, which can be easily replaced with a mobile phase.

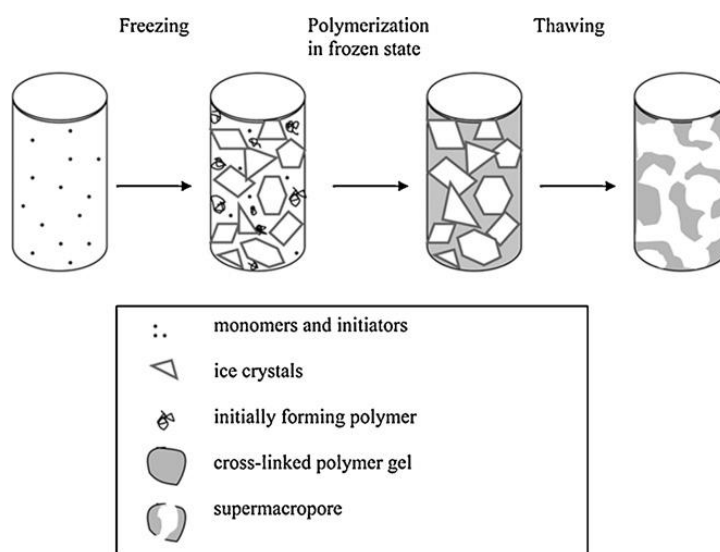


Figure 1-13 Schematic of formation of cryogels (Plieva et al., 2004).

A variety of cryogels have been made from monomers including poly(vinyl alcohol) (Lozinsky et al., 2001) and acrylamide (AAm) (Plieva et al., 2004, Yilmaz et al., 2009, Yao et al., 2006). Polymerisation of the cryogels can occur by the

process of free-radical polymerisation (Yao et al., 2006). Pore sizes for cryogels are larger than monoliths, with a large distribution of pore sizes, up to approximate 100 μm and as low as 5 μm (Chen et al., 2008, Plieva et al., 2004, Yilmaz et al., 2009). Recovery of the captured macromolecule can be removed by flow-induced elution or detachment of cells by compressing the matrix (*Figure 1-14*) (Dainiak et al., 2006, Kumar and Srivastava, 2010).

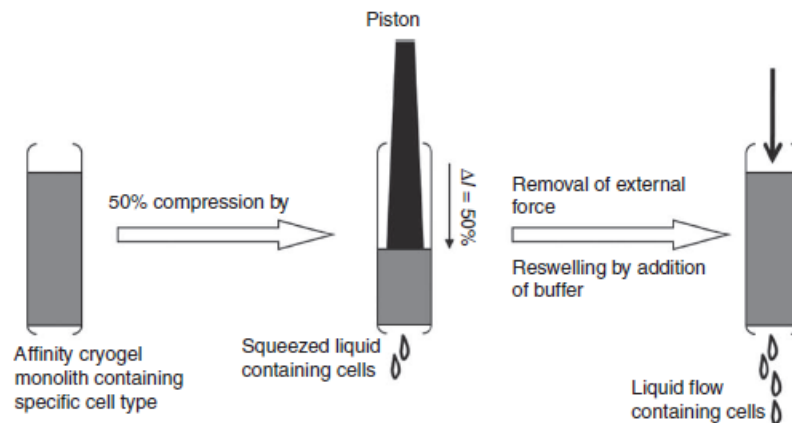


Figure 1-14 Mechanical squeezing of the cryogel matrix for the recovery of bound cells. Affinity-bound cells on cryogel matrix were removed by compressing the cryogel column up to 50% of its original length by using an external piston that squeezes out the liquid that contains cells. In the next step, the buffer was added to re-swell the affinity cryogel matrix and then the column was flushed with fresh cold buffer.

The pores of a cryogel are controlled by the size and shape of ice crystals which are formed. Therefore the temperature the cryogel is formed at, and the speed this temperature is reached, is very important in determining the flow characteristics of the column. Cryogels are formed at a range of temperatures, including -12°C (Arvidsson et al., 2002, Plieva et al., 2004), -16°C (Yilmaz et al., 2009) and -20°C (Chen et al., 2008, Yao et al., 2006). Plieva et al. (2004) studied the effect of temperature on acrylamide (AAM)-based cryogels. Very different cryogels were formed if the temperature was at -12°C or -18°C. This was a result of the different morphology of the ice crystals that were formed during the freezing process; at -12°C the cryogel had large interconnected pores around 5-100 μm , whereas at -18°C

the gel showed a bimodal pore size distribution with pores at several hundred micrometres in size and 0.1-3 μ m. This variability was due to the different cooling rates; the -18°C column was formed over 4-6 minutes, whereas the -12°C was over 12-15 minutes.

Yao et al. (2006) looked at the effect of the cooling time to -20°C on the pore formation. They saw that the most favourable cryogel was formed over 2 hours and contained well connected pores and smooth walls. If the mixture was cooled too quickly (in this case over 1 hour) then inhomogeneous ice blocks were formed which gave irregular ice crystals, and a cryogel with rough walls. The column did not perform as well as the 2 hour cryogel.

Thanks to the large pores in cryogels they are particularly useful as a matrix for a variety of macromolecules. As the pore sizes can be from 5-100 μ m they have proven to be excellent for cell separation from crude or processed material, such as with *E.coli* and *Saccharomyces cerevisiae* (Dainiak et al., 2006, Arvidsson et al., 2002, Lozinsky et al., 2003, Plieva et al., 2004). The purification of the hepatitis B surface antibody (anti-HBs) was achieved on a cryogel by embedding some anti-HBs imprinted particles into the cryogel structure. This increased the specific surface area, and gave large inter-connected flow channels (Asliyuce et al., 2012).

Cryogels can be modified for very specific separation technologies, either by attaching a ligand or using a particular monomer in the production process. Specific affinity ligand separation includes IMAC (Arvidsson et al., 2002), Cu²⁺-IDA (iminodiacetate) to remove His-tagged recombinant lactate dehydrogenase (Plieva et al., 2004) and protein A to capture IgG specific-labelled cells (Kumar and Srivastava, 2010). The cryogel with protein A ligands proved to be better for cell separation than flow cytometry or magnetic affinity cell sorting (Kumar and Srivastava, 2010). The separation of lysozyme from egg white was achieved by using a tryptophan containing hydrophobic adsorbent (Yilmaz et al., 2009). The cryogel was made using a monomer of *N*-methacryloyl-L-tryptophan (PHEMAtrp).

1.6 CHARACTERISTICS OF PROCESS CHROMATOGRAPHY PERFORMANCE

The performance of the chromatography column must be monitored throughout the operation of the column. In a manufacturing process this is to ensure consistency between each run, and in the lab this is to obtain information in the research and development of the unit operation. During chromatographic runs the profile during the loading, washing, elution and cleaning steps will be monitored on-line. Typical methods include looking at the UV absorbance profile of the material post-column, as proteins are visible at a wavelength of 280nm, checking the back pressures, or other characteristics such as conductivity or pH. Monitoring the process will indicate if there are any deviations from a standard run and allows the operator to make any changes. Off-line monitoring gives further details about the run and the protein, antibody or macromolecule being purified.

This section describes a few of the characteristics and methods of monitoring performance that were encountered during the project, and is not a comprehensive list.

1.6.1 Fouling of chromatographic resins

Ideally a chromatographic run will be identical to the one before it, and the one after. The method of purification will produce a molecule which is unaffected by the process, with no variation on the final elution pool in terms of its purity profile. To achieve this resin in the column must remain unchanged during the chromatographic runs, either from the feed material, the elution process, or the cleaning steps. It is important to understand the cycles of use as replacement of resins can have a considerable impact on manufacturing costs (Shepard et al., 2000). Limited work has been published on fouling in chromatography, although comparisons can be made with research from membranes to understand the characteristics and mechanisms (Kelly and Zydney, 1997, Meng et al., 2009).

Unfortunately fouling of resins can occur by contaminants in the feed material, in particular residual proteins, lipids, nucleic acids, and endotoxins. The

consequences of fouling includes reduction in DBC and product yield, increase in backpressure, loss of signal resolution and medium discolouration (Shepard et al., 2000, Siu et al., 2006a, Siu et al., 2006b, Levison, 1997, Boushaba et al., 2011, Levison et al., 1999, Nash et al., 1997). Even cell wall have been shown to increase the degree of fouling by exhibiting characteristics of ion-exchange medium (Shaeiwitz et al., 1989).

The most common, and noticeable consequence from fouling, is the reduction in binding capacity. Foulants can block pores or layer on the resin (Jiang et al., 2009, Siu et al., 2006b). If breakthrough curves are compared between fresh resins and used resins the curves are shifted on the used resins so that breakthrough occurs earlier, probably as a result of mass transfer limitations on beads due to deposits (Bracewell et al., 2008, Siu et al., 2006a, Pampel et al., 2007, Jiang et al., 2009, Boushaba et al., 2011). The degree of fouling, and hence the percentage reduction in binding capacity, is dependent on the feed material on to the column. When a “dirty” feed stream (with many foulants present) is compared to a “cleaner” feed stream, the greatest reduction occurs with the dirty stream (Fee and Chand, 2005, Staby et al., 1998, Muller-Spath et al., 2009, Jin et al., 2010). Bracewell et al. (2008) looked at the impact of clarification strategies before a chromatography step to remove some or most of the foulants. They found that it had a positive impact on the capacity.

With *Saccharomyces cerevisiae* yeast the foulant with the most impact is lipids. The commonest lipids in are the neutral lipids – triacylglycerol (TAG) and steryl esters (SE). They are sequestered from the rest of the cell by forming the hydrophobic core of so-called lipid particles (LP), in particular lipoproteins (Czabany et al., 2007). The tails of lipid particles are non-polar and therefore act as a site for hydrophobic interaction (Levison, 1997). The chromatographic separation of products from milk clearly illustrates the issue of lipid fouling (Pampel et al., 2007, Fee and Chand, 2005). Pampel et al. (2007) showed that the back pressure in the column increased as chromatography runs were undertaken, and that removal of the lipids (skimmed milk) had less effect of the pressure.

HIC columns are very susceptible to lipid fouling as the lipid molecules are hydrophobic and therefore binding easily and irreversible to the columns. Work at

UCL has highlighted the effect of lipids on resin binding capacities (Jin, 2010). SEM shows the build-up of the lipids on a resin bead after ten cycles using a yeast homogenate feed, see *Figure 1-15*.

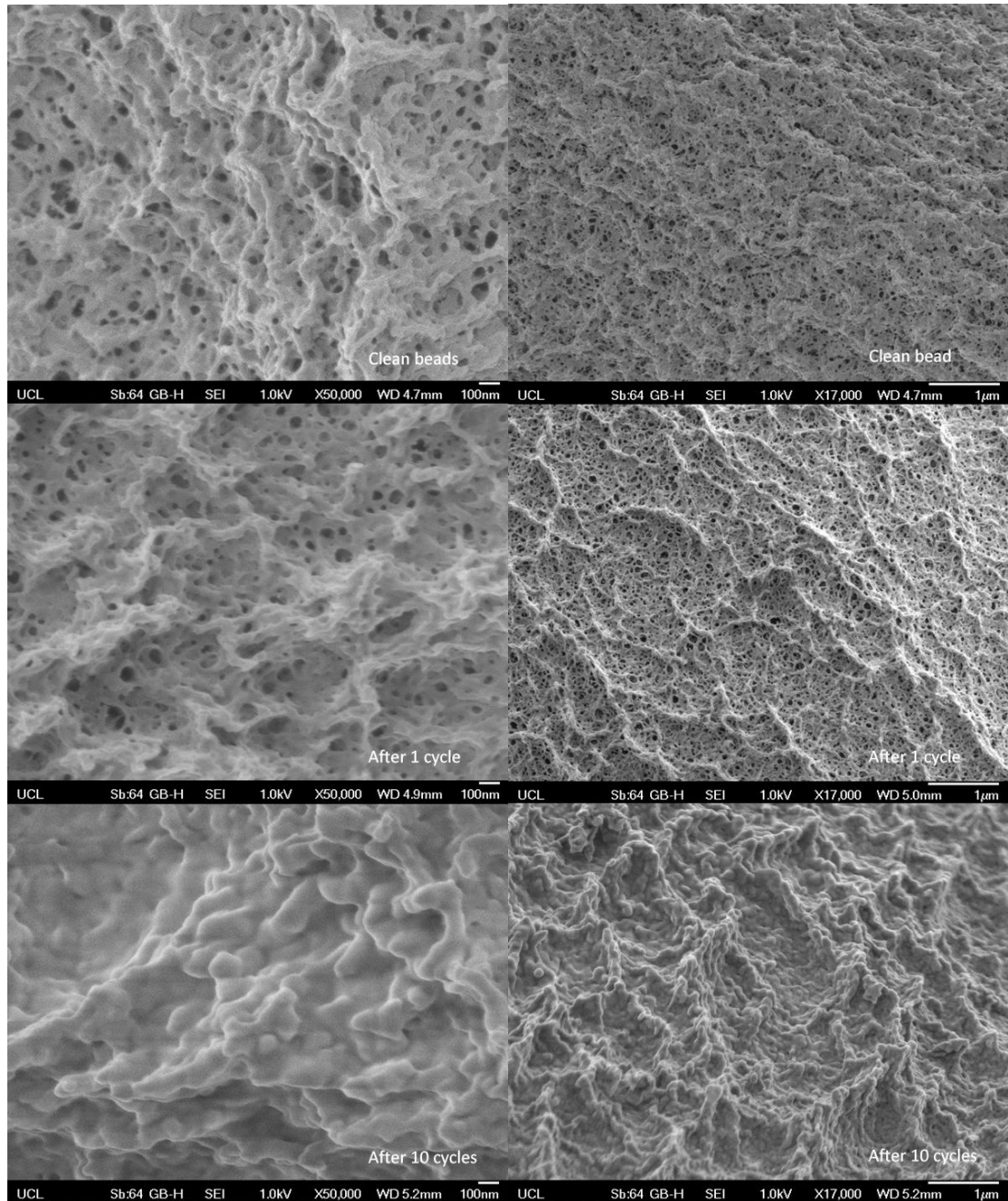


Figure 1-15 Fouling of 6 Sepharose FF beads (GE Healthcare, Sweden) by lipids in a yeast homogenate feed after 10 cycles, including CIP, as visualised by electron microscopy (Courtesy of Jing Jin, UCL).

1.6.2 Cleaning-in-place (CIP)

After each chromatographic run, or a set of number of runs, cleaning of the column will occur to remove any contaminants that have become tightly bound to the column and are not removed during any other stage. Cleaning can help restore a column to its previous capacity, or reduce the degree of DBC reduction (Siu et al., 2006a, Levison et al., 1996, Grongberg et al., 2011, Nash et al., 1997). Sometimes CIP methods cannot restore a resin to its “new” DBC value due to irreversible binding of foulants (Siu et al., 2006b, Muller-Spath et al., 2009)

Common methods of removing foulants include (Ng and McLaughlin, 2007, Levison, 1997):

Method	Example chemicals used
Ionic strength	NaCl (sodium chloride)
Elevated pH	NaOH (sodium hydroxide)
Reduce pH down	Hydrochloric acid, citric acid
Alcohols	Isopropanol, ethanol
Detergents	Tween
Denaturants	Guanidine hydrochloride, urea,
Elevated temperatures	

The most common cleaning solution used is NaOH, as it removes proteins, nucleic acids, endotoxins and viruses. Removal of lipids is often by alcohols, such as isopropanol, but can be through guanidine hydrochloride, urea and ethanol. Metal ions are removed with citric acid and EDTA.

Cleaning solutions can be used in combination, such as NaOH and NaCl together to improve the range of contaminants removed. Ideally the cleaning procedure should be one step only, as this ensures that the step time is kept short, but for more challenging feeds a two-step process may be needed. The order of the steps has been shown by GE Healthcare to be important, as the wrong order may in fact reduce the effect of cleaning. For example they saw that using a reducing agent and then NaOH removed all traces of protein impurities, but if the reducing agent

was used after the NaOH it did not show any improved efficiency compared to NaOH alone (Grongberg et al., 2011).

A chromatographic performance test can be performed before and after the CIP regime to assess the effect. Not only is the degree of removal of the foulants important but the effect of the cleaning solution on the resin and/or ligand must also be analysed. The CIP step may cause a degree of ligand leakage and therefore decrease the life of the resin (Levison et al., 1996, Jiang et al., 2009).

1.6.3 Confocal microscopy

The graphic visualisation of contamination effects on chromatographic matrix is possible through the use of Confocal Laser Scanning Microscopy (CLSM). Confocal microscopes were developed in the 1950's at Harvard by Marvin Minsky, who patented it in 1957, and this was modified in the 1980's into CLSM for biological specimens (Pawley, 2006). Built around a conventional light microscope a laser is used instead of a light source.

The molecule of interest is labelled using a fluorescent dye, such as Cy5 on BSA or PicoGreen on DNA. The choice of fluorescent dye is important as it should not change the binding affinity of the labelled molecule compared to an unlabelled molecule. Teske et al. (2005) studied the effect of labelling on lysozyme and concluded that there were changes in the binding patterns on the resin, if it was fluorescently labelled. Therefore it is important to have a method of monitoring which may indicate if changes have occurred.

A laser beam is focused on a specimen and fluorescent light returns through the microscope along the same ray path as the excitation light (Forsgren et al., 1990). Illumination and detection is confined to a single diffraction limited point in the specimen and is focused by an objective lens. Points of light from the specimen are detected by a photomultiplier behind a pinhole or slit (Paddock, 1999). The pinhole aperture effectively blocks light from out-of-focus planes (Linden et al., 1999). Three dimensional pictures are achieved by scanning consecutive sections with a change of focus setting between each section (Forsgren et al., 1990).

CLSM has been used to study the kinetics and mechanisms of uptake in resin beads, mainly with IEX ligands. The use of a labelled molecule or molecules enables researchers to look at the rate of diffusion into the bead pores, and verify experimental results on the kinetics of binding, see *Figure 1-16* (Linden et al., 1999, Ljunglof et al., 1999, Ljunglof and Hjorth, 1996, Ljunglof and Thommes, 1998). It has also been used to look at dynamic capacity data for Sartobind Q and S membranes, and the accessibility of binding sites in the membrane (Wickramasinghe et al., 2006).

Looking at time related scanning has also enabled visualisation of phenomena which cannot be explained on experimental data alone, such as exclusion mechanisms in IEX (Harinarayan et al., 2006), pore hindrance of MAb in HIC (Susanto et al., 2007), and the low binding capacity of DNA (Hubbuch et al., 2003). Labelling the foulants as well as the molecule of interest can help visualise where they bind on to the chromatography matrix, indicating how they can reduce its binding capacity (Siu et al., 2006b, Jin et al., 2010). For example the work by Jin et al. (2010) showed that lipids slowly build up on the beads of Sepharose 6 FF, and gradually penetrate into the centre (see *Figure 1-17*). Further work showed the degree of fouling along the column length, over repeated cycles (Jin, 2010).

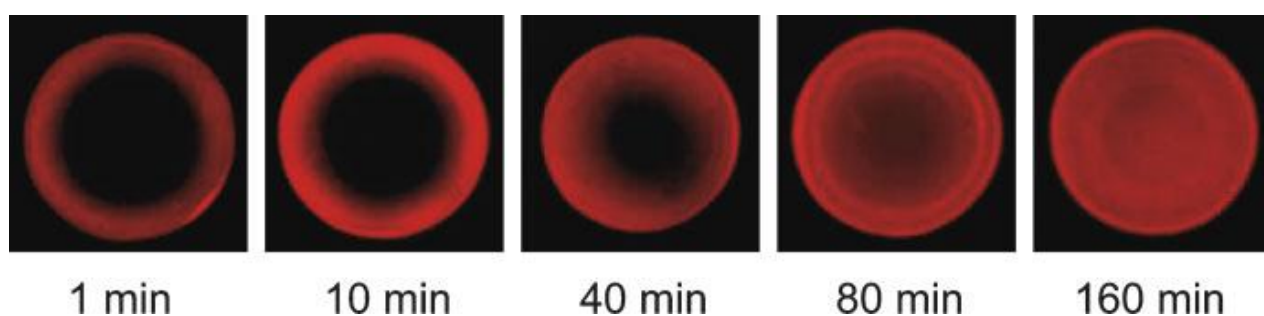


Figure 1-16 Confocal study of the rate of adsorption of Cy5.5-labelled BSA to fresh Q Sepharose FF. The BSA and resin were mixed for different times before being analysed (as indicated below pictures). (Siu et al., 2006b)

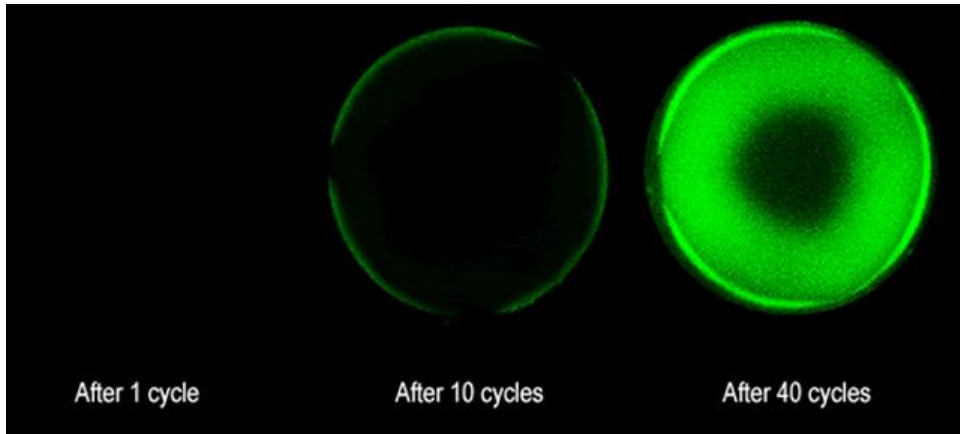


Figure 1-17 Confocal laser scanning microscopy image of Sepharose Butyl-S 6 FF beads after repeated loading cycles with a crude yeast feed. Neutral lipids in the feed were labelled green by BODIPY 493/503 dye (Jin et al., 2010).

1.6.4 Dynamic Light Scattering

Dynamic light scattering (DLS) is used for measuring the size of particles in the sub-micron range. DLS measures Brownian motion and relates this to the size of the particles. Brownian motion is the random motion that particles make in a solution as a result of their bombardment by fast-moving molecules in the solvent around them. The larger the particle the slower the Brownian motion will be. Temperature will have the greatest effect on the degree of Brownian motion, via viscosity of the solution, and therefore must be stable on measurement.

The size is calculated from the translational diffusion coefficient by using the Stokes-Einstein equation.

Stokes – Einstein equation:
$$D = \frac{KT}{3\eta D_H}$$

D = hydrodynamic diameter,

D_H = translational diffusion coefficient,

K= boltzmanns constant,

T = ab temp,

η = viscosity.

Notice that the size is not an absolute diameter but a hydrodynamic diameter. The hydrodynamic diameter of particles in the solution measured is equal to the diameter of a sphere that has the same translational diffusion coefficient as the particle. The result can result in the particle being smaller or larger than seen through other methods, such as electron microscopy, if the particle is not spherical and has surface modification. Any changes in the surface of a particle will affect the diffusional speed and correspondingly change the apparent size of the particle. The ionic strength of the medium also has a large effect on the apparent hydrodynamic diameter of the particle. A low conductivity media will result in a higher hydrodynamic diameter, with the opposite effect in high conductivity media.

The sizing capability of the Zetasizer Nano S, from Malvern Instruments, uses NIBS (Non-invasive back-scatter) technology, which detects the scattering information caused by the particle of a 4mW He-Ne 633nm laser at 173°.

The key results obtained from the Zetasizer Nano are:

- *Intensity* – this is proportional to the molecular weight. Intensity distributions can be dominated by small amount of aggregates or larger particles.
- *Polydispersity (Pd)* – Describes the width of the particle size distribution. Derived from the polydispersity index, a parameter calculated from a cumulants analysis of the DLS measured intensity autocorrelation function. In the cumulants analysis, a single particle size is assumed and a single exponential fit is applied to the autocorrelation function. The coefficient of variation of %Pd is the most used term for protein analysis. Due to the small degree of polydispersity always seen samples with a %Pd <~20% are considered to be monodispersed. But results can be incorrect if the sample is composed of a mixture and the Zetasizer' s DTS program shows the %Pd of each peak obtained instead of the sample as a whole.
- *Count rate and attenuator level* – The derived count rate values are displayed by the software and allow comparison of the relative intensities of the samples before attenuation, i.e. how many particles are in the sample.

1.6.5 Zeta potential

A net surface charge is generated through the absorption of specific ions from solution (Hughes, 1977). *Figure 1-18* shows a model for the surface charges surrounding a particle in an aqueous system (Malvern website www.malvern.com). There are two layers which form, with the charge of each layer depending on the charge of the particle. The zeta potential is an important value as it can be measured and gives an indication of the potential existing between the bulk phase and the shear plane (Hughes, 1977) and can be regarded as the controlling parameter for charged-particle interactions (Lin et al., 2006).

The zeta potential is regarded as the controlling parameter for charged particles (Lin et al., 2006), and, as the zeta potential reaches zero, particles in the fluid become unstable and can flocculate together (Hughes, 1977). Values of the zeta potential are measured in millivolts and can be positive or negative. A high value will indicate stability in the solution. The zeta potential of a particle depends on both the surface charge of the particle as well as the environmental conditions. Altering in the zeta potential can come about from changing the pH, conductivity or concentration of a formulation component. The most important variable is the pH as the zeta potential is related to the isoelectric point of a molecule.

Measuring the zeta potential has proved a useful tool in looking at the adhesion of biomass in EBA (Lin et al., 2006), bioadhesion (Tur and Ch'ng, 1998), cell immobilisation (Thonart et al., 1982), and the surface charge on bacterial cells (Wilson et al., 2001, van der Wal et al., 1997), which can model cell function and behaviour. Zeta potential can also be used in the formation of complexes, for example surface charge on DNA polyplex formation to determine if the complex had been formed correct and therefore give information on the transfection efficiency of the DNA vector (Dhanoya et al., 2012).

Determining the zeta potential of a molecule during process development can provide information about the characterisation of the molecule and how it will perform during unit operations. Ion-exchange chromatography relies on the use of pH for binding and elution and so zeta potential can be used to look at the degree of protein absorption in IEX chromatography (Jonsson and Stahlberg, 1999). The pH of a solution will also have an effect on the aggregation of a molecule, so this needs

to be analysed in relation to an IEX step (Trilisky and Lenhoff, 2007) or stability studies (Biddlecombe et al., 2009). This makes zeta potential an attractive parameter to study in formulation studies.

The zeta potential value is measured by using laser Doppler electrophoresis within a special designed machine, such as the Zetasizer Nano from Malvern Instruments, UK. Electrophoresis is defined as the potential gradient applied to dispersion and the movement of the charged particles relative to the bulk stationary phase is measured (Hughes, 1977). The stability of a particle at varying conditions can then be effectively and easily measured.

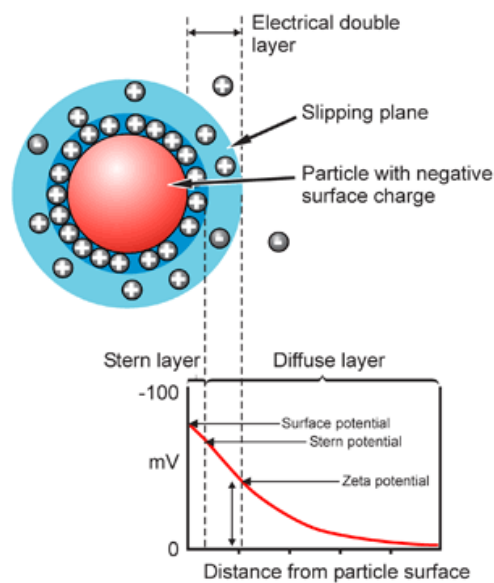


Figure 1-18 The colloidal model for net electronegative particle. (Malvern Instruments, UK. www.malvern.com)

1.7 HYDROPHOBIC INTERACTION CHROMATOGRAPHY

Hydrophobic interaction chromatography (HIC) is a common method in the purification of proteins. It is similar to affinity chromatography as it utilises a function of the protein to enable separation, in this case it is the hydrophobicity of the protein or patches on the protein. This hydrophobicity is the result of non-polar amino acids on the surface of the protein.

1.7.1 Theory

Although the concept of hydrophobic interaction has been around since the 1940's the 1970's saw an increase in the amount of research conducted and the introduction of chromatographic resins. Despite the amount of research into the phenomena there is still no one solid theory to describe the action. Many theories have been proposed (Queiroz et al., 2001), but two main theories have emerged as the most popular; the solvophobic theory (Melander and Horvath, 1977, Melander et al., 1984) and preferential interaction theory (Arakawa and Timasheff, 1982).

Hydrophobicity in proteins comes about from non-polar amino acids or groups, which tend to cluster together in water. Hydrophobic attractions are a major driving force in the folding of macromolecules, the binding of substrates to enzymes, and the formation of membranes (Stryer, 1999). The common non-polar amino acid found in proteins are detailed in *Table 1.7-1* (Ochoa, 1978).

Amino acid	Structure	Amino acid	Structure
Alanine	$ \begin{array}{c} \text{COO}^- \\ \\ {}^+\text{H}_3\text{N} - \text{C} - \text{H} \\ \\ \text{CH}_3 \end{array} $	Proline	$ \begin{array}{c} \text{COO}^- \\ \\ {}^+\text{H}_2\text{N} - \text{C} - \text{H} \\ \quad \\ \text{H}_2\text{C} \quad \text{CH}_2 \\ \diagdown \quad / \\ \text{CH}_2 \end{array} $

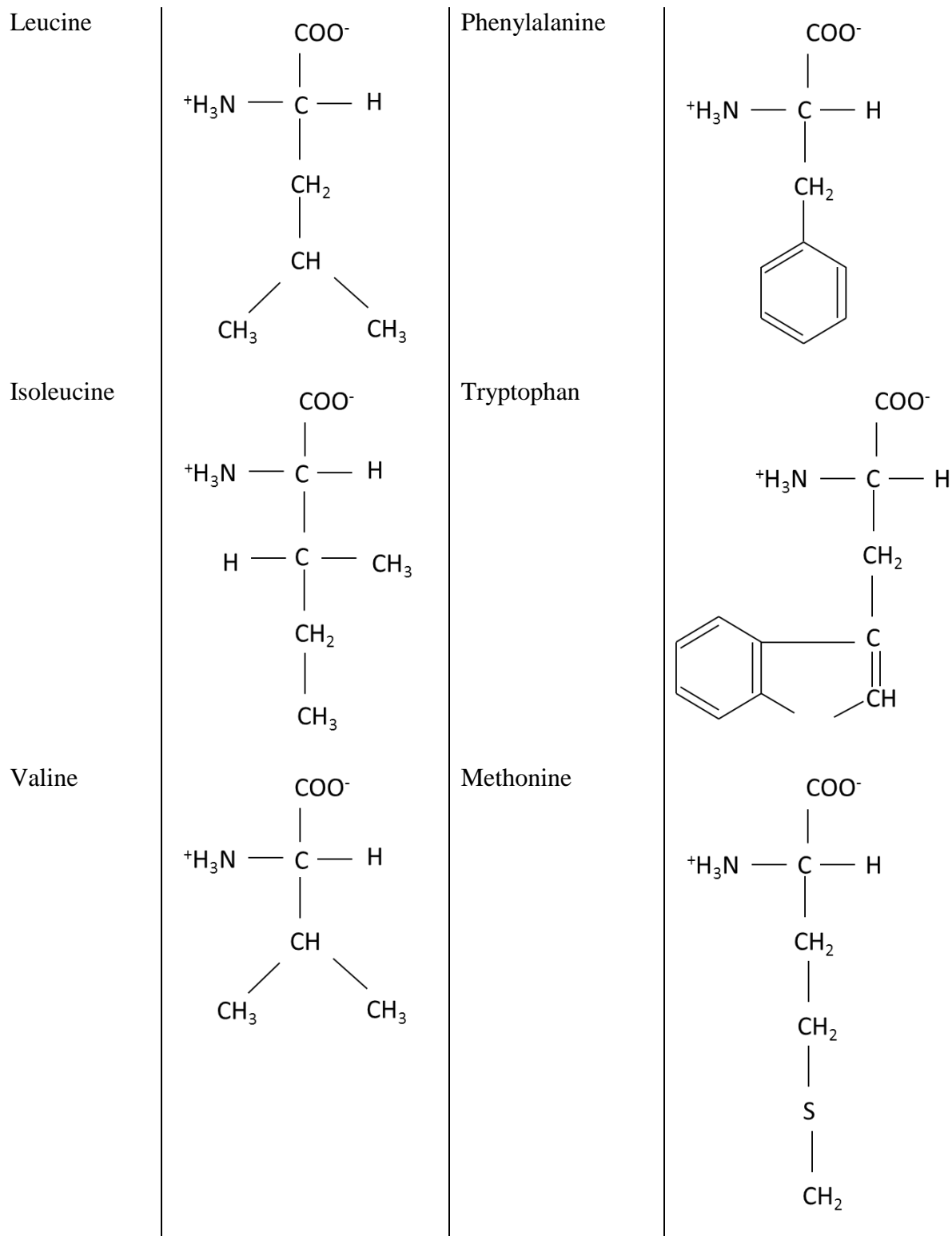


Table 1.7-1 Non-polar amino acids which contribute to the hydrophobicity of proteins.

Porath et al. (1973) named the chromatographic method as “hydrophobic salting-out chromatography” and often early papers noted the similarities of the

method to salting-out of proteins for precipitation. Theoretical equations for both principles also show their similarities (Melander and Horvath, 1977).

Hydrophobic interactions can only occur in the presence of water (a polar solvent), which is a poor solvent for nonpolar molecules. This promotes the nonpolar molecules/proteins to want to aggregate in order to achieve the lowest thermodynamic energy (McCue, 2009). An increase in entropy is observed as ordered water molecules are displaced from around the non-associated hydrophobic groups to the more unstructured bulk water (Queiroz et al., 2001). Formation constants are governed by the gain in entropy following the reorganisation of the water (Porath, 1990). In HIC the attraction is between a protein and a ligand, whereas in precipitation it is between two proteins (*Figure 1-19*).

The thermodynamic relationships in the binding (free energy ΔG) can be expressed as a function of enthalpy change (ΔH) and entropy (ΔS) according to the equation:

$$\Delta G = \Delta H - T\Delta S$$

Equation 1.7-1

An increase in entropy ($\Delta S > 0$) is observed, due to the displacement of the ordered water molecules, resulting in a negative change in the free energy ($\Delta G < 0$) and a thermodynamically favourable process.

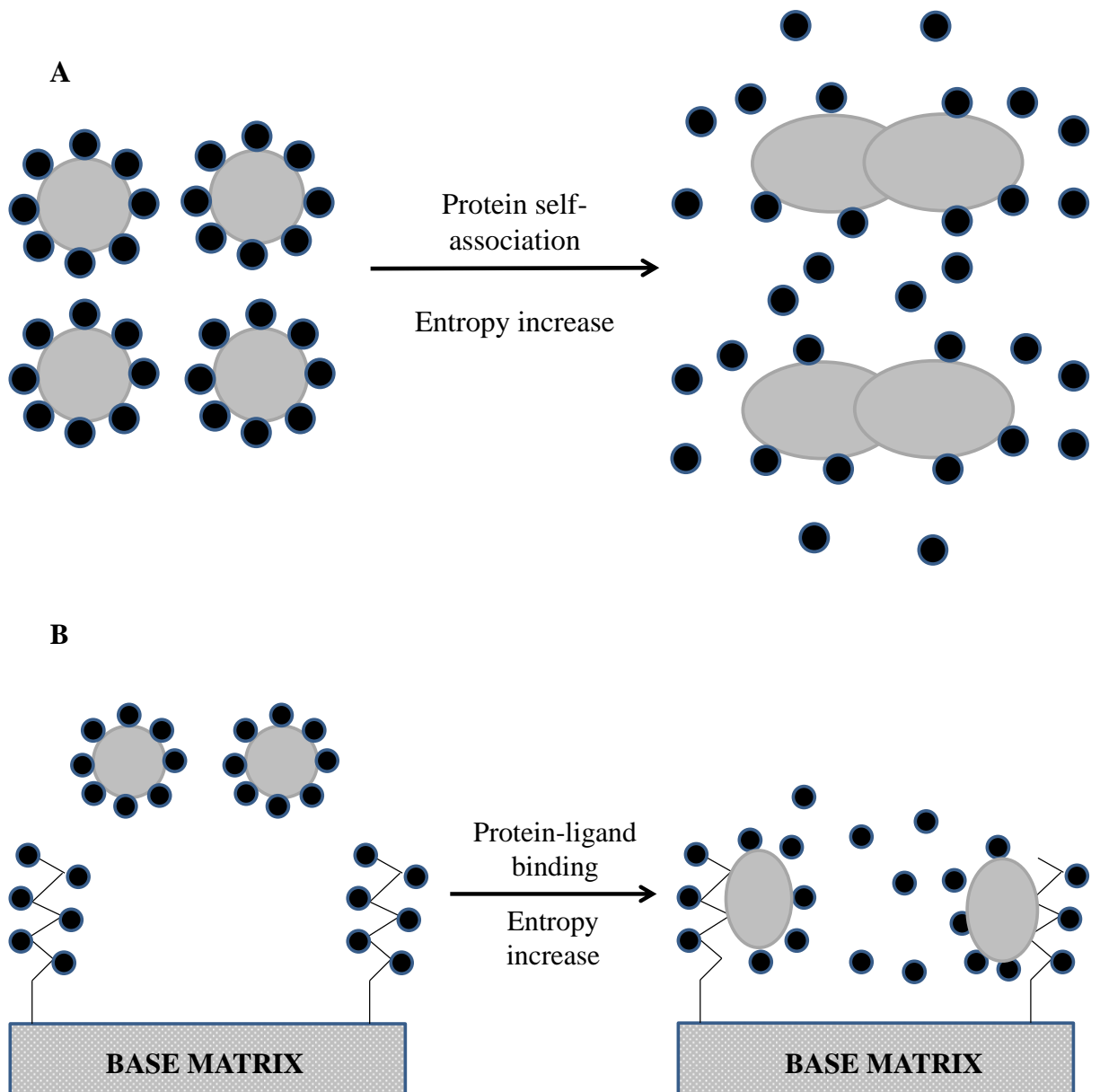


Figure 1-19 Schematic diagram showing hydrophobic interaction between proteins in solution (A) and between proteins and a hydrophobic ligand on HIC absorbent (B). As detailed in McCue (2009).

The polarity of the solvent can be controlled through the addition of salts or organic solvents, which can strengthen or weaken hydrophobic interactions (McCue, 2009). In 1888 Hofmeister defined a series of anion and cations that can precipitate proteins out from whole egg white. Almost all Hofmeister ions salt out non-polar molecules from aqueous solution (Baldwin, 1996). Ions which promote hydrophobic interactions are called lyotropes or antichaotropic salts and those which disrupt

(weaken) hydrophobic interactions are called chaotropes. (McCue, 2009). The series of anions and cations is as follows (Pahlman et al., 1977):

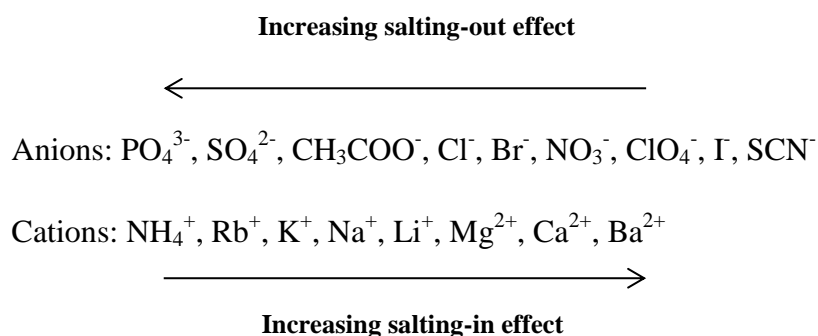


Figure 1-20 Hofmeister series of cations and anions.

The denaturant action of Hofmeister ions like SCN^- results from the fact that they salt in the peptide group, and consequently they interact much more strongly with the unfolded form of a protein than with its native form (Baldwin, 1996). Arakawa and Timasheff (1982) notes that the preferential interaction parameter for KSCN , MgCl_2 or CaCl_2 is very small in contrast to NaCl , CH_3COONa and Na_2SO_4 and they cause destabilising effects.

There are three kinds of adsorption or affinity chromatography based on this principle, using salt promoted interaction (Porath, 1990), although HIC has proved the most popular:

- 1) Hydrophobic interaction chromatography (HIC);
- 2) EDAC (electron donor-acceptor chromatography, including thiophilic chromatography)
- 3) TAC and IMAC (immobilised metal ion affinity-based chromatography).

1.7.2 HIC columns

The stationary phase of a HIC column consists of a base matrix coupled to a hydrophobic ligand. The ligand is important as this controls the hydrophobicity of the column. The early development of an ideal adsorbent required that three fundamental problems be addressed (Porath, 1986):

- 1) Finding a matrix material of desirable physical properties with no affinity for any of the substances present in the sample to be fractionated;
- 2) Finding a ligand substance to form the adsorption centre such that only one separation parameter will be operative;
- 3) Finding a method to introduce the ligand into the matrix without sacrificing those properties that define ligand specificity and affinity for the receptor.

1.7.3 Column resins

Ideally the base matrix of the column needs to be neutral so binding is with the ligands only. Early HIC base matrix materials would also promote binding within the column by electrostatic interactions. The development of neutral absorbents, such as the coupling of alcohols, instead of aliphatic and aromatic amines, to sepharose produced an ideal base matrix (Hjerten, 1974), and helped address problem 1 detailed above.

Common base matrices in use include hydrophilic carbohydrates (such as agarose), methacrylate, polystyrene-divinylbenzene and silica (Queiroz et al., 2001, McCue, 2009). Silica is used in high pressure applications as it is a harder material and therefore not affected by the high pressure (Kato et al., 1983, Kato et al., 1986).

1.7.4 Column ligands

Hydrophobicity of the ligand comes not only from the type of ligand but also the density of the ligand on the base matrix. The ligands consist of alkyl and aryl derivatives (Hjerten, 1974). As the length of the alkyl chain increases, so does its hydrophobicity. Straight alkyl chains (butyl, octyl, ether, isopropyl) show pure hydrophobic character, whereas aryl ligands (phenyl) show a mixed mode behaviour (GE Healthcare HIC handbook) and interact with compounds through “ π - π interactions” (McCue, 2009). The common HIC ligands include:

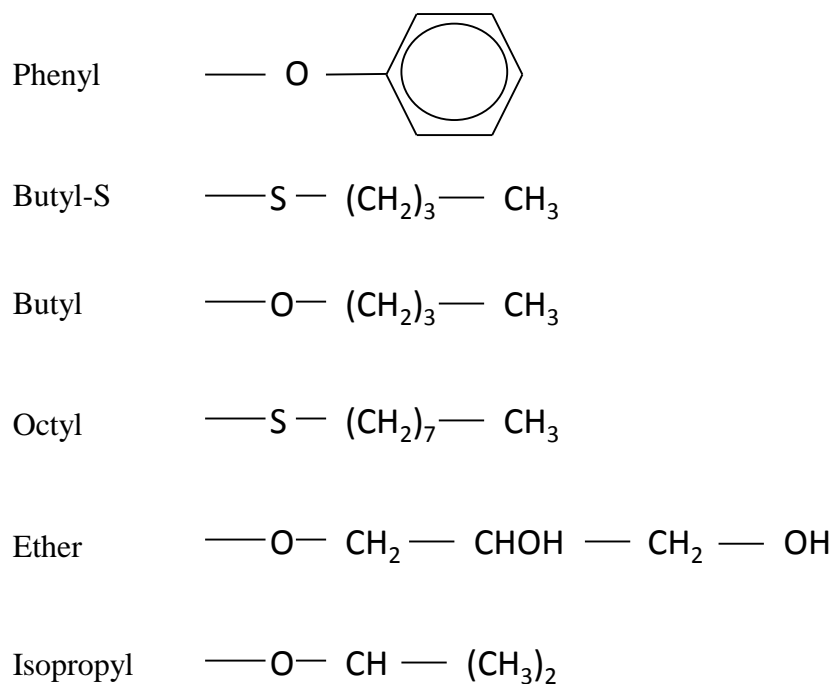


Figure 1-21 Ligands substituted on HIC media. Reproduced from Hydrophobic Interaction and Reverse Phase Chromatography handbook available from GE Healthcare.

The ligand density can be manipulated to obtain a variety of stationary phases with different selectivity and capacity. HIC matrices with a higher ligand density show a greater degree of hydrophobicity which results in a higher binding capacity. This increase could be attributed to the higher probability of forming multipoint attachment (Lienqueo et al., 2007). Changes in the ligand density can alter the retention time of a protein, as seen when different lots of the same media with varying ligand densities were compared (Jiang et al., 2010, Vicente et al., 2011a, Hahn et al., 2003, To and Lenhoff, 2011), or the phenomena can be exploited for processes such as monomer and aggregate separation of antibodies (Mccue et al., 2009) and when combined with the type of ligand can optimise the process (Lin et al., 2000).

1.7.5 Optimising a HIC step

The main purpose of optimising the chromatographic step in a process is to ensure the highest possible recovery and yield from a step. To do this the most suitable combination of the critical parameters must be selected. In the case of a HIC step these parameters include type of buffer, salt concentration, buffer pH and temperature. Other parameters associated with chromatography in general include bed height, flow rate, gradient shape and gradient slope.

1.7.5.1 Salt

The process of adsorption in HIC is driven by the use of salts at a concentration which allows reversible binding. Common salts used are ammonium sulphate and sodium chloride. As the salt concentration is increased the product develops a stronger interaction with the column, promoting a higher binding affinity and yield (To and Lenhoff, 2011, Bonomo et al., 2006, Mccue et al., 2009). The type of salt and concentration must be selected experimentally, as it is difficult to determine these parameters theoretically, because they are affected by other parameters such as ligand type, and protein hydrophobicity. Often a high concentration of salt is required and this can result in extra processing steps after to reduce the salt concentration. Kato et al. (2002) proposed that if the hydrophobicity of the support is correctly adjusted for each individual protein then a low salt concentration can be used. Obviously this would not be possible for every company to impose this on every process but does illustrate how parameters in the step are closely related.

The salt in the mobile phase helps to change the underlying thermodynamics of adsorption and more water is released as it goes into the unordered bulk water. Salts which increase the preferential hydration of hydrophobic surfaces have the greatest impact on retention time (Perkins et al., 1997). All of this is seen in the change in the $\ln(k')$ value (*Equation 1.7-4*).

1.7.5.2 Temperature

Temperature also has an influence on the binding affinity between the protein and ligand. As the temperature in the column is increased the hydrophobic forces also increase. Temperatures above 30°C increases the retention time for cytochrome C, reducing the amount of salt needed to promote binding and a high yield (Goheen and Engelhorn, 1984). The hydrophobic patches buried in protein molecules are exposed when the temperature increases enhancing the hydrophobic forces of the protein (Lin et al., 2001).

Increases in temperature result in the decrease of the Gibbs free energy released (ΔG^0) (Bonomo et al., 2006). The effect of temperature can also be viewed as it is a parameter in the capacity factor, as detailed in (Queiroz et al., 2001).

1.7.5.3 pH

The influence of pH on the binding in HIC columns is unclear and not straightforward. The binding affinity between the column is particular to each individual protein (Queiroz et al., 2001) and has no general trend (McCue, 2009). The general thought is that an increase in pH can weaken hydrophobic interactions (Porath et al., 1973). With monoclonal antibodies the pH becomes important as binding increases as the pH of the mobile phase approaches the pI (Valliere-Douglass et al., 2008). When the pH is close to a proteins pI, net charge on a protein is zero and hydrophobic interactions are maximum, due to the minimum electrostatic repulsion between protein molecules allowing them to get closer (Lienqueo et al., 2007).

1.7.5.4 Additives

Additives can be added into the elutant buffer to assist desorption of the product from the column (Goheen and Engelhorn, 1984), especially if the binding affinity is strong and low yields are achieved. Common additives include water miscible alcohols (e.g. ethanol), detergents (e.g. Triton X-100) and aqueous solutions of chaotropic salts (Queiroz et al., 2001).

1.7.6 Protein unfolding on HIC columns

During the development of a HIC process the focus is often on the various parameters which can be altered to promote a high yield and purity in the final eluent. But research has shown, particularly from the groups of Jungbauer and Hahn in Austria and O'Connell and Fernandez in the States, that proteins can unfold during the operation of the column. This can reduce the percentage recovery of a product, although the degree of reduction for each product must be determined individually as there is no general model.

In an attempt to understand the unfolding mechanism various models have been presented in the literature. One theory looks at the unfolding as in terms of first-rate reaction kinetics (Ueberbacher et al., 2008), with the rate constant k for the reaction of partial unfolding,

$$k = -\frac{\ln\left(\frac{Y}{Y_0}\right)}{t}$$

Equation 1.7-2

Where Y_0 represents the amount of native protein applied, Y is the amount of native protein in isocratic elution, and t is the residence time of the protein on the column.

Haimer et al. (2007) (*Equation 1.7-3*) looked at the unfolding reaction rate k_2 in relation to a spreading process on the column. The amount of spread protein (q_2) was estimated by integration a second peak, eluted during the regeneration phase. The native fraction (q_1) was estimated by integration of the first peak. The second peak is assumed to have undergone conformational change. The unfolding rate constant can be derived by assuming that the maximal binding capacity q_m exceeds the actual surface coverage by the native and spreading protein.

$$\frac{q_2}{q_1} = k_2 q_1 q^* t \text{ where } q^* = q_m - q_1 - \beta q_2$$

Equation 1.7-3

The four-state model described by Xiao et al. (2007b) considers the adsorbed and desorbed states of two protein conformations (*Figure 1-22*). The states are assumed to be reversible and the proteins undergo conformational change in either the mobile phase or at the liquid-solid interface. If all the states are in rapid equilibrium then a single peak should be observed, if any transformations are slow then two peaks will be observed. The free energy of unfolding (ΔG_{unf}) increases linearly with salt concentration and if this is looked at in terms of the four different states the unfolding free energy on the surface would be:

$$\Delta G_{unf,s} = \Delta G_{unf}^{sf} + \Delta G_{ads,U}^{sf} - \Delta G_{ads,N}^{sf} + \beta_U - \beta_N - m C_{salt}$$

Equation 1.7-4

The unfolding free energy on the surface ($\Delta G_{unf,s}$) is determined from adding the free energy difference of the salt independent terms (*sf*) of free energy of unfolding and adsorption in the native (N) and unfolded (U) forms. The salt effect on adsorbed protein stability depends on the salt dependence of stability in solution (*m*) and for adsorption of both native (β_N) and unfolded (β_U) forms to determine whether a salt will be stabilising (positive coefficient) or destabilising (negative coefficient).

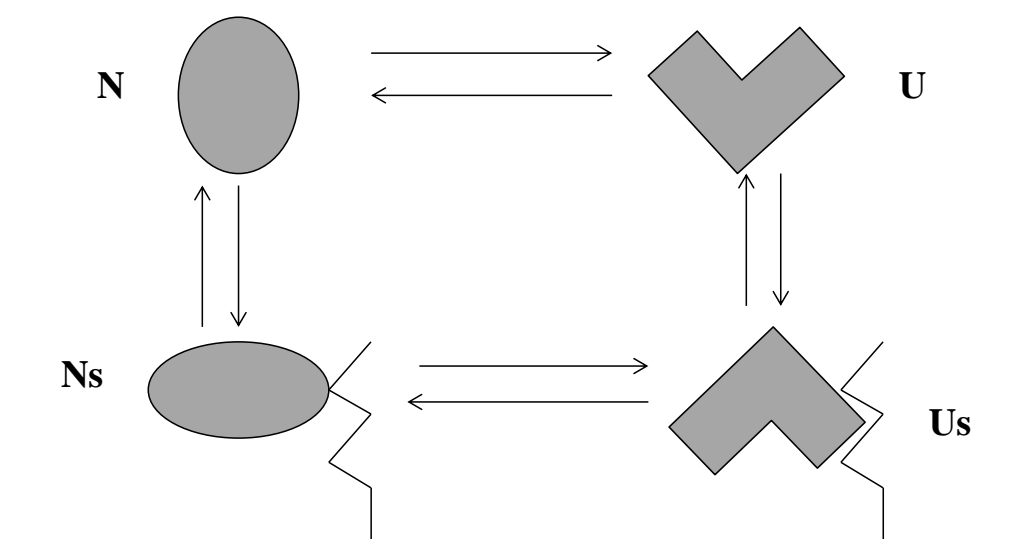


Figure 1-22 The four state model. N = native protein and U = unfolded protein. S indicates the form in the stationary phase. Reproduced from (Xiao et al., 2007b).

Conformational change can be seen as a drop in the recovery of a product in the elution material. This would be evident in the chromatogram traces at 280nm during the elution stage (as seen in figure 1 of Xiao et al. (2007b)). If pulse experiments are conducted, or if the elution profile has two peaks, the first peak is assumed to be native protein and the second the unfolded protein, as it is known that unfolded proteins will bind stronger to the column (Haimer et al., 2007, Ueberbacher et al., 2008). Hydrogen exchange, detected by mass spectrometry (MS), can look at structural changes related to conformational change and determine the amount of solvent exposure. This can give an indication of the degree and percentage of unfolding (Jones and Fernandez, 2003, Xiao et al., 2007a, Oroszlan et al., 1990).

A separate study by Ueberbacher et al. (2010) also looked at the thermodynamic quantities associated with conformational changes using isothermal titration calorimetry (ITC). The study looked at two common parameters which have an effect on conformational change in HIC. These are temperature and salt concentration (in this case ammonium sulphate). As explained in a previous section higher temperatures and salt concentrations lead to greater protein-surface interactions and a higher binding strength. Looking at literature the trend is that higher temperatures and salt concentrations (especially with ammonium sulphate due to its increased binding affinities when compared to sodium chloride) cause a greater degree of unfolding (Ueberbacher et al., 2008, Ueberbacher et al., 2010, Xiao et al., 2007a, Benedek, 1988, Bonomo et al., 2006, Wu et al., 1986, McNay et al., 2001, Fogle et al., 2006).

Another factor which can influence the degree or amount of unfolding in a protein sample is the time spent on the column. Benedek et al. (1984) studied unfolding on reverse-phase columns and noted that there was two steps; first a kinetically rapid initial contact of the protein with the surface and a second step which is kinetically slow and includes all further conformational events until elution. Hydrophobic interaction is weaker than reverse-phase but it would be expected that these phenomena would also occur, although possible at a slower rate. Hahn et al. (2003) saw that the unfolding of *cis-trans* prolyl-peptidyl isomerisation or intermediate formation took place within a time span from seconds to minutes and Jungbauer et al. (2005) noted that to look at unfolding conditions for a selection of proteins the residence time had to be kept constant to remove the time dependence

effects. McNay et al. (2001) also noted that on reverse-phase columns broadened peak shapes were observed at longer hold times and that loss occurred after 5 minutes.

It is the column ligands that dictate the degree of hydrophobicity in the column. Hydrophobicity can be increased by using a longer chained ligand (i.e. Octyl) or increasing the ligand density. Altering either of these parameters can cause an increase in hydrophobicity and therefore increase the degree of unfolding by the protein (Jungbauer et al., 2005, Oroszlan et al., 1990, Fogle et al., 2006). Increasing loading on the column seems to help to counteract any unfolding of the protein (Fogle et al., 2006, Ueberbacher et al., 2010).

1.8 CIM MONOLITHS

BIA Separations was founded in 1998 to develop and manufacture short monolithic chromatography columns, and are based in Austria and Slovenia. Production and R&D is carried out in a new facility in Ajdovscina, Slovenia. The company manufactures and sells a range of laboratory and industrial sized monolithic chromatographic columns based on technology called CIM or Convective Interaction Media technology.

1.8.1 Principles

Research on methacrylate monoliths was first conducted in 1967, but unfortunately the research did not prove favourable and development stopped for around 20 years. In the 1980s methacrylate monoliths were prepared as disks and the outcome of the development looked more promising, with the first commercialisation of the monoliths in 1991 partially successful. BIA took over their commercialisation in 1996 and introduced CIM technology (Barut et al., 2005).

Preparation of a CIM monolith involves the free-radical polymerization of two monomers glycidyl-methacrylate and ethylene-dimethacrylate, inert porogens dodecanol and cyclohexanol and an initiator, benzoyl peroxide-BPO, to produce a GMA-EDMA polymer (Mihelic et al., 2003). Changing the ratio of the monomers results in a different mean pore radius of the column (Podgornik et al., 2003). The optimal CIM disk has a porosity of 62% and a maximum pore size of 1.5 μ m (Podgornik et al., 2003), with an average pore radius of 600-750nm (BIA Separations information sheets).

The pressure drop is a linear function of flow rate, indicating a laminar flow regime. A linear relation between the pressure drop and the flow rate also proves that the porous monolithic structure is stable and does not contract at higher flow rates (Mihelic et al., 2005). The porosity of the CIM column equates to an equivalent particle diameter of 0.63 μ m. A column with these size particles would have a pressure drop that is 2.75 times higher than the monolith (Mihelic et al., 2005).

CIM monoliths are available in 3 different formats (*Figure 1-23*). There are the small 0.1ml analytical monoliths in a stainless steel housing (*Figure 1-23A*), disks (0.34ml volume), which can be put into a PEEK or POM housing (*Figure 1-24*), and tubes (1ml-8L). The cGMP tube columns are available in sizes 8ml to 8L. These columns come in a stainless steel housing ready for use within the manufacturing process. Columns are available with a large range of IEX, HIC and affinity ligands, see *Table 1.8-1*. The chemistry of the column is indicated by the coloured plastic ring, either around the disk or the housing. Not all chemistries are available at all sizes, although specific columns and specific ligands are available on request.

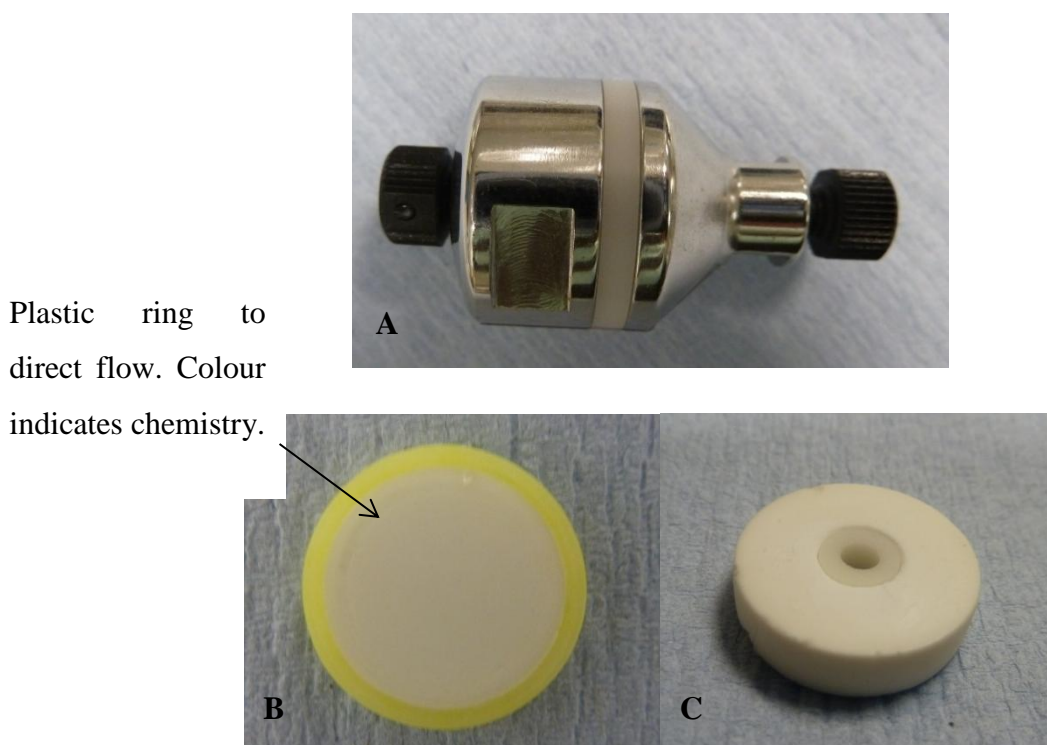


Figure 1-23 Different format of CIM monolith columns available from BIA Separations. (A) Analytical columns, 0.1ml; (B) Disks, 0,34ml (C) Radial monolith, 1ml. The yellow plastic ring around the disk indicates that the column chemistry is C4 HIC. The white ring on the analytical column indicates the column chemistry is OH HIC.

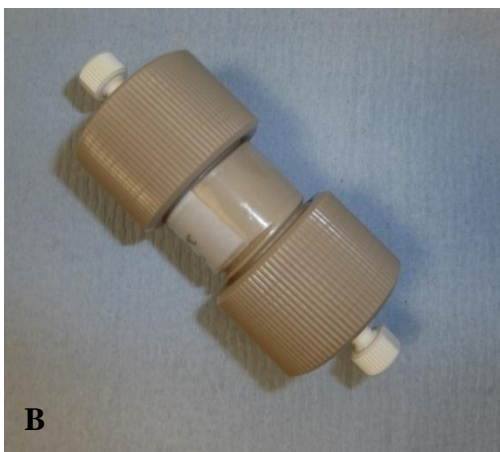
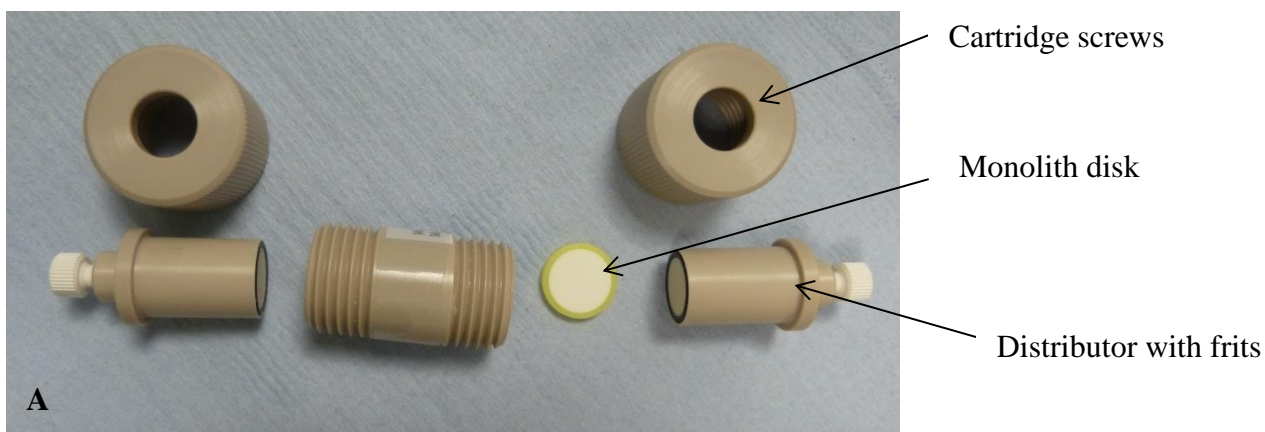


Figure 1-24(A) CIM monolith disk (0.34ml) and disk housing available from BIA separation. (B) A complete disk housing.

<i>Chemistry type</i>	<i>Ligands</i>
Ion exchange	Strong anion: QA Weak anion: DEAE, EDA Strong cation: SO3 Weak cation: CM
Hydrophobic/hydrophilic interaction	OH, C4
Affinity	Protein A, Protein G, Protein L, iminodiacetic acid (IDA with/without Cu ²⁺)
Activated chromatography (for ligand coupling)	Epoxy, CDI (carbonyldiimidazole), EDA (ethylene diamino)

Table 1.8-1 The range of ligand chemistries for CIM Monoliths available from BIA separations. List from www.biaseparations.com.

Use of the 0.34ml disk monoliths is by a cartridge device, made from PEEK (polyether ether ketone) or POM (polyoxymethylene) (*Figure 1-24B*). The difference in materials is that the PEEK cartridge is autoclavable and compatible with most organic solvents, whereas the POM can only be used up to 50°C and with aqueous mobile phases. The cartridge is able to hold up to 4 disks, allowing conjoint liquid chromatography (CLC). (Barut et al., 2003). A combination of different chromatography modes can be used in a single run by stacking up two to four disks. A suitable cartridge was designed by Josic et al. (1992) and BIA separations to enable connection of the disks to a common HPLC system (Barut et al., 2003). The cartridge was designed to avoid three main problems:

1. Leakage and by-passing of the mobile phase;
2. Poor distribution of mobile phase;
3. Limited mechanical stability of thin and wide rigid disks.

The first problem was eliminated by using O-rings at both the top and bottom of the disk, sealing the perimeter. Poor distribution over the disk resulted in a jet of liquid leaving the inlet tube and only using the centre of the disk for separation. This also resulted in the centre of the disk experiencing a much higher pressure that reduced the life of the unit. Distributors made of PAT (PEEK alloy with Teflon) frits with a thickness of 0.78mm and a porosity of 5µm are used to spread the liquid entering the cartridge over the disks. The cartridge developed by BIA separations allowed the easy exchange of disks.

1.8.2 Applications

Monoliths have been used for the concentration, separation and analysis of a large variety of macromolecules. These include plasmid DNA (Urthaler et al., 2005, Branovic et al., 2004, Bencina et al., 2004b, Smrekar et al., 2010), viruses and viral-like particles (Urbas et al., 2011a, Urbas et al., 2011b, Whitfield et al., 2009, Kramberger et al., 2007, Kramberger et al., 2004, Forcic et al., 2011), enzymes (Zmak et al., 2003), small proteins (Podgornik et al., 1999) and clotting factor IX

(Branovic et al., 2003). Monoliths have also been used for enzymatic immobilisation and conversions (Bencina et al., 2004a, Josic et al., 1998).

A variety of monolith sizes and chemistries have also been used with macromolecules. The first process to be scaled up on a monolith to a production scale was with plasmid DNA, in collaboration with Boehringer Ingelheim Austria GmbH, for use in gene-therapy and genetic vaccination (Urthaler et al., 2005) (see section 1.8.3). The advantage of using the monolith to BI was a more cost effective process.

Although most academic papers and other literature focuses on the replacement of traditional chromatographic media by monoliths for production processes involving plasmid DNA, viruses and other large macromolecules, monoliths can also be used for in-process or product analysis. BIA separations, in conjunction with Agilent, have released small monolithic columns under the name of CIMac® or BioMonolith. The use of a QA (quaternary amine) analytical CIMac® or Bio-monolith columns have been used for the in-process monitoring of adenovirus VLP (Whitfield et al., 2009, Urbas et al., 2011a). The CIM 0.34ml disk has also been reported for the in-process monitoring of plasmid DNA (Branovic et al., 2004). The analytical columns are 100µl in size and are housed in a metal casing (*Figure 1-23A*), enabling their use within a HPLC system. The use of HPLC assays can complement imprecise, costly and time consuming biological assays (Withka et al., 1987).

1.8.3 Scale up

Initially CIM monoliths were produced as disks with a column volume of 0.34ml. A maximum of four columns can be placed inside the holder to increase the column volume total to 1.36ml. As with any chromatographic technique monoliths must be scaled up, to above column volumes greater than four disks, to handle larger liquid volumes and more concentrated solutions. There are three options to scale up a monolithic disk, but each have disadvantages (Mihelic et al., 2003), as detailed in *Table 1.8-2*. Ultimately all CIM monoliths from 1mL to 8L are tubular in shape.

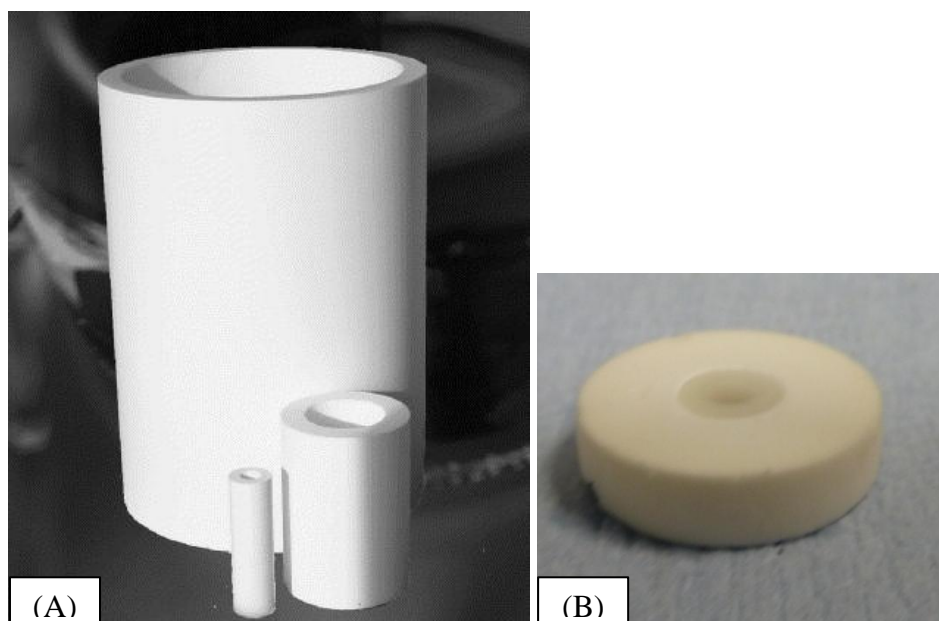


Figure 1-25 (A) Shape of CIM monoliths at 80ml, 800ml and 8L; (B) Shape of 1ml CIM monolith.

Option	Scale up method	Disadvantages
1	Increase diameter	Mechanical unstable and issues with uniform distribution across the column.
2	Increase length	High pressure drops causing compression
3	Tube columns one inside each other	Joining together of the columns may cause problems

Table 1.8-2 Scale up options for monolithic columns.

The production of the methacrylate monoliths by the process of free radical polymerisation also contributes to the issues surrounding the scale up of the columns from a 0.34mL disks. Free radical polymerisation is a highly exothermic process, with temperature controlling the rate of initial decomposition. A high temperature increases the number of nuclei and results in smaller pores (Podgornik et al., 2003). As the dimensions of the monolith mould increases the amount of heat inside the mixture also increases but the heat cannot be dissipated efficiently if a disk shape is maintained (Podgornik et al., 2003). Mapping of the temperature over different

radial positions in the column shows that the temperature can vary between positions over the mould. Natural convective flow inside the mould causes enhancement of the heat transfer influencing the radial temperature distribution and rate of polymerisation. Overall this results in a non-homogenic structure to the column which affects separation of molecules (Mihelic et al., 2003). The construction of a tube with a limited thickness enables the control of the temperature during production and subsequently the reproducibility of the columns with a consistent pore size.

As the columns are produced as tubes there is also a change in the flow of the mobile phase from axial to radial flow, as detailed in *Figure 1-26*. The bed height of the column remains short, and therefore so does the footprint of the unit (Carta and Jungbauer, 2010). With a radial column the mobile phase flows from outside to the inside. Inward flow provides a sharper concentration profile (Gu et al., 1991). As the inside is smaller there is a change in the linear velocity and flux, as modelled by Huang et al. (1988) and Gu et al. (1991). This change is not an issue with monoliths as they show flow independent resolution (Podgornik et al., 2000).

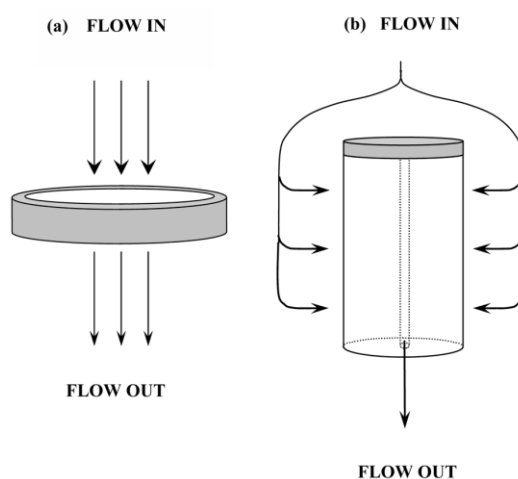


Figure 1-26 Schematics of the flow of the mobile phase and the sample through CIM disk (a) and CIM tube (b).

The use of a gradient elution is often used in chromatographic separation and the transfer of the method is not necessarily based on the constant column length. If

the optimal gradient for a small column is known then the gradient time for the large column can be calculated using the following equation (Podgornik et al., 2003):

$$t_{g,large} = t_{g,small} \cdot \left(\frac{V_{large}}{V_{small}} \right) \cdot \left(\frac{F_{small}}{F_{large}} \right) \cdot \left(\frac{L_{small}}{L_{large}} \right)$$

Where t_g is the gradient time (s), V is the total column volume (m³), F is the flow rate (m³/s) and L is the column length (m). The porosities of the two columns are presumed equal.

Scale up of various processes from disks to radial tube monoliths have proved successful and research shows that there is little or no variability between the chromatographic profiles (Podgornik et al., 2003, Zmak et al., 2003, Barut et al., 2005). Large CIM monoliths have been used for the commercial production of plasmid DNA, up to 8L (Urthaler et al., 2005).

2 METHODS AND MATERIALS

2.1 MATERIALS

2.1.1 Chemicals

All chemicals were purchased from Sigma-Aldrich (Poole, UK) unless stated.

2.1.2 2.1.2 HBsAg Cell line

The cell line used to produce the Hepatitis B Surface Antigen (HBsAg) was a recombinant *Saccharomyces cerevisiae* donated by Merck & Co. Inc. (West Point, PA, USA).

2.2 FERMENTATION OF SACCHAROMYCES CEREVISIAE

The fermentation media was taken from US patent 5,820,870 (Joyce et al., 1998) which was developed for the production of the HPV vaccine in *S cerevisiae*.

2.2.1 Media

Defined media was used in both seed and the HBsAg production stages. The components were as follows (per L): 8.5g Difco yeast nitrogen base without amino acids and ammonium sulphate (BD, Oxford, UK); 0.2g adenine; 0.2g uracil; 10g succinic acid; 5g ammonium sulphate; 0.25g L-tyrosine; 0.1g L-arginine; 0.3g L-isoleucine; 0.05g L-methionine; 0.2g L-tryptophan; 0.05g L-histidine; 0.2g L-lysine and 0.3g L-phenylalanine. Glucose was added at 40g/L to all 3 stages, with 40g/L galactose added at stage 3 only. The pH of the media was adjusted to 5.5 using 4M NaOH prior to sterilisation. Antifoam was added to the 75L fermenter before sterilisation.

2.2.2 Evaluation of yeast extract

To evaluate the effect of yeast extract on the growth of *S cerevisiae* and production of VLP cultures were only grown in 250ml and 2L shake flasks, using the recipe from 2.2.1. The addition of galactose added to the 2L flasks promoted VLP production. All other ingredients were the same as stated in section 2.2.1. Half the shake flasks contained yeast nitrogen base without amino acids and ammonium sulphate from Difco and the other half had a Sigma-Aldrich variety (Poole, UK).

2.2.3 Fermentation protocol

Cultures were grown in three stages; stage 1 and 2 were the seed stages in 250ml and 2L shake flasks respectively and stage 3 was in a fermenter. The initial seed stage involved the inoculation of two 250ml flasks containing 50ml of media and glucose with two frozen seed vials (1ml). Both flasks with incubated in a shaker at 28°C for 24 hours. The 2L flasks were inoculated with 4ml of this culture into 396ml of media and grown for a further 24 hours under the same conditions. Stage 3 was either in a 75L fermenter (Inceltech High containment fermenter, Maidenhead, UK), with a working volume of 45L, or a 20L fermenter (Applikon Biobench 20, Holland), with a 12L working volume, operated at 28°C, and 1vvm. Mixing was at an average of 250rpm in the 75L or 350rpm in the 20L to maintain a DO level over 20% in the fermenter. DO levels were liable to drop in the first 12-36 hours of fermentation, during the growth phase.

The sugar stocks of glucose and galactose were added to either fermenter before inoculation. Inoculation of the fermenters was at 10% working volume, with 12 shake flasks used for the 75L and 3 used for 20L. Adjustment in the fermenter was by 4M NaOH and 2M H₂SO₄ to maintain a pH 5.5 ± 0.1 before and during fermentation. A foam probe was used to monitor the fermentation level and automated for any additions, although antifoam was rarely used during fermentation. On-line measurements were carried out by using the ProPack data logging and acquisition software (Acquisition systems, Hampshire UK), which was later changed to GasWorks, version 1.0 (Thermo Electron Corporation, USA) and enVigil (Pharmagraph, Berkshire, UK). Samples were removed via the sample port to allow

regular off-line measurements of OD 600nm, glucose and galactose levels, pH and dry cell weight.

Fermentations were carried out when new materials was required, which was approximately every five months, due to the low amount of cells produced during fermentation.

2.2.4 Fermentation harvest

Fermentation broth from the 75L fermenter was harvested at 72 hours and centrifuged in a tubular bowl centrifuge (CARR Powerfuge P6, Pneumatic Scale Corporation, Florida, USA) at 15000 rpm at a flow rate of 1mL/min until all harvest material had passed though. Due to the low volume of cells all material was centrifuged in one go. This would on the day of the fermentation harvest.

Fermentation broth from the 20L fermenter was also harvested at 72 hours but centrifuged in an ultracentrifuge at 6300rpm at 4°C for 30 minutes (Beckman Coulter, Brea, USA). After centrifugation the supernatant was poured off and the cells collected by hand.

The centrifugation step produced a cell paste which was reasonably dry. The cell paste was stored in double layered plastic laboratory bags in a lab freezer at -80°C. A set quantity of frozen cell paste was removed to be thawed before primary recovery of the VLP, as detailed in Section 2.3, was carried out to ensure a set of experiments had the same starting material.

The VLP is an intracellular product and so freezing of the product would have had limited effect on the VLP as the concentration in the starting material, after primary recovery, was often at the same levels. Samples of the experimental starting material were tested during ELISA assays of post-experimental samples (Section 2.11.4) to ensure that no adverse effect of the VLP had occurred during the harvest or primary recovery stage.

2.3 PRIMARY RECOVERY OF VLP

The primary purification process carried out is detailed in (Kee, 2009) and was adapted from Kee et al. (2008). Frozen cell paste was resuspended at 25% (w/v) in 0.1M sodium phosphate, 0.5M sodium chloride and 2mM phenylmethylsulfonyl fluoride (dissolved in isopropanol). Cell disruption was carried out in a homogenizer at 1200 bar for three passes (Gaulin Micron Lab 40, APV Gaulin GmbH, Germany) or 400 bar for eight passes (Gaulin Lab 60, APV Gaulin GmbH, Germany). The detergent triton X-100 in 10mM sodium phosphate, pH 7, was added to the homogenate to a final volume of 0.4% (v/v) and incubated for 4 hours at 20°C. Centrifugation was carried out at 3000g for 5 minutes (Eppendorff, UK) to remove cell debris. Removal of the Triton X-100 was by XAD-4 beads in a batch mode at 0.5g triton per g XAD-4 (in accordance to values specified on Sigma product information sheet) for 2 hours at 20°C. This was followed by filtration to remove the beads at 1.0µm and 0.7µm (Whatman, Kent, UK).

2.3.1 Reduced lipid feed

A reduced lipid feed was produced by adding 0.3g/ml of XAD-4 (Amberlite) to the feed material for 30 minutes and gently mixing on the shaker at 100rpm. The beads were removed by filtration at 1.0µm, 0.7µm (Whatman, Kent, UK) and 0.45µm (Millipore, UK). The level of lipid was analysed as per the method in section 2.11.7.

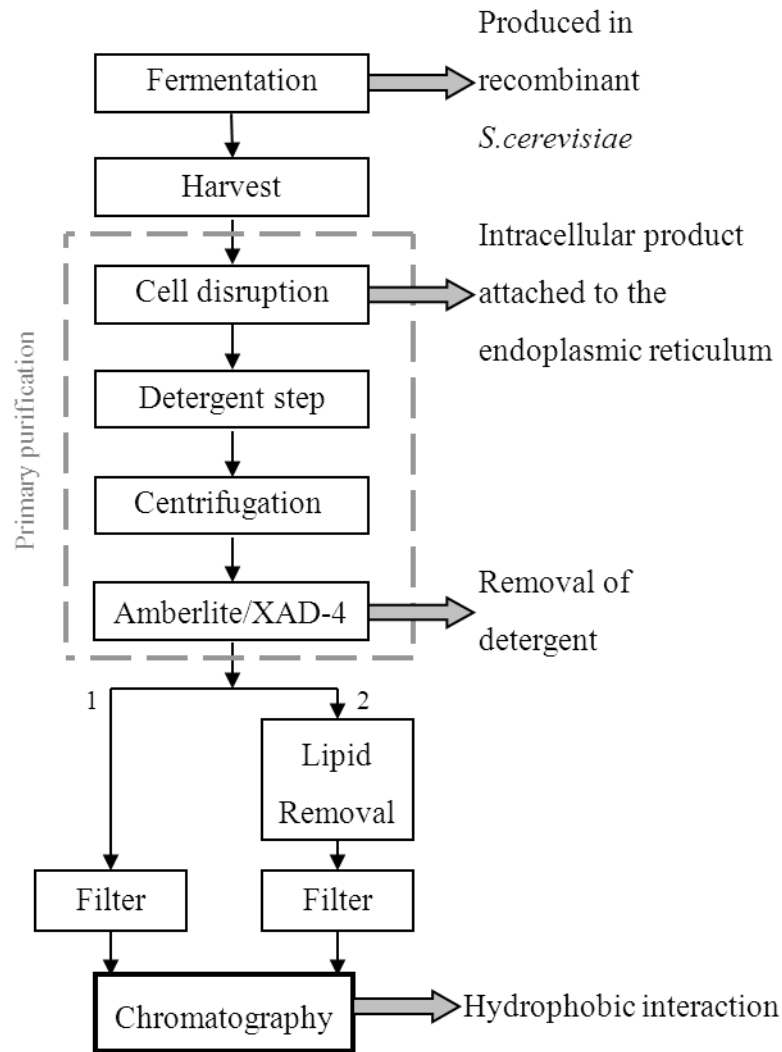


Figure 2-1 Flow sheet of primary purification and pre-chromatography preparation steps. Material can then follow two different routes; route one is for crude material and is filtered before the column, route two is for a reduced lipid feed where a lipid removal method is applied before filtration.

2.4 CONVENTIONAL CHROMATOGRAPHY

Butyl-S Sepharose 6 FF 1ml/5ml HiTrap columns (GE Healthcare, Bucks, UK) in the pre-packed format were used in a capture mode. The method of use is detailed by Jin et al. (2010) and was carried out on an Akta Explorer 100 (GE Healthcare) controlled by Unicorn Version 4.0 software and monitored at 280nm.

The feed was adjusted to 0.6M ammonium sulphate using a 3M concentrated stock in a 4:1 ratio (sample:salt). As per the method binding was carried out with 0.6M ammonium sulphate in 20mmol⁻¹ sodium phosphate, pH 7.0, elution conditions were 20mmol⁻¹ sodium phosphate, pH 7.0 and regeneration was 30% isopropanol in the elution buffer. Cleaning was carried out with 0.5M sodium hydroxide either after 1 or 5 consecutive runs, depending on the experiment undertaken. The flow rate was set to 1CV/ml (156 cm/h), and loading was approximately 2CV. Fractions were collected during loading and elution, either 1ml or 10ml samples.

2.5 MONOLITHIC ABSORBENTS

All monoliths were obtained from BIA Separations (Ljubljana, Slovenia).

2.5.1 CIM[®] disks and tubes

The monolithic chromatographic process was carried out using CIM[®] 0.34mL disk or 1mL tube monoliths with either C4 or OH ligands. Flow of the mobile phase and sample in the disks is axial, whereas the 1mL column is tube shaped and the flow is radial. The method was adapted from section 2.4. Buffer conditions were (unless stated) as follows; Buffer A, 20mmol⁻¹ sodium phosphate, 1.0M ammonium sulphate, pH 7.0; Buffer B, 20mmol⁻¹ sodium phosphate, pH 7.0; Buffer C, 30% isopropanol in Buffer B. Cleaning-in-place was with 1M sodium hydroxide. The samples were filtered with a 0.45µm filter (Millipore, UK) and then equilibrated to the salt level in Buffer A by adding ammonium sulphate to the feed. Feed volumes were adjusted depending on column size and material type, with 2mL for the 0.34mL disks and 5 or 10mL for the 1mL columns for the lipid and reduced lipid feed respectively. The 1mL columns were equilibrated with 20CV of Buffer A followed by loading and a wash step totalling 20 or 25CV (for a 5ml or 10ml loading volume). Elution was carried out with 10CV of Buffer B, with regeneration of the columns using Buffer C for 10CV to remove tightly bound material. A CIP was carried out after every run, which was followed by a water wash. The 0.34mL columns were loaded and washed with Buffer A for 10CV, elution with buffer B was for 7CV and regeneration with Buffer C for 10 CV. All chromatography was carried

out on an AKTA Explorer 100 system controlled with Unicorn Version 4.0 (GE Healthcare, Bucks, UK)) and monitored using 280nm. Flow rates were at 3 ml/min (139 cm/h) unless stated.

2.5.2 CIMac™ OH columns

Columns were used on an Agilent 1100 (Berkshire, UK) high-performance liquid chromatography (HPLC) system, controlled with ChemStation for LC Systems. The columns are 0.1ml volume, encased in stainless steel housing. Columns were run at 2ml/min for 9 minute runs. Material was adjusted to 0.8M ammonium sulphate using a stock solution of 3.4M and 100µl was loaded on to the column. Samples were bound with buffer A, 0.8M ammonium sulphate in 20mmol⁻¹ sodium phosphate, pH 7 and eluted with buffer B, 20mmol⁻¹ sodium phosphate, pH 7. Elution was conducted in a step elution mode as illustrated in *Figure 2-2* at 80% and 100% B for 3 minutes each before equilibration in buffer A. The column was regenerated and cleaned with 30% isopropanol in buffer B after 1 or 3 runs, with triplicates for each sample where available. The column was cleaned with 1M NaOH in a reverse flow direction at 0.2ml/min for 1 hour.

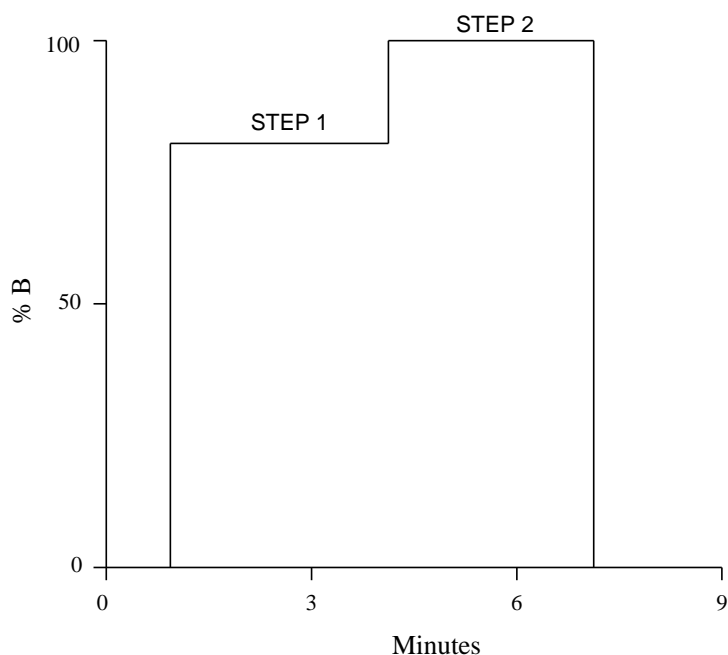


Figure 2-2 Schematic illustrating the elution steps of CIMac monolith method for VLP analysis.

2.6 CONFOCAL LASER SCANNING MICROSCOPY (CLSM)

Neutral lipids were labelled with BODIPY 493/503 dye solution (Invitrogen, Paisley, UK) to give a final ratio of $8\mu\text{mol L}^{-1} \text{g}^{-1}$ lipids. The solution was incubated at 20°C overnight before use. The C4 monolith disks (0.34mL) were challenged for 3 chromatography runs with a crude feed containing the fluorescently labelled lipids. The columns were cut into vertical sections using a razor blade and placed onto a microscope slide. Images were acquired using a confocal microscope (Pseemore upright SP1, Leica Microsystem GmbH, Mannheim, Germany) with a 10x objective lens.

2.7 LIPID REMOVAL METHODS

Lipid removal was carried out in a batch process using material which was prepared from the purification process (section 2.3). For the ammonium sulphate precipitation saturated solutions were added to the sample in equal volume with the crude yeast material. Samples were mixed for 20 minutes and then spun at 14K rpm

for 10 minutes to remove any precipitate. Both lipid removal absorbent (Advance Mineral Corp, California, USA) and XAD-4 (Amberlite) were added at the relevant w/v concentrations to the sample and mixed for 30 minutes. The sample was then filtered with a 1.0µm filter (Whatman, Kent, UK) to remove the LRA and XAD-4. Cuno Zeta Plus[®] BC25 capsule filters (Cuno 3M, Bracknell, UK) were run at varying flow rates using an AKTA Crossflow system controlled by Unicorn version 4.0 (GE Healthcare, Bucks, UK). Filters were equilibrated with a solution of equal parts homogenisation buffer and 0.01M sodium phosphate, pH 7.0 at a 1:1 ratio. A new filter was used at each flow rate. All filtrates and the supernatants were collected and analysed for VLP and lipid levels.

2.8 TRANSMISSION ELECTRON MICROSCOPY (TEM)

Chromatography elution samples were concentrated and diafiltered with 0.01M PBS pH 7 using 7mL Pierce protein concentrators, MWCO 150,000 (Thermo Scientific, Loughbough, UK). Electron microscopy was carried out in UCL department of Cell and Developmental biology, using a JEOL 1010 transmission electron microscope, (Jeol, UK). Samples were placed onto a carbon grid and the sample was left to dry. The carbon grid was stained with 2% uranyl acetate for approximately 1 minute (Yamaguchi et al., 1998). The grid was viewed at x300K for proteins or x120K for lipid particles.

2.9 ATOMIC FORCE MICROSCOPY (AFM)

Glass slides were cleaned with ethanol and silanised with trichloro (1H, 1H, 2H, 2H-perfluorooctyl) silane vapours to make it hydrophobic and encourage the VLP to bind to the surface, Kol et al. (2006). The silanised glass slides were attached to magnetic holders (Agar Scientific, UK) using a protocol from Muller and Engel (2007). The glass slide with the VLP was prepared in a similar method to that stated by Milhiet et al. (2011), with the VLP samples concentrated and diafiltered into Tris-HCl 20mM, NaCl 150mM, pH 7.4, using 7mL Pierce protein concentrators (Thermo Scientific, Loughbough, UK). The VLP was incubated onto the glass slides, for two hours and fixed with 5% glutaraldehyde. AFM was performed in a

tapping/intermittent mode using a Multimode SPM (Veeco, Mannheim, Germany), with a J scanner and NSC15 cantilevers (Mikromasch, Estonia) and Nanoscope 5.3 software.

2.10 ZETA POTENTIAL MEASUREMENTS

To measure the net electrical charge on a particle the Zetasizer Nano ZS (Malvern Instruments, UK) was used to look at the Zeta potential on a sample. Zeta potential is determined from electrophoretic mobility and then applying the Henry equation. Samples were analysed in Zeta folded capillary cells (DTS 1060, Malvern, UK), which were first cleaned out using 100% ethanol and Milli-Q water. The sample was loaded via a syringe, as per instructions, and equilibrated for approximately 5 minutes. If needed samples were diluted using 20mmol^{-1} sodium phosphate, pH 7, to ensure that the conductivity of the sample was low (preferably under 10 mS/cm). Any samples which were above 5 mS/cm were analysed by monomodal analysis, which only gives the mean zeta potential value, instead of a distribution. Three measurements were made of each sample and the number of runs within each measurement was determined by the instruments software.

2.11 ANALYTICAL TECHNIQUES

2.11.1 Optical density measurements

Optical density (OD) measurements were carried out on fermentation samples at a wavelength of 600nm using spectrometer Biomate 3 (Thermo Sepctronic, UK). Disposable 1ml cuvettes (Sarstedt, Germany) were used and the machine blanked with Milli-Q water (Millipore, UK) before use. Any samples above 1 Au were diluted with Milli-Q water to be in the range of 0.1 – 1 Au.

2.11.2 Dry cell weight analysis

Dry cell weight (DCW) analysis of fermentation samples were measured by filtering media through a $0.7\mu\text{m}$ Whatman Glass Microfibre Filter Grade GF/F

(Whatman, Maidstone, UK), using a vacuum filtration device. Both the filter and sample container were weighed before use. Around 5-10ml of media was filter and the container reweighed. The filter was then dried in an oven at 100°C overnight and reweighed. The DCW was calculated using where F1 is the filter before use, F2 is the filter after use, M1 is the mass of sample before use and M2 is the mass of sample after use (assuming that the density of the sample is equal to water).

$$DCW = \frac{F2 - F1}{M2 - M1}$$

Equation 2-1 Dry cell weight analysis

2.11.3 Glucose and galactose measurements

Offline glucose and galactose measurements were analysed using YSI bioanalyser (YSI life sciences, Hampshire, UK). Both glucose and galactose were calibrated to 2.5g/L. Samples were diluted to be in the range of 2-4 g/L using Milli-Q water and were measured in duplicate.

2.11.4 Enzyme Linked Immunosorbent Assay (ELISA) for HBsAg

Quantification of the VLP was carried out using the Abbott-Murex HBsAg Version 3 96-well plate ELISA kit (Dartford, UK). An HBsAg standard was obtained from Aldevron GENOVAC GmbH (Freiburg, Germany) to produce the calibration curve. The HBsAg standard was stored at +4°C, as per instructions from the manufacturer, and mixed well before use. Serial dilution was carried out to produce a calibrate curve on each plate, and a minimum of 3 samples at each point were used to produce the curve. A trendline was applied to get the value of the slope and intercept which were applied to produce the results. The use of a robotic system was used to produce the calibration curves and ensured a higher R² value. The R² value was between 0.85 and 0.98 on the calibration curves.

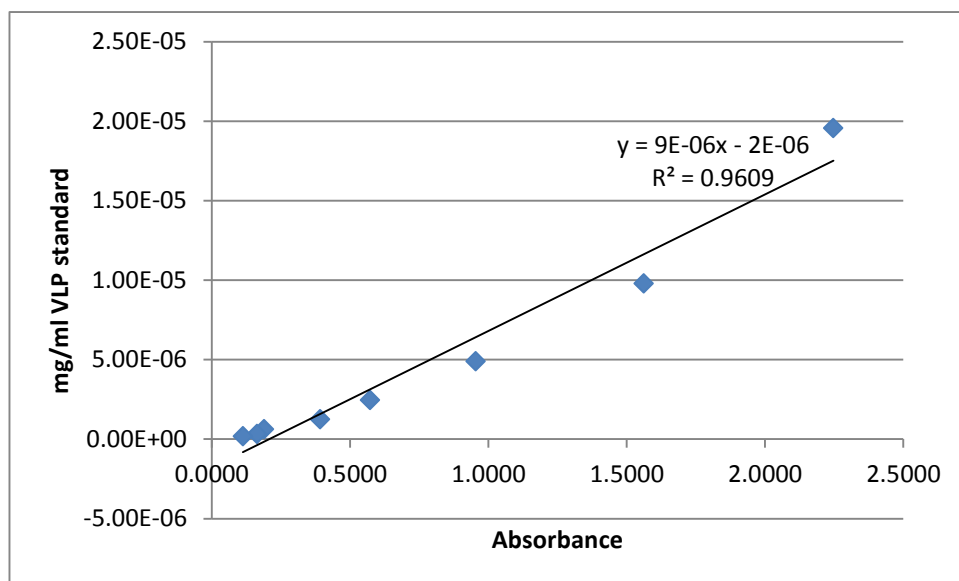


Figure 2-3 Example of a calibration curve used for ELISA analysis of VLP samples post experiment.

Samples were pre-diluted 1000 fold by serial dilution using 20mmol^{-1} sodium phosphate, pH 7.0, to ensure that results would lie within the range of 7.81×10^{-5} and 1.53×10^{-7} mg/ml. A minimum of 3 samples were used for each sample point. A minimum of five samples were used from each experiment for analysis of the results. The plates were read using Tecan Safire II microplate reader (Tecan Group Ltd, Switzerland).

The percentage of error seen in results was as much as 50% (as can be observed in graphs within chapters 3-5), which could vary across the plate. This is a standard problem seen with ELISA tests. Any analysis was repeated if it was felt that no clear conclusions from the samples could be drawn or the error bars were too large. The ELISA plates were purchased as part of a kit and as such were pre-coated. It was observed over time that plates would not necessarily produce like-for-like results, and some variation could be seen between plates or rows within a plate. Sample analysis from an experiment was kept to one plate to reduce any variation, as comparison between plates was a source of error.

2.11.5 Total protein assay using Bicinchonic acid assay (BCA)

Total soluble protein in samples was analysed using a Bicinchonic acid (BCA) assay kit (Thermo Scientific Pierce, Leicestershire, UK). The assay was carried out in 96-well plates (Sardstedt AG & Co, Leicester, UK) using the method as detailed in the kit handout. Calibration was performed by using dilutions of a 2.0 mg/ml BSA solution provided with the kit in the range 20 - 2000 $\mu\text{g/ml}$. Samples were diluted 2 – 10 fold with 20 mmol^{-1} sodium phosphate, pH 7.0, depending on the starting concentration to lie within the calibration range. Plates were read using Tecan Safire II microplate reader (Tecan Group Ltd, Switzerland).

2.11.6 Total protein assay using Coomassie Blue reagent (Bradford)

Another method to analyse total protein in samples was using Bio-rad dye reagent concentrate (Bio-rad, Herts, UK) as per instructions for microtiter plates, either standard or microassay format. Testing was carried out on 96-well plates (Sardstedt AG & Co, Leicester, UK). Calibration was performed with BSA in the ranges stated in the instructions, 0.05 mg/ml to 0.5 mg/ml for microtiter assay and 8.0 $\mu\text{g/ml}$ to 80 $\mu\text{g/ml}$ for microassay. Samples were diluted 5 to 10 fold with 20 mmol^{-1} sodium phosphate, pH 7.0, to ensure that the readings were within the calibration range and to remove any interference from detergents. Plates were read using Tecan Safire II microplate reader (Tecan Group Ltd, Switzerland).

2.11.7 Lipid quantification by HPLC

The concentration and types of lipids within samples was analysed using a Jordi Gel Glucose- DVB 500 Å column (Grace, Lancashire, UK). The method has previously been described by Jin et al. (2010). Samples were applied to the column using a mobile phase of chloroform, methanol and 0.15% TFA (in water) in the ratio 50:43:7. Samples were prepared by adding 70 μl of the required sample to 930 μl of extraction solution, which is the same composition as the mobile phase without water. Mixtures were centrifuged 30 minutes after extraction solution addition to remove any solids. The column was operated at 1 mL/min on an Agilent 1100 HPLC system (Agilent, Wokingham, UK) with an injection volume of 50 μL . After the column samples were passed through an Evaporative Light Scattering

detector (ELSD), (Grace, Lancashire, UK) operating at 39.8°C, a gas flow of 1.4 mL⁻¹ and gain 1 to obtain a chromatogram. Calibration had been carried out using standards of triacylglycerol, Triton X-100, ergosterol and phospholipids at various concentrations.

2.11.8 Dynamic light scattering (DLS)

Size analysis of a sample using dynamic light scattering was carried out on a Zetasizer Nano ZS (Malvern, UK) with DTS Nano software. Dynamic light scattering measures the Brownian motion of particles in a liquid and relates this via the Stokes-Einstein equation to a particle size. Brownian motion is measured by illuminating the particles using a laser (in this case 633nm) and analysing the intensity fluctuations in the scattering light, using a detector set at 173°. Samples were measured in a small volume (45µl) quartz cuvette (Hellman, Germany), which was cleaned with 50% ethanol v/v and Milli-Q water or Hellmanex III and Milli-Q water. Initial test runs on the material determined the attenuation level (ideal is a level of 5-8) and polydispersity (ideal is below 0.5) the samples and if necessary they were diluted 5-10 fold with 20mmol⁻¹ sodium phosphate, pH 7. The software can give expert advice if the sample is not ideal for DLS. Samples were measured in triplicate and the number of runs per measurement was determined by the software. Results were analysed using intensity measurements (raw data) or volume, which is generated from the intensity data.

2.11.9 SDS-PAGE

Electrophoresis gels were run under reducing conditions using 4-12% Bis-Tris gels (Invitrogen, UK). The gel was used to separate proteins from 3.3 to 160KDa with MES buffer (Invitrogen, UK). Samples were concentrated to an approximate value of 1mg/ml, dependant on results from a Bradford assay, using Amicon Ultra centrifugal filters (Millipore, UK) with a 3K MWCO. Samples were diluted with an equal volume of a mixture of sample buffer and reducing agent. Gels were loaded with 20µL of the sample and buffer mix. The mixture was heated up to 100°C for 2 minutes and then centrifuged to precipitate any particulates. One lane was for protein standard Novex sharp pre-stained (Invitrogen, UK), to indicate

molecular weights. The gel was run at 0.8Volts for 1 hour and then removed from the holder and washed with RO water for 5 minutes. This was repeated twice more. Staining of the bands within the gel was with Coomassie Blue stain (Bio-rad, UK) for 1 hour and left in RO water overnight for destaining. Pictures of the gel were obtained and were left drying overnight with Gel-Dry drying solution (Invitrogen, UK).

2.11.10 Size Exclusion Chromatography (SEC)

All SEC work was carried out on Agilent 1100 HPLC system (Agilent, Wokingham, UK) using a Tosoh Hass G5000 PWXL column (7.8mm x 300mm) (Tosoh Bioscience, Germany). This column has been previously used by Tleugabulova et al. (1997) to separate HBsAg. A PWXL guard column (Tosoh Bioscience, Germany) was used before the column to extend the column lifespan. To increase the peak size 100 μ L of the sample was loaded onto the column from the autosampler. Samples were run at a flow rate of 0.5ml/min for 60 minutes using a 100mM PBS mobile phase.

3 DEVELOPMENT OF A PURIFICATION PROCESS FOR VIRUS-LIKE PARTICLE ON A MONOLITHIC ADSORBENT

3.1 INTRODUCTION

The earliest production of a Hepatitis B vaccine relied on the purification of Hepatitis B surface antigen (HBsAg) from infected human plasma. This restricted supply reduced the possible number of vaccines available and so laboratories looked for an alternative source. The HBsAg genes from the Hepatitis B virus were placed in a bacterial system but production failed even with a powerful bacterial promoter (Valenzuela et al., 1982). Placing the genetic code for the HBsAg into a yeast host system resulted in the production of HBsAg (Mcaleer et al., 1984, Petre et al., 1987) and enabled the manufacture of larger quantities of vaccine.

Yeast are an ideal host system for vaccines as they are non-pathogenic to humans, relatively free of endotoxins and have been grown at industrial scale for centuries (Carty et al., 1989). The genes for HBsAg were placed into the yeast *Saccharomyces cerevisiae* via a plasmid. Literature reported that the yeast produced particles which were similar to those produced in humans (Valenzuela et al., 1982, Miyanochara et al., 1983) and that the particles were as antigenic in mice as human-derived HBsAg.

The expression of the HBsAg was found to be easily controlled in *S.cerevisiae* by a galactose regulated system (Carty et al., 1989). The *GAL1*, *GAL7* and *GAL10* promoters are all useful to regulate high-level expression in yeast (Schultz et al., 1987). Glucose is used to increase the mass of the yeast, and is preferentially used before the galactose promotes the production of HBsAg.

Monoliths are an alternative stationary phase format to conventional particle based media for large biomolecules. Conventional resins suffer from limited capacities and flow rates when used for viruses, virus-like particles (VLP) and other nanoplex materials. Particle based adsorbents require the transport of molecules

though their pores via diffusion which can be slow and may even prevent large molecules accessing the large internal surface area (Svec and Frechet, 1999). Conventional particle resins were designed for small proteins and as such the pores in the resin beads are around 10-100nm. As most proteins have a diameter of below 3nm the pore size is not a hindrance (Jungbauer, 2005).

The open pore structure in monoliths uses flow to improve the mass transfer to the sites of adsorption. By containing large wide pores the column shows flow-independent performance, which would be unachievable with a conventional resin column, indicating that the adsorption is not mass transfer limited. The advantages of this can be seen in reduced processing times, although the flow rate becomes limited by the high-pressures formed at very high rates (Hahn and Jungbauer, 2000, Mihelic et al., 2000, Jungbauer and Hahn, 2008).

Zeta potential is used to characterise the electrical double layer on a molecule or cell. A net surface charge on a molecule is generated through the absorption of specific ions from solution. There are two layers which form, with the charge of each layer depending on the charge of the particle. The zeta potential is an important value as it can be measured and gives an indication of the potential existing between the bulk phase and the shear plane (Hughes, 1977).

As the zeta potential reaches zero, particles in the fluid become unstable and can flocculate together (Hughes, 1977). Measuring the zeta potential has proved a useful tool in looking at the adhesion of biomass in EBA (Lin et al., 2006), protein absorption in IEX chromatography (Jonsson and Stahlberg, 1999), MAb DBC on CIEX (Faude et al., 2007), bioadhesion (Mahrag Tur and Ch'ng, 1998), cell immobilisation (Thonart et al., 1982) and the surface charge on bacterial cells (Wilson et al., 2001, van der Wal et al., 1997), which can model cell function and behaviour.

This chapter focuses the production of the VLP via fermentation of recombinant yeast and the subsequent primary purification steps. Although the fermentation conditions had already been defined by a previous colleague, some media development had to be undertaken when the fermentations started to fail and the cells subsequently lysed in the fermenter.

A new monolithic process was developed as an initial chromatography step to purify the VLP from a crude feed. A selection of weak hydrophobic interaction columns were tested to find the column which gave the highest yield. The process was then modified further to maximise the VLP recovery. Comparing the monolith process to a conventional process shows how more effective the monolith is at purifying the VLP. The VLP produced was visualised and analysed using various methods, including dynamic light scattering and size exclusion chromatography. These methods would determine whether the VLP was produced correctly and if any aggregation had occurred. The use of zeta potential was tested to see if a screening mechanism to determine the ideal binding conditions and degree of binding affinity of the VLP to the chromatography column could be developed.

3.2 MATERIALS AND METHODS

Production of the Virus-like particle was carried out by fermentation as defined in **Section 2.2**, using a recombinant cell line (**Section 2.1.2**). The fermentation was analysed for growth using optical density (**2.11.1**), dry cell weight (**2.11.2**), and for glucose and galactose use (**2.11.3**). The HBsAg was purified using the primary recovery protocol (**Section 2.3**). The chromatographic steps were carried out as per **Sections 2.4** and **2.5**. Experiments were quantified using ELISA for VLP (**Section 2.11.4**) and protein using Bradford (**2.11.6**) or BCA (**2.11.5**). The size of the VLP was determined by DLS (**2.11.8**), EM (**2.8**) and AFM (**2.9**). Size exclusion was carried out as per **Section 2.11.10**. Experiments to determine the zeta potential were performed as per **Section 2.10**.

3.3 RESULTS AND DISCUSSION

3.3.1 Fermentation of *Saccharomyces cerevisiae*

The Virus-like Particle was produced intracellularly in a recombinant *Saccharomyces cerevisiae* by fermentation in the pilot plant at UCL either in a 75L or 20L fermenter. Development of the fermentation process is described in full by (Kee, 2009).

3.3.1.1 75L fermentations

The fermentation process produces a low concentration of cells, reaching peak optical density values around 48 hours (*Figure 3-1*). The OD is low compared to wild type *S.cerevisiae* growth. Fermentations were carried out when new material was required, and due to variation in the fermentation batches experimental sets were carried out with material from the same batch to ensure consistency.

The media was sterilised at 121°C inside the fermenter. Samples were taken from the fermenter by the operator at time intervals during the working day and material was analysed immediately for glucose and OD. Dry cell weight (DCW) was carried out after glucose and OD readings, or samples were stored at 4°C before this was carried out. On-line analysis of the off-gas was carried out by mass spectrometer. After immediate off-line analysis the remaining volume of timed samples were aliquoted out and stored at -20°C to analyse material for galactose concentration and VLP production at a later date.

In the initial 24 hours the yeast increases steadily in mass by using glucose as a carbon source, after a lag phase of around 8 hours. The RQ value peaks around 18 hours, resulting in a drop in the dissolved oxygen level which can be seen on the on-line monitoring. If necessary the stirrer speed was increased from 250rpm to ensure that the DO remained above 30%. The OD continued to increase up to 48 hours before decreasing slightly until the material is harvested at 72 hours as natural cell death occurs. The consumption of galactose is minimal until depletion of glucose,

around 24 hours, when the rate increases.

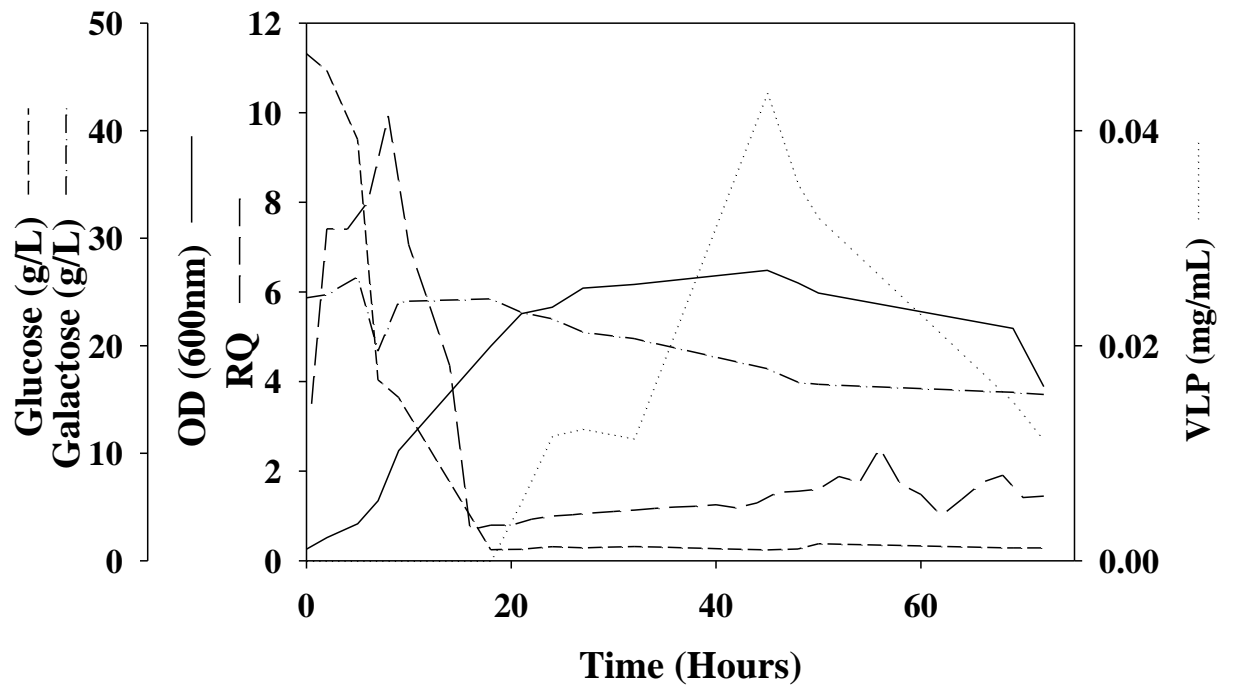


Figure 3-1 Example fermentation data for the production of the VLP in the 75L fermenter.

3.3.1.2 20L fermentations

Some fermentations were carried out in a 20L fermenter as the 75L was not available. The media components remained at the same concentrations, including glucose and galactose. The OD reached a higher value in the smaller fermenter (Figure 3-2), perhaps due to higher oxygen transfer rates or better mixing. The VLP production level was similar from both fermenters

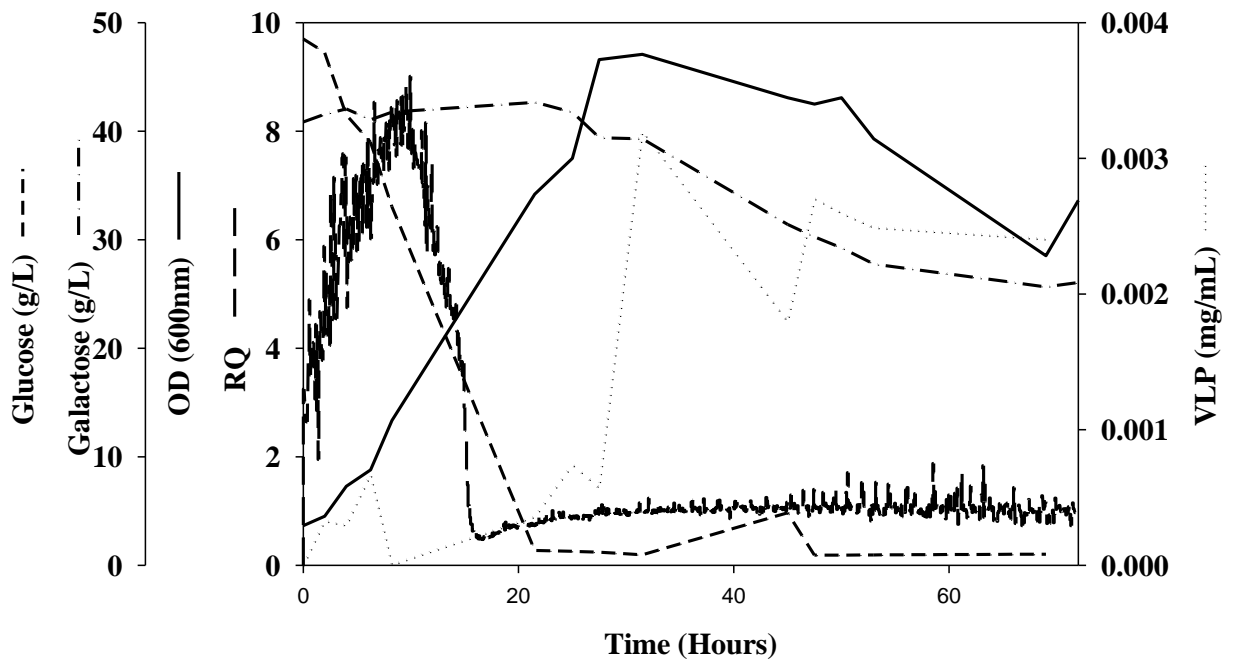


Figure 3-2 Example fermentation data for VLP production in the 20L fermenter.

3.3.2 Change of yeast extract and effect on VLP production

Due to the nature of fermentations batch to batch variation can occur and this can then have a knock on result on the downstream processing steps. To prevent this it was decided to produce a large batch of material using the 450L pilot scale fermenter. With a working volume of 300L it would have produced enough material for the entire project timescale. A new batch of yeast extract was purchased along with all the amino acids and sugars needed. The seed steps were carried out in shake flasks and 75L fermenter to achieve a 10% inoculum volume for the 450L.

The shake flasks and 75L fermenter grew as expected and the 450L fermenter was inoculated from the 75L at 22 hours growth. From the fermentation graph it can be seen that the OD and glucose use is slower than expected and the glucose does not become depleted, as usual (*Figure 3-3*). Foaming occurred at 30 hours whereas normally there is no foaming at all and therefore no antifoam was connected. When sampled at 71 hours the sample showed the fermenter was contaminated (as seen by the sharp increase in OD on *Figure 3-3*).

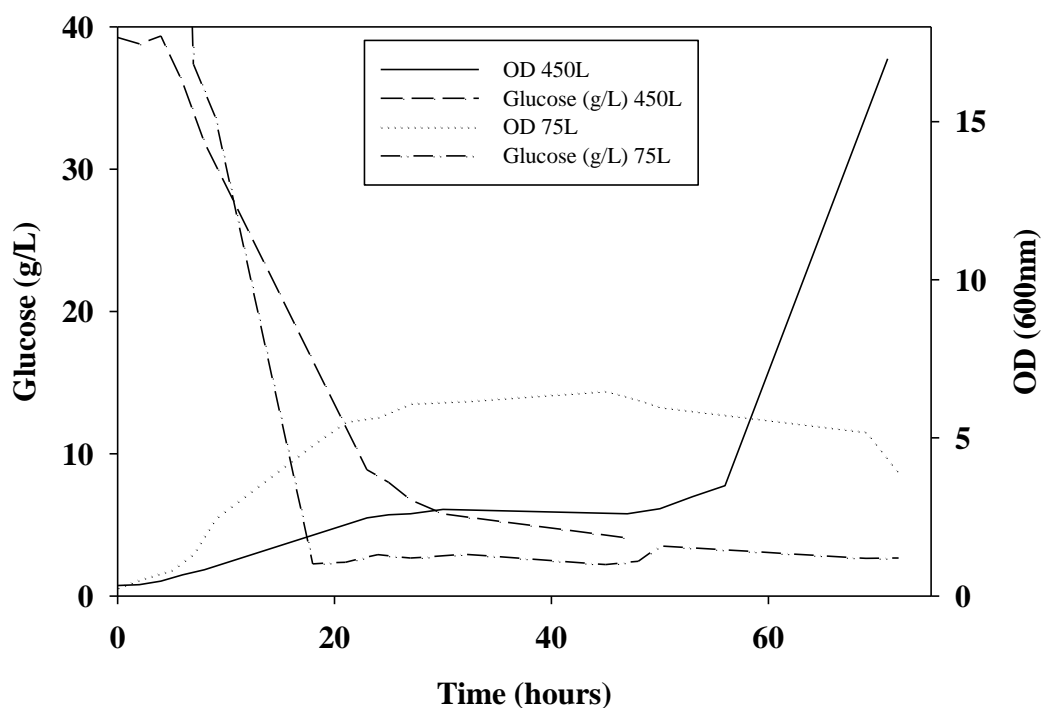


Figure 3-3 Fermentation data for OD and glucose in the 450L fermenter.

Further fermentations in the 75L showed the same growth pattern until the addition of some general yeast extract restarted the growth. This indicated that the yeast extract used in the media was limiting the growth of the yeast. To test this theory yeast extract was purchased from a different supplier and in this case the yeast extract was switched from Sigma-Aldrich to BD Difco.

Comparing the two yeast extracts in shake flasks over 72 hours, the BD Difco media showed higher growth and full consumption of glucose (*Figure 3-4*). With the addition of galactose the BD Difco media showed production of VLP, while the Sigma-Aldrich media only produced about 10% of the VLP amount made by the BD Difco media (*Figure 3-5*). Due to the results seen in the comparison study BD Difco media was subsequently used in any further fermentations.

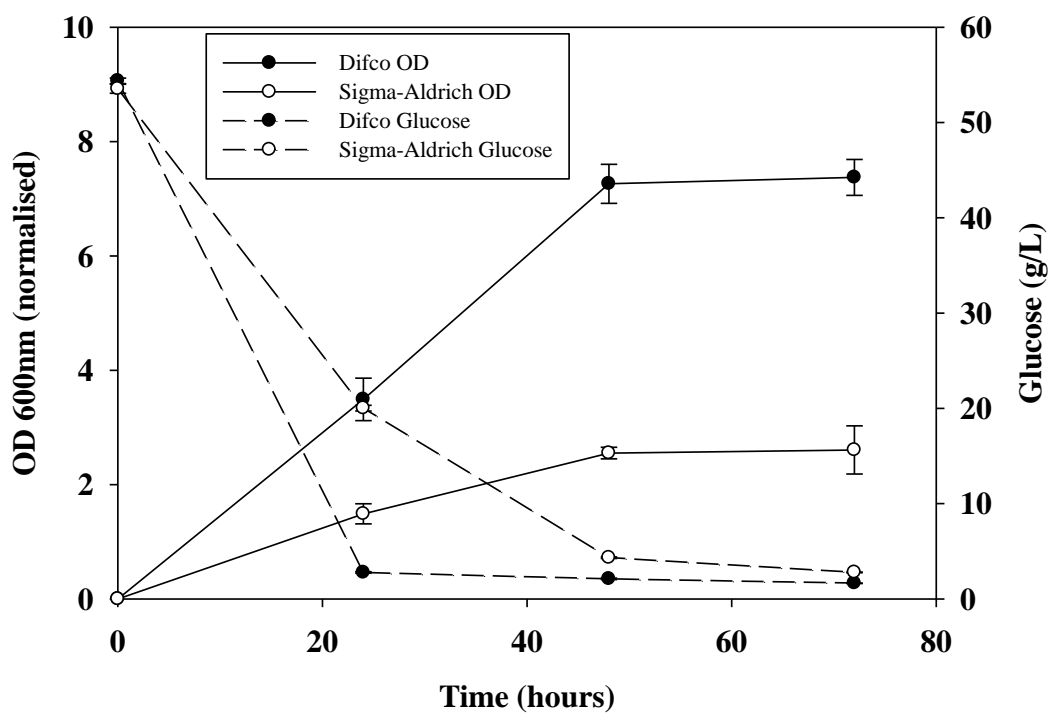


Figure 3-4 Comparison of OD and glucose consumption in shake flasks with either Sigma-Aldrich (●) or BD Difco media (○) (n=3).

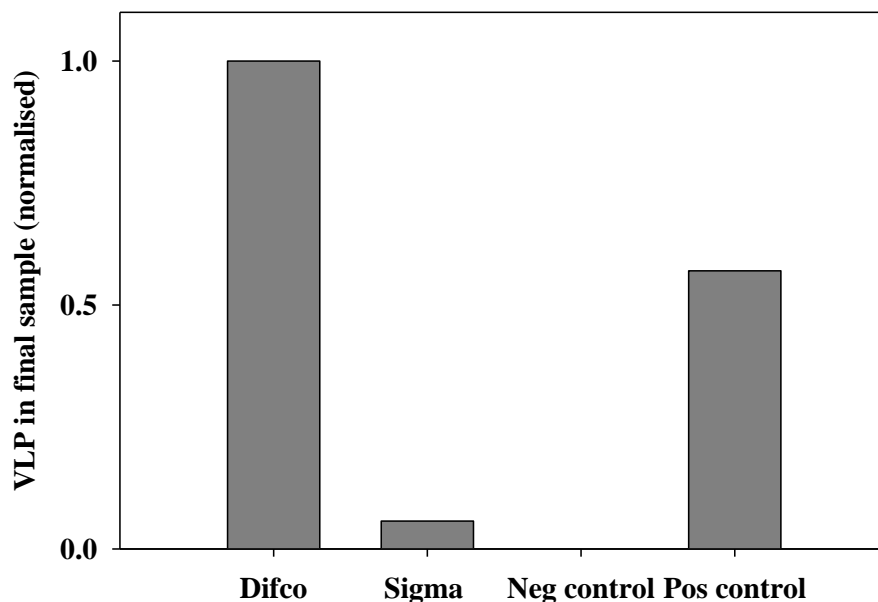


Figure 3-5 Comparison of VLP production by yeast extract supplier. The negative and positive control samples were purchased as part of the ELISA kit.

3.3.3 Primary Purification

Primary purification steps involve the homogenisation of the yeast cells and the use of detergent to remove the VLP from the endoplasmic reticulum (ER). The issue with this is that the detergent also removes other material on the ER, in particular lipids, and contributes to the amount of contaminants in the crude feed. The purification process must ensure that the maximum amount of VLP is recovered but that it does not have an effect on the VLP and/or promote aggregation. The three main variables thought to be important in the detergent step are:

1. Type of detergent
2. Temperature during extraction
3. Time of extraction step.

These were investigated to ensure that the step is optimised to ensure a high yield of VLP is obtained from the ER.

3.3.3.1 *Effect of detergent in primary purification*

Triton X-100 has been shown to be an effective detergent to remove the VLP from the ER (Kee et al., 2008). Other detergents chosen to compare were Tween 20 (polysorbate 20), CHAPS and glycol butyl ether. The amount of VLP removed from the ER by the detergents was compared against a control sample with no detergent (*Figure 3-6*). The sample with no detergent had a very low amount of VLP, showing that detergent is needed to remove the VLP from the homogenate material. Triton showed that it was most effective at 20°C, with the yield of VLP reduced at 50°C. Tween 20 presented a near 100% recovery of VLP at 50°C for over 2 hours, but the level was similar to triton at 20°C after 4 hours. It is possible that this is a false result as follow up experiments did not confirm the high level. Therefore triton was chosen to remain as the detergent of use in the purification process, although it possibly might also have a high recovery for impurities as well as the VLP.

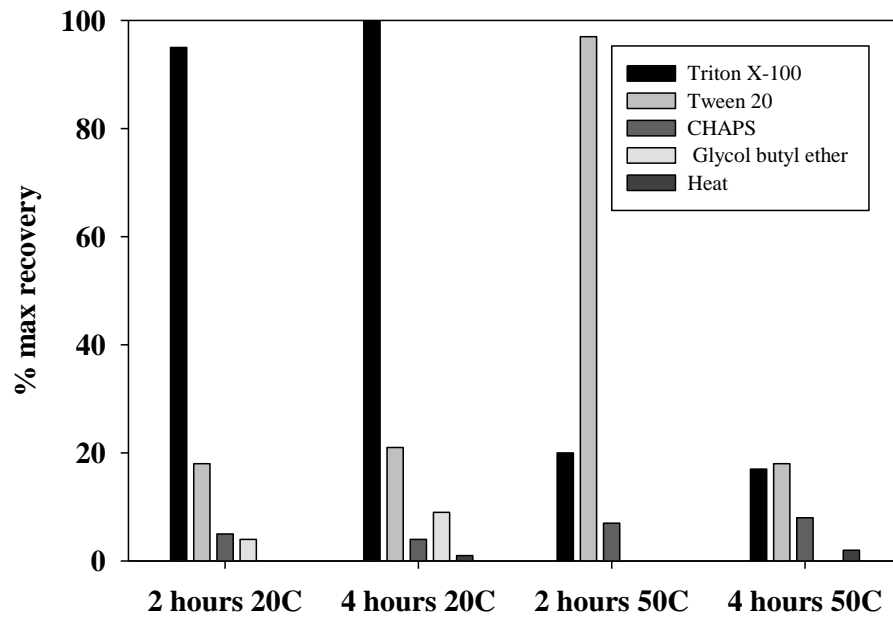


Figure 3-6 Comparison of VLP recovery between different detergents and heat (no detergent). The recovery was compared at 2 and 4 hours, at 20°C and 50°C. The XAD-4 was carried out at 20°C for all samples.

Figure 3-6 shows that the temperature of the extraction step could affect the effectiveness of the detergent to remove the VLP and contaminants. Figure 3-7 shows the effect of temperature on the DLS results using triton as a detergent. The DLS shows the size distribution of the sample (for more information see Section 3.3.10). At the lower temperatures most of the material is around 100nm, whereas the size reduces to 10nm at 50°C. Neither of the samples shows any material at 20nm-30nm (size of the VLP) but it is assumed that large impurities block out the VLP. This supports the ELISA results in indicating that the VLP is altered by the heat, either it is destroyed or does not maintain its antigenic structure.

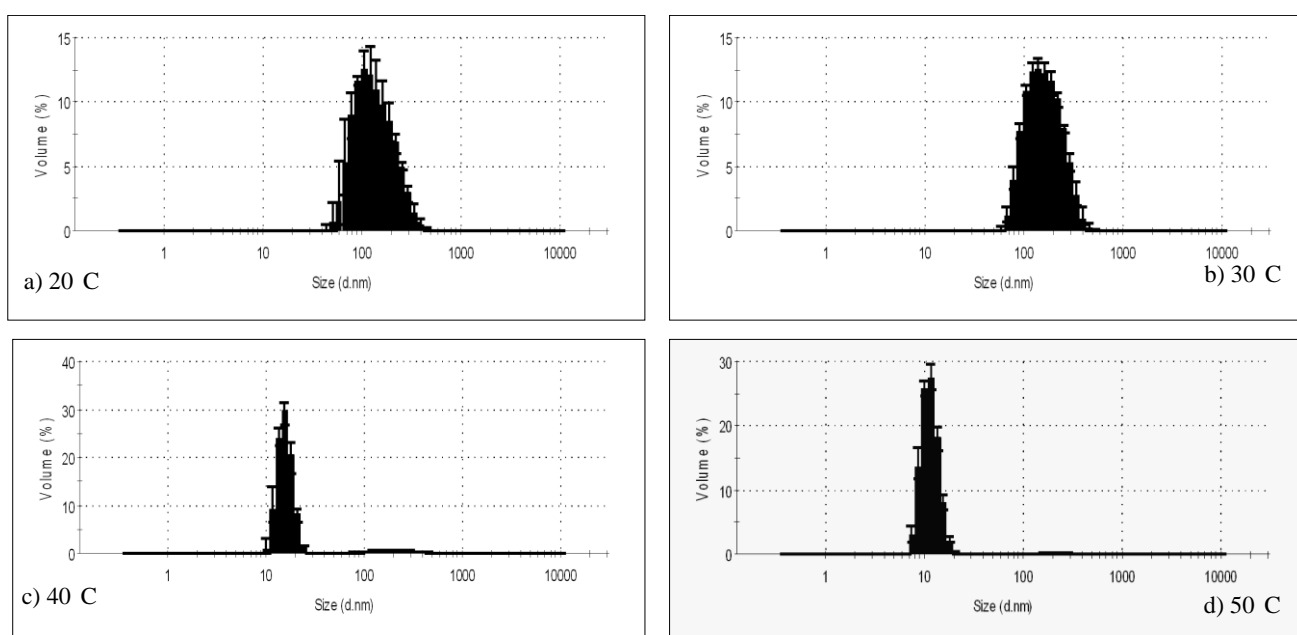


Figure 3-7 DLS results from extraction steps using Triton X-100 at 20°C to 50°C.

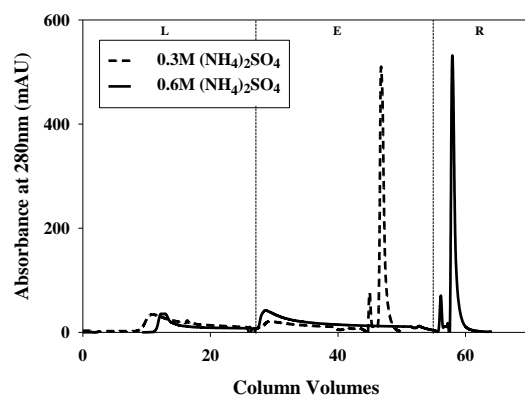
3.3.4 Selection of monolith chemistry for VLP separation

The current chromatographic method of VLP separation uses a weak hydrophobic column (Belew et al., 1991). The purification process was transferred to a 1mL poly (butyl methacrylate-co-ethylene diamethacrylate) monolith chromatography column. Three commercially available columns from BIA Separations were tested; a high density C4 column, low density C4 column and hydroxyl (OH) column. A prototype column was selected as well, which had 50% C4 butyl and 50% OH ligands. Initial scoping work on the columns was carried out using purified VLP, obtained by passing the crude VLP feed through a Butyl-S 6 Sepharose FF column, using a known chromatography process (Jin et al., 2010). The elution fraction, containing the VLP from the column, was loaded on to the monoliths with a mobile phase containing 0.6M or 0.3M ammonium sulphate. If the elution peak was smaller than the peak for the regeneration step then this was an indication that the VLP had bound too tightly to the column and was only being removed using isopropanol in the regeneration buffer. The isopropanol renders the VLP unusable and so the amount of VLP lost to this fraction must be minimised. The salt levels were tested at two points as reducing the amount of salt in the loading

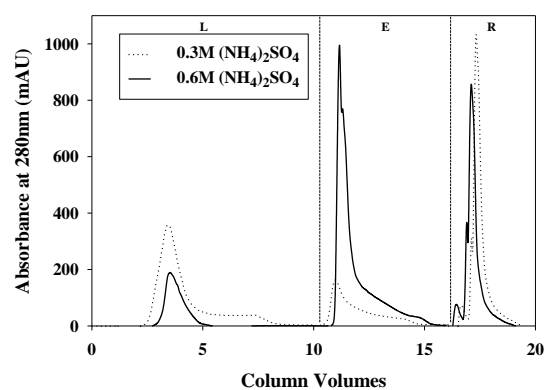
buffer decreases the binding affinity of the VLP to the column which could help to reduce the VLP being lost in the regeneration step.

The three columns with the C4 ligands proved to be unsuitable for the purification of the VLP (*Figure 3-8*). The reduction in the ligand density from high (*Figure 3-8a*) to low (*Figure 3-8b*) did result in an increased amount of VLP eluted from the column but recovery was only increased to around 45% (see *Table 3-1*), with most VLP was removed from the column in the regeneration step. Reducing the salt level to 0.3M resulted in a lower amount of VLP, possibly as the low salt did not promote sufficiently strong binding. The prototype column using 50% C4 ligands with 50% OH ligands should theoretically have had the lowest hydrophobicity of the three columns with C4 ligands but it was evident during use that it still retained high hydrophobic properties.

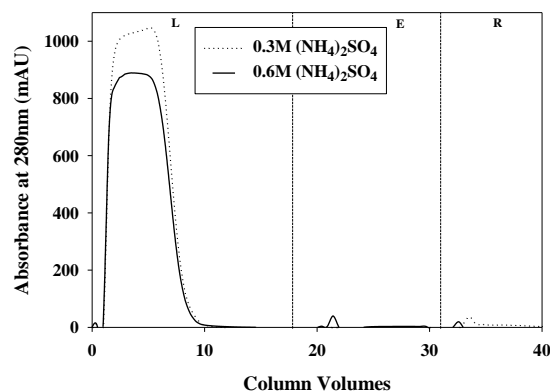
The only column to perform the purification effectively, with recoveries around 85% was the OH column (*Figure 3-8d*), which is comparable to the Butyl-S 6 Sepharose FF column (*Figure 3-8e*). This column has a weak hydrophobic ligand. The salt level was only run at 0.6M on the OH monolith as it was felt that using 0.3M would not produce any significant result.



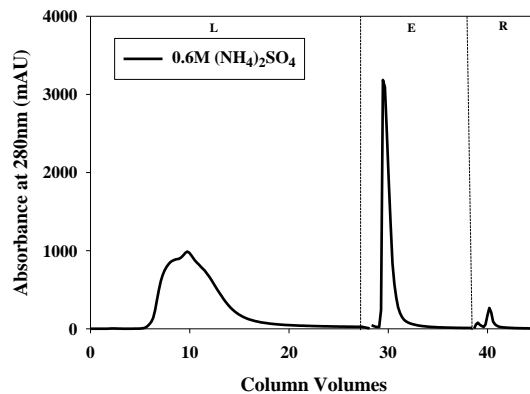
A



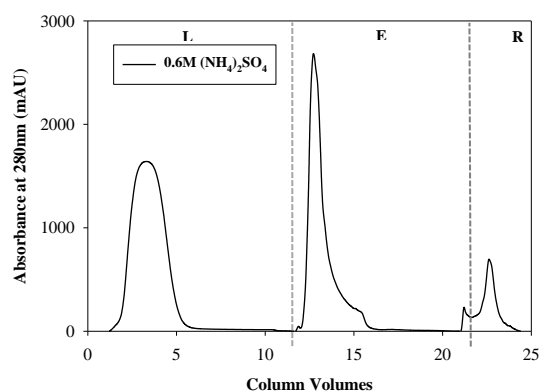
B



C



D



E

Figure 3-8 Chromatograms obtained during screening for a suitable monolith column ligand with post-hydrophobic interaction chromatography material. Material was loaded on to C4 and OH column at 0.6M $(\text{NH}_4)_2\text{SO}_4$ and 0.3M $(\text{NH}_4)_2\text{SO}_4$ to adjust binding affinities within in the column. Absorbance profiles at 280nm are shown with peaks marked out for (L) Loading Zone; (E) Elution Zone and (R) Regeneration. Graphs correspond to (A) High ligand density (HLD) C4 1mL monolith columns, (B) Low ligand density (LLD) C4 disks, (C) 50% C4 and 50% OH 1mL monolith columns, (D) OH 1mL monolith columns. Columns A/B/D are commercially available. Column C was a gift from BIA Separations.

Column type	0.6M (NH₄)₂SO₄ Recovery of VLP (%)	0.3M (NH₄)₂SO₄ Recovery of VLP (%)
High ligand density C4	2 - 5	1 - 3
Low ligand density C4	40 - 50	20 - 23
50% C4 and 50% OH ligands	0 - 1	0 - 1
Hydroxyl ligands	85	-
Butyl-S Sepharose 6 FF[24]	90	-

Table 3-1 The recovery levels of VLP from each of the five columns tested at the two salt levels of 0.6M and 0.3M ammonium sulphate.

3.3.5 Determination of salt concentration in mobile phase

Hydrophobic interaction chromatography is driven by the addition of salt in the mobile phase, so changes to the salt concentration can have a great effect on the binding affinity on the column. The initial process used 0.6M ammonium sulphate but the level of salt in the mobile phase buffer was increased in increments to 1.2M.

Chromatograms of the different runs show that the flow-through peak is reduced as the salt level increases, indicating that more material is bound to the monolith (*Figure 3-9*). The elution peak also increases with the salt concentration, but the regeneration peak remains the same. The regeneration peak includes irreversibly bound VLP and proteins, and the lack of change over the various salt concentrations would indicate that the increase in salt does not promote any additional irreversible binding to the column. Breakthrough curves show that more VLP binds as the salt concentrations in the mobile phase is increases (*Figure 3-10*).

Figure 3-11 shows that over the increased salt concentration the amount of VLP and protein also increases. The protein increase is more substantial than the VLP increase. There is limited difference in VLP elution concentration between the runs using 1.0M and 1.2M ammonium sulphate in the mobile phase. As the amount of protein increases the purity of the elution material is decreased. Subsequent steps

in the purification process would then be used to remove any protein impurities. The use of 1.0M ammonium sulphate was accessed to be the best salt level for the process and will be used for all future studies.

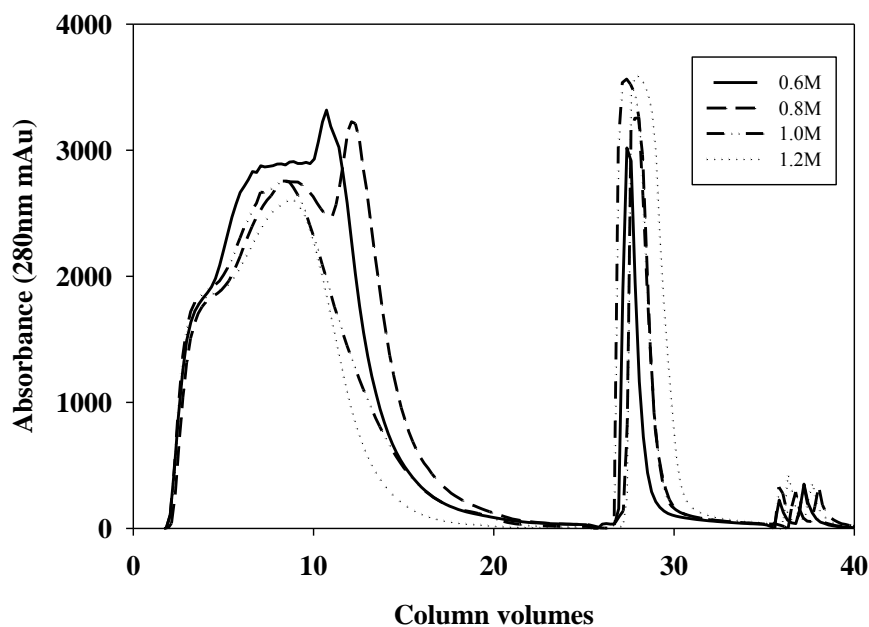


Figure 3-9 Chromatograms of monolith runs with mobile phase of 0.6M to 1.2M ammonium sulphate. The first peak corresponds to binding, the second to elution and third to the regeneration step.

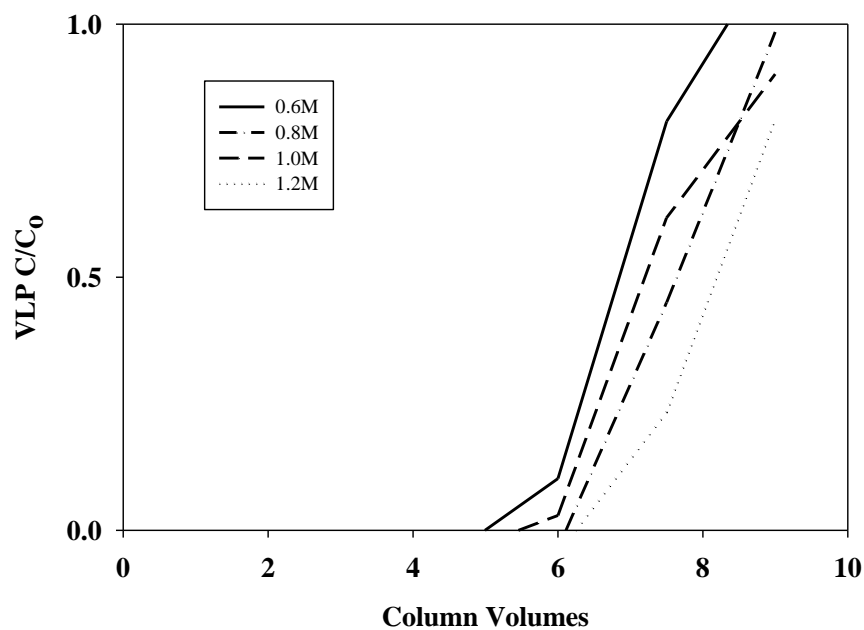


Figure 3-10 Breakthrough curves for VLP binding to an OH monolith at 0.6M to 1.2M ammonium sulphate.

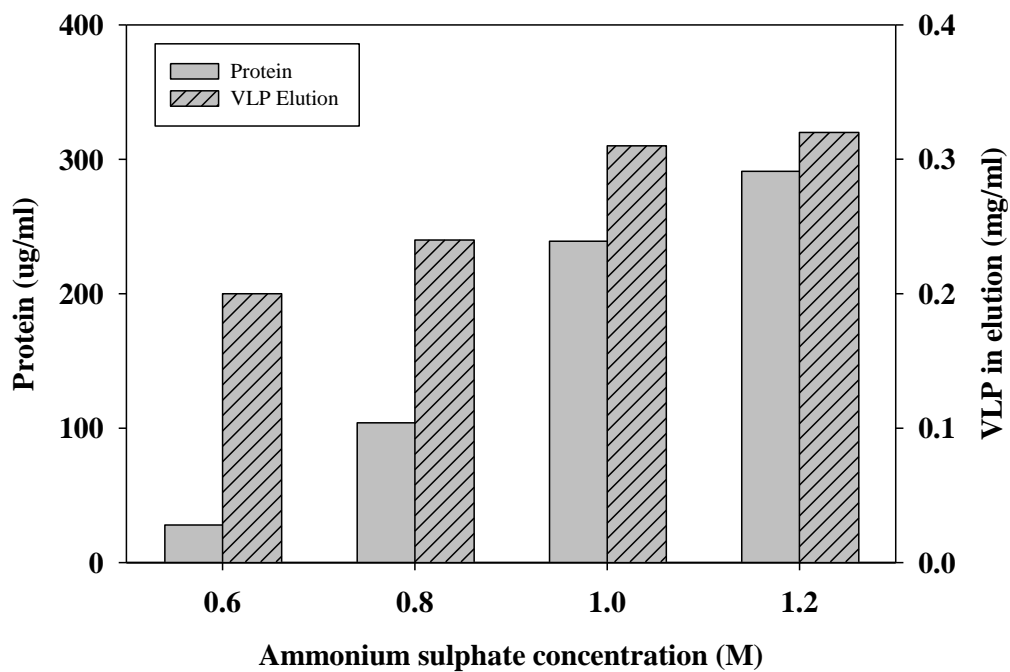


Figure 3-11 Comparison of VLP and protein levels in elution samples over increasing salt levels in the mobile phase buffer.

3.3.6 Dynamic binding capacity of CIM 1mL OH columns

The DBC study was using crude yeast homogenate. The column was overloaded with material to ensure that the completely filled with VLP. The 10% breakthrough point for the VLP on the column is around 4CV as seen on *Figure 3-12*.

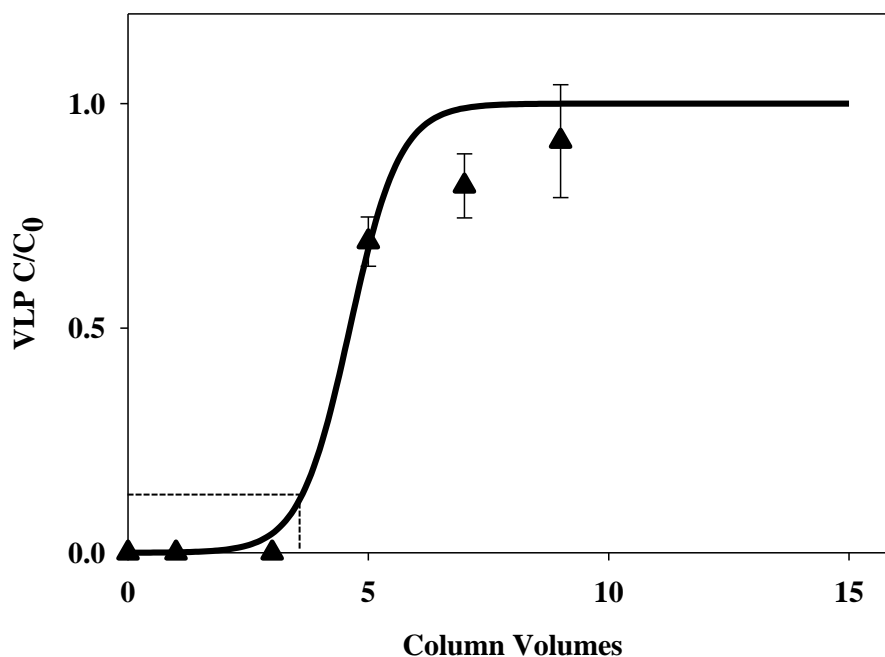


Figure 3-12 Breakthrough curve for crude feed at 1.0M ammonium sulphate on an OH monolith. (n=3). 10% breakthrough is indicated by the dotted line. (Please see Section 9 Figure 9-1 for raw VLP data)

When the breakthrough curve was analysed by ELISA it can be seen that two separate breakthrough peaks appear (*Figure 3-13*). The first peak reached $C/C_0=1$ after approximately 10 ml of material had flowed through, indicating that the column had reached capacity and no more VLP was binding. Then the amount of VLP coming out of the columns drops to 0, and another peak appears. This occurs over all 3 runs. As the material contains lipid it is probable that during the initial part of loading lipid is deposited on the column and secondary binding occurs onto either the column or other bound material, i.e. VLP. To prevent this no more than 10mL of crude feed should be loaded on to the column.

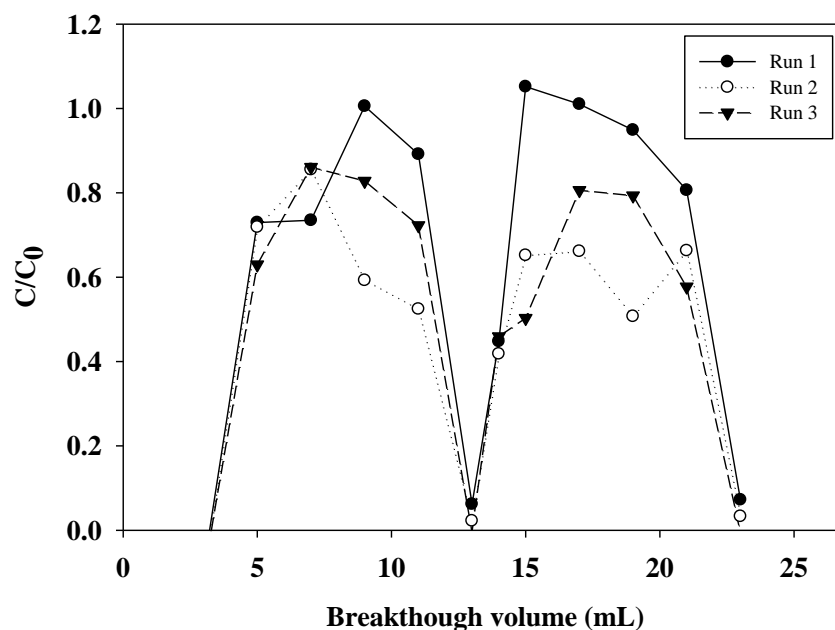


Figure 3-13 Breakthrough curves using 25mL of crude feed material over 3 consecutive run on a new column. The amount of VLP was monitored using ELISA. (Please see Section 9 Figure 9-2 for raw VLP data)

3.3.7 Comparison of monoliths and conventional resin chromatography

The characteristics of a monolith are designed as an improved medium over resin beads for the purification of nanoplex molecules. To determine the additional dynamic binding capacity of the OH monolith the breakthrough curve was compared to a conventional resin butyl-S column using the same feed material.

Figure 3-14 shows that the 10% breakthrough on the Butyl-S column was at approximately 1.5CV, whereas with the monolith it was at approximately 4CV. Both columns show recovery of the VLP around 85-90%. In total the monolith has a three to four times greater binding capacity for the VLP than the conventional resin.

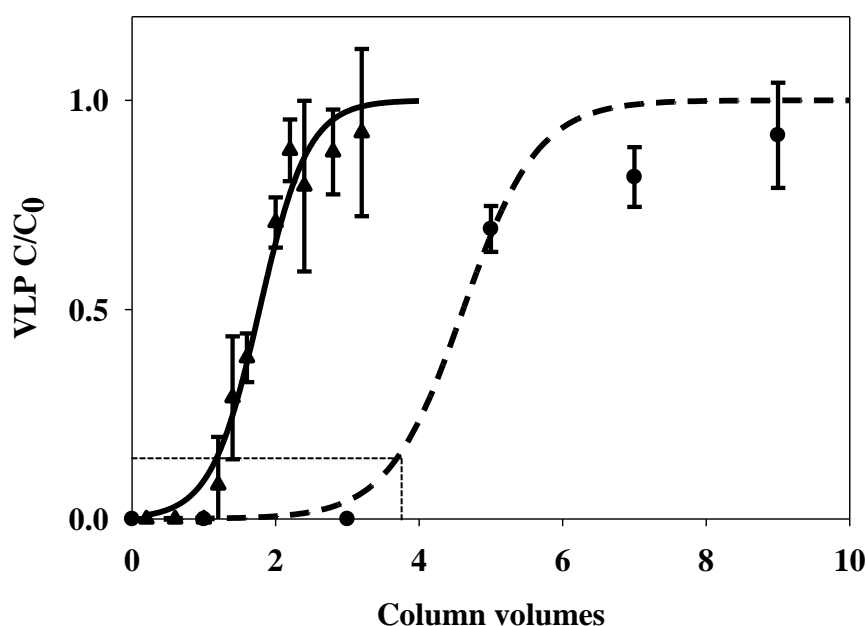


Figure 3-14 Comparison of dynamic binding capacity of butyl-S Sepharose 6 FF 1mL HiTrap column (▲) and a monolith OH 1mL column (●). 10% breakthrough is indicated by the dotted line. The columns were loaded with untreated homogenised yeast and the VLP breakthrough was monitored using ELISA. ($n=2$ for butyl-S column and $n=3$ for OH monolith. Error bars are 1 S.D.) (Please see Section 9 Figure 9-3 for raw VLP data)

3.3.8 Comparison of standard and large pore CIM 1mL monoliths

The pores of the monolith are produced during the production process and so therefore can be adjusted accordingly. A large pore monolith was compared to the standard monolith to see if the pore diameter would affect the binding capacity. The standard pore size of a monolith is 600-700nm, whereas the large pore monolith has a pore size around 6 μ m. Using crude feed 3 consecutive sample runs were loaded on the column (Figure 3-15). The results show an earlier breakthrough on the column and a lower yield. The breakthrough is also much steeper, indicating limited adsorption reactions on the column. Recovery was around 60%, although due to the low value it is possible that the final recovery level is higher as the amount of VLP may not have been within the suitable range for the test. This can be seen due to the large error bars.

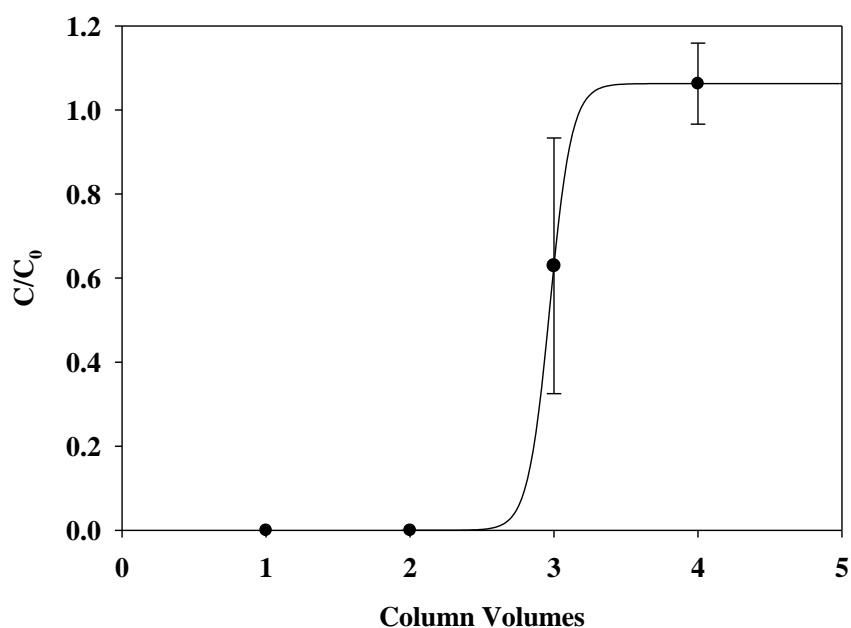


Figure 3-15 Breakthrough curve of VLP on a large pore OH monolith, analysed by ELISA. ($n=3$). (Please see Section 9 Figure 9-4 for raw VLP data).

3.3.9 Topography of HBsAg particle

Post-monolith samples were examined under electron microscopy (TEM) and atomic force microscopy (AFM) to investigate the topography of the VLP (Figure 3-16). The elution buffer was exchanged for low salt buffers to ensure no salt interference during the techniques. It is assumed the buffers will have no effect on the particle. Both techniques show a majority of circular VLP particles and a few larger unknown masses. The VLP was found to be around 30-35nm under TEM and around 25-30nm with AFM. These differences in size may be due to the different techniques used to capture the VLP onto the sampling surface. The TEM sample was dried onto the carbon grid and resulted in the VLP being condensed together, whereas AFM involved capture onto a hydrophobic surface and fixation by glutaraldehyde. It is unknown what effects they have on the structure of the VLP. Both methods indicate that most of the VLP is in monomeric form, although no distinct topography can be seen on individual particles. The sizes of the particles correlate to that in the literature (Milhiet et al., 2011).

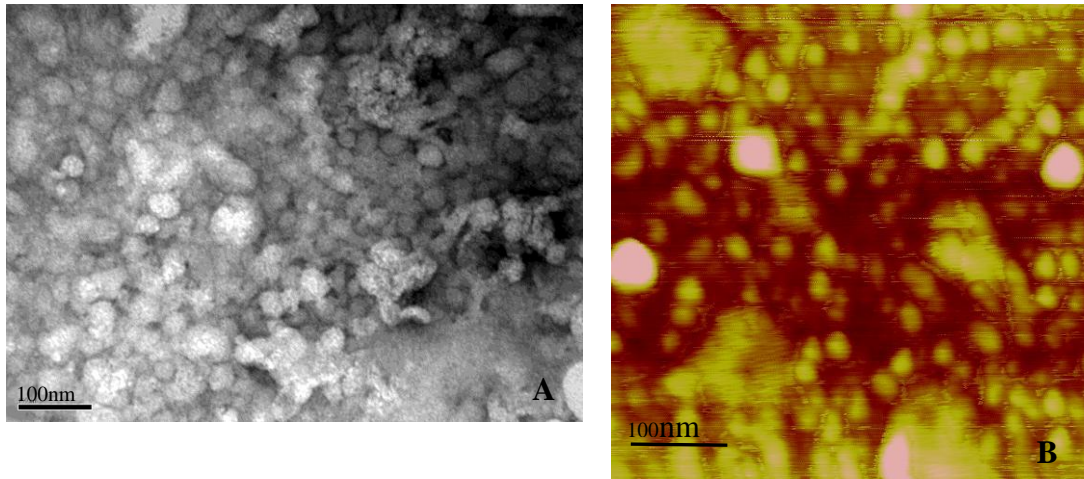


Figure 3-16 Pictures of HBsAg from elution samples after hydrophobic interaction chromatography using an OH monolith. The black bar is equal to 100nm on both pictures. A) Transmission electron microscope (TEM). Samples were negatively stained with 2% uranyl acetate on carbon grid. B) Atomic force microscopy picture (AFM). Samples were adhered to a silanised glass slide. AFM was in tapping mode.

3.3.10 Analysis of VLP using dynamic light scattering

There are limited methods to analyse the size of particles, especially something as large as a VLP. Dynamic light scattering can be used but will give a size distribution of all particles in the sample. It is quick and easy to use and does not affect the sample, i.e. the sample can be retained afterwards and stored, which is especially important if there is limited amounts available. The sample may require dilution if the concentration is high, but most of the samples used did not require any dilution.

But looking at the results from samples taken either before or after the chromatography step it became apparent that DLS does not show the VLP as an individual peak. Often there is only one peak around 100nm (*Figure 3-17*). As the VLP level in the samples is low, compared to the amount of proteins or other impurities, the other particles seem to prevent detection of the VLP. It may also indicate that the VLP temporarily exists as dimers or larger, although this has not been proved. This means that DLS is not ideal to look at aggregation of the VLP, unless the sample is a lot purer. It can be used to look at the amount of particles in

the sample (both VLP and impurities) as it gives an indication of the amount of particles through the attenuator level.

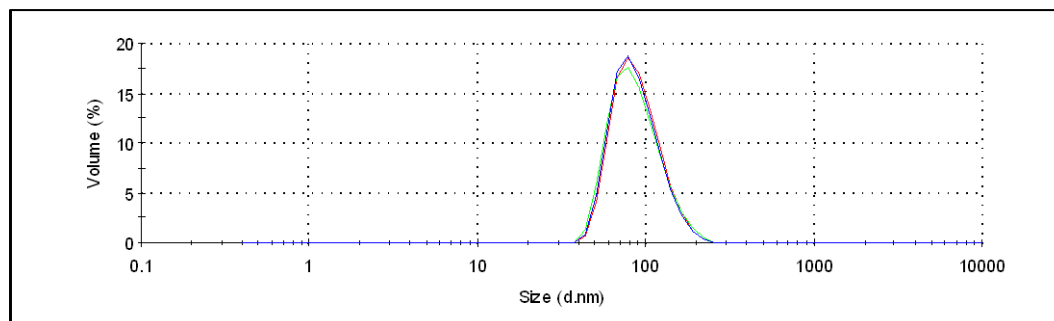


Figure 3-17 An example DLS size graph on a post-chromatography sample. Size distribution is by volume ($n=3$).

3.3.11 Analysis of VLP using Zeta potential

Zeta potential is affected by pH and ionic strength, which are two factors which can also influence the binding affinity of the VLP on the HIC monolith. Using the Malvern Zetasizer ZS, with the addition of an autotitrator, a range of pH and salt concentrations could be tested.

Initial work focused on determining the ideal dilution factor for the material, as zeta potential does not require as high as concentration as DLS to produce a result. It soon became apparent that the material was not ideal for producing results *Figure 3-18*. From the DLS results it can be seen that there are other materials in the sample, which would all have individual zeta potentials. The zeta potential distribution was then very broad and it was difficult to determine which peak was the one from the VLP.

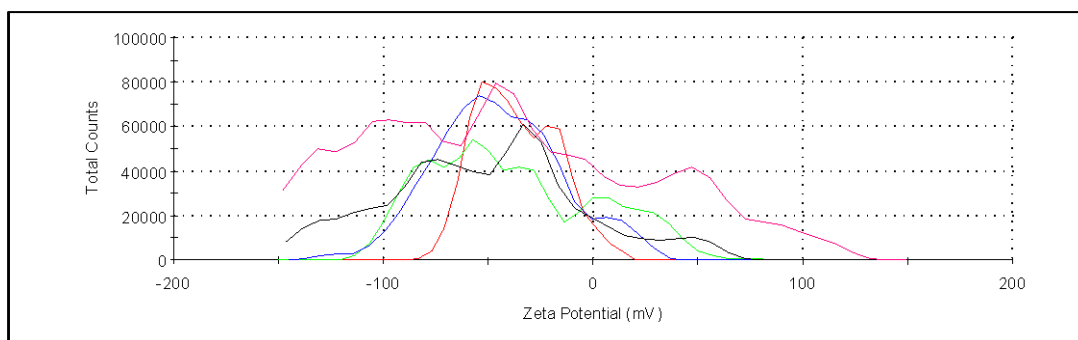


Figure 3-18 Graph showing zeta potential results for five measurements on a VLP sample. The sample was diluted x15 with 10mM Sodium phosphate, pH 7.

Measurement of zeta potential uses an electrical field applied to attract particles in a specially designed flowcell, which in turn determines the electrophoretic mobility. Addition of any salt into a sample before zeta potential measurement will change the conductivity of the sample. The conductivity is ideally kept at a low level of 10 μ S or less, as noted by the manufacturer, so an accurate zeta potential can be determined. Unfortunately the addition of ammonium sulphate significantly increases the conductivity to levels which are not compatible with the equipment. Therefore the salt level was not used above 0.3M and therefore could not show any zeta potential results at salt levels used in the column (*Figure 3-19*).

Using the titrator the zeta potential of the sample from pH 4 to 9 was analysed and it showed that the zeta potential increases as the pH increases (*Figure 3-20*). An increase in zeta potential should make the sample more likely to repel each other and not aggregate. The use of zeta potential with changing pH can indicate the pI of a protein or virus (Trilisky and Lenhoff, 2007). The addition of acid or base into the purified VLP sample showed variable results and did not show any point which could be the pI point.

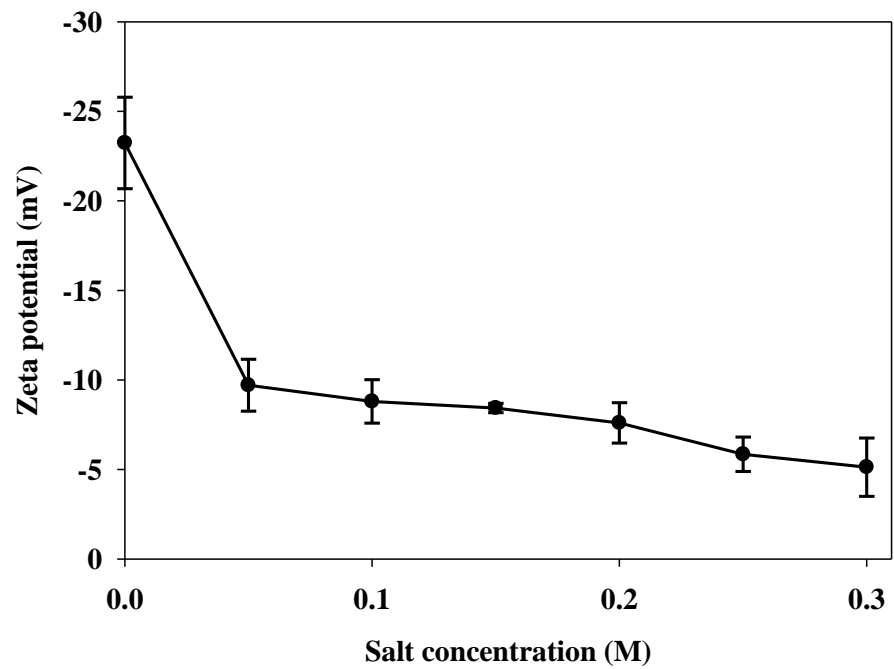


Figure 3-19 Zeta potential results for purified VLP samples over a range of salt concentrations. The samples were diluted with 20mM sodium phosphate pH 7.0 to 7% v/v (n=3).

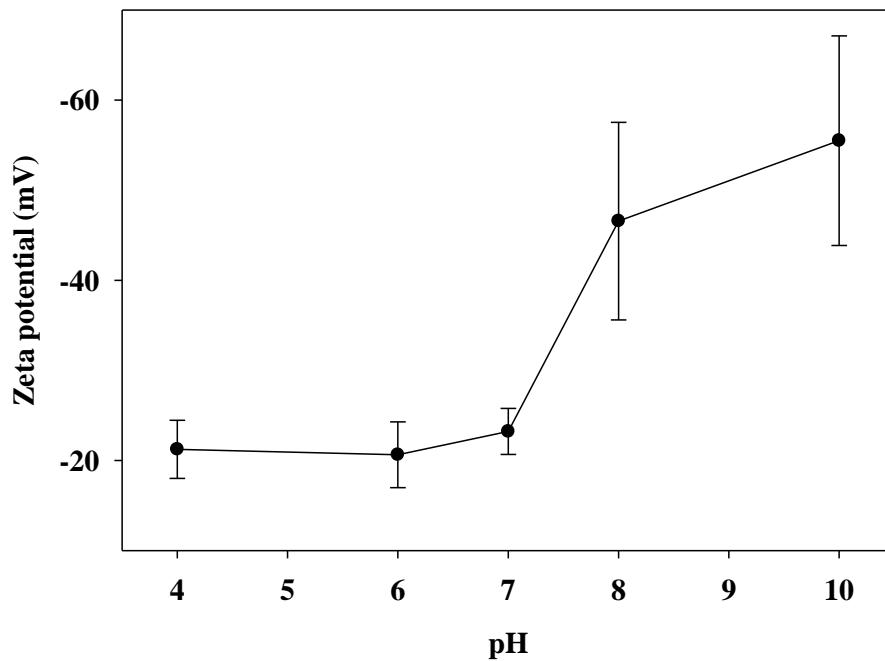


Figure 3-20 Titration graphs showing the zeta potential over a range of pH values from pH 4 to 9. The samples were diluted to 7% v/v (n=3).

3.3.12 Analysis of VLP using Size Exclusion Chromatography

SEC has been used to look at aggregation of HBsAg VLP. The group used a Tosho Bioscience G5000 PWWL size exclusion column, as it had a suitable calibration range and has an exclusion limit of $>1 \times 10^7$ (HBsAg is 3.5×10^6). To calibrate the column a range of protein standards were used (*Table 3-2*). As the VLP standard is expensive a cheaper alternative was substituted in the form of low density lipoprotein (LDL). It is very similar to HBsAg as it is around the same size at 26nm and the same molecular weight at 3.5M Da, so is ideal for use. The only difference is that it contains 22% protein and 78% lipids, whereas HBsAg has 75% protein and 25% lipid.

All the proteins eluted in the correct formation apart from the LDL which eluted later than the carbonic anhydrase (*Figure 3-21*). This is unexpected as large particles should elute before smaller particles. The literature for the column stated that if there were any hydrophobic interactions to use the buffer 0.1 mol/l NaNO_3 with 20% ACN. When the LDL was run on the column in this buffer its elution time changed to 16.8 minutes, eluting just before any of the proteins. This indicates that there are some secondary interactions between the column and VLP. Literature on the column stated that it is made from hydroxylated polymethacrylate and is slightly hydrophobic. Therefore it will interact with the VLP and LDL as they are both hydrophobic though the lipids and proteins in each.

Standard	Molecular weight (Daltons)
Carbonic anhydrase	29,000
Albumin	66,000
ADH	150,000
Amylase	200,000
Apoferritin	443,000
Thyroglobulin	669,000
LDL	3,500,000

Table 3-2 Standards used to calibrate the SEC column.

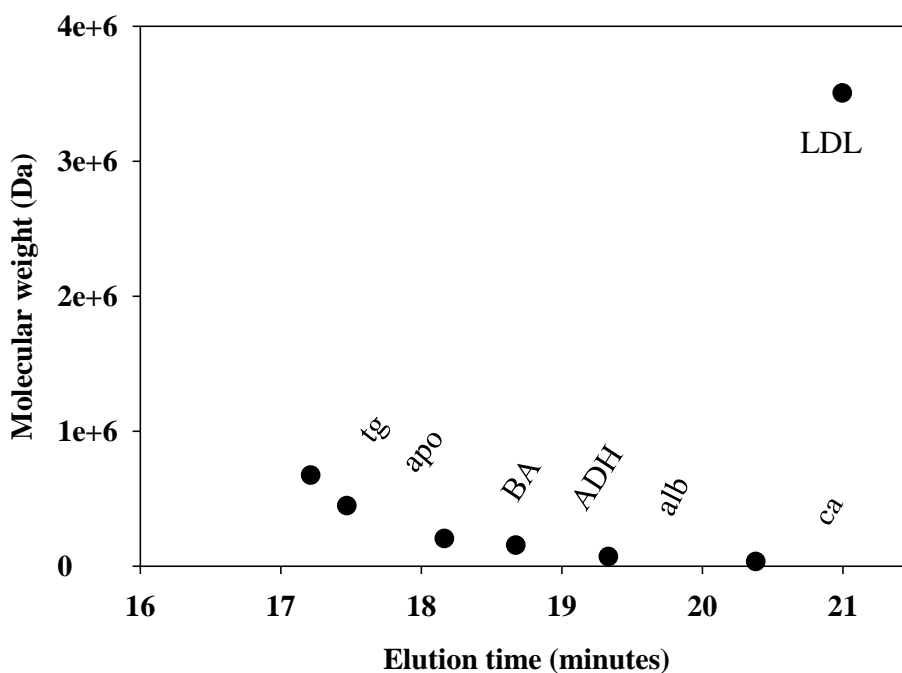


Figure 3-21 Calibration curve for proteins and LDL using PBS as the mobile phase. LDL = low density lipoprotein; tg = thyroglobulin (669 KDa); apo = apoferritin (443 KDa); BA = β -amylase (200 KDa); ADH = ADH (150 KDa); alb = albumin (66 KDa); ca = carbonic anhydrase (29 KDa).

The sample material loaded was very crude and due to the limit amount of VLP in comparison to impurities made it difficult to define where the VLP emerged. A VLP standard run down the column showed a peak at 23 minutes but chromatograms did not necessarily show a peak at the same time (data not shown). Samples were taken on a run between the points of 20 and 30 minutes to try and determine the elution time for the VLP (Figure 3-22). But there was no distinct VLP peak on the ELISA or consistency over where the peaks were seen and therefore it is difficult to know where the VLP will emerge on each run. It increasingly became apparent that the column was not going to be effective for use with the material either pre or post chromatography as the mobile buffer would have to contain a solvent to remove any hydrophobic interactions with the VLP. Therefore this would affect the VLP structure and possibly change any aggregates etc.

Looking at the literature on the use of this column for SEC the samples loaded are pure, enabling easy detection of the VLP peak. Therefore the column was not used for any further work with the crude material as the interactions between the column and material cannot provide any consistent results. If needed for future use the column would be used only for pure VLP samples.

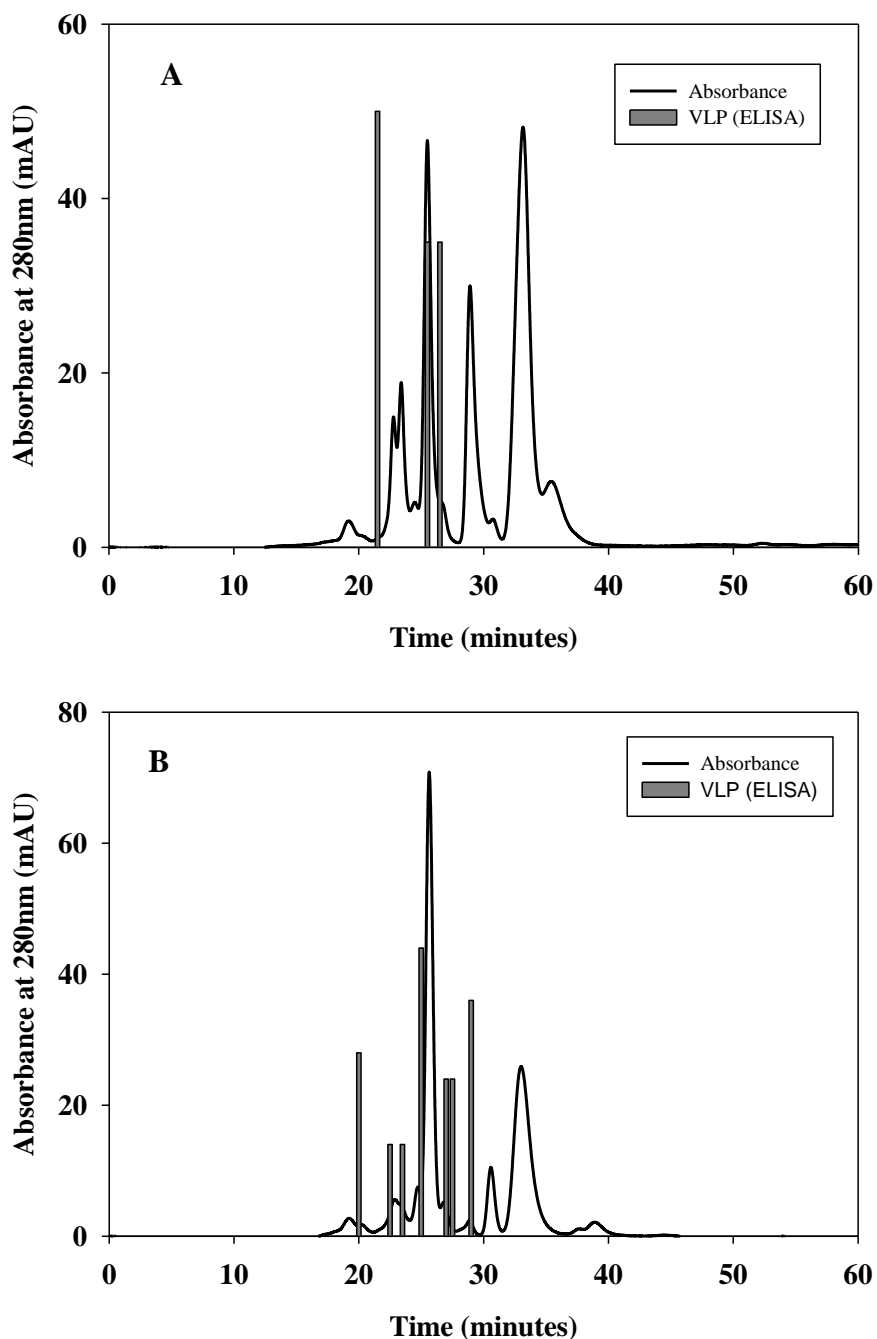


Figure 3-22 Graphs comparing absorbance at 280nm for the size exclusion chromatography and VLP ELISA results from collected samples. (A) 20°C; (B) 30°C.

3.3.13 Analysis of VLP using Bradford or BCA assays – comparison of methods

To determine the purity of the elutant the amount of protein in a sample must be quantitatively measured. Often this can be done using the 280nm trace on a chromatogram, but unfortunately this requires knowledge of the particular protein or proteins being eluted so that the extinction coefficient can be used and a concentration related to an absorbance value. Another easy and effective way of doing this is to use a protein assay. Common assays in use are the Bradford Assay, using Coomassie Brilliant Blue G-250, or the BCA assay, using Bicinchonic Acid. Calibration curves are determined for both using Bovine Serum Albumin (BSA), over a set range.

The Bradford Assay looks at an absorbance shift of Coomassie Brilliant Blue G-250 from 465nm to 595nm. This is carried out on a spectrophotometer, using a microwell plate or cuvettes. The shift occurs when the acidic dye binds to proteins, mainly basic and aromatic amino acid residues, especially arginine (Bio-rad information sheet).

The BCA assay is by colorimetric detection but uses the reduction of Cu^{2+} to Cu^+ . First of all copper is chelated with the protein with three or more amino acid residues, in an alkaline environment containing sodium potassium tartrate (biuret reaction), which forms a coloured chelate complex. The bicinchonic acid is added to the sample, and reacts with the reduced cuprous cation creating a purple coloured reaction of 2 BCA to 1 cuprous ion. There is a strong influence on this assay from cysteine/cysteine, tyrosine and tryptophan amino acids.

Comparing the results of the Bradford Assay to the BCA assay it can be seen in *Figure 3-23* that the assays give very different results for the same sample. Although both assays can be affected by reagents in the sample buffer, this is not the case with these samples. It is unknown why the two assays give very different results, but must arise from the amino acids which the copper or Coomassie blue binds too. Literature tells us that the HBsAg contains cysteine and tryptophan residues in the 'a' antigenic region (Hemling et al., 1988, Mangold and Streeck, 1993, Bruce and Murray, 1995, Greiner et al., 2010) and as such should therefore

react with the BCA assay. It may be possible that these are blocked by non-specific interactions with impurities within the samples.

These results shows that care must be taken when choosing a protein assay for this process as an analytical tool and other methods must be used to verify the results. It also shows that it is difficult to correctly determine the purity of a sample and in reality only trends can be looked at.

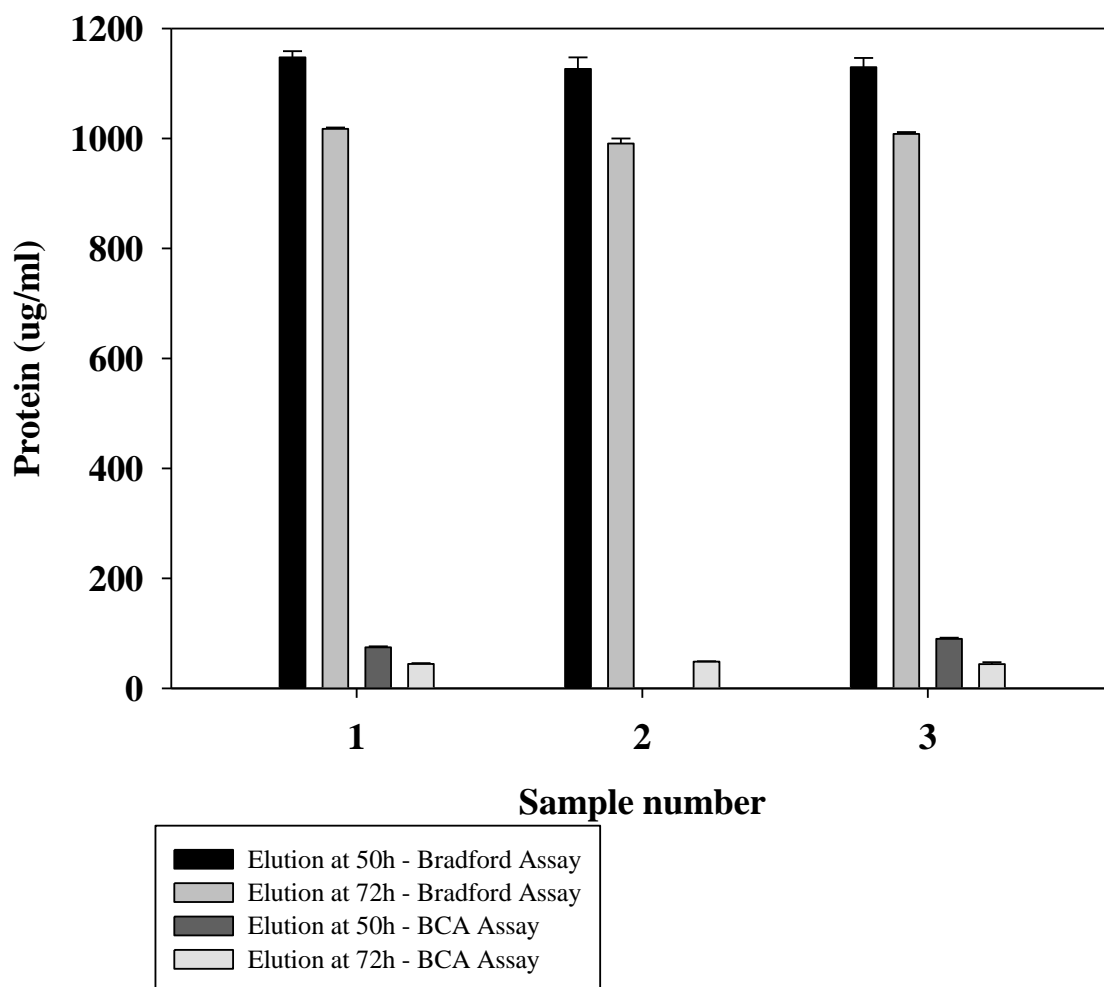


Figure 3-23 Comparison between Bradford Assay and BCA Assay for three elution samples. The box below indicates which sample each column corresponds to. Each sample was analysed in triplicate.

3.4 CONCLUSIONS

Production of the VLP (HBsAg) was possible in both a 75L and 20L fermenter. The production method is not optimised, as shown by greater growth in the 20L fermenter, although the media components were like-for-like with the 75L. The changes from the yeast extract were never understood, even with the issue was looked at by Sigma-Aldrich.

The use of a detergent is important in the extraction of VLP from attachment from the ER. In comparative tests Triton proved the best detergent as it removed the most VLP from the ER, which is important due to the low levels of VLP produced by the yeast.

It was shown that the VLP can be successfully purified by hydrophobic interaction using a monolith format. The use of a weakly hydrophobic interaction OH ligand gave the best performance. This is due to the highly hydrophobic nature of the VLP which binds too strongly to more hydrophobic chemistries. Analysing the loading of the crude feed material by ELISA showed that the column bound an initial amount of VLP before full loading, but then secondary interactions occurred. This phenomenon indicates that the feed is very crude and other impurities may have an effect on the process. Comparison with the standard Butyl-S resin column indicated that the monolith had a capacity around four times greater.

Examination of the VLP under the electron microscope and by atomic force microscopy showed particles around 25-35nm. The VLP was difficult to examine using DLS and zeta potential due to the feed post-chromatography still containing many contaminants. Size-exclusion chromatography proved difficult due to the range of contaminating proteins that are also present in the material. The concentration of VLP is very low compared to these and due to the hydrophobic nature of the SEC column a good separation was not achievable.

4 PRE-TREATMENT OF A VLP-YEAST HOMOGENATE AND THE EFFECT ON THE CHROMATOGRAPHIC STEP

4.1 INTRODUCTION

The use of crude feeds on chromatography columns can cause problems of fouling from various impurities such as lipids, proteins and DNA. As the VLP is produced in *Saccharomyces cerevisiae*, which is later homogenised, lipids have proved to be the main foulant in the feed stream. Lipids are used by the yeast for energy storage, with the majority of them being Triacylglyceride (TAG) (Sorger and Daum, 2003). They are stored within the endoplasmic reticulum (ER), the same place where the VLP is made (Huovila et al., 1992, Patzer et al., 1986, Simon et al., 1988). The purification process uses detergents to remove the VLP from the ER. The addition of detergents into lipid mixtures causes micelles to form and aggregates of the detergents and lipids (Lichtenberg et al., 1983).

Fouling has been noted to occur with other chromatographic resins in the presence of material containing a high amount of lipids. Studies on ion-exchange resins show that this can be experienced with cell cultures (Staby et al., 1998), yeast homogenate (Siu et al., 2006a), whole milk (Pampel et al., 2007, Fee and Chand, 2005) or during expanded bed use (Fernandez-Lahore et al., 1999). The application of yeast homogenate on a DEAE-sepharose FF resin decreased in the breakthrough point but surprisingly increased the amount of BSA to bind per run, indicating that the lipid foulant increased the binding area available in the column for BSA. Pampel et al. (2007) noted that when a feed containing a high level of lipids was fed onto a Sepharose SP columns an increase in column backpressure was observed but Fee and Chand (2005) noted they could avoid this by heating the milk feed up to 35°C.

Jin et al. (2010) studied lipid fouling using a homogenised yeast feed and also noted the amount of VLP eluted decreased but the amount of VLP bound per run increased. It is possible that lipid fouling increased the surface area for binding

under hydrophobic conditions. Confocal microscopy on individual beads confirmed that the lipids in the feed bound irreversibly to the beads over consecutive runs by slowly diffusing into the pores. Confocal microscopy is a useful tool to look at the position of foulants which can be fluorescently labelled. A number of labelled foulants and proteins can be applied to the beads, as each is excited at different wavelengths. Using an *E.coli* feed and labelling the foulant host cell proteins and DNA Siu et al. (2006b) showed that BSA was unable to penetrate into the beads when fouling occurred, and subsequently the binding capacity was reduced.

Pre-treatment of the crude feed before the chromatography column could help to reduce the amount of lipids. The amount of lipid reduction can be measured by evaporative light scattering detection, combined with normal phase HPLC (Jin et al., 2010, Narvaez-Rivas et al., 2011). Lipid removal methods have been used as pre-chromatographic steps for transgenic proteins in milk, including centrifugation, filtration and precipitation using salts, acids and polyethylene glycol (Nikolov and Woodard, 2004). Bracewell et al. (2008) showed that centrifugation with ammonium sulphate and filtration methods were able to remove lipids from a yeast homogenate and increase the capacity of a HIC column to ADH.

In this chapter the effect of lipids in the crude feed on the chromatographic separation of the VLP was studied. Using confocal microscopy the degree and placement of fouling in the monolith from the lipids was studied. A number of lipid removal methods were accessed to determine which method would remove lipid but ensure maximum VLP yield. Using the chosen method the effect of the lipid removal was studied on both the monolith and the conventional resin columns.

4.2 MATERIALS AND METHODS

The VLP yeast material used in this section was produced by fermentation (**Section 2.2**) and primary purification steps were conducted as per **Section 2.3**. Chromatography experiments were conducted on the monolith (**Section 2.5**) and on a conventional Butyl-S resin column (**Section 2.4**). Confocal experiments to visualise the lipid fouling were undertaken at UCL using the method stated in **Section 2.6**. Four different lipid removal methods were tested to determine the ideal method (**Section 2.7**) and the amount of lipid and VLP were analysed using a lipid quantification method (**Section 2.11.7**) and an ELISA assay (**Section 2.11.4**). The material from the loading, elution and flow through were analysed using SDS-PAGE (**Section 2.11.9**).

4.3 RESULTS AND DISCUSSION

4.3.1 Effect of lipid fouling on monoliths

The effect of lipid fouling on a monolith can be seen when consecutive loads are pass through the column. The pressures over both the loading phase and the elution phase both show incremental increases after a number of runs. The column is regenerated after each elution by 30% isopropanol to remove hydrophobic material and the cleaning (CIP) is carried out with 1M NaOH. The use of isopropanol is often recommended by column manufacturers for the removal of lipids. The pressure increase over then runs using crude feed can be seen in *Figure 4-1*.

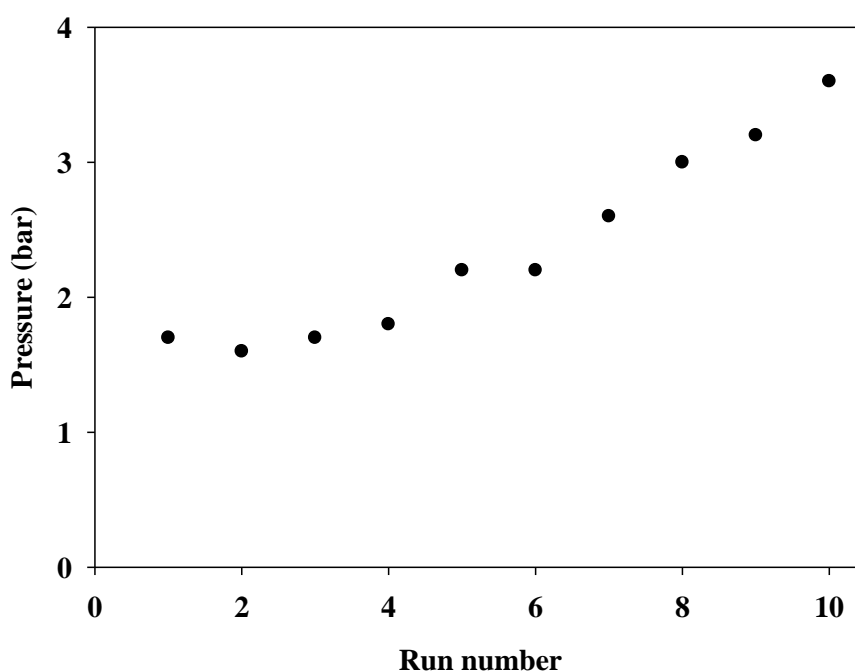


Figure 4-1 Pressure increases over 10 consecutive runs during loading. The column is a 1mL OH monolith column run with a crude feed at 1.0M ammonium sulphate.

Although the monolith can deal with pressures up to 20 bar, the increase on pressures and the notably fouling can result in a reduce life span of the column.

4.3.2 Visualisation of lipid fouling on monoliths

Previous research on resin beads showed that lipids in the crude feed would bind irreversibly to the beads and were not removed by the regeneration or CIP steps (Jin et al., 2010). The lipid builds up in layers on the beads and pores preventing the VLP entering the pores. Lipids are very hydrophobic, more so than the Butyl-S ligands in the column. As a layer of lipids builds up it increases the hydrophobic nature of the column increasing the amount of VLP bound to the column on loading. But the lipids have a stronger affinity for the VLP and so less is eluted off the column, reducing the yield.

To see how lipids foul the monolith lipids in a crude feed were fluorescently labelled so that they would be visible under a confocal microscope. Three standard chromatography runs were carried out on a C4 monolith disk (0.34mL), including regeneration and CIP steps after each run (*Figure 4-2*). The column was removed from its holder and cut into thin cross-sections to enable both the top and bottom of the column to be seen.

Confocal pictures show that the lipids build up into a thin layer on top of the column. This would explain the increase in pressure as the pores in the monolith become restricted, reducing the ability of feed to enter the column. It is unknown whether the pores would eventually block up entirely. The lipid may deposit on top of the column by two mechanisms, binding to the ligands and column or an inability to enter the pores of the column (similar to a filter). The dye is present throughout the column, although at a much reduced level indicating that there is some affinity between the column/ligands and lipids. Having fluorescence in the column also shows lipids can get in the pores. It is possible that as the material enters the column holder through the frit lipids are attracted to the top of the column with some binding and the rest carried into the pores where they are either deposited or carried through.

The study was carried out on a C4 monolith, a more hydrophobic column than the OH monolith. Using the C4 monolith highlighted the issue much better than the OH monoliths. Both columns show an increase in pressures over consecutive runs, indicating that the same problems occur on both columns. The experiments were designed to show the location and characteristics of lipid fouling, and to help improve understanding of this phenomenon on a new separation media.

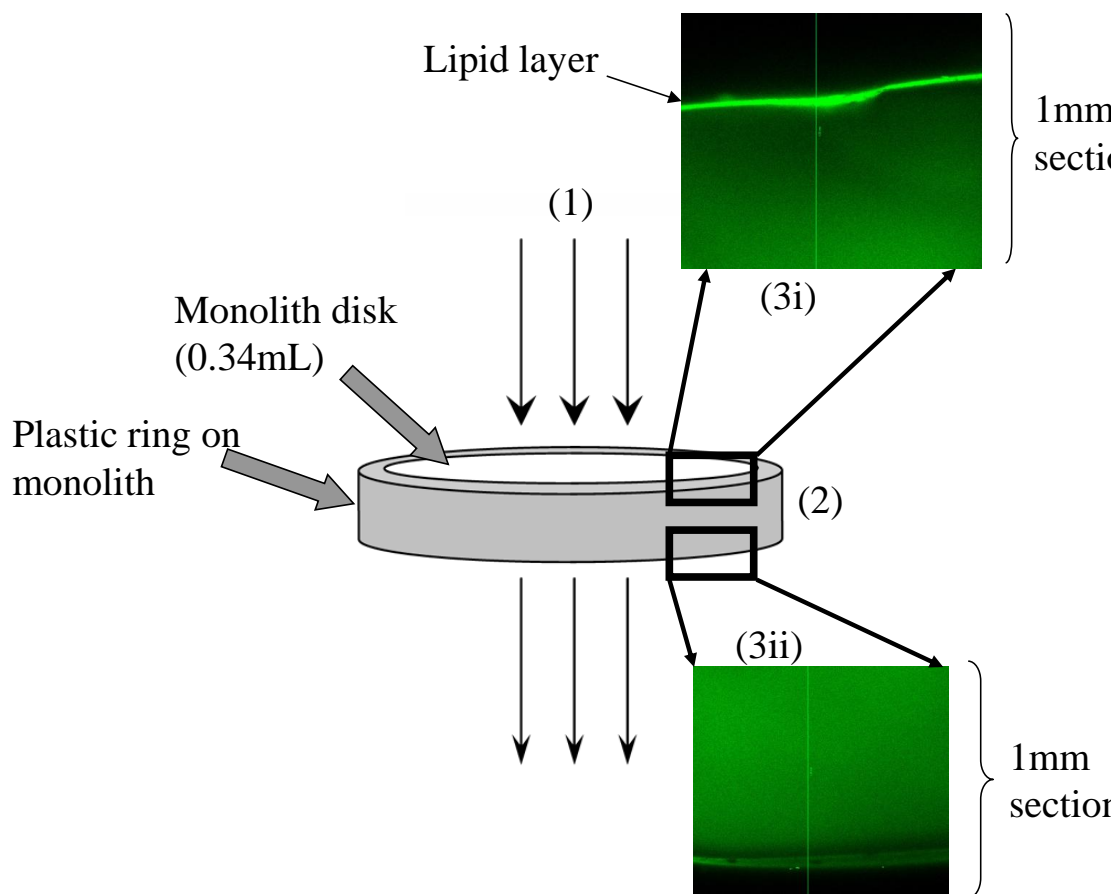


Figure 4-2 Confocal microscopy showing the fouling of lipids in a C4 disk monolith. The lipids were fluorescently labelled with BODIPY 493/503 dye (Invitrogen, Paisley, UK). (1) The column was challenged with the labelled crude VLP material; (2) the column was cut into sections and placed under the confocal microscope; (3i) the lipids form a layer on top of the column, causing an increase in pressure and reducing the recovery; (3ii) the lipids move throughout the column too, affecting the VLP recovery.

4.3.3 Lipid removal methods

Four lipid removal methods were studied to determine which would be useful as a pre-chromatography removal step. By removing the lipid in the feed it should reduce fouling in the column. The different methods were all run in a batch mode, although the lipid removal absorbent (LRA) and XAD-4 can be run in a continuous column format if necessary. The methods chosen were:

- Ammonium sulphate precipitation
- Lipid removal absorbent

- Delipid filters
- XAD-4/Amberlite

4.3.3.1 Ammonium sulphate precipitation

The addition of a saturated ammonium sulphate solution to the crude material causes the precipitation of lipids out of solution. Unfortunately it also causes the co-elution of VLP at the same time (*Figure 4-3*) and so would not be an appropriate method. Lipid reduction does not occur until at least 20% w/v saturation and full removal of the VLP happens at 35% w/v. The method would also be difficult to scale up, and the high level of ammonium sulphate in the resultant solution may cause issues in the next unit operation steps. In this method though the material is then placed on a hydrophobic chromatography column so the salt level would only need to be adjusted to 1M for the method.

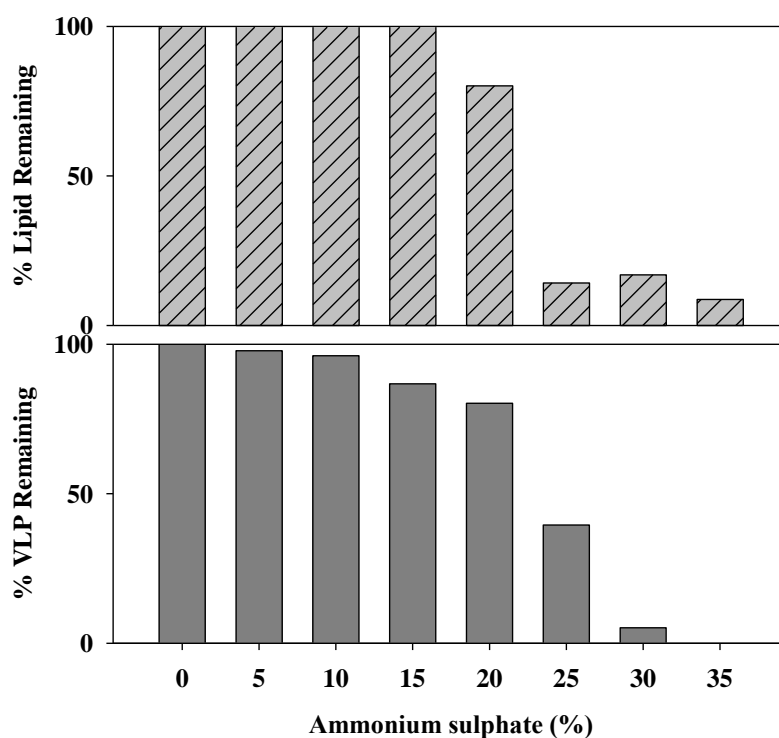


Figure 4-3 Amount of VLP and lipid remaining in samples after ammonium sulphate precipitation from 0-35% w/v.

4.3.3.2 Lipid removal adsorbent (LRA)

Lipid removal adsorbent (LRA) media is a synthetic calcium silicate hydrate adsorbent which is effective for lipids, lipopolysaccharides and lipoproteins. Lipid and VLP are reduced after the addition of 2.5mg/mL of LRA (*Figure 4-4*). Reduction in lipid levels corresponded to a similar reduction in the amount of VLP which remained, suggesting that co-removal has occurred. As the VLP is essentially a lipoprotein, this reduction is understandable. The method is therefore also not appropriate for use as a lipid reduction method for this feed.

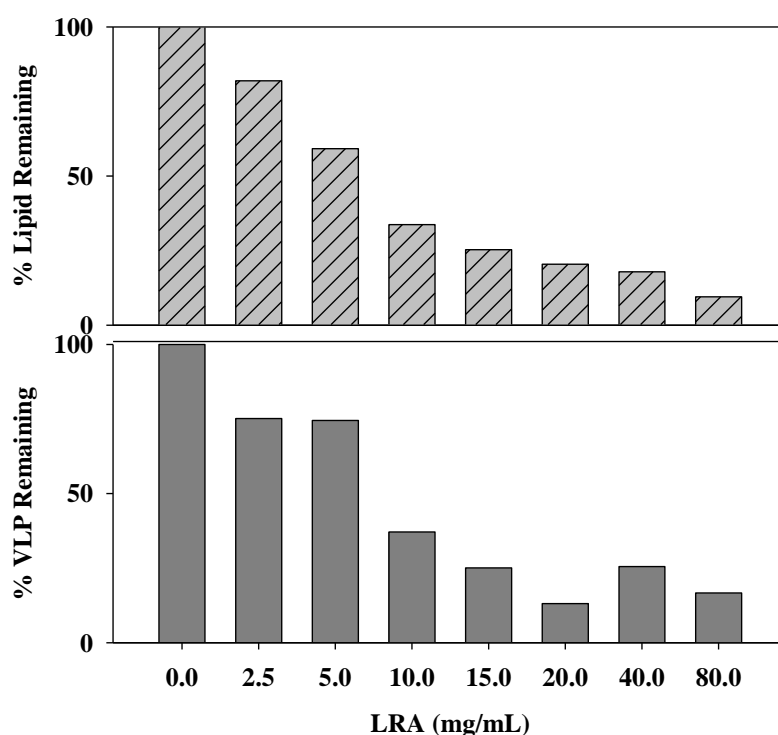


Figure 4-4 Amount of VLP and lipid remaining in the feed after the addition of LRA from 0 – 80 mg/mL.

4.3.3.3 Delipid filters

Cuno Zeta Plus Filters (DELI) are depth filter capsules using diatomaceous earth as an adsorbent. Three different flow rates, 6.5/20/65 mL/min were chosen to study their performance (*Figure 4-5*). At 6.5 mL/min the greatest reduction in lipid was seen, as expected due to the longer residence time, although the highest amount of VLP was also retained. An increase in flow rate to 65mL/min only decreased the

amount of lipid removed and VLP retained by approximately 10%, showing that this method is robust. On average around 50% of lipid is removed, while 80% of VLP is retained. The method can be easily scaled up using the larger filters available in the range and could be integrated into the current protocol with a minimal yield loss over the step.

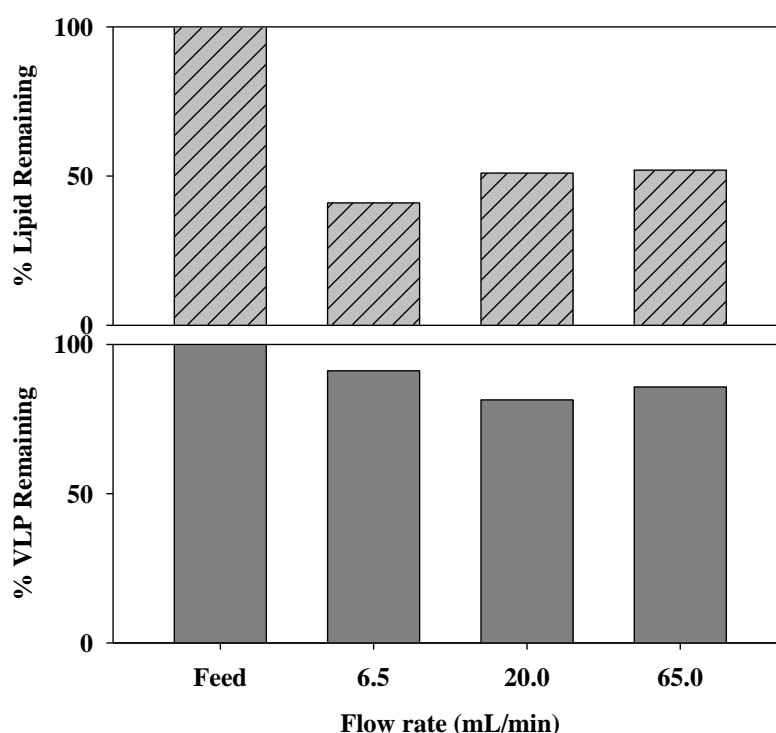


Figure 4-5 Lipid and VLP remaining in the pooled filtrate after filtration through Zeta Plus delipid filters at 6.5/20/65 mL/min.

4.3.3.4 XAD-4/Amberlite

Currently XAD-4 is used to remove the detergent Triton X-100 from the crude material. It is a non-ionic styrene-divinylbenzene polymer that adsorbs and releases ionic species through hydrophobic and polar interactions. Using the XAD-4 in a batch mode it was able to remove the lipid from the crude feed without removing VLP as well (Figure 4-6). The results indicate that the adsorbent has a good specificity for lipids in the feed. At concentrations above 0.3g/mL the amount of lipids in the feed was significantly reduced by around 70% but had little impact on the VLP remaining, ensuring that the loss of VLP was less than 20%.

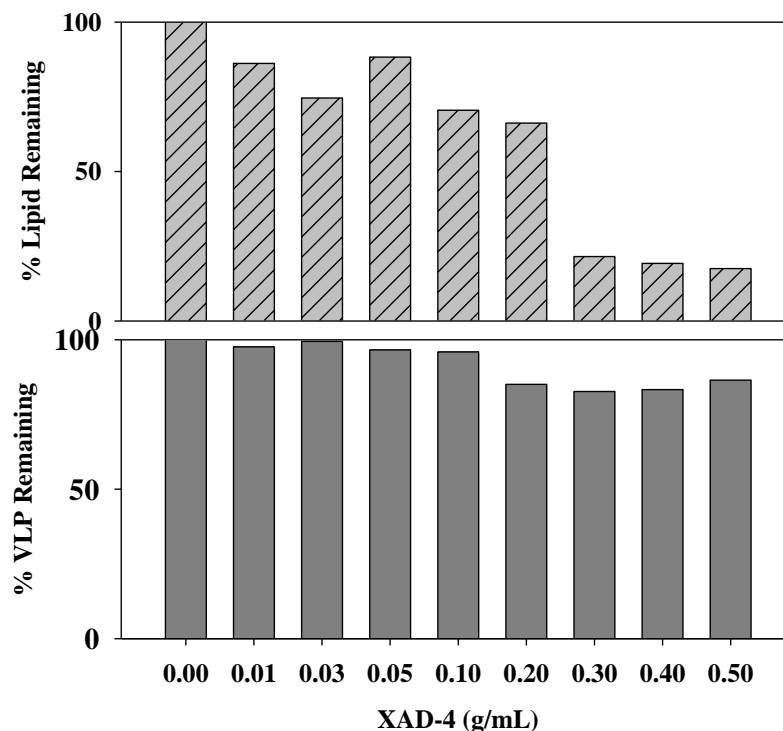


Figure 4-6 Lipid and VLP remaining in the crude feed after the addition of XAD-4 to the material and subsequent filtration.

4.3.3.5 Integration of lipid removal method

Using the VLP to lipid ratio the favourable lipid removal method could be chosen (Figure 4-7). The XAD-4 method comes out as the method which achieves the highest ratio of VLP to lipid. It was decided to use this method in future experiments to achieve a reduced lipid feed. Although there are some conditions which have a favourable ratio value, such as ammonium sulphate 25% w/v, the loss yields of VLP also need to be taken into account.

The addition of an extra step into the current purification method was very simple, especially as XAD-4 already appears in an earlier step in the method. As the XAD-4 is only left for 30 minutes and at ambient temperature there was limit effects on the time of the purification process, which already took between 6 and 9 hours, depending on the homogenisation step. Removal of the XAD-4 was via filtration, included as part of the process anyway before the chromatography columns. For

scale-up the XAD-4 can be packed into a column and the feed flowed through, with the lipid binding to the beads. The beads can then be regenerated to enable reuse. This was not investigated for this study though.

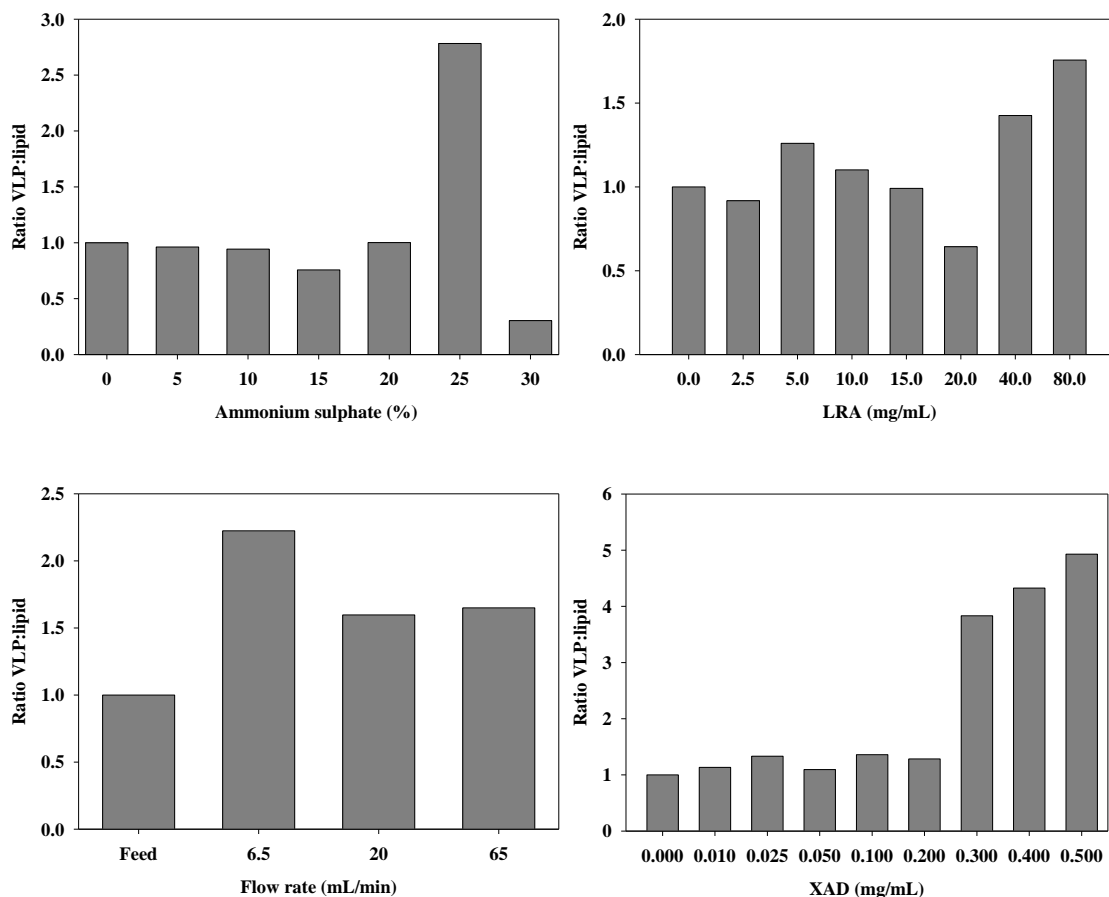


Figure 4-7 Analysis of the VLP:Lipid ratios for each of the lipid removal methods to determine the ideal method of use.

4.3.4 Effect of reduced lipid feed on the dynamic binding capacity in monoliths

The reduced lipid feed was applied on a 1mL OH monolith to determine the effects of removing lipid from the feed (*Figure 4-8*). Removal of the lipid should increase the binding capacity of the column as there will be less competition, and hence less inhibition on the ligands between the lipids and VLP. Over consecutive runs less fouling should occur from the lipids, allowing extended use of the column.

The dynamic binding capacity of the column is increased approximately 2.5 times, at a value of 0.1 C/C_0 . With the crude feed the column has a DBC of approximately 4 CV, whereas the reduced lipid feed DBC is approximately 10CV. The results of the ELISA test also confirm a doubling in the amount of VLP binding, with an increase in the VLP from 0.11mg to 0.25mg.

The curves are very similar in shape and length, indicating that there is no change in the methods of binding within the column. Around 80% of the proteins remain in the feed after lipid removal, and as most of the proteins do not bind to the column this decrease would not be attributed to the increase in DBC between the two feeds.

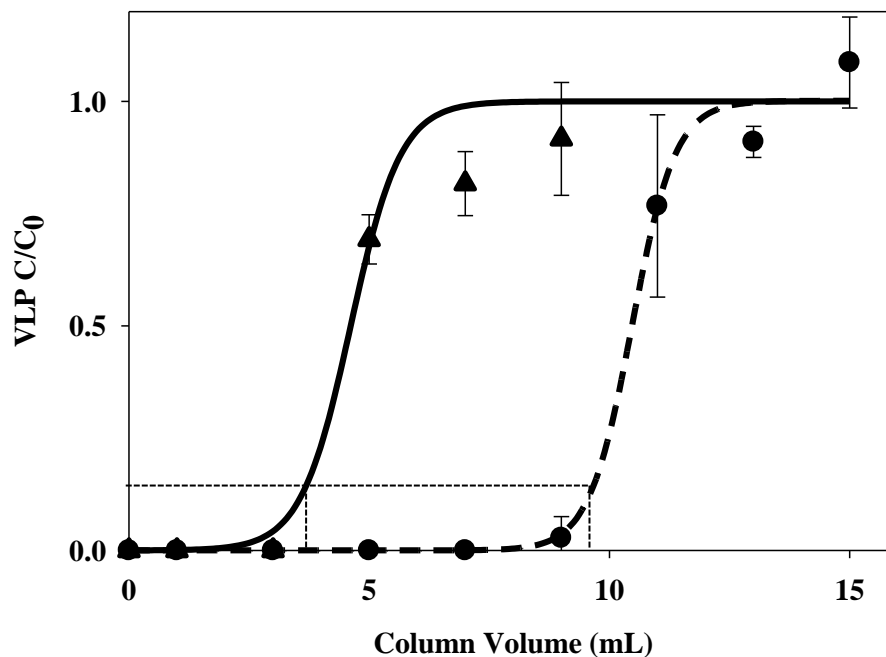


Figure 4-8 Comparison of the dynamic binding capacity of the 1mL OH monolith when a crude feed (▲) and a reduced lipid feed (●) are applied to the column. 10% breakthrough is indicated by the dotted line.(See Section 9 Figure 9-5 for raw VLP data)

4.3.5 Effect of reduced lipid feed on dynamic binding capacity in Butyl-S - a comparison.

The effect of removing the lipid from the VLP feed should also increase the DBC on the conventional Butyl-S resin column in the same way as the monolith. *Figure 4-9* shows that the application of a reduced lipid feed changes the binding dynamics within the column, as seen by the change in the binding curve when the crude and reduced lipid feeds are compared. The effect on the DBC in the column is minimal but overall the column does have an increase in binding capacity. This is a different effect from the monoliths where the binding curves remain similar suggesting that the binding dynamics are not affected by any contaminants. Overall the amount of VLP bound onto the column with a reduced lipid feed was approximately 0.11mg, an increase of nearly 3 times from the crude feed.

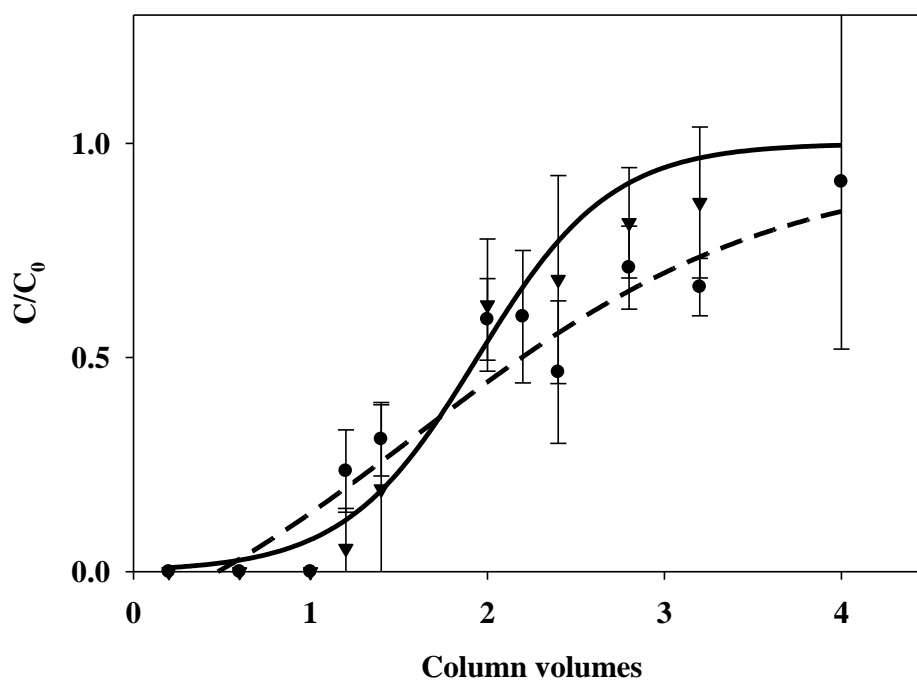


Figure 4-9 Comparison of the dynamic binding capacity on a Butyl-S resin column when a crude feed (solid line ▲) and reduced lipid feed (dotted line ●) are applied to the column. (See section 9 Figure 9-6 for raw VLP data)

4.3.6 Effect of lipid removal on the life span of the monolith column

Due to the cost of chromatography resins they will often be used for a number of batches before disposal. As previously seen in section 4.3 one effect of

the crude feed on the monolith was an increase in pressure over consecutive runs. When a reduced lipid feed is applied to the column the pressure increase over the 10 runs is reduced compared to the crude feed (*Figure 4-10*). The crude feed had a pressure increase around 2 bar, but the reduced lipid feed only increases by 0.8bar. As the feeds are from the same starting material it can be assumed that the reduced pressure increase with the reduced lipid feed is the result of the removal of the lipid.

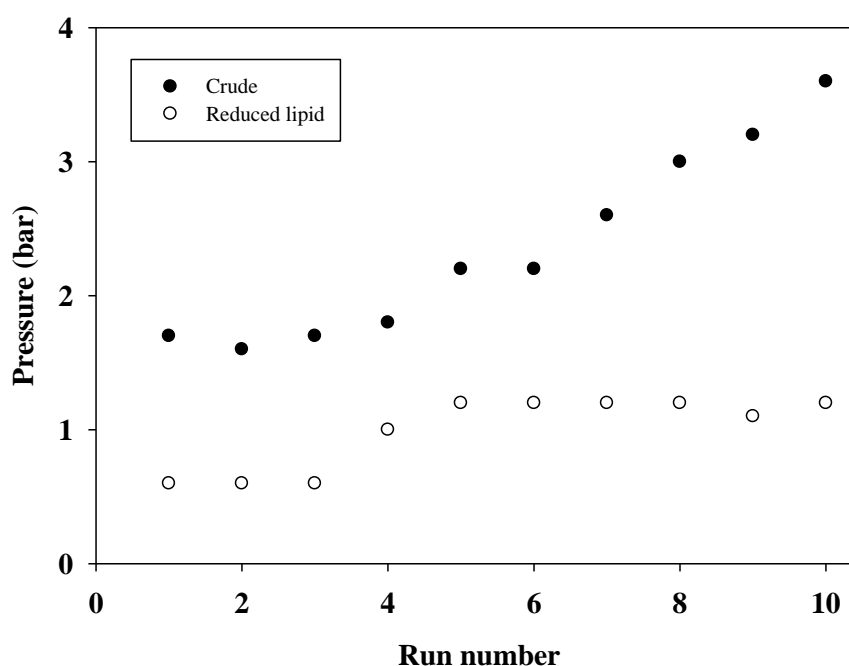


Figure 4-10 Comparison of the pressure increase over consecutive runs in a monolith column when a crude feed (●) or reduced lipid feed (○) is applied.

4.3.7 Sample purity after monolithic process from SDS-PAGE

As the monolithic process was developed to be used as an initial capture step for crude material, it was important to maximise the VLP binding capacity and elution yield. But it is also important to look at the purity of the elutant, and determine the amount of impurities which remain. Often these contaminants can go on to influence how subsequent steps in the downstream process will work. In the case of yeast the contaminants will commonly be host proteins, lipids and nucleic acids. For this study triton can also be counted as a contaminant within the feed stream.

To look at contaminant removal after the monolith column a number of tests were used, including SDS-PAGE, DLS and protein assays (Bradford and BCA). The use of the protein assay has been discussed in Section 3.3.13 and DLS in 3.3.10. Material from the elution and feeds were concentrated down and run on a SDS-PAGE gel, as seen in *Figure 4-11*. From this it can be seen that there are more bands in the feed and flow through lines than in the elution lines, indicating that more material does not bind during loading. On a chromatogram this would relate to a flow through peak at 280nm. The gels confirmed that this is probably protein in the feed not binding to the column as many of the bands are similar in both lines. The heavily dyed areas at the bottom of the gels indicate that some material has been dyed but not separated out on the SDS gels. As this is greater in those wells related to a crude feed it is assumed to be lipids (Gavilanes et al., 1982).

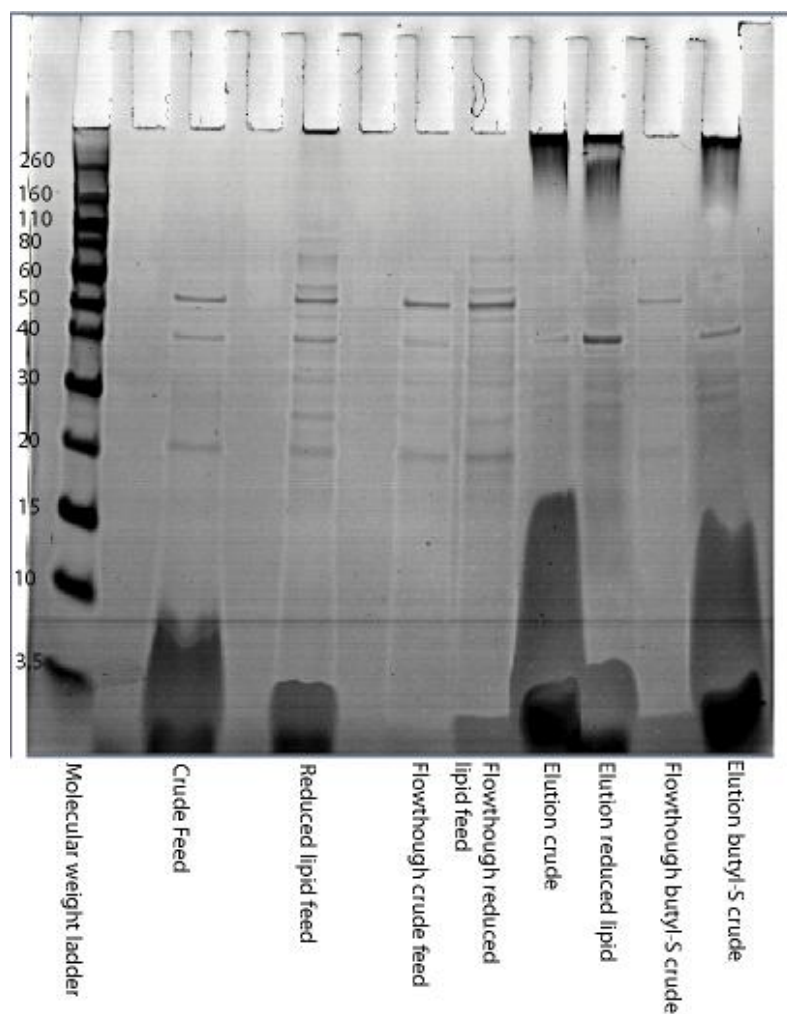


Figure 4-11 SDS-PAGE of material from a 1ml OH monolith separation process. The feed, flow through (breakthrough) and elution material were collected and concentrated down to approximately 1mg/ml before loading. Material from an equivalent run with crude material on a butyl-S resin column has been added for comparison.

4.4 CONCLUSION

The above study shows that the lipids in the yeast homogenate crude feed can greatly affect the chromatographic process. The effect of the lipids on the column can be seen in the increases in pressure seen over consecutive runs. Fouling on the monolith column was observed using confocal microscopy with fluorescently labelled lipids. Although the fluorescent dye was observed throughout the column, a distinct layer was observed on the entry side of the column. This fouling was not removed by the isopropanol regeneration steps, as it was observed after 3 consecutive runs, confirming that the lipid is irreversibly bound. To increase the life span of the column fouling needs to be reduced.

A lipid removal method before the chromatography step should reduce the amount of lipid reaching the column. Removing the lipid using XAD-4 beads resulted in a 70% decrease in the lipid content of the crude feed. Using XAD-4 is easy to fit into the current process, either in batch form or as a flow-through column. Applying the reduced lipid feed to the column increased the breakthrough point from 4CV to 10CV. Consecutive runs using the reduced lipid feed resulted in a smaller increase in pressure between the first and the tenth run, indicating a reduced amount of lipid is deposited on the column.

5 INVESTIGATION OF THE BEHAVIOUR OF A VLP ON MONOLITHS

5.1 INTRODUCTION

Previously it has been shown that hydrophobic interaction chromatography (HIC) is a useful step in the purification of the HBsAg VLP from crude yeast homogenate material. But as previously mentioned in Section 1.8 hydrophobic interaction chromatography can cause unfolding and denaturation of proteins upon adsorption onto the column. This can decrease the yield of the step, and also affect the structure or conformation of a protein. Therefore conditions of the process must be carefully considered during evaluation of conditions for the step.

As part of the continuous development of the monolithic purification process gradient runs were undertaken to look at purity of the feed material. A gradient elution is often used during initial process development to determine the ideal conditions for step elution or for high-resolution separation and analysis. Application of gradient elutions on the monolith resulted in a very low elution titre for the VLP in comparison to a step elution which has a 90% yield. McNay et al. (2001) showed that the hold time before elution in reverse phase chromatography affected both the protein structure and chromatographic behaviour. Studies conducted into the influence of the HIC ligands on conformational changes during separation found in the literature have increased in numbers in recent years (>10 years) but the mechanisms are still poorly understood. These studies have shown that other components of the process, such as salt and loading can have an effect as well.

The use of salt in the mobile phase is important for promoting binding and retention in a HIC column. Papers have shown that an increase in the salt concentration within the mobile phase results in a higher amount of unfolding on the column, particularly with the salt ammonium sulphate, the most commonly used salt in HIC (Jungbauer et al., 2005, Fogle et al., 2006, Xiao et al., 2007a, McNay et al., 2001). Fogle et al. (2006) also concluded that higher loadings of the protein BLA onto the HIC resins resulted in more BLA retaining a native-like structure. But in

reality it is difficult to produce a model of unfolding as proteins differ greatly in their structures and ultimately their stability. Different proteins can react to the same conditions in contradictory ways, for example Ueberbacher et al. (2008) saw that the rigid structure of lysozyme was not affected by HIC ligands in comparison to BSA and β -lactoglobulin which are much “softer” proteins.

Often HIC is used in processing for the removal of protein aggregates in a polishing step, as monomeric proteins display less hydrophobicity than aggregates. (Li et al., 2005, Kuczewski et al., 2010). Membrane absorbers from Sartorius Stedim Biotech have been shown to remove monoclonal antibody aggregates using four elution steps with decreasing salt levels, to separate monomer and aggregates (Ebert and Fischer-Fruhholz, 2011). Ligand density in a Phenyl Sepharose Fast Flow resin can also be used to influence the binding strength of aggregates and therefore monomer/aggregate separation (McCue et al., 2009). As the ligand density increased less aggregates appeared in the eluate pool at the same elution salt level. An increase in the elution buffer salt concentration also had the same effect as ligand density in reducing aggregate elution. Earlier work had shown that the irreversible adsorption of the aggregate species, and not differences in the binding properties between monomer and aggregates, contributed to the significant separation between the two (McCue et al., 2008).

This chapter focuses on the effect of using chromatography within a purification process for the VLP, specifically in relation to the use of a monolith. The first half of the chapter describes how loading conditions can affect the behaviour of the VLP, to try and understand why a gradient elution was not possible with the HIC column and the VLP. Initial work focused on the binding time or residence time of the VLP in the column and see how the elution recovery might be affected. Later the influence of the binding affinity and interactions in the feed material were studied.

At the end there is a focus on analysing the elution material. A small 0.1mL monolith column was used on a HPLC system to run a fast two-step separation of the elution material. Using a HPLC system a short method was developed to achieve a new analytical method to infer information about the VLP.

5.2 MATERIALS AND METHODS

Crude feed and reduced lipid material for the chromatography runs was produced from frozen material produced by fermentation (**Section 2.2.3**), by the methods stated in **Sections 2.3** and **2.3.1**. Initial capture step chromatography experiments were carried out on both CIM 1mL OH columns (BIA Separation, Slovenia) and Hi-Trap columns with Butyl-S resin (GE Healthcare, UK). The method for the CIM column is described in **Section 2.5.1** and the resin column in **Section 2.4**. Modifications of these methods were needed to analyse the behaviour of the VLP on the columns and any changes are detailed in the relevant Results and Discussion section.

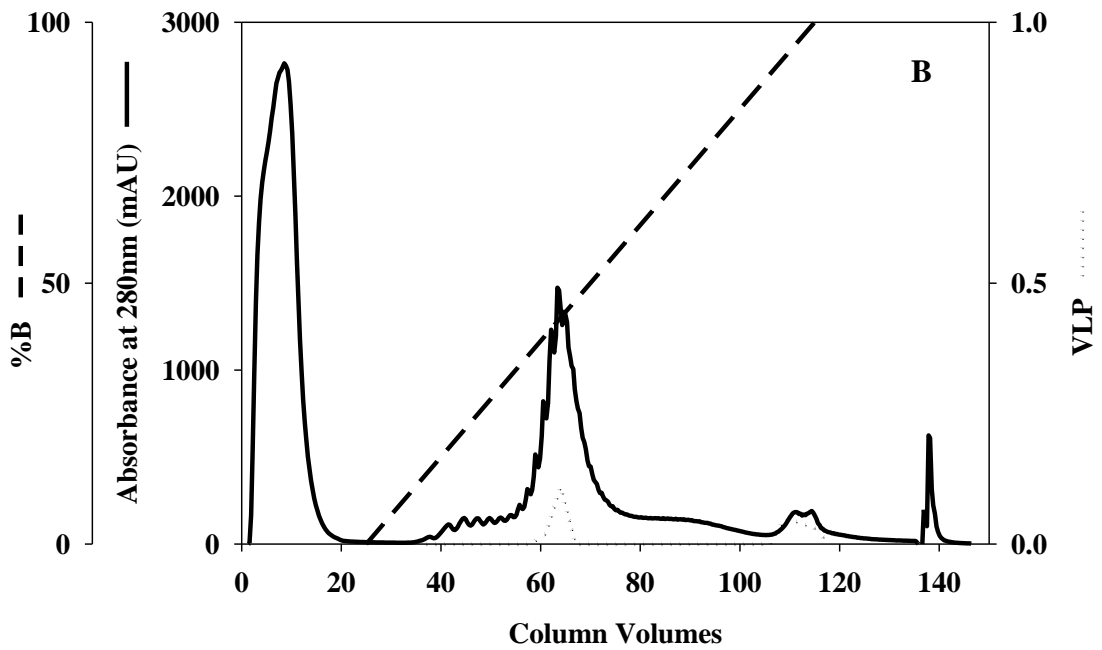
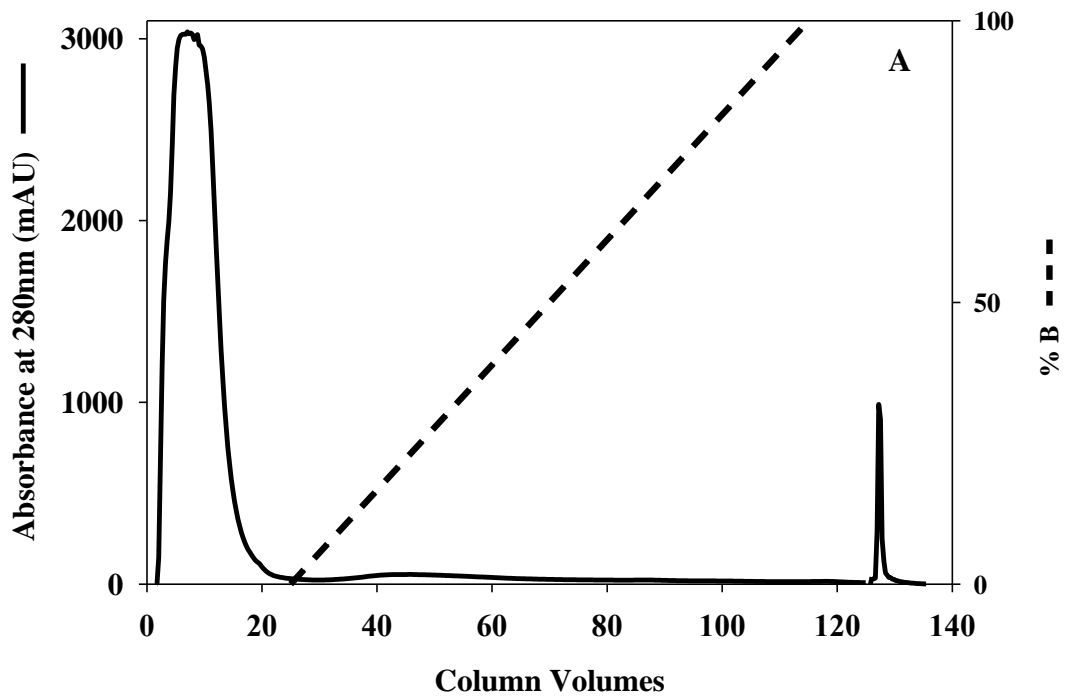
A method to study the elution samples was developed on a CIMac® column, to evaluate the amount of VLP and protein and indicate the structure of the VLP. The method for this is described in **Section 2.5.2**. Other analytical techniques were used to analysis the samples and include the determination of the quantity of VLP via ELISA (**Section 2.11.4**), the quantity of protein by BCA assay (**Section 2.11.5**) or Bradford (**Section 2.11.6**), and the size of material in the samples by DLS (**Section 2.11.8**).

5.3 RESULTS AND DISCUSSION

5.3.1 Gradient and step elutions on the monolith

The elution sample(s) from the monolith contains a large amount of impurities and contaminants as well as VLP, as previously shown in *Figure 4-11*. It is important to understand the ratio between the VLP and contaminants to determine the degree of purity achieved during the step. The use of a gradient elution during adsorption chromatography enables the separation of different molecules and molecular species into individual peaks.

To determine the percentage of impurities contained in the sample, and to understand about the binding affinity of these impurities, a gradient elution was carried out at a flow rate of 3 ml/min for 30 minutes (total flow of 90ml). During elution the absorbance profile (280nm) was used to determine where material (VLP or protein) was eluted. Fractions of the elution were collected and analysed for VLP off-line. The gradients were attempted using two different ammonium sulphate concentrations in the mobile phase, 0.6M and 1.2M. With the 0.6M (*Figure 5-1A*) mobile phase the elution gradient showed little evidence of any elution (protein or VLP) from the column. Whereas a mobile phase with 1.2M salt (*Figure 5-1B*) shows a number of overlapping peaks are visible. Some VLP was detected in the ELISA assay but the levels of it were very low and overall recovery was less than 30%. As we would expect recovery levels of around 90% from an isocratic elution this indicates that a large amount of the VLP must somehow become irreversible bound to the column.



B

Figure 5-1 Gradient elutions on a OH 1mL column using crude material. (A) 0.6M (B) 1.2M. Only graph B contains any VLP as nothing was seen on the ELISA assay for graph A.

5.3.2 The effect of wash time on the elution profile

It was unclear why a gradient elution would have such a dramatic decrease in VLP recovery. The only changes in a gradient elution compared to an isocratic elution were the time the VLP spent on the column and the step buffer change at the time of elution. To mimic the binding time during gradient elution a wash step was introduced for up to 40 minutes, at 10 minute intervals. The chromatographic runs were conducted at 1.0M ammonium sulphate using a crude feed.

The chromatographic profiles under the five different time conditions are very similar (*Figure 5-2A & B*). Looking particularly at the regeneration peak (R) the peak areas are consistent. Any change in the peak area would indicate that the VLP has changed its binding conditions. Comparing the elution peak at 0 and 40 minutes wash time does indicate a broadening of the peak. Often this indicates that material bound to the column has changed in conformation and as a subsequent result these particles will have a higher binding affinity for the column. Elution (desorption) will therefore occur at different rates, depending on the degree of alteration, causing a tailing on the elution curve. The ELISA test shows that the amount of VLP is consistent up to 40 minutes. (*Figure 5-3*).

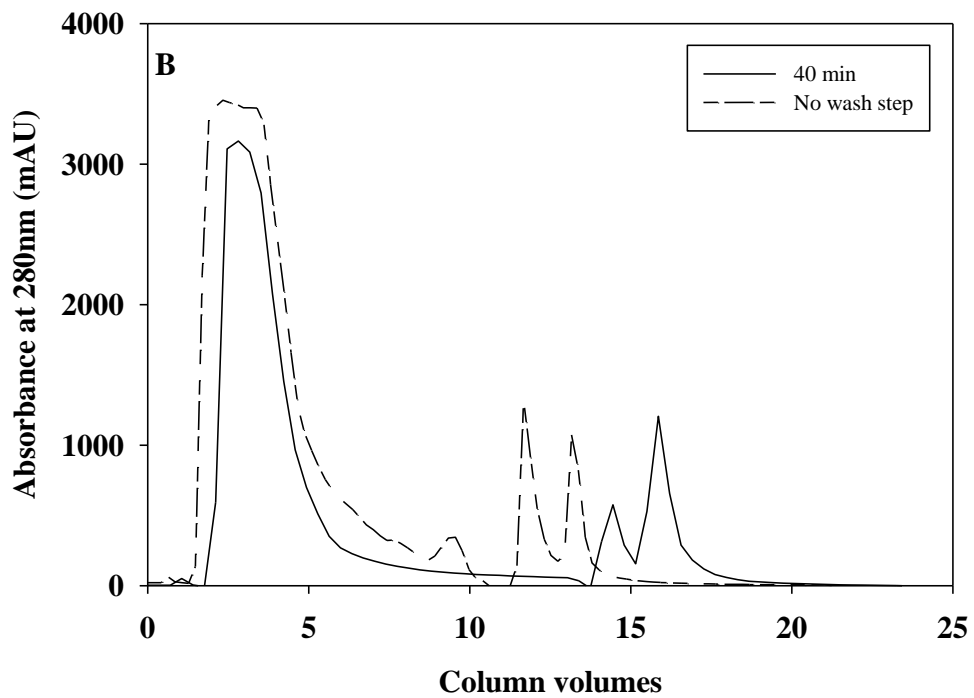
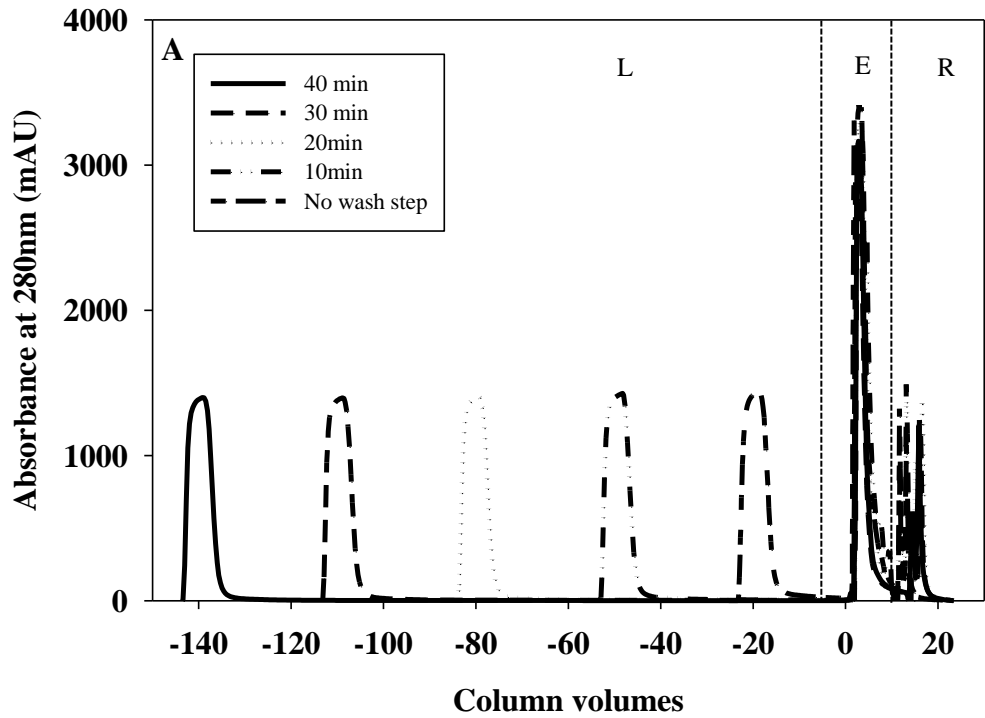


Figure 5-2 Chromatographic profile for runs on a 1mL OH monolith column with crude homogenate material bound at 1.0M ammonium sulphate. The wash step was increased from 0 to 40 minutes (25CV to 145 CV). (A) Full profile for absorbance at 280nm. L=loading, E = elution, R=regeneration; (B) Elution and regeneration peaks at absorbance 280nm for no wash step (0 min) and 40 minutes.

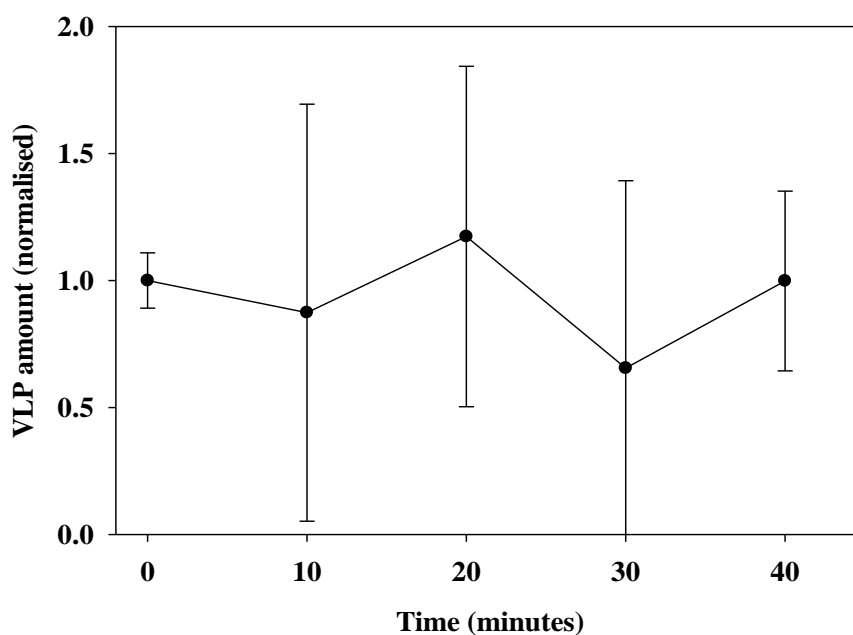


Figure 5-3 ELISA results from elutions with crude material with binding buffer with 1.0M ammonium sulphate. Samples were collected after a wash time from 0 (no additional wash time) to 40 minutes. (n=3).

The experiments were carried out on Butyl-S columns as well. This was to confirm that any changes could be associated with a HIC ligand and not the monolith column itself. The VLP decrease over the 40 minutes was actually higher on the resin column although no decrease was seen until after 20 minutes (*Figure 5-4*). The Butyl-S ligand is slightly more hydrophobic than the OH ligand in the monolith and so may explain the decrease.

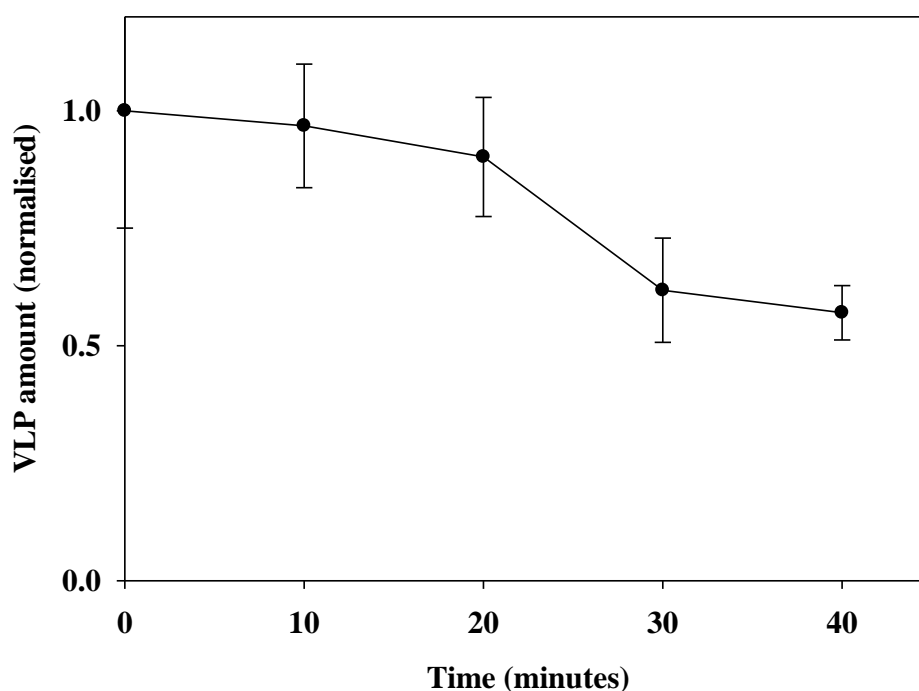


Figure 5-4 ELISA results for VLP on the effect of wash time on the VLP elution profile on a 1mL Butyl-S HiTrap column, using a crude homogenate VLP feed, binding at 0.6M ammonium sulphate . Increased wash time was from 0 minutes to 40 minute.) (n=3). L=loading, E=elution, R= regeneration.

5.3.3 Influence of binding strength on the elution profile

In this chromatography process the two factors which have the greatest influence on the column are salt in the mobile phase and lipids. We decided to study the effect of both of these on the elution profile if the VLP was allowed to remain on the column for an extended length of time.

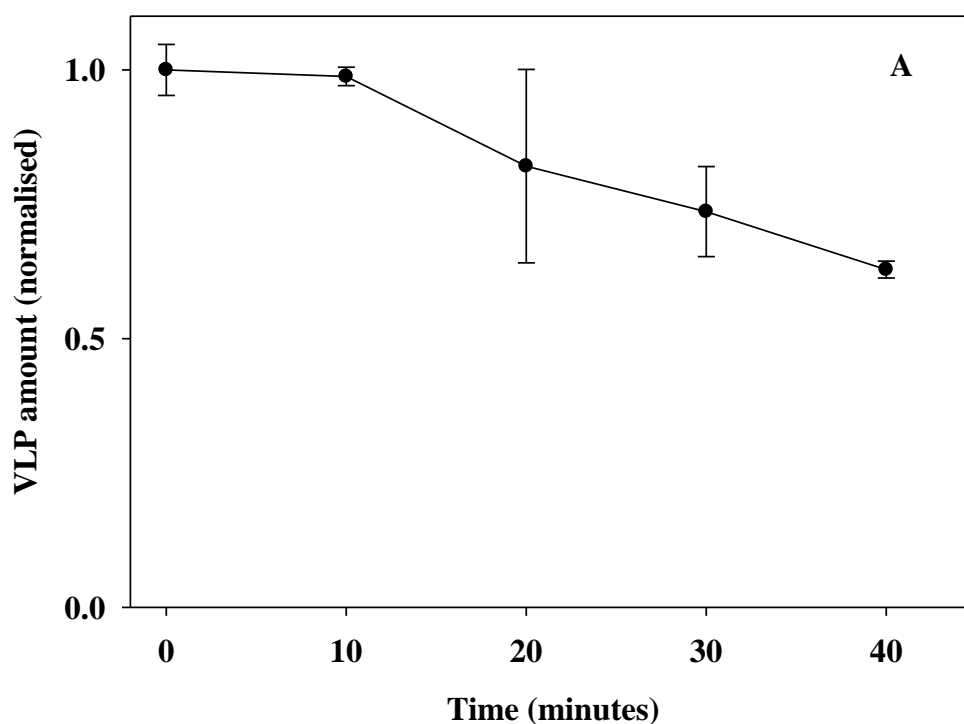
Literature describes how the level of salt, and therefore binding strength, can have an effect on a protein during binding/elution on a HIC column. An ammonium sulphate salt level in the mobile phase of 0.6M causes a reduction in the amount of VLP that binds, as the binding affinity is reduced between the VLP and the column.

Figure 5-5 A shows that the VLP concentration decreases over the 40 minutes by approximately 40%. This is evident from the absorbance profile for the

elution peak, (Figure 5-5 B) which is significantly smaller after a wash time of 40 minutes.

In section 5.3.2 the use of 1.0M in the mobile phase resulted in no effect on the VLP over a 40 minutes wash time. The higher affinity and great binding capacity achieved with the higher salt level could have stabilised the VLP on the column and reduced any effect from the hydrophobic ligands. The higher binding capacity can also reduce protein spreading. Fogle et al. (2006) showed that decreasing the loading amount with α -lactoalbumin increased the conformational effects seen on the protein.

Haimer et al. (2007) state that HIC adsorption should be considered a multiple stage reaction mainly consisting of adsorption and spreading. They recommend that HIC adsorption should be performed at high salt concentrations in order to yield high adsorption rate constants and therefore decouple this from protein spreading. If this is indeed the case then it is not unsurprising that the ideal condition is at 1.0M and not 0.6M for ammonium sulphate in the mobile phase.



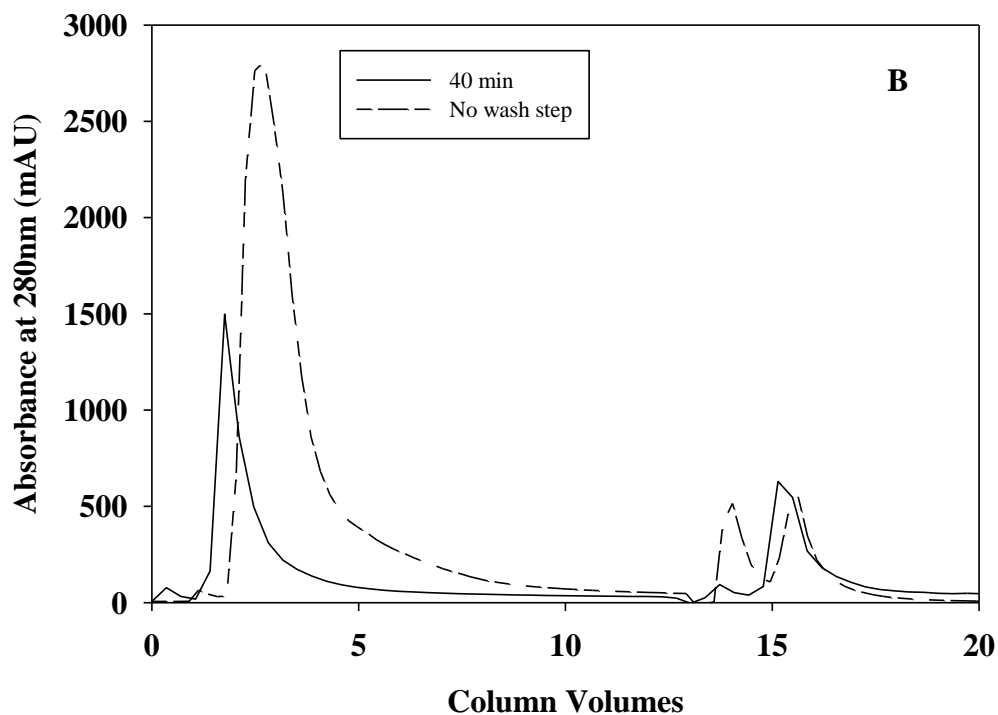


Figure 5-5 The effect of residence time with a crude yeast homogenate VLP feed, at 0.6M ammonium sulphate on a 1mL monolith column . (A) ELISA results (n=3); (B) Elution and regeneration peaks.

5.3.4 Influence of lipids on the elution profile

The lipids found in the crude homogenate material are highly hydrophobic and can cause irreversible binding of the VLP onto the column (Jin et al., 2010). A comparison was made between a crude feed and reduced feed to see if the addition of lipids enhanced the effects of unfolding on the column due to lipid:VLP interactions. In Figure 5-6 the VLP levels at both the 1.0M and 0.6M salt levels both show a small change over hold times for the VLP on the column. Again the level drops more when the salt is 0.6M in the mobile phase, but the decrease is not as extensive as with the crude feed indicating that VLP are also subject to the degree of hydrophobicity in the column environment in the same way as proteins are.

These results show that not only is the salt level important but also other factors within the feed, in this case it is lipids, which can have an effect on the elution concentration for VLP. Therefore it is important that the make-up of the feed is understood and how these components can affect the chromatography process, particularly during scale up as factors, such as binding time, can change.

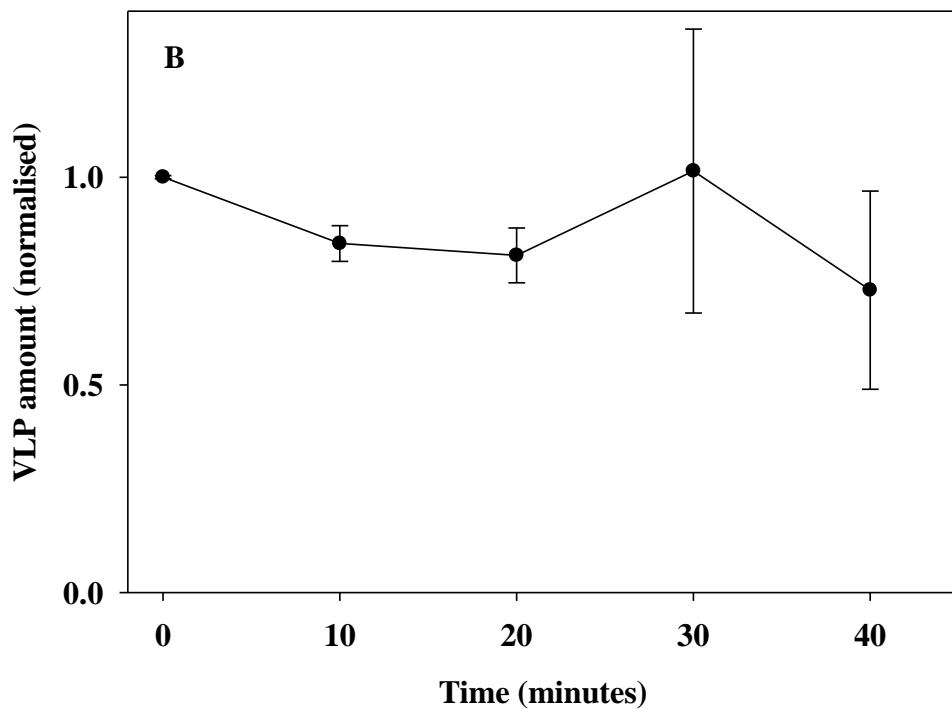
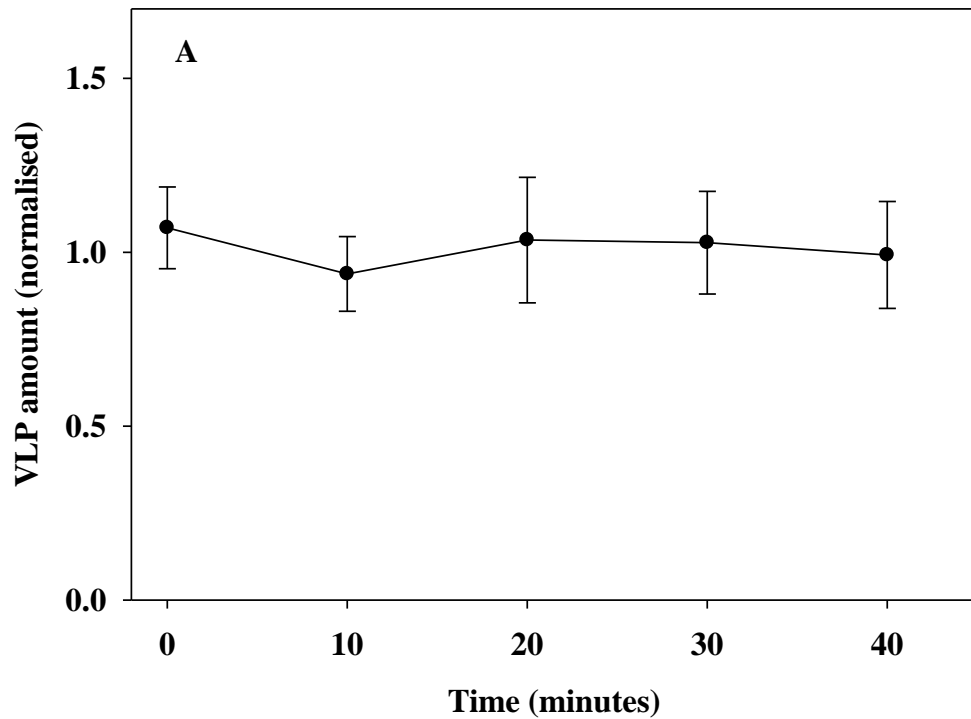


Figure 5-6 Residence time on OH monolith with reduced lipid yeast homogenate VLP feed material at loading salt concentration of 1.0M (A) and 0.6M (B) ammonium sulphate. (ELISA results n=3).

5.3.5 Reduction of residence time on the column

One way of decreasing the residence time in a column is to increase the flow rate of the loading and elution stages. By increasing the flow rate in relation to the column size it would keep any residence time consistent and ensure that there is comparable recovery over scale-up.

The advantage of monoliths is their ability to run at very high flow rates compared to standard resin columns, with no effect on the binding capacity. The 1mL OH column was run at flow rates of 1 ml/min (average linear velocity 46 cm/h) to 12 ml/min (average linear velocity 566 cm/h) (*Figure 5-7*). The maximum flow rate achievable for the column is 16 ml/min. The pressure drop during loading increased with the flow rate. As VLP binds to the column it will reduce the width of the pores inside the column. The crude material had the higher pressure increase due to the nature of the feed material being more viscous, (*Table 5-1*), but if the flow rate was decreased the pressures did too and so therefore these effects are reversible. Although the ELISA test has a significant degree of error it can be seen clearly that the VLP binding capacity does not change over time (*Figure 5-7*). The absorbance profile was also consistent over the flow rates (results not shown).

Flow rate (ml/min)	Pressure drop (bar)	
	Crude	Reduced lipid
1	0.5	0
3	3.0	0
4	3.5	-
5	5.0	4.0
6	5.5	4.5
8	7.5	6.0
10	9.0	5.5
12	11.0	7.0

Table 5-1 Pressure drop seen over flow rates with 1ml OH monolith column at 1M ammonium sulphate.

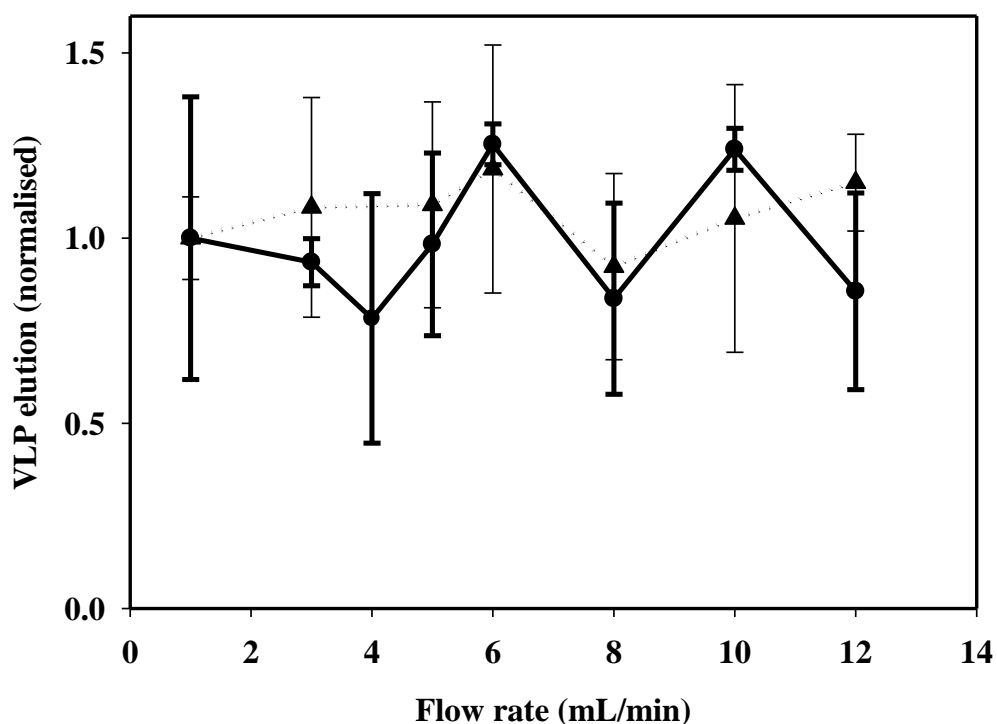


Figure 5-7 Comparison of the amount of VLP in the elution peak from a 1mL monolith, using 1M ammonium sulphate in the binding buffer, with crude (●) and reduced lipid (▲) material. The column was run from 1ml/min to 12ml/min.

5.3.6 Use of a monolith column as an advanced analytical method

It is important that any method to quantify the amount of VLP in material is reliable and has a low degree of error. Currently the ELISA assay used to quantify the VLP produces high error rates, up to 50%. The error rates are very variable, as evident by past graphs, even over the same ELISA plate or between different plates with the same sample. It prevents the accurate determination of a quantitative value and it is therefore more meaningful to examine the trend of VLP over different conditions. Combined with the difficulty in determining any structural changes in the VLP, or separate the VLP from impurities, development of another analytical method is needed.

The hydrophobicity of particles can be exploited in HIC to elute different species at different times (as described with the Sartorius Stedim phenyl membrane absorbers, Sartobind, for removal of MAb aggregates). At first this was tried on the 1mL OH column on the Akta system but the large volume resulted in a slow process,

which required large quantities of loading material. An ideal analytical method needs to work on small quantities of material, and be automated so that large numbers of samples can be processed. It did show a separation of particles when the elution was carried out at two different percentages of elution buffer *Figure 5-8*. The first step involves a reduction in the salt level and is intended to remove any material which was weakly bound to the column. The second step is 100% elution buffer and therefore contains no salt. This step should remove material which is more strongly bound to the column.

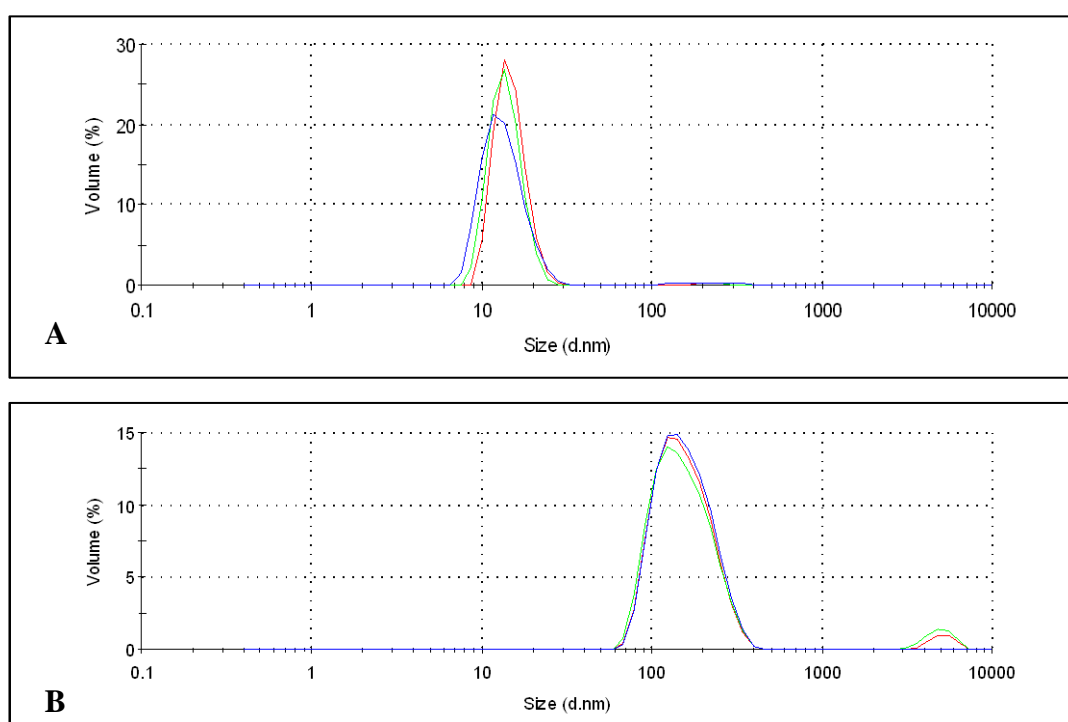


Figure 5-8 Dynamic light scattering graphs of material eluted during a two step process on a OH 1mL column, using 1M ammonium sulphate in the binding buffer. Step 1 is at 60% B (A) and step 2 at 100% B (B). The peaks correspond to 13nm for step 1 and 210nm for step 2. (n=3).

It was decided to try and implement the two-step method as an analytical method using small analytical monoliths, named CIMac or Bio-monoliths, that BIA Separations produce and are currently marketed by Agilent. These are only 0.1ml in

volume and can be run on a HPLC system, which has an advantage of enabling automation of samples and the use of small sample loadings. As BIA Separations does not produce a commercially available CIMac column with the OH ligand, or any HIC ligand, the column was specially produced for this study.

The runs were carried out using 0.8M ammonium sulphate as a loading buffer. Initial runs indicated that as the column was slightly more hydrophobic, possibly due to smaller scale, and 1.0M salt in the mobile phase bound the material a little too tightly to enable a good separation when the elution steps were run.

To increase the signal response at 280nm and enable accurate analysis of the sample the maximum sample volume of 100µl was injected in each run (*Figure 5-9*). There is a small loading peak which appears, but this does not contain any VLP (data not shown). The elution was carried out at 80% and 100% elution buffer. At 80% the material which is less tightly bound will elute off before the remaining material.

Ideally an analytical method will be fast, enabling results to be produced quickly and almost in “real-time”. As the samples to be used had come from the chromatographic step, and therefore contained little or no yeast material which would cause pressure issues, the method was run at 2 ml/min. This also allowed a high resolution of the peaks and enabled a run to be completed in 8 minutes. The short contact time should prevent any effects from the column on the VLP.

Triplicates were run of each sample to ensure that the results were consistent and reliable. But when three samples were run back to back the height of peak 1 decreased and peak 2 increased. This indicated that the binding affinity for the column was changing over the three runs and resulted in retention of material. In past work with the standard monolithic columns this meant that fouling was occurring on the column, either reversible or irreversibly, and the column was becoming more hydrophobic. This was confirmed when samples were repeated after a run using 30% isopropanol, the standard buffer used to regenerate the larger columns. By incorporating a wash step between each run the consistency of the peak areas is maintained (*Figure 5-10*). Further work needs to be conducted to determine how this phenomenon occurs and what the foulant material is, but as regeneration conferred the column to its original binding affinity it can be assumed it was strongly

bound VLP or proteins and not irreversibly bound lipids. It may be possible to eliminate the foulant from the feed in future and remove the need for a wash run.

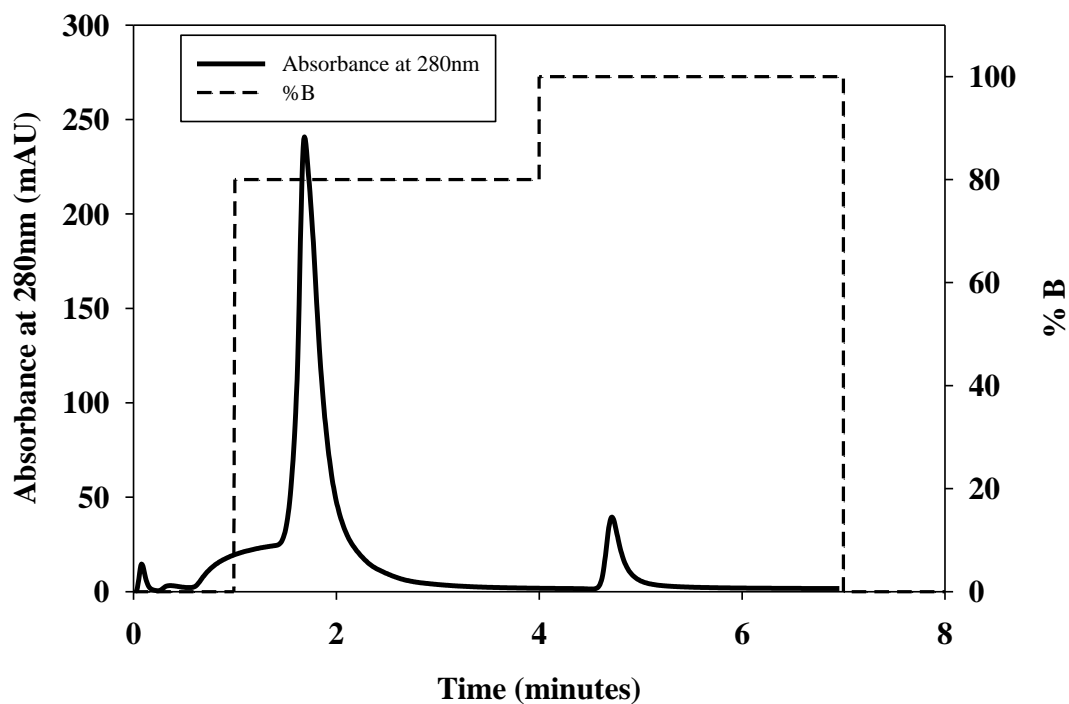


Figure 5-9 Final analytical method on the CIMac using a two-step process at 80% and 100% steps. The binding buffer was 0.8M ammonium sulphate and 100 μ l was loaded. The absorbance profile at 280nm shows the majority of material was eluted in the first step at 80%.

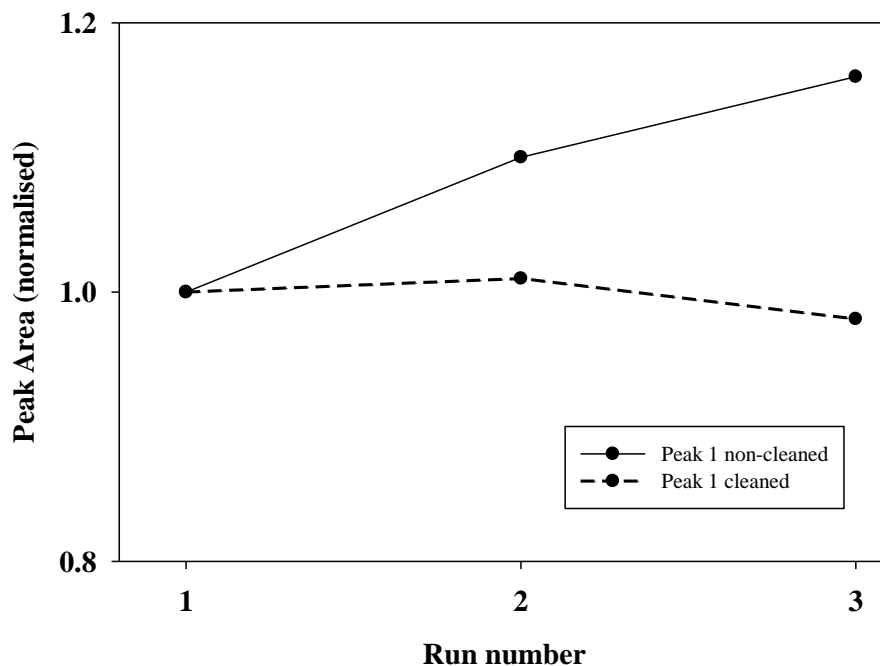


Figure 5-10 Initial runs on 0.1M CIMac at 0.8M ammonium sulphate, loading 100 μ L using triplicate samples showed a shift in peak sizes over successive runs, with or without cleaning between each sample run. As the size of peak 1 decreased peak 2 increased indicating that the binding affinity within the column was changing over runs, probably due to fouling.

5.3.7 Use of monolith analytical method to investigate the influence of residence time on monoliths

Samples were taken from the elution samples of all previous experiments looking at the residence time of the VLP on the HIC column. The samples were run on the CIMac column using the method developed. Using the Bradford and VLP ELISA assays on the elution samples taken from some of the runs a profile of the method was seen (Figure 5-11). Both peaks contain VLP, as seen by the ELISA profile. This would indicate that the VLP binds more weakly to the column in these samples.

The areas of the peaks decrease as the wash time was increased from 0 to 40 minutes as seen in Figure 5-12. Although the method cannot currently differentiate between protein and VLP the decrease in peak area, by as much as 50%, must indicate that the material in the samples has changed in concentration.

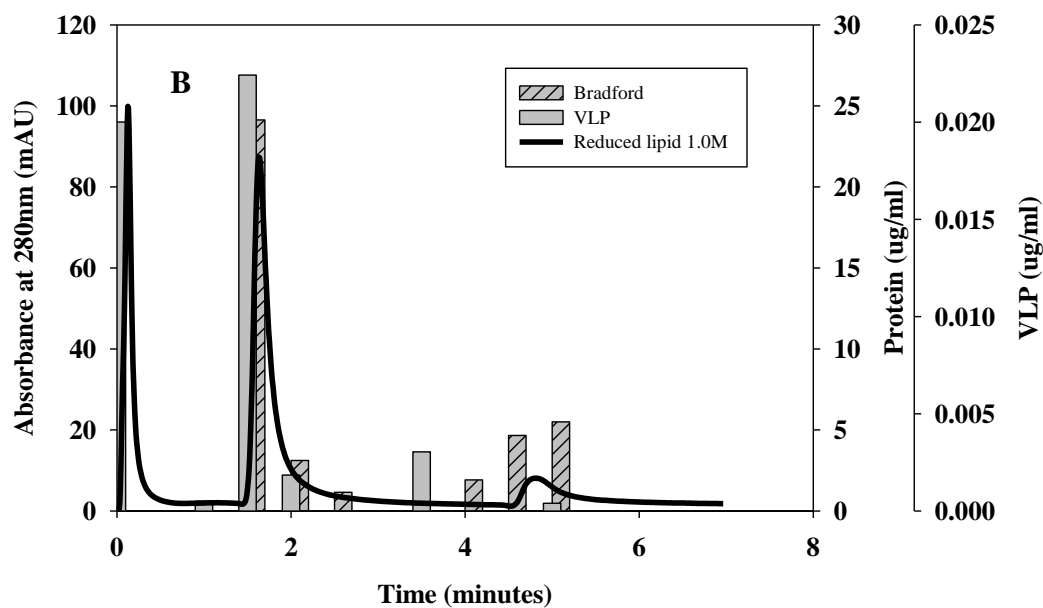
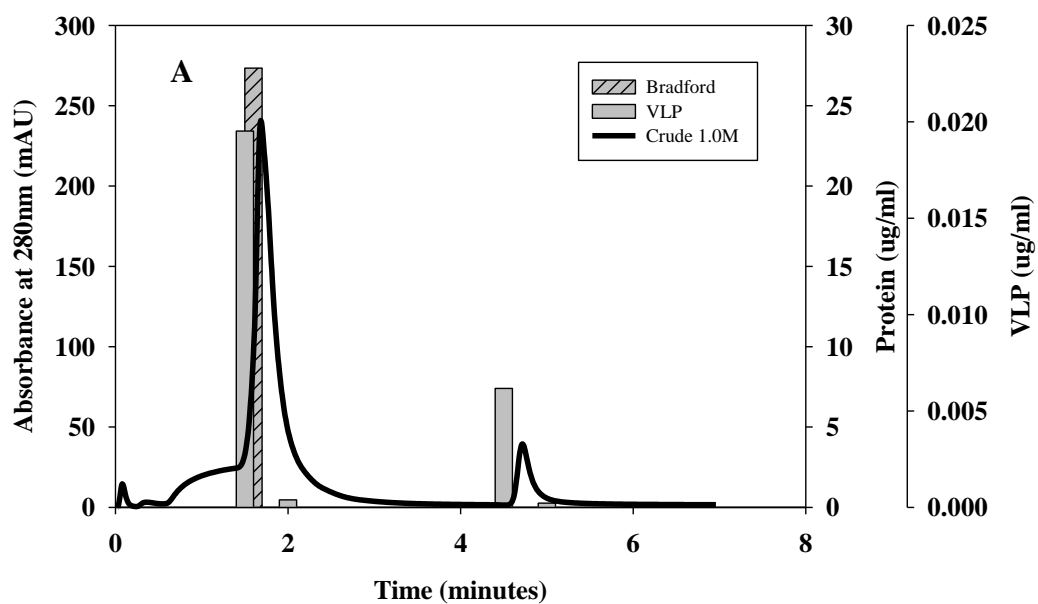


Figure 5-11 Graphs showing the absorbance trace seen at 280nm and comparisons with samples collected and tested for protein and VLP. (A) Crude sample 0 minutes; (B) Reduced lipid sample 0 minutes

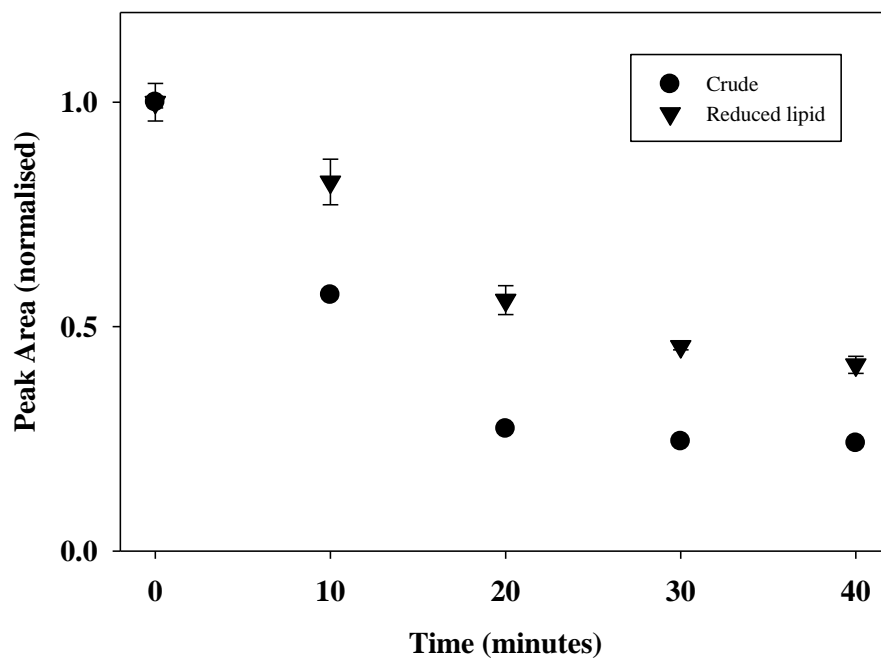
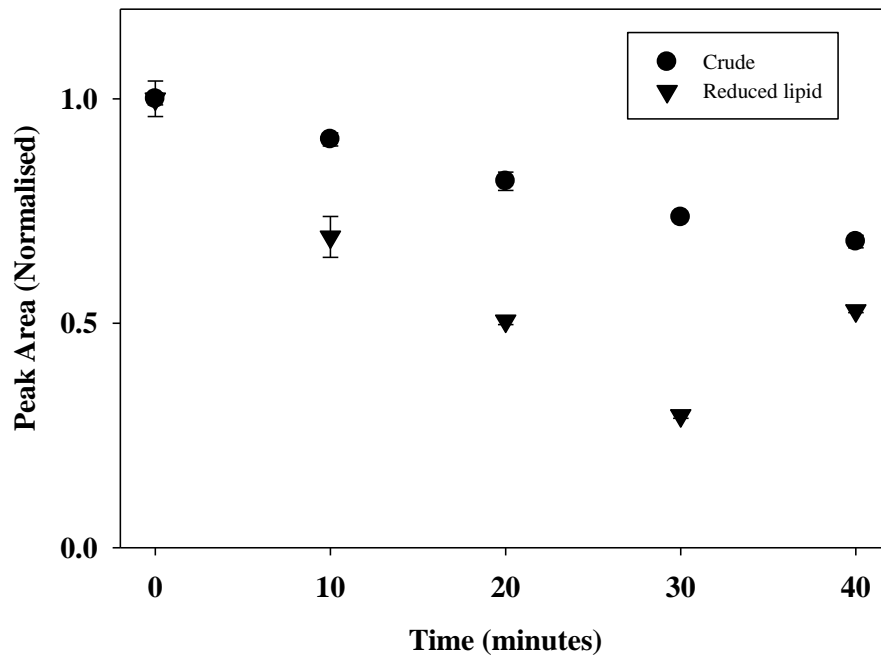


Figure 5-12 Results from CIMac column for elution samples after a wash time of 0 (standard elution profile) to 40 minute with crude (●) and reduced lipid (▼) feed material. (A) 1.0M binding buffer; (B) 0.6M binding buffer.

These results indicate that a high amount of lipid in the crude feed seems to have a stabilising effect on the molecule during the extended wash period when the

salt is at 1.0M. As seen by looking at the CIMac absorbance profiles the VLP and protein seem to form complexes, and it is possible that the lipid helps with this by increasing the hydrophobicity in the mixture. Further work needs to be carried out to see if any additives could be added in to the feed material to reduce the unfolding effects on the VLP, or if an extra processing step, (Zhao et al., 2006).

The data in *Figure 5-12* still shows a large decrease for the crude feed material at the low salt level of 0.6M ammonium sulphate. The reduced lipid feed at this salt concentration also decrease, although not as much as the crude feed. As the level of salt controls the degree of affinity of the column for the VLP it shows that this is the overriding force in changing the conformation of the VLP.

5.3.8 Comparison of analytical monolith method to the ELISA and Bradford assays

The CIMac method was developed as a complimentary method to the ELISA and Bradford assays currently used to analyse the material. Although the method has not been fully developed to enable quantification of the amount of VLP and protein it can still indicate if there is an increase or decrease in the amount of VLP or protein. When comparing all three methods it can be seen that the CIMac method has the possibility of reducing the degree of error (*Figure 5-13*). When compared to the ELISA assay we see similar trends, showing the method has promise to be used as an alternative. As the HPLC method can be run almost immediately after a chromatography run this would allow quick feedback on sample results. Whereas with the ELISA assay any chromatography runs must be completed before the assay can be run and the assay itself takes around 4 hours.

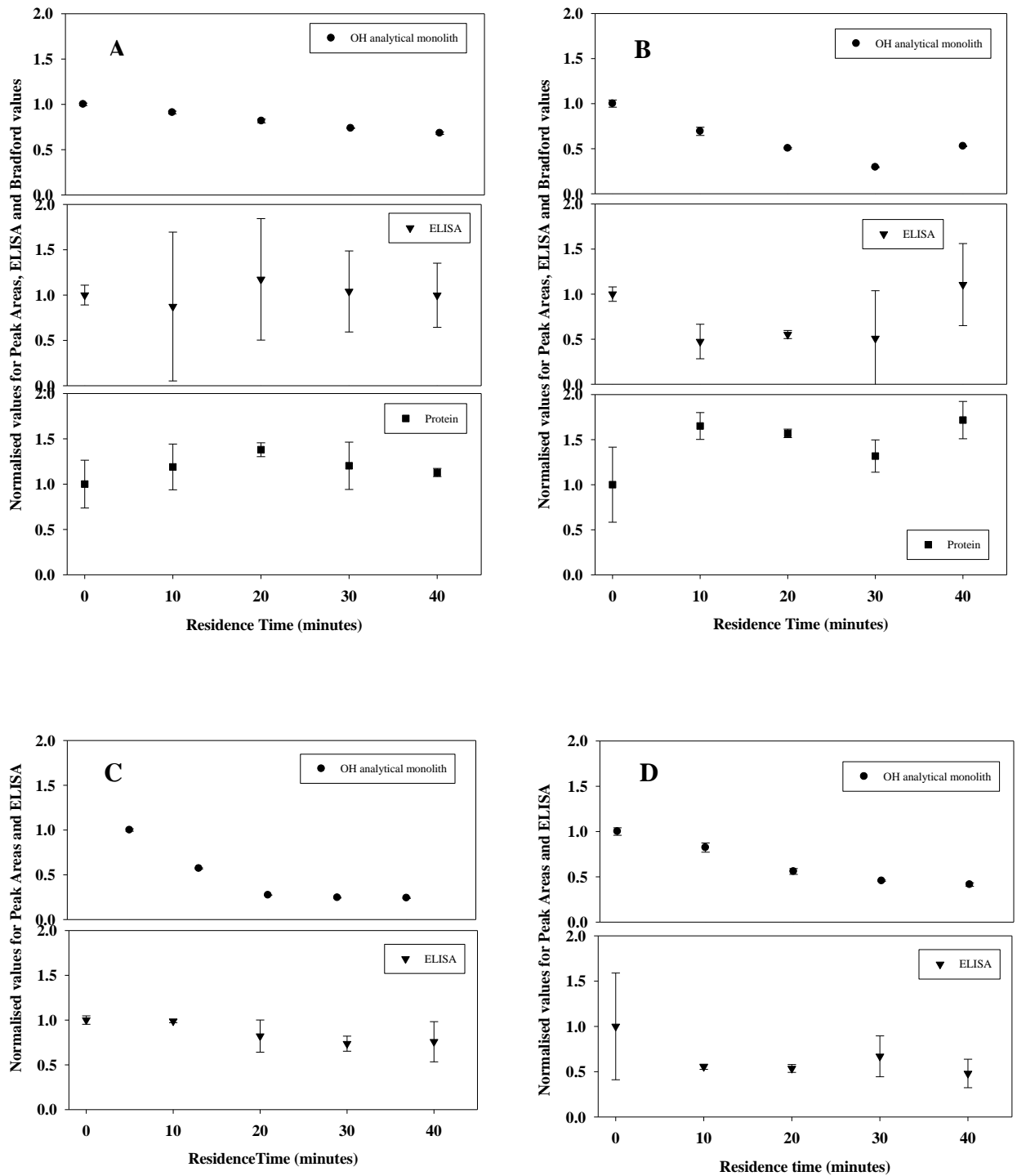


Figure 5-13 Comparisons for each residence time condition (salt level and lipid content) between all three assays (CIMac, ELISA and protein). (A) 1.0M Crude feed; (B) 1.0M Reduced lipid feed; (C) 0.6M Crude feed; (D) 0.6M Reduced lipid feed. Protein was unavailable for 0.6M as the level was below assay limits.

5.4 CONCLUSION

Early work on the monolith showed that the VLP would not elute off as expected during a gradient elution. The yield dropped to around 30% of the amount loaded, a decrease of 60% on the recovery value of an isocratic elution. The first half of this chapter focused on the effect of a hold time on the monolith column on the VLP elution profile to investigate why a gradient elution changed the recovery profile.

The effect of the hydrophobic ligands on proteins has been studied with the result that some of proteins can become unfolded on binding and the chromatographic process is then less effective (Xiao et al., 2007b). To determine if this mechanism occurs for VLP on the monolith the hold time of up to 40 minutes was added to the run during the loading step.

Overall four conditions were looked at, two salt levels (1.0M and 0.6M ammonium sulphate) and then crude and reduced lipid feeds. Previous work showed that the VLP binds stronger at the higher salt concentration and that the lipid in the feed can change the binding environment of the column. When the feed (either crude or reduced lipid) was loaded at the higher salt of 1.0M little decrease in the amount of VLP eluted was seen in the ELISA assay, over the 40 minutes. But when the lower salt concentration of 0.6M was used the ELISA assay showed a decrease with both the crude and reduced lipid feed, especially after 20 minutes. The effect was greater with the crude feed, with the yield of VLP decreasing to around 60%. Using a high salt level in the mobile phase conveys a greater binding affinity for the VLP to the column. The lipid in the feed contributes to the unfolding possibly by exacerbating the effect of the hydrophobic environment.

It was possible to study the elution profile for the VLP using a CIMac column or Bio-monolith. The method needs further development to understand how to separate the protein and VLP in the feed to produce individual peaks and therefore gain concentration information about the VLP. The elution samples were run on the analytical monolith, and the peak areas gave an indication of the protein, lipid and VLP concentrations. Running the samples showed increases and decreases of

amounts of the materials. At the current level it was assumed that the VLP and protein would be affected in the same way and therefore a peak decrease equalled a VLP decrease.

A comparison of the three different analytical methods showed that the degree of error from the chromatographic method was very small in comparison to the ELISA and Bradford methods. Combined with an ability to automate the process on the HPLC it makes it an attractive and viable alternative.

Samples analysed on DLS shows that most particles are around the size of 100nm, and proteins would not be expected to be around this size. As DLS looks for a hydrodynamic diameter of particles it is probably that these are aggregates of the material in the sample. It is rare to see any particles around the size of the VLP (22nm), even though they are visible in AFM or EM. It is more probable that the VLP is interacting with the protein to create these large aggregate particles.

6 PROJECT CONCLUSIONS AND FUTURE WORK

6.1 REVIEW OF PROJECT OBJECTIVES

6.1.1 Development of a monolithic VLP separation

Monoliths were originally developed as an alternative form of media, suitable for large macromolecules including viruses (Urbas et al., 2011a, Whitfield et al., 2009, Forcic et al., 2011, Kramberger et al., 2007, Kramberger et al., 2004, Jungbauer and Hahn, 2008, Jungbauer and Hahn, 2004). This project initially focused on the development of a monolith separation process for the VLP Hepatitis B Surface Antigen, which is a lipoprotein approximately 22nm in size (Gavilanes et al., 1982), and can be purified by conventional resin chromatography (Belew et al., 1991).

Knowing that the VLP is highly hydrophobic a weakly hydrophobic ligand is required to reversibly bind the VLP. A number of commercial and novel columns were tried in collaboration with BIA separations, including those with C4 (butyl) and OH (hydroxyl) ligands. The modification of the salt levels in hydrophobic interaction chromatography altered the degree of ligand and product interaction to help improve the capacity and yield.

This resulted in a new chromatography process using an OH monolith column, with 1M ammonium sulphate in the binding buffer. Comparison with the conventional column showed that the monolith had a binding capacity approximately 3-4 times greater. The yield of each column was comparable at around 90%.

A variety of analytical techniques were used to study the VLP. These included looking at the size and shape of the VLP with DLS, AFM and SEC, as well as zeta potential and the protein content. These enabled insights into the purification process and the effect on the VLP assembly and structure. The development of an AFM protocol confirmed that the VLP was the same size as detailed in literature.

At the process scale the increase in binding capacity for the monolith, in comparison to the equivalent volume resin column, would contribute to an increased

throughput of VLP during purification. If the same throughput was maintained, exchanging a resin column to a monolith would result in a decrease in facility footprint. Unfortunately the biggest commercially available column currently available is only 8L. This would impose limits on how large the processing volume could be to ensure the column does not become a bottleneck.

Another aspect to consider in the use of a monolith as a replacement for the resin is the economic comparison between the two methods. This would involve analysing the cost of goods for the unit operations, including the variable costs such as consumables, materials and labour, and the non-variable costs such as capital. A new technique is more likely to be adopted if it results in the overall process being more economically viable.

6.1.2 Interactions of impurities with hydrophobic monoliths

Previous work from confocal microscopy had shown that lipids in an HBsAg yeast homogenate caused irreversible fouling on conventional butyl-S HIC resins (Jin et al., 2010). Fouling the column with fluorescently labelled lipids showed irreversible fouling on monolith columns too. Labelling the lipids indicated that the structure of the monolith caused a different fouling pattern than on beads, with the column acting like a filter and building up lipids on the top of the column. A result of this was an increase in backpressure over subsequent runs.

A lipid removal technique using XAD-4/Amberlite reduced the lipid content by 70% but removed less than 20% of VLP. The current purification process already contained a XAD-4/Amberlite step to remove triton detergent, used in an earlier step. Use of a lipid removal filter was also successful as the level of VLP post use remained about 80% but it removed a lower percentage of lipid.

The ultimate goal in removing impurities is to improve a chromatographic process, by increasing capacity and throughput. The work demonstrated that removing the lipids from the feed had a significant effect on the binding capacity, increasing the DBC (10%) 2.5 times, supporting findings detailed in literature (Bracewell et al., 2008, Pampel et al., 2007, Kee et al., 2010). Related to this the pressure increase seen in loading over 10 runs using a reduced lipid feed was 65%

lower, when compared to a crude feed. Pressure increases can indicate a reduction in the width of the pores in the monolith and hence a build-up of fouling impurities (Zochling et al., 2004).

Increasing the binding capacity even greater, by removing any foulant material competing for binding space would further enhance the rate of VLP throughput on the column, reducing the overall time of the step. The reduction in the amount of lipid would also result in a longer life span for the column, as the column will experience less irreversible fouling, hence retaining its maximum binding capacity over a greater number of cycles. Ultimately the implementation of lipid removal would reduce the cost of goods, for the initial capture step.

6.1.3 Interactions and loss of product on hydrophobic monoliths

Study of the chromatogram using a gradient elution showed that the VLP had reduced in peak area as the length of time on column due to the gradient used is increased. Yield values decreased significantly with only 30% eluting over the longest gradient time interval of 30 minutes. Using a step elution after binding produces a 90% yield so the time factor was studied by leaving the VLP on the column for an increasing length of time, up to 40 minutes to observe a decrease in the VLP concentration after elution. The salt concentration in the binding buffer and the percentage of lipids in the material were also altered.

Altering the salt concentration changes the binding capacity and affinity within the column. When the salt was reduced to 0.6M ammonium in the binding buffer the effect of the hold time had a greater effect on the rate of unfolding, seen by a decrease in elution concentration. No change was seen with 1.0M ammonium sulphate, under conditions of greater affinity, or binding strength, of VLP to the column possibly conferring stability on binding. It had been seen that lipids in the feed material reduced the DBC on the column (Chapter 4), as well as increasing the hydrophobicity in the column (Jin et al., 2010). Removing the lipids prevented the decrease in VLP elution concentration seen with 0.6M ammonium sulphate, and again no effect was seen with 1.0M.

Overall having a high salt concentration of 1.0M in the mobile phase resulted in no VLP losses obtained even after 40 minutes additional contact time with the column with both the crude and reduced lipid feeds. This would suggest that any influence from the lipid, in terms of increasing on column hydrophobicity, has a limited effect and that the strength of binding is the dominant force. At 0.6M the adsorption reaction and strength of binding to the column is decreased, as seen by a reduced binding capacity. For low salt concentrations the reaction rate constants for adsorption and spreading are within the same order or magnitude. Thus the spreading reactions affect the adsorption equilibrium (Haimer et al., 2007). Reduced binding strength may allow flexibility of the VLP when attached to ligand. Previous work has seen that the concentration on loading had an influence (Fogle et al., 2006). Further work would try to evaluate whether the VLP concentration on loading at 1.0M would have any effect on the VLP structure over contact time.

Manipulating the flow rate in the column showed that the concentration of the VLP remained consistent as flow rates were increased up to four times above the original flow rate. This confirmed that the VLP acted as expected and that this could be used to reduce any hold time of the VLP on the column. The only issue would be the increase in pressure seen over the increased flow rate, but this was a factor of the feed material itself and not the column.

This work begins to illustrate the importance of understanding how other factors, not only the known ones such as salt, can affect the recovery in chromatography. In this case the column VLP contact time and feed material composition proved to also exert an influence. As the process is scaled it becomes even more important to ensure that recovery yields are high and the VLP integrity is unaffected, namely to ensure the process is efficient and cost effective.

6.2 FUTURE WORK

The objective of the project was to look at the use of a monolithic absorbent to use as a capture step for a virus-like particle. Development work on understanding both the influence of various factors on the chromatographic process has shown that these need to be controlled to ensure a successful separation process. Future work would seek to further develop knowledge on the chromatographic separation process by focusing on the difficulties encountered so far and expanding the breadth of understanding on both the chromatographic side and the VLP.

Any future work would focus on either controlling the chromatography media to alter the adsorptive environment, or look at manipulating the VLP feed material; both equally important in ensuring a full understanding a capture step using a monolithic absorbent.

6.2.1 Controlling and understanding the adsorptive environment

- Use confocal microscopy to study the binding of the VLP to the column. CLSM is a valuable and powerful tool as it is non-destructive and can be used to monitor binding of a fluorescently labelled molecule on an adsorptive surface. Work has been published which looked at the binding pattern of lysozyme on a membrane absorber (Sartobind) (Wang et al., 2008). As the monolith has a very similar structure to membranes the method could be adapted. Using CLSM could allow visualisation of phenomena such as the binding pattern of VLP on monoliths and how the lipid fouling changes the binding pattern.
- Study the degree of product unfolding which occurs during adsorption. Further work is needed to determine if the unfolding which occurs on the HIC column is reversible or irreversible. The VLP is made up of a lipid layer with the S protein imbedded in it. When the unfolding occurs it is unknown whether the lipid layer is moving or it is the protein which is deforming. Previous work has used hydrogen exchange or fluorescence studies on amino acids to study the degree of unfolding (Jones and Fernandez, 2003, Xiao et al., 2007a, Oroszlan et al., 1990). Another effect which can be studied would

be the concentration of VLP on binding. Reducing the concentration of VLP could encourage the spreading of VLP on the column as the ligand/VLP would be increased and therefore the increase of forces on the VLP would increase (Haimer et al., 2007).

- Control the binding affinity of the column for the VLP. Increasing or reducing the binding affinity of the VLP to the column can have an influence on the capacity and yield in the chromatography step. Variables which can be manipulated in the column include the ligand density or the pore size to determine the optimum to maximum values which would ensure maximum capacity and stability for the VLP but still allow desorption from the column.
- Use a 100µl analytical monolith as a tool to allow fast analysis. The CIMac column can be used with a HPLC enabling easy manipulation of the chromatography protocol for short, fast runs to provide insight on conformation and quantity. Current analytical methods to quantify the VLP are limited and may involve breaking the VLP apart and looking at the amount of protein. Size exclusion chromatography is very difficult to undertake due to the size of the VLP, whereas the monolith has already been proven to allow easy passage of the VLP.

6.2.2 Adjustment of VLP feed material

- Stabilise the binding of the VLP before the chromatography step. Research highlighted that when the VLP resides on the column for a significant period of time it is liable to unfold, reducing the amount of viable VLP which is eluted. Stabilising the VLP before using it on the column may prevent the unfolding phenomenon that occurs. Merck have shown the VLP can be stabilised by increasing the amount of disulphide bonding in the molecule (Zhao et al., 2006).
- Control the binding affinity of the VLP for the column. Changing the conditions of the feed can also affect the affinity of the VLP for the ligands, such as the pH of the mobile phase or by including stabilising amino acids. Varying the conditions can be used to manipulate the binding capacity and the stability of the VLP on the column.

- Adapt the method of using XAD- 4/Amberlite from a batch process to a continuous process. The batch process was ideal for small batches in the lab but would not scale up easily. XAD-4 can be packed into a column so that material is flowed through.
- Develop a CIP regime to remove the lipid that irreversible binds on to the column. Currently the use of 30% isopropanol is recommended but this did not remove any lipid, as seen during the use of preparing the column for confocal microscopy. Further work would need to identify any reagents, such as reducing agents or lipases, which would remove the lipid from the column pores but not the ligands. An effective CIP regime would allow regeneration of the column to its pre-use form, increasing the number of resin uses for the column and therefore the lifetime of the monolith.
- The lipids contained in the feed material are a natural component of the yeast cells used to produce the VLP. Yeast use lipids for energy storage and are closely associated with the VLP in the ER. Besides from removing the lipids before chromatography a long term strategy could be cell line engineering to reduce the lipid content in the cell.

7 VALIDATION AND PROCESS ECONOMICS OF A CHROMATOGRAPHY UNIT OPERATION

7.1 PROCESS VALIDATION

To ensure that any drug produced and sold is safe companies have to abide by guidelines set down by a number of regulatory bodies. These guidelines are known as Process Validation and cGMP (current good manufacturing process).

The cGMP regulations require that a manufacturing process is designed in such a way that it can consistently produce a product which is within predetermined and acceptable criteria. Process validation is an important part of cGMP, to verify that the process performs as stated. The EMEA regulations describe validation as:

“Process validation can be defined as documented evidence that the process, operated within established parameters, can perform effectively and reproducibly to produce a medicinal product meeting its predetermined specifications and quality attributes.”

Regulatory bodies such as the FDA (USA), EMEA (EU), and the cross collaboration ICH (International Conference for Harmonisation) publish guidelines for manufacturers and industry so that they can understand current thinking. The FDA guidance was published in 2011, and the EMEA document is currently under consultation to update it. Without a full and complete process validation in a regulatory submission a drug may not meet approval and therefore be unsellable.

Process validation is applicable from the design of the process to the commercial production and beyond. The FDA defines it into three parts:

- Stage 1 – Process Design: The commercial manufacturing process is defined during this stage based on knowledge gained through development and scale-up activities.

- Stage 2 – Process Qualification: During this stage, the process design is evaluated to determine if the process is capable of reproducible commercial manufacturing.
- Stage 3 – Continued Process Verification: On-going assurance of the process.

Stage 1, process design, does not have to be run under cGMP conditions and is often carried out in small-scale laboratories. Once the process has been defined stage 2 involves the design of the facility, and qualifying the equipment and utilities. The second part of stage 2 involves producing batches of product using the facility, equipment, testing methods, and trained personnel just like the real process. If the process performs as predicted in the protocol it can assumed it is in a state of control. Once the commercial process is producing product the process validation enters stage 3. During this stage a manufacturer wants to show that the process is under control (the validated state) and that they also are aware of sources of variability. The addition of continuous PQ has resulted in new EMEA regulations.

The validation program within a company or with a product will be successful if information and knowledge on the product is gained in process development and applied in the correct manner to the manufacturing process. It enables manufacturers to:

- a) Understand sources of variation,
- b) Detect the presence and degree of variation,
- c) Understand the impact of variation on the process and product attributes,
- d) Control variation with the degree dependant on the risk it represents.

Validation of the chromatography step would involve producing data detailing the elution results including the impurity carryover and/or physical changes to the VLP using analytical tools. Details of the specification limits would need to be not too restrictive or too wide to ensure the column could consistently produce material within the ranges. Too restrictive and a large number of failed batches would occur, too loose and it indicates a lack of control over the column.

7.2 POST-APPROVAL CHANGES TO A COMMERCIAL MANUFACTURING PROCESS

Once a product is approved by the regulatory authorities the manufacturing process is fixed. Any change to the manufacturing process, i.e. consumables or equipment, will require reporting or notification to the relevant regulatory authority. Part of the validation plan is to have clearly defined procedures to control any changes. The EMEA states that “such procedures should tightly control planned changes, ensuring sufficient supporting data is generated to demonstrate that the revised process will result in a product of the desired quality, consistent with the approved specification and ensure that all aspects are thoroughly documented and approved including whether regulatory approval is needed by way of variation.”

Comparing the monolith to traditional resin columns showed it had a higher capacity and, with a faster flow rate, throughput was increased. If a company wanted to change the resin for a monolith post approval they would have to go through a procedure to see what effect the change has on the safety and effectiveness of the product.

The FDA has draft guidance for industry on manufacturing chromatography systems post approval changes (October 2004). It clearly details the steps and validation needed by a company to show the impact of the change, such as the reassessment of the critical controls, which are important to control to ensure that the drug meets its predefined specification. This may include stability studies.

The guidelines recognise that there are two major factors for determining comparability; 1) the impurity profile and 2) physical/structural properties. The impurity profiles, for unit op or multiple unit ops, between the old and new process must be compared to evaluate old and new impurities which may arise. Analytical technology must be adequate to perform the task, especially if new tests are needed for new impurities. Impurities may be process and/or product related. A profile is considered comparable by the FDA after 3 similar batches if:

- a) No new impurity exceeds ICH Q3A id threshold of 0.1%,

- b) Level of each specified or existing impurity doesn't exceed current or historical specification limits,
- c) Total level of impurities doesn't exceed current or historical specification.

If the impurity profile is different pre-clinical studies, including safety and PIC studies may be required.

Physical properties include aggregates, glycosylation patterns, variants etc. The analytics need to detect these changes and therefore bioassays and/or PK/PD studies may be required. Animal test may be needed if bioassays are not accurate to detect small tertiary changes. Long term stability data may also be needed.

The FDA categorizes changes into three levels

- Minimal – reported in the company's annual report
- Moderate – report to FDA for approval,
- Substantial – report to FDA for approval.

Using the recommended actions from the FDA guidance for industry (chromatography-PAC), documents, and tests, in the guidance the following table details the changes in moving from a resin to a monolith column. There are no changes in the mobile phase, equipment, addition/subtraction of columns, or site changes from the resin process. When multiple related changes occur, with different reporting categories for individual changes, the filing should be in accordance with the most restrictive of those recommended for the individual changes.

Change from resin column	Change category	Reason for category (changes in process)	Test Documentation
Stationary phase	Moderate	<p>Change in manufacturer of the packing material.</p> <p>Change in composition of the solid support (sepharose to polyacrylamide)</p>	<p>Evaluate leachables, capacity and yield.</p> <p>Prospective or concurrent resin lifetime studies to level of previously used resin. Assessment of impact on carry-over of impurities or impact on viral clearance.</p> <p>Three consecutive batches made using new stationary phase, compared to historical data and description of source of historical data.</p> <p>Stability testing required.</p>
Chromatographic conditions	Moderate	<p>Change in flow rate for the elution, cleaning and/or regeneration phase</p> <p>Changes in load composition (conductivity)</p>	<p>Revalidation of lifetimes of resin might be required to show increased load does not adversely impact the ability of the resin to clear impurities.</p> <p>Assessment of impact on carry-over of impurities or impact on viral clearance.</p> <p>Three consecutive batches made using new chromatographic conditions compared to historical data, and source for historical data, to demonstrate no adverse impact of change on drug substance.</p> <p>Stability testing.</p>

Changes in column size	Substantial potential	Increased/decreased column size – changing bed height and column diameter and/or making changes to the load or washes to the column	<p>Assessment of no impact on carry-over of impurities or impact on viral clearance. Revalidation of the column lifetimes and process required as the proportions of load and washes are changing, or the bed height is different.</p> <p>Three consecutive batches made using new columns, historical data for comparison and description of source of historical data.</p> <p>Stability testing.</p>
------------------------	-----------------------	---	--

Table 7.2-1 Table of validation documents needed for post-approval changes switching from resin columns to a monolith

7.3 PROCESS ECONOMICS

Alongside the validation of a process it is also important to look at the economics behind each unit operation. The cost of goods for each unit can be broken down into fixed costs and variable costs. The fixed costs include the capital, i.e. equipment costs and facility costs. Fixed costs will be the same no matter how many batches are run as the equipment has to be brought regardless. The variable costs include materials, consumables and labour, which will depend on the number of batches run.

There are a variety of models which are now used in process development to look at the process economics of a chromatography step. Models can be used by process development to look at different scenarios (e.g. resin type, binding capacity, cycles, and diameter) and give insights into how one change can have an overall effect on the process. These can include cost of goods models for the overall economics, simulation models or statistical models, such as those for design of experiments (DoE). DoE help reduce the overall time and cost of process development by reducing the number of experiments needed to acquire statistical relevant results.

There are a number of variables which need to be considered for a chromatography step, which will affect the process economics of the step. These include:

- Binding capacity of the chromatography resin - this will determine the size of the column required, and hence volume and cost of resin, to complete the purification of a molecule in a predetermined number of cycles;
- Number of cycles – as the number of cycles is increased the amount of material needed to bind on each cycle is reduced, reducing the volume of resin needed;
- Volume of column – as determined by the binding capacity and the number of cycles;
- Time of the chromatography phases and unit operation – this is dependent on the flow rate during the phases and the number of phases in each run.

- Reuses/lifetime of the resin – this will determined how often the column must be replaced.

It is these variables which can be used to compare the resin column and the monolith. The binding capacity of the monolith was shown to be greater than the resin. This would reduce the number of cycles that would be needed on a column and would therefore reduce the length of time for the unit operation. It would also mean a smaller column could be used. The flow rates in a monolith can be increased compared to a resin column. This would directly reduce the time of the unit operation. Combined these variables would result in a higher throughput for the column and an overall reduction in the process time.

These benefits though have to be used in collaboration with the cost of the column and the column lifetime. If the column is more expensive compared to the conventional resin and has a shorter lifetime, the reduction in cost from the higher binding capacity and time may not be enough to make the unit operation economically cheaper. This will be product and feed dependant. Considering that many of the macromolecules have very low binding capacities with conventional resins it is likely that changing to monoliths will produce a process which is more economically viable.

8 REFERENCES

- AFEYAN, N. B., GORDON, N. F., MAZSAROFF, I., VARADY, L., FULTON, S. P., YANG, Y. B. & REGNIER, F. E. 1990. Flow-through Particles for the High-Performance Liquid-Chromatographic Separation of Biomolecules - Perfusion Chromatography. *Journal of Chromatography*, 519, 1-29.
- ALMEIDA, J. D. & WATERSON, A. P. 1969. Immune complexes in hepatitis. *Lancet*, 2, 983-6.
- ARAKAWA, T. & TIMASHEFF, S. N. 1982. Preferential interactions of proteins with salts in concentrated solutions. *Biochemistry*, 21, 6545-52.
- ARVIDSSON, P., PLIEVA, F. M., SAVINA, I. N., LOZINSKY, V. I., FEXBY, S., BULOW, L., GALAEV, I. Y. & MATTIASSON, B. 2002. Chromatography of microbial cells using continuous supermacroporous affinity and ion-exchange columns. *Journal of Chromatography A*, 977, 27-38.
- ASLIYUCE, S., UZUN, L., RAD, A. Y., UNAL, S., SAY, R. & DENIZLI, A. 2012. Molecular imprinting based composite cryogel membranes for purification of anti-hepatitis B surface antibody by fast protein liquid chromatography. *Journal of Chromatography B-Analytical Technologies in the Biomedical and Life Sciences*, 889-890, 95-102.
- BAILEY, J. E. & OLLIS, D. F. 1986. *Biochemical Engineering Fundamentals*, New York; London, McGraw-Hill.
- BALDWIN, R. L. 1996. How Hofmeister ion interactions affect protein stability. *Biophysical Journal*, 71, 2056-63.
- BARTON, R. J. 1977. Examination of Permeation Chromatography on Columns of Controlled Pore Glass for Routine Purification of Plant-Viruses. *Journal of General Virology*, 35, 77-87.

BARUT, M., PODGORNIK, A., BRNE, P. & STRANCAR, A. 2005. Convective Interaction Media short monolithic columns: Enabling chromatographic supports for the separation and purification of large biomolecules. *Journal of Separation Science*, 28, 1876-1892.

BARUT, M., PODGORNIK, A., MERHAR, M. & STRANCAR, A. 2003. Short Monolithic Columns - Rigid Disks. In: SVEC, F., TENNIKOVA, T. & DEYL, Z. (eds.) *Monolithic Materials: Preparation, properties and applications*. The Netherlands: Elsevier Science B.V.

BAYER, M. E., BLUMBERG, B. S. & WERNER, B. 1968. Particles associated with Australia antigen in the sera of patients with leukaemia, Down's Syndrome and hepatitis. *Nature*, 218, 1057-9.

BELEW, M., YAFANG, M., BIN, L., BERGLOF, J. & JANSON, J. 1991. Purification of recombinant hepatitis B surface antigen produced by transformed Chinese hamster ovary (CHO) cell line grown in culture. *Bioseparation*, 1, 397-408.

BELLIER, B., DALBA, C., CLERC, B., DESJARDINS, D., DRURY, R., COSSET, F. L., COLLINS, M. & KLATZMANN, D. 2006. DNA vaccines encoding retrovirus-based virus-like particles induce efficient immune responses without adjuvant. *Vaccine*, 24, 2643-2655.

BENCINA, K., PODGORNIK, A., STRANCAR, A. & BENCINA, M. 2004a. Enzyme immobilization on epoxy- and 1,1'-carbonyldiimidazole-activated methacrylate-based monoliths. *Journal of Separation Science*, 27, 811-818.

BENCINA, M., PODGORNIK, A. & STRANCAR, A. 2004b. Characterization of methacrylate monoliths for purification of DNA molecules. *Journal of Separation Science*, 27, 801-810.

BENEDEK, K. 1988. Thermodynamics of Alpha-Lactalbumin Denaturation in Hydrophobic-Interaction Chromatography and Stationary Phases Comparison. *Journal of Chromatography*, 458, 93-104.

- BENEDEK, K., DONG, S. & KARGER, B. L. 1984. Kinetics of Unfolding of Proteins on Hydrophobic Surfaces in Reversed-Phase Liquid-Chromatography. *Journal of Chromatography*, 317, 227-243.
- BIDDLECOMBE, J. G., SMITH, G., UDDIN, S., MULOT, S., SPENCER, D., GEE, C., FISH, B. C. & BRACEWELL, D. G. 2009. Factors Influencing Antibody Stability at Solid-Liquid Interfaces in a High Shear Environment. *Biotechnology Progress*, 25, 1499-1507.
- BLANCHE, F., BARBOT, A. & CAMERON, B. 2003. *Method of separating viral particles*. United States patent application.
- BLANCHE, F., CAMERON, B., BARBOT, A., FERRERO, L., GUILLEMIN, T., GUYOT, S., SOMARRIBA, S. & BISCH, D. 2000. An improved anion-exchange HPLC method for the detection and purification of adenoviral particles. *Gene Therapy*, 7, 1055-62.
- BLANCHET, M. & SUREAU, C. 2007. Infectivity determinants of the hepatitis B virus pre-S domain are confined to the N-terminal 75 amino acid residues. *Journal of Virology*, 81, 5841-9.
- BONOMO, R. C. F., MINIM, L. A., COIMBRA, J. S. R., FONTAN, R. C. I., DA SILVA, L. H. M. & MINIM, V. P. R. 2006. Hydrophobic interaction adsorption of whey proteins: Effect of temperature and salt concentration and thermodynamic analysis. *Journal of Chromatography B-Analytical Technologies in the Biomedical and Life Sciences*, 844, 6-14.
- BOUSHABA, R., BALDASCINI, H., GERONTAS, S., TITCHENER-HOOKER, N. J. & BRACEWELL, D. G. 2011. Demonstration of the Use of Windows of Operation to Visualize the Effects of Fouling on the Performance of a Chromatographic Step. *Biotechnology Progress*, 27, 1009-1017.
- BRACEWELL, D. G., BOYCHYN, M., BALDASCINI, H., STOREY, S. A., BULMER, M., MORE, J. & HOARE, M. 2008. Impact of clarification strategy on

chromatographic separations: Pre-processing of cell homogenates. *Biotechnology and Bioengineering*, 100, 941-9.

BRANOVIC, K., BUCHACHER, A., BARUT, M., STRANCAR, A. & JOSIC, D. 2003. Application of semi-industrial monolithic columns for downstream processing of clotting factor IX. *Journal of Chromatography B-Analytical Technologies in the Biomedical and Life Sciences*, 790, 175-182.

BRANOVIC, K., FORCIC, D., IVANCIC, J., STRANCAR, A., BARUT, M., KOSUTIC GULIJA, T., ZGORELEC, R. & MAZURAN, R. 2004. Application of short monolithic columns for fast purification of plasmid DNA. *J Chromatography B-Analytical Technologies in the Biomedical and Life Sciences*, 801, 331-7.

BRIGHT, R. A., CARTER, D. M., CREVAR, C. J., TOAPANTA, F. R., STECKBECK, J. D., COLE, K. S., KUMAR, N. M., PUSHKO, P., SMITH, G., TUMPEY, T. M. & ROSS, T. M. 2008. Cross-Clade Protective Immune Responses to Influenza Viruses with H5N1 HA and NA Elicited by an Influenza Virus-Like Particle. *Plos One*, 3.

BRUCE, S. A. & MURRAY, K. 1995. Mutations of Some Critical Amino-Acid-Residues in the Hepatitis-B Virus Surface-Antigen. *Journal of Medical Virology*, 46, 157-161.

BRUSS, V. & GANEM, D. 1991a. Mutational analysis of hepatitis B surface antigen particle assembly and secretion. *Journal of Virology*, 65, 3813-20.

BRUSS, V. & GANEM, D. 1991b. The role of envelope proteins in hepatitis B virus assembly. *Proceeding of the National Academy of Science of the United States of America*, 88, 1059-63.

BUCKLAND, B. C. 2005. The process development challenge for a new vaccine. *Nat Med*, 11, S16-9.

BUNDY, B. C. & SWARTZ, J. R. 2011. Efficient disulfide bond formation in virus-like particles. *Journal of Biotechnology*, 154, 230-9.

BURNS, N. R., SAIBIL, H. R., WHITE, N. S., PARDON, J. F., TIMMINS, P. A., RICHARDSON, S. M., RICHARDS, B. M., ADAMS, S. E., KINGSMAN, S. M. & KINGSMAN, A. J. 1992. Symmetry, flexibility and permeability in the structure of yeast retrotransposon virus-like particles. *EMBO J*, 11, 1155-64.

CARTA, G. & JUNGBAUER, A. 2010. Lab and process columns and equipment. In: CARTA, G. & JUNGBAUER, A. (eds.) *Protein Chromatography: process development and scale-up*. Austria: Wiley-VCH.

CARTY, C. E., TEKAMPOLSON, P., ROSENBERG, S., MCALEER, W. J. & MAIGETTER, R. Z. 1989. Galactose-Regulated Expression of Hepatitis-B Surface-Antigen by a Recombinant Yeast. *Biotechnology Letters*, 11, 301-306.

CHAMBERS, S. D., GLENN, K. M. & LUCY, C. A. 2007. Developments in ion chromatography using monolithic columns. *Journal of Separation Science*, 30, 1628-45.

CHEN, Z., XU, L., LIANG, Y., WANG, J., ZHAO, M. & LI, Y. 2008. Polyethylene glycol diacrylate-based supermacroporous monolithic cryogel as high-performance liquid chromatography stationary phase for protein and polymeric nanoparticle separation. *Journal of Chromatography A*, 1182, 128-31.

CHENG, K.-S., RAMASWAMY, S., BIAN, N., GAGNON, B., UMANA, J. & SOICE, N. P. 2010. *Method and Apparatus for Making Porous Agarose Beads*.

CHIOU, H. L., LEE, T. S., KUO, J., MAU, Y. C. & HO, M. S. 1997. Altered antigenicity of 'a' determinant variants of hepatitis B virus. *Journal of General Virology*, 78 (Pt 10), 2639-45.

COLEMAN, P. F. 2006. Detecting hepatitis B surface antigen mutants. *Emerging Infectious Diseases*, 12, 198-203.

COOK, J. 2003. *Process for purifying human papillomavirus virus-like particles*.

- COOK, J. C., JOYCE, J. G., GEORGE, H. A., SCHULTZ, L. D., HURNI, W. M., JANSEN, K. U., HEPLER, R. W., IP, C., LOWE, R. S., KELLER, P. M. & LEHMAN, E. D. 1999. Purification of virus-like particles of recombinant human papillomavirus type 11 major capsid protein L1 from *Saccharomyces cerevisiae*. *Protein Expression and Purification*, 17, 477-484.
- CRAWFORD, S. E., LABBE, M., COHEN, J., BURROUGHS, M. H., ZHOU, Y. J. & ESTES, M. K. 1994. Characterization of Virus-Like Particles Produced by the Expression of Rotavirus Capsid Proteins in Insect Cells. *Journal of Virology*, 68, 5945-5952.
- CZABANY, T., ATHENSTAEDT, K. & DAUM, G. 2007. Synthesis, storage and degradation of neutral lipids in yeast. *Biochimica Et Biophysica Acta-Molecular and Cell Biology of Lipids*, 1771, 299-309.
- DAINIAK, M. B., GALAEV, I. Y. & MATTIASSON, B. 2006. Affinity cryogel monoliths for screening for optimal separation conditions and chromatographic separation of cells. *Journal of Chromatography A*, 1123, 145-50.
- DANE, D. S., CAMERON, C. H. & BRIGGS, M. 1970. Virus-like particles in serum of patients with Australia-antigen-associated hepatitis. *Lancet*, 1, 695-8.
- DANQUAH, M. K. & FORDE, G. M. 2007. The suitability of DEAE-Cl active groups on customized poly (GMA-co-EDMA) continuous stationary phase for fast enzyme-free isolation of plasmid DNA. *Journal of Chromatography B-Analytical Technologies in the Biomedical and Life Sciences*, 853, 38-46.
- DANQUAH, M. K. & FORDE, G. M. 2008. Large-volume methacrylate monolith for plasmid purification - Process engineering approach to synthesis and application. *Journal of Chromatography A*, 1188, 227-233.
- DESAI, M. A. & MERINO, S. P. 2000. Application of Density Gradient Ultracentrifugation Using Zonal Rotors in the Large-Scale Purification of

Biomolecules. In: DESAI, M. A. (ed.) *Downstream Processing of Proteins: Methods and Protocols*. USA: Humana Press Inc.

DESOMBERE, I., WILLEMS, A., GIJBELS, Y. & LEROUX-ROELS, G. 2006. Partial delipidation improves the T-cell antigenicity of hepatitis B virus surface antigen. *Journal of Virology*, 80, 3506-3514.

DHANOYA, A., CHAIN, B. M. & KESHAVARZ-MOORE, E. 2012. Role of DNA topology in uptake of polyplex molecules by dendritic cells. *Vaccine*, 30, 1675-1681.

DIMINSKY, D., MOAV, N., GORECKI, M. & BARENHOLZ, Y. 2000. Physical, chemical and immunological stability of CHO-derived hepatitis B surface antigen (HBsAg) particles. *Vaccine*, 18, 3-17.

DIMINSKY, D., SCHIRMBECK, R., REIMANN, J. & BARENHOLZ, Y. 1997. Comparison between hepatitis B surface antigen (HBsAg) particles derived from mammalian cells (CHO) and yeast cells (*Hansenula polymorpha*): composition, structure and immunogenicity. *Vaccine*, 15, 637-47.

DOAN, L. X., LI, M., CHEN, C. Y. & YAO, Q. Z. 2005. Virus-like particles as HIV-1 vaccines. *Reviews in Medical Virology*, 15, 75-88.

EBERT, S. & FISCHER-FRUHHOLZ, S. 2011. Efficient aggregate removal from impure pharmaceutical active antibodies. *BioProcess International*, 9, 36-42.

EBLE, B. E., LINGAPPA, V. R. & GANEM, D. 1986. Hepatitis B surface antigen: an unusual secreted protein initially synthesized as a transmembrane polypeptide. *Molecular and Cellular Biology*, 6, 1454-63.

EON-DUVAL, A. & BURKE, G. 2004. Purification of pharmaceutical-grade plasmid DNA by anion-exchange chromatography in an RNase-free process. *Journal of Chromatography. B-Analytical Technologies in the Biomedical and Life Sciences*, 804, 327-35.

ETZEL, M. R. & RIORDAN, W. T. 2009. Viral clearance using monoliths. *Journal of Chromatography A*, 1216, 2621-2624.

FAUDE, A., ZACHER, D., MULLER, E. & BOTTINGER, H. 2007. Fast determination of conditions for maximum dynamic capacity in cation-exchange chromatography of human monoclonal antibodies. *Journal of Chromatography A*, 1161, 29-35.

FEE, C. J. & CHAND, A. 2005. Design Considerations for the Batch Capture of Proteins from Raw Whole Milk by Ion Exchange Chromatography. *Chemical Engineering Technology*, 28, 1360-1366.

FERNANDEZ-LAHOIRE, H. M., KLEEF, R., KULA, M. & THOMMES, J. 1999. The influence of complex biological feedstock on the fluidization and bed stability in expanded bed adsorption. *Biotechnology and Bioengineering*, 64, 484-96.

FERREIRA, G. N., MONTEIRO, G. A., PRAZERES, D. M. & CABRAL, J. M. 2000. Downstream processing of plasmid DNA for gene therapy and DNA vaccine applications. *Trends in biotechnology*, 18, 380-8.

FOGLE, J. L., O'CONNELL, J. P. & FERNANDEZ, E. J. 2006. Loading, stationary phase, and salt effects during hydrophobic interaction chromatography: alpha-lactalbumin is stabilized at high loadings. *Journal of Chromatography A*, 1121, 209-18.

FORCIC, D., BRGLES, M., IVANCIC-JELECKI, J., SANTAK, M., HALASSY, B., BARUT, M., JUG, R., MARKUSIC, M. & STRANCAR, A. 2011. Concentration and purification of rubella virus using monolithic chromatographic support. *Journal of Chromatography B-Analytical Technologies in the Biomedical and Life Sciences*, 879, 981-986.

FORSQREN, P.-O., FRANKSSON, D. & LILJEBORG, A. 1990. Software + Electronics for a digital 3D microscopy. In: WILSON, T. (ed.) *Confocal Microscopy*. UK: Academic Press Ltd.

- FREITAS, S. S., SANTOS, J. A. & PRAZERES, D. M. 2006. Optimization of isopropanol and ammonium sulfate precipitation steps in the purification of plasmid DNA. *Biotechnology Progress*, 22, 1179-86.
- FU, J., VANDUSEN, W. J., KOLODIN, D. G., O'KEEFE, D. O., HERBER, W. K. & GEORGE, H. A. 1996a. Continuous culture study of the expression of hepatitis B surface antigen and its self-assembly into virus-like particles in *Saccharomyces cerevisiae*. *Biotechnology Bioengineering*, 49, 578-86.
- FU, J., VANDUSEN, W. J., KOLODIN, D. G., O'KEEFE, D. O., HERBER, W. K. & GEORGE, H. A. 1996b. Continuous culture study of the expression of hepatitis B surface antigen and its self-assembly into virus-like particles in *Saccharomyces cerevisiae*. *Biotechnology and Bioengineering*, 49, 578-586.
- GAGNON, P. 2006. Monoliths Seen to Revitalize Bioseparations. *Genetic Engineering News*, 26.
- GALARZA, J. M., LATHAM, T. & CUPO, A. 2005. Virus-like particle (VLP) vaccine conferred complete protection against a lethal influenza virus challenge. *Viral Immunology*, 18, 244-251.
- GAVILANES, F., GOMEZGUTIERREZ, J., ARACIL, M., GONZALEZROS, J. M., FERRAGUT, J. A., GUERRERO, E. & PETERSON, D. L. 1990. Hepatitis-B Surface-Antigen - Role of Lipids in Maintaining the Structural and Antigenic Properties of Protein-Components. *Biochemical Journal*, 265, 857-864.
- GAVILANES, F., GONZALEZROS, J. M. & PETERSON, D. L. 1982. Structure of Hepatitis-B Surface-Antigen - Characterization of the Lipid Components and Their Association with the Viral-Proteins. *Journal of Biological Chemistry*, 257, 7770-7777.
- GILBERT, R. J. C., BEALES, L., BLOND, D., SIMON, M. N., LIN, B. Y., CHISARI, F. V., STUART, D. I. & ROWLANDS, D. J. 2005. Hepatitis B small

surface antigen particles are octahedral. *Proceedings of the National Academy of Sciences of the United States of America*, 102, 14783-14788.

GOHEEN, S. C. & ENGELHORN, S. C. 1984. Hydrophobic Interaction High-Performance Liquid Chromatography of Proteins. *Journal of Chromatography*, 317, 55-65.

GREINER, V. J., EGELE, C., ONCUL, S., RONZON, F., MANIN, C., KLYMCHENKO, A. & MELY, Y. 2010. Characterization of the lipid and protein organization in HBsAg viral particles by steady-state and time-resolved fluorescence spectroscopy. *Biochimie*, 92, 994-1002.

GRGACIC, E. V. L. & ANDERSON, D. A. 2006. Virus-like particles: Passport to immune recognition. *Methods*, 40, 60-65.

GRONGBERG, A., ERIKSSON, M., ERSOY, M. & JOHANSSON, H. J. 2011. A tool for increasing the lifetime of chromatography resins. *mAbs*, 3, 192-202.

GU, T. Y., TSAI, G. J. & TSAO, G. T. 1991. A Theoretical-Study of Multicomponent Radial Flow Chromatography. *Chemical Engineering Science*, 46, 1279-1288.

GUAN, Z. J., GUO, B., HUO, Y. L., GUAN, Z. P. & WEI, Y. H. 2010. Overview of expression of hepatitis B surface antigen in transgenic plants. *Vaccine*, 28, 7351-7362.

GUIOCHON, G. 2007. Monolithic columns in high-performance liquid chromatography. *Journal of Chromatography A*, 1168, 101-168.

HABER, C., SKUPSKY, J., LEE, A. & LANDER, R. 2004. Membrane chromatography of DNA: Conformation-induced cavity and selectivity. *Biotechnology and Bioengineering*, 88, 26-34.

HAHN, R., DEINHOFER, K., MACHOLD, C. & JUNGBAUER, A. 2003. Hydrophobic interaction chromatography of proteins. II. Binding capacity, recovery

and mass transfer properties. *Journal of Chromatography. B-Analytical Technologies in the Biomedical and Life Sciences*, 790, 99-114.

HAHN, R. & JUNGBAUER, A. 2000. Peak broadening in protein chromatography with monoliths at very fast separations. *Analytical Chemistry*, 72, 4853-4858.

HAIMER, E., TSCHELIESSNIG, A., HAHN, R. & JUNGBAUER, A. 2007. Hydrophobic interaction chromatography of proteins IV - Kinetics of protein spreading. *Journal of Chromatography A*, 1139, 84-94.

HAMEL, J.-F. P., HUNTER, J. B. & SIKDAR, S. K. 1990. *Downstream processing and bioseparation: Recovery and purification of biological products*, US, American Chemical Society.

HAN, B. B., SPECHT, R., WICKRAMASINGHE, S. R. & CARLSON, J. O. 2005. Binding Aedes aegypti densovirus to ion exchange membranes. *Journal of Chromatography A*, 1092, 114-124.

HANSEN, L. C. & SIEVERS, R. E. 1974. Highly Permeable Open-Pore Polyurethane Columns for Liquid-Chromatography. *Journal of Chromatography*, 99, 123-133.

HARINARAYAN, C., MUELLER, J., LJUNGLOF, A., FAHRNER, R., VAN ALSTINE, J. & VAN REIS, R. 2006. An exclusion mechanism in ion exchange chromatography. *Biotechnology and Bioengineering*, 95, 775-787.

HARPER, D. M. 2009. Currently approved prophylactic HPV vaccines. *Expert Review of Vaccines*, 8, 1663-1679.

HEMLING, M. E., CARR, S. A., CAPIAU, C. & PETRE, J. 1988. Structural Characterization of Recombinant Hepatitis-B Surface-Antigen Protein by Mass-Spectrometry. *Biochemistry*, 27, 699-705.

HERBST-KRALOVETZ, M., MASON, H. S. & CHEN, Q. 2010. Norwalk virus-like particles as vaccines. *Expert Review of Vaccines*, 9, 299-307.

- HILBRIG, F. & FREITAG, R. 2003. Protein purification by affinity precipitation. *Journal of Chromatography B-Analytical Technologies in the Biomedical and Life Sciences*, 790, 79-90.
- HJERTEN, S. 1974. Hydrophic Interaction Chromatography; The Synthesis and the Use of Some Alkyl and Aryl Derivatives of Agarose. *Journal of Chromatography*, 101, 281-288.
- HJERTEN, S., LI, Y. M., LIAO, J. L., MOHAMMAD, J., NAKAZATO, K. & PETTERSSON, G. 1992. Continuous Beds - High-Resolving, Cost-Effective Chromatographic Matrices. *Nature*, 356, 810-811.
- HJERTEN, S., LIAO, J. L. & ZHANG, R. 1989. High-Performance Liquid-Chromatography on Continuous Polymer Beds. *Journal of Chromatography*, 473, 273-275.
- HJERTEN, S., MOHAMMAD, J. & NAKAZATO, K. 1993a. Improvement in Flow Properties and Ph Stability of Compressed, Continuous Polymer Beds for High-Performance Liquid-Chromatography. *Journal of Chromatography*, 646, 121-128.
- HJERTEN, S., NAKAZATO, K., MOHAMMAD, J. & EAKER, D. 1993b. Reversed-Phase Chromatography of Proteins and Peptides on Compressed Continuous Beds. *Chromatographia*, 37, 287-294.
- HONORATI, M. C. & FACCHINI, A. 1998. Immune response against HBsAg vaccine. *World Journal of Gastroenterology*, 4, 464-466.
- HUANG, S. H., LEE, W. C. & TSAO, G. T. 1988. Mathematical-Models of Radial Chromatography. *Chemical Engineering Journal and the Biochemical Engineering Journal*, 38, 179-186.
- HUBBUCH, J., LINDEN, T., KNIEPS, E., LJUNGLOF, A., THOMMES, J. & KULA, M. R. 2003. Mechanism and kinetics of protein transport in chromatographic media studied by confocal laser scanning microscopy - Part I. The interplay of

sorbent structure and fluid phase conditions. *Journal of Chromatography A*, 1021, 93-104.

HUGHES, M. 1977. Coagulation and Flocculation. *In: SVAROVCSKY, L. (ed.) Solid-liquid separation*. Oxford: Butterworth-Heinemann.

HUOVILA, A. P., EDER, A. M. & FULLER, S. D. 1992. Hepatitis B surface antigen assembles in a post-ER, pre-Golgi compartment. *The Journal of Cell Biology*, 118, 1305-20.

INGLIS, S., SHAW, A. & KOENIG, S. 2006. HPV vaccines: Commercial research & development. *Vaccine*, 24, 99-105.

JIANG, C. P., FLANSBURG, L., GHOSE, S., JORJORIAN, P. & SHUKLA, A. A. 2010. Defining Process Design Space for a Hydrophobic Interaction Chromatography (HIC) Purification Step: Application of Quality by Design (QbD) Principles. *Biotechnology and Bioengineering*, 107, 985-997.

JIANG, C. P., LIU, J., RUBACHA, M. & SHUKLA, A. A. 2009. A mechanistic study of Protein A chromatography resin lifetime. *Journal of Chromatography A*, 1216, 5849-5855.

JIN, J. 2010. *Lipid foulant interactions during the chromatographic purification of virus-like particles from Saccharomyces cerevisiae*. PhD, UCL.

JIN, J., CHHATRE, S., TITCHENER-HOOKER, N. J. & BRACEWELL, D. G. 2010. Evaluation of the impact of lipid fouling during the chromatographic purification of virus-like particles from *Saccharomyces cerevisiae*. *Journal of Chemical Technology and Biotechnology*, 85, 209-215.

JOHNSON, K. B., LARSSON, P. O., NYLEN, U. T. G., WIKSTROM, P. I. O. & ZETTERSTRAND, I. K. 1990. *Method of Coating Solid Particles with a Hydrophilic Gel*.

- JONES, T. T. & FERNANDEZ, E. J. 2003. alpha-Lactalbumin tertiary structure changes on hydrophobic interaction chromatography surfaces. *Journal of Colloid and Interface Science*, 259, 27-35.
- JONSSON, B. & STAHLBERG, J. 1999. The electrostatic interaction between a charge sphere and an oppositely charge polar surface and its application to protein adsorption. *Colloid Surface B*, 14, 67-75.
- JOSEFSBERG, J. O. & BUCKLAND, B. 2012. Vaccine process technology. *Biotechnology and Bioengineering*, 109, 1443-60.
- JOSIC, D. & BUCHACHER, A. 2001. Application of monoliths as supports for affinity chromatography and fast enzymatic conversion. *Journal of Biochemical and Biophysical Methods*, 49, 153-174.
- JOSIC, D., BUCHACHER, A. & JUNGBAUER, A. 2001. Monoliths as stationary phases for separation of proteins and polynucleotides and enzymatic conversion. *Journal of Chromatography B*, 752, 191-205.
- JOSIC, D., REUSCH, J., LOSTER, K., BAUM, O. & REUTTER, W. 1992. High-Performance Membrane Chromatography of Serum and Plasma-Membrane Proteins. *Journal of Chromatography*, 590, 59-76.
- JOSIC, D., SCHWINN, H., STRANCAR, A., PODGORNIK, A., BARUT, M., LIM, Y. P. & VODOPIVEC, M. 1998. Use of compact, porous units with immobilized ligands with high molecular masses in affinity chromatography and enzymatic conversion of substrates with high and low molecular masses. *Journal of Chromatography A*, 803, 61-71.
- JOYCE, J. G., GEORGE, H. A., HOFMAN, K. J., JANSEN, K. U. & NEEPER, M. P. 1998. *Recombinant Human Papillomavirus Type 18 Vaccine*. United States patent application. Oct. 13, 1998.
- JUNGBAUER, A. 2005. Chromatographic media for bioseparation. *Journal of Chromatography A*, 1065, 3-12.

JUNGBAUER, A. & HAHN, R. 2004. Monoliths for fast bioseparation and bioconversion and their applications in biotechnology. *Journal of Separation Science*, 27, 767-78.

JUNGBAUER, A. & HAHN, R. 2008. Polymethacrylate monoliths for preparative and industrial separation of biomolecular assemblies. *Journal of Chromatography A*, 1184, 62-79.

JUNGBAUER, A., MACHOLD, C. & HAHN, R. 2005. Hydrophobic interaction chromatography of proteins. III. Unfolding of proteins upon adsorption. *Journal of Chromatography A*, 1079, 221-8.

KALASHNIKOVA, I. V., IVANOVA, N. D. & TENNIKOVA, T. B. 2008. The use of monolithic polymeric sorbents to simulate virus-cell interactions. *Russian Journal of Applied Chemistry*, 81, 867-873.

KATO, Y., KITAMURA, T. & HASHIMOTO, T. 1983. High-Performance Hydrophobic Interaction Chromatography of Proteins. *Journal of Chromatography*, 266, 49-54.

KATO, Y., KITAMURA, T. & HASHIMOTO, T. 1986. New Resin-Based Hydrophilic Support for High-Performance Hydrophobic Interaction Chromatography. *Journal of Chromatography*, 360, 260-265.

KATO, Y., NAKAMURA, K., KITAMURA, T., MORIYAMA, H., HASEGAWA, M. & SASAKI, H. 2002. Separation of proteins by hydrophobic interaction chromatography at low salt concentration. *Journal of Chromatography A*, 971, 143-149.

KEE, G. S. 2009. *A rational approach to the development of future generation processes for lipoprotein VLP vaccine candidates*. Ph.D., University College London.

KEE, G. S., JIN, J., BALASUNDARAM, B., BRACEWELL, D. G., PUJAR, N. S. & TITCHENER-HOOKER, N. J. 2010. Exploiting the intracellular

compartmentalization characteristics of the *S. cerevisiae* host cell for enhancing primary purification of lipid-envelope virus-like particles. *Biotechnology Progress*, 26, 26-33.

KEE, G. S., PUJAR, N. S. & TITCHENER-HOOKER, N. J. 2008. Study of detergent-mediated liberation of hepatitis B virus-like particles from *S. cerevisiae* homogenate: identifying a framework for the design of future-generation lipoprotein vaccine processes. *Biotechnology Progress*, 24, 623-31.

KELLY, S. T. & ZYDNEY, A. L. 1997. Protein fouling during microfiltration: comparative behavior of different model proteins. *Biotechnology and Bioengineering*, 55, 91-100.

KIM, H. J., LIM, S. J. & KWAG, H. L. 2012. The choice of resin-bound ligand affects the structure and immunogenicity of column-purified human papillomavirus type 16 virus-like particles. *PLoS One*, 7, e35893.

KNUDSEN, H. L., FAHRNER, R. L., XU, Y., NORLING, L. A. & BLANK, G. S. 2001. Membrane ion-exchange chromatography for process-scale antibody purification. *Journal of Chromatography A*, 907, 145-154.

KOKU, H., MAIER, R. S., CZYMMEK, K. J., SCHURE, M. R. & LENHOFF, A. M. 2011. Modeling of flow in a polymeric chromatographic monolith. *Journal of Chromatography A*, 1218, 3466-75.

KOL, N., GLADNIKOFF, M., BARLAM, D., SHNECK, R. Z., REIN, A. & ROUSSO, I. 2006. Mechanical properties of murine leukemia virus particles: effect of maturation. *Biophysical Journal*, 91, 767-74.

KRAMBERGER, P., PETERKA, M., BOBEN, J., RAVNIKAR, M. & STRANCAR, A. 2007. Short monolithic columns - A breakthrough in purification and fast quantification of tomato mosaic virus. *Journal of Chromatography A*, 1144, 143-149.

- KRAMBERGER, P., PETROVIC, N., STRANCAR, A. & RAVNIKAR, M. 2004. Concentration of plant viruses using monolithic chromatographic supports. *Journal of Virological Methods*, 120, 51-57.
- KUCZEWSKI, M., FRAUD, N., FABER, R. & ZARBIS-PAPASTOITSIS, G. 2010. Development of a Polishing Step Using a Hydrophobic Interaction Membrane Adsorber With a PER.C6 (R)-Derived Recombinant Antibody. *Biotechnology and Bioengineering*, 105, 296-305.
- KUMAR, A. & SRIVASTAVA, A. 2010. Cell separation using cryogel-based affinity chromatography. *Nature Protocols*, 5, 1737-47.
- KUN, K. A. & KUNIN, R. 1968. Macroreticular Resins .3. Formation of Macroreticular Styrene-Divinylbenzene Copolymers. *Journal of Polymer Science Part a-1-Polymer Chemistry*, 6, 2689-&.
- LANDER, R. J., WINTERS, M. A., MEACLE, F. J., BUCKLAND, B. C. & LEE, A. L. 2002. Fractional precipitation of plasmid DNA from lysate by CTAB. *Biotechnology and Bioengineering*, 79, 776-84.
- LANGER, E. S. 2011. Alleviating Downstream Process Bottlenecks. *GEN*, 31.
- LAVANCHY, D. 2004. Hepatitis B virus epidemiology, disease burden, treatment, and current and emerging prevention and control measures. *Journal of Viral Hepatitis*, 11, 97-107.
- LECHNER, F., JEGERLEHNER, A., TISSOT, A. C., MAURER, P., SEBBEL, P., RENNER, W. A., JENNINGS, G. T. & BACHMANN, M. F. 2002. Virus-like particles as a modular system for novel vaccines. *Intervirology*, 45, 212-7.
- LESCH, H. P., LAITINEN, A., PEIXOTO, C., VICENTE, T., MAKKONEN, K. E., LAITINEN, L., PIKKARAINEN, J. T., SAMARANAYAKE, H., ALVES, P. M., CARRONDO, M. J., YLA-HERTTUALA, S. & AIRENNE, K. J. 2011. Production and purification of lentiviral vectors generated in 293T suspension cells with baculoviral vectors. *Gene Therapy* 18, 531-8.

- LEVISON, P. R. 1997. Ion Exchange Chromatography and Secondary Absorption effects. In: VERREL, M. S. (ed.) *Downstream Processing of Natural Products - A Practical Handbook*. England: John Wiley & Sons, Ltd.
- LEVISON, P. R., HOPKINS, A. K. & HATHI, P. 1999. Influence of column design on process-scale ion-exchange chromatography. *Journal of Chromatography A*, 865, 3-12.
- LEVISON, P. R., STREATOR, M., JONES, R. M. H. & PATHIRON, N. D. 1996. Validation Studies in the Regeneration of Ion-Exchange Celluloses. In: SHILTERIN, J. K. (ed.) *Validation Practices for Biotechnology Products*. USA: American Society for Testing and Materials.
- LEVY, J., FRAENKEL-CONTRAT, H. & OWENS, R. 1994. *Virology*, Prentice-Hall International (UK) Limited, London.
- LEVY, S., O'KENNEDY, R., AYZAZI-SHAMLOU, P. & DUNNIL, P. 2000. Biochemical engineering approaches to the challenges of producing pure plasmid DNA. *Trends in Biotechnology*, 18, 296-305.
- LI, F., ZHOU, J. X., YANG, X., TRESSEL, T. & LEE, B. 2005. Current therapeutic antibody production and process optimization. *Bioprocessing Journal*, 4, 1-8.
- LI, Y., BI, J. X., ZHOU, W. B., HUANG, Y. D., SUN, L. J., ZENG, A. P., MA, G. H. & SU, Z. G. 2007. Characterization of the large size aggregation of Hepatitis B virus surface antigen (HBsAg) formed in ultrafiltration process. *Process Biochemistry*, 42, 315-319.
- LIAO, J. L., ZHANG, R. & HJERTEN, S. 1991. Continuous Beds for Standard and Micro High-Performance Liquid-Chromatography. *Journal of Chromatography*, 586, 21-26.
- LICHTENBERG, D., ROBSON, R. J. & DENNIS, E. A. 1983. Solubilization of phospholipids by detergents. Structural and kinetic aspects. *Biochimica et Biophysica Acta*, 737, 285-304.

LIENQUEO, M. E., MAHN, A., SALGADO, J. C. & ASENJO, J. A. 2007. Current insights on protein behaviour in hydrophobic interaction chromatography. *Journal of Chromatography. B-Analytical Technologies in the Biomedical and Life Sciences*, 849, 53-68.

LIN, D. Q., ZHONG, L. N. & YAO, S. J. 2006. Zeta potential as a diagnostic tool to evaluate the biomass electrostatic adhesion during ion-exchange expanded bed application. *Biotechnology and Bioengineering*, 95, 185-91.

LIN, F. Y., CHEN, W. Y. & HEARN, M. T. W. 2001. Microcalorimetric studies on the interaction mechanism between proteins and hydrophobic solid surfaces in hydrophobic interaction chromatography: Effects of salts, hydrophobicity of the sorbent, and structure of the protein. *Analytical Chemistry*, 73, 3875-3883.

LIN, F. Y., CHEN, W. Y., RUAAN, R. C. & HUANG, H. M. 2000. Microcalorimetric studies of interactions between proteins and hydrophobic ligands in hydrophobic interaction chromatography: effects of ligand chain length, density and the amount of bound protein. *Journal of Chromatography A*, 872, 37-47.

LINDEN, T., LJUNGLOF, A., KULA, M. R. & THOMMES, J. 1999. Visualizing two-component protein diffusion in porous adsorbents by confocal scanning laser microscopy. *Biotechnology and Bioengineering*, 65, 622-630.

LIU, R. S., LIN, Q. L., SUN, Y., LU, X. Y., QIU, Y. L., LI, Y. & GUO, X. G. 2009. Expression, Purification, and Characterization of Hepatitis B Virus Surface Antigens (HBsAg) in Yeast *Pichia Pastoris*. *Applied Biochemistry and Biotechnology*, 158, 432-444.

LJUNGLOF, A., BERGVALL, P., BHIKHABHAI, R. & HJORTH, R. 1999. Direct visualisation of plasmid DNA in individual chromatography adsorbent particles by confocal scanning laser microscopy. *Journal of Chromatography A*, 844, 129-135.

LJUNGLOF, A. & HJORTH, R. 1996. Confocal microscopy as a tool for studying protein adsorption to chromatographic matrices. *Journal of Chromatography A*, 743, 75-83.

LJUNGLOF, A. & THOMMES, J. 1998. Visualising intraparticle protein transport in porous adsorbents by confocal microscopy. *Journal of Chromatography A*, 813, 387-395.

LOZINSKY, V. I., GALAEV, I. Y., PLIEVA, F. M., SAVINA, I. N., JUNGVID, H. & MATTIASSON, B. 2003. Polymeric cryogels as promising materials of biotechnological interest. *Trends in Biotechnology*, 21, 445-51.

LOZINSKY, V. I., PLIEVA, F. M., GALAEV, I. Y. & MATTIASSON, B. 2001. The potential of polymeric cryogels in bioseparation. *Bioseparation*, 10, 163-88.

LUTKEMEYER, D., BRETSCHEIDER, M., BUNTEMEYER, H. & LEHMANN, J. 1993. Membrane Chromatography for Rapid Purification of Recombinant Antithrombin-Iii and Monoclonal-Antibodies from Cell-Culture Supernatant. *Journal of Chromatography*, 639, 57-66.

LYDDIATT, A. 2002. Process chromatography: current constraints and future options for the adsorptive recovery of bioproducts. *Current Opinion in Biotechnology*, 13, 95-103.

LYDDIATT, A. & O'SULLIVAN, D. A. 1998. Biochemical recovery and purification of gene therapy vectors. *Current Opinion in Biotechnology*, 9, 177-85.

MAHMOOD, K., BRIGHT, R. A., MYTLE, N., CARTER, D. M., CREVAR, C., ACHENBACH, J. E., HEATON, P. M., TUMPEY, T. M. & ROSS, T. M. 2008. H5N1VLP vaccine induced protection in ferrets against lethal challenge with highly pathogenic H5N1 influenza viruses. *Vaccine*, 26, 5393-5399.

MAHRAG TUR, K. & CH'NG, H.-S. 1998. Evaluation of possible mechanism(s) of bioadhesion. *International Journal of Pharmaceuticals.*, 160, 61-74.

- MALLIK, R. & HAGE, D. S. 2006. Affinity monolith chromatography. *Journal of Separation Science*, 29, 1686-1704.
- MANGOLD, C. M. T. & STREECK, R. E. 1993. Mutational Analysis of the Cysteine Residues in the Hepatitis-B Virus Small Envelope Protein. *Journal of Virology*, 67, 4588-4597.
- MANGOLD, C. M. T., UNCKELL, F., WERR, M. & STREECK, R. E. 1995. Secretion and Antigenicity of Hepatitis-B Virus Small Envelope Proteins Lacking Cysteines in the Major Antigenic Region. *Virology*, 211, 535-543.
- MARTIN, C., COYNE, J. & CARTA, G. 2005. Properties and performance of novel high-resolution/high-permeability ion-exchange media for protein chromatography. *Journal of Chromatography A*, 1069, 43-52.
- MCALEER, W. J., BUYNAK, E. B., MAIGETTER, R. Z., WAMPLER, D. E., MILLER, W. J. & HILLEMANN, M. R. 1984. Human Hepatitis-B Vaccine from Recombinant Yeast. *Nature*, 307, 178-180.
- MCALLISTER, C., KARYMOV, M. A., KAWANO, Y., LUSHNIKOV, A. Y., MIKHEIKIN, A., UVERSKY, V. N. & LYUBCHENKO, Y. L. 2005. Protein interactions and misfolding analyzed by AFM force spectroscopy. *Journal of Molecular Biology*, 354, 1028-1042.
- MCCUE, J. T. 2009. Theory and use of hydrophobic interaction chromatography in protein purification applications. *Methods in Enzymology*, 463, 405-14.
- MCCUE, J. T., ENGEL, P., NG, A., MACNIVEN, R. & THOMMES, J. 2008. Modeling of protein monomer/aggregate purification and separation using hydrophobic interaction chromatography. *Bioprocess and Biosystems Engineering*, 31, 261-75.
- MCCUE, J. T., ENGEL, P. & THOMMES, J. 2009. Effect of phenyl sepharose ligand density on protein monomer/aggregate purification and separation using

hydrophobic interaction chromatography. *Journal of Chromatography A*, 1216, 902-909.

MCNAY, J. L., O'CONNELL, J. P. & FERNANDEZ, E. J. 2001. Protein unfolding during reversed-phase chromatography: II. Role of salt type and ionic strength. *Biotechnology and Bioengineering*, 76, 233-40.

MELANDER, W. & HORVATH, C. 1977. Salt effect on hydrophobic interactions in precipitation and chromatography of proteins: an interpretation of the lyotropic series. *Archives of Biochemistry and Biophysics*, 183, 200-15.

MELANDER, W. R., CORRADINI, D. & HORVATH, C. 1984. Salt-mediated retention of proteins in hydrophobic-interaction chromatography. Application of solvophobic theory. *Journal of Chromatography A*, 317, 67-85.

MENG, F., CHAE, S. R., DREWS, A., KRAUME, M., SHIN, H. S. & YANG, F. 2009. Recent advances in membrane bioreactors (MBRs): membrane fouling and membrane material. *Water Research*, 43, 1489-512.

MEYERS, J. J. & LIAPIS, A. I. 1999. Network modeling of the convective flow and diffusion of molecules adsorbing in monoliths and in porous particles packed in a chromatographic column. *Journal of Chromatography A*, 852, 3-23.

MIHELIC, I., KOLOINI, T. & PODGORNIK, A. 2003. Temperature distribution effects during polymerization of methacrylate-based monoliths. *Journal of Applied Polymer Science*, 87, 2326-2334.

MIHELIC, I., KOLOINI, T., PODGORNIK, A. & STRANCAR, A. 2000. Dynamic capacity studies of CIM (Convective Interaction Media)(R) monolithic columns. *Hrc-Journal of High Resolution Chromatography*, 23, 39-43.

MIHELIC, I., KRAJNC, M., KOLOINI, T. & PODGORNIK, A. 2001. Kinetic model of a methacrylate-based monolith polymerization. *Industrial & Engineering Chemistry Research*, 40, 3495-3501.

- MIHELIC, I., NEMEC, D. A., PODGORNIK, A. & KOLOINI, T. 2005. Pressure drop in CIM disk monolithic columns. *Journal of Chromatography A*, 1065, 59-67.
- MILHIET, P. E., DOSSET, P., GODEFROY, C., LE GRIMELLE, C., GUIGNER, J. M., LARQUET, E., RONZON, F. & MANIN, C. 2011. Nanoscale topography of hepatitis B antigen particles by atomic force microscopy. *Biochimie*, 93, 254-9.
- MIYANOHARA, A., TOHE, A., NOZAKI, C., HAMADA, F., OHTOMO, N. & MATSUBARA, K. 1983. Expression of Hepatitis-B Surface-Antigen Gene in Yeast. *Proceedings of the National Academy of Sciences of the United States of America-Biological Sciences*, 80, 1-5.
- MOTOKAWA, M., KOBAYASHI, H., ISHIZUKA, N., MINAKUCHI, H., NAKANISHI, K., JINNAI, H., HOSOYA, K., IKEGAMI, T. & TANAKA, N. 2002. Monolithic silica columns with various skeleton sizes and through-pore sizes for capillary liquid chromatography. *Journal of Chromatography A*, 961, 53-63.
- MULLER-SPATH, T., AUMANN, L. & MORBIDELLI, M. 2009. Role of Cleaning-in-Place in the Purification of mAb Supernatants Using Continuous Cation Exchange Chromatography. *Separation Science and Technology*, 44, 1-26.
- MULLER, D. J. & ENGEL, A. 2007. Atomic force microscopy and spectroscopy of native membrane proteins. *Nature Protocols*, 2, 2191-7.
- NAKANISHI, K. & SOGA, N. 1991. Phase-Separation in Gelling Silica Organic Polymer-Solution - Systems Containing Poly(Sodium Styrenesulfonate). *Journal of the American Ceramic Society*, 74, 2518-2530.
- NARVAEZ-RIVAS, M., GALLARDO, E., RIOS, J. J. & LEON-CAMACHO, M. 2011. A new high-performance liquid chromatographic method with evaporative light scattering detector for the analysis of phospholipids. Application to Iberian pig subcutaneous fat. *Journal of Chromatography A*, 1218, 3453-8.
- NASH, D. C., MCCREATH, G. E. & CHASE, H. A. 1997. Modification of polystyrenic matrices for the purification of proteins - Effect of the adsorption of

poly(vinyl alcohol) on the characteristics of poly(styrene-divinylbenzene) beads for use in affinity chromatography. *Journal of Chromatography A*, 758, 53-64.

NG, P. K. & MCLAUGHLIN, V. 2007. Regeneration Studies of Anion-Exchange Chromatography Resins. *BioProcess International*, 5, 52-56.

NIKOLOV, Z. L. & WOODARD, S. L. 2004. Downstream processing of recombinant proteins from transgenic feedstock. *Current Opinion in Biotechnology*, 15, 479-86.

NOAD, R. & ROY, P. 2003. Virus-like particles as immunogens. *Trends in Microbiology*, 11, 438-444.

NORDER, H., COUROUCE, A. M. & MAGNIUS, L. O. 1992. Molecular basis of hepatitis B virus serotype variations within the four major subtypes. *Journal of General Virology*, 73 (Pt 12), 3141-5.

O'GRADY, J. 2002. Liver and Biliary Tract Disease. In: SOUHAMI, R. & MOXHAM, J. (eds.) *Textbook of medicine*. 4th Edition ed.: Churchill Livingstone.

OCHOA, J. L. 1978. Hydrophobic (interaction) chromatography. *Biochimie*, 60, 1-15.

OROSZLAN, P., BLANCO, R., LU, X. M., YARMUSH, D. & KARGER, B. L. 1990. Intrinsic Fluorescence Studies of the Kinetic Mechanism of Unfolding of Alpha-Lactalbumin on Weakly Hydrophobic Chromatographic Surfaces. *Journal of Chromatography*, 500, 481-502.

PADDOCK, S. W. 1999. *Confocal Microscopy Methods and Protocols*, USA.

PAHLMAN, ROSENGREN, J. & HJERTEN, S. 1977. Hydrophobic interaction chromatography on uncharged Sepharose derivatives. Effects of neutral salts on the adsorption of proteins. *Journal of Chromatography*, 131, 99-108.

PALSSON, E., SMEDS, A. L., PETERSSON, A. & LARSSON, P. O. 1999. Faster isolation of recombinant factor VIII SQ, with a superporous agarose matrix. *Journal of Chromatography A*, 840, 39-50.

PAMPEL, L., BOUSHABA, R., UDELL, M., TURNER, M. & TITCHENER-HOOKER, N. 2007. The influence of major components on the direct chromatographic recovery of a protein from transgenic milk. *Journal of Chromatography A*, 1142, 137-47.

PATTENDEN, L. K., MIDDELBERG, A. P., NIEBERT, M. & LIPIN, D. I. 2005. Towards the preparative and large-scale precision manufacture of virus-like particles. *Trends in Biotechnology*, 23, 523-9.

PATZER, E. J., NAKAMURA, G. R., SIMONSEN, C. C., LEVINSON, A. D. & BRANDS, R. 1986. Intracellular assembly and packaging of hepatitis B surface antigen particles occur in the endoplasmic reticulum. *Journal of Virology*, 58, 884-92.

PAWLEY, J. B. 2006. *Handbook of Biological Confocal Microscopy*, USA, Springer Science & Business Media LLC.

PEIXOTO, C., SOUSA, M. F., SILVA, A. C., CARRONDO, M. J. & ALVES, P. M. 2007. Downstream processing of triple layered rotavirus like particles. *Journal of Biotechnology*, 127, 452-61.

PEREZ, O. & PAOLAZZI, C. C. 1997. Production methods for rabies vaccine. *Journal of Industrial Microbiology & Biotechnology*, 18, 340-347.

PERKINS, T. W., MAK, D. S., ROOT, T. W. & LIGHTFOOT, E. N. 1997. Protein retention in hydrophobic interaction chromatography: Modeling variation with buffer ionic strength and column hydrophobicity. *Journal of Chromatography A*, 766, 1-14.

PERSSON, P., BAYBAK, O., PLIEVA, F., GALAEV, I. Y., MATTIASSON, B., NILSSON, B. & AXELSSON, A. 2004. Characterization of a continuous

supermacroporous monolithic matrix for chromatographic separation of large bioparticles. *Biotechnology and Bioengineering*, 88, 224-236.

PETERSON, D. L. 1987. The Structure of Hepatitis-B Surface-Antigen and Its Antigenic Sites. *Bioessays*, 6, 258-262.

PETRE, J., VANWIJNENDAELE, F., DENEYS, B., CONRATH, K., VANOPSTAL, O., HAUSER, P., RUTGERS, T., CABEZON, T., CAPIAU, C., HARFORD, N., DEWILDE, M., STEPHENNE, J., CARR, S., HEMLING, H. & SWADESH, J. 1987. Development of a Hepatitis-B Vaccine from Transformed Yeast-Cells. *Postgraduate Medical Journal*, 63, 73-81.

PINHEIRO, H. & CABRAL, J. M. 1992. Centrifugation. *In*: KENNEDY, J. F. & CABRAL, J. M. (eds.) *Recovery Processes for Biological Materials*. UK: John Wiley & Sons.

PLIEVA, F. M., SAVINA, I. N., DERAZ, S., ANDERSSON, J., GALAEV, I. Y. & MATTIASSON, B. 2004. Characterization of supermacroporous monolithic polyacrylamide based matrices designed for chromatography of bioparticles. *Journal of Chromatography B-Analytical Technologies in the Biomedical and Life Sciences*, 807, 129-37.

PODGORNIK, A., BARUT, M., JANCAR, J., STRANCAR, A. & TENNIKOVA, T. 1999. High-performance membrane chromatography of small molecules. *Analytical Chemistry*, 71, 2986-2991.

PODGORNIK, A., BARUT, M., MIHELIC, I. & STRANCAR, A. 2003. Tubes. *In*: SVEC, F., TENNIKOVA, T. B. & DEYL, Z. (eds.) *Monolithic Materials; preparation, properties and applications*. Netherlands: Elsevier Science B.V.

PODGORNIK, A., BARUT, M., STRANCAR, A., JOSIC, D. & KOLOINI, T. 2000. Construction of large volume monolithic columns. *Analytical Chemistry*, 72, 5693-5699.

- PORATH, J. 1986. Salt-promoted adsorption: recent developments. *Journal of Chromatography*, 376, 331-41.
- PORATH, J. 1990. Salt-promoted Adsorption Chromatography. *Journal of Chromatography*, 510, 47-48.
- PORATH, J., SUNDBERG, L., FORNSTEDT, N. & OLSSON, I. 1973. Salting-out in amphiphilic gels as a new approach to hydrophobic adsorption. *Nature*, 245, 465-6.
- POUS-TORRES, S., TORRES-LAPASIO, J. R., RUIZ-ANGEL, M. J. & GARCIA-ALVAREZ-COQUE, M. C. 2010. Origin and correction of the deviations in retention times at increasing flow rate with Chromolith columns. *Journal of Chromatography A*, 1217, 5440-3.
- PRATHER, K. J., SAGAR, S., MURPHY, J. & CHARTRAIN, M. 2003. Industrial scale production of plasmid DNA for vaccine and gene therapy: plasmid design, production, and purification. *Enzyme and Microbial Technology*, 33, 865-883.
- PRAZERES, D. M., SCHLUEP, T. & COONEY, C. 1998. Preparative purification of supercoiled plasmid DNA using anion-exchange chromatography. *Journal of Chromatography A*, 806, 31-45.
- QUEIROZ, J. A., TOMAZ, C. T. & CABRAL, J. M. 2001. Hydrophobic interaction chromatography of proteins. *Journal of Biotechnology*, 87, 143-59.
- REIF, O. W. & FREITAG, R. 1993. Characterization and Application of Strong Ion-Exchange Membrane Adsorbers as Stationary Phases in High-Performance Liquid-Chromatography of Proteins. *Journal of Chromatography A*, 654, 29-41.
- RICHTER, L. J., THANAVALA, Y., ARNTZEN, C. J. & MASON, H. S. 2000. Production of hepatitis B surface antigen in transgenic plants for oral immunization. *Nature Biotechnology*, 18, 1167-71.

- ROLDÃO, A., MELLADO, M. C. M., CASTILLO, L. R., CARRONDO, M. J. & ALVES, P. M. 2010. Virus-like particles in vaccine development. *Expert Review of Vaccines*, 9, 1149-1176.
- ROLLAND, D., GAUTHIER, M., DUGUA, J. M., FOURNIER, C., DELPECH, L., WATELET, B., LETOURNEUR, O., ARNAUD, M. & JOLIVET, M. 2001. Purification of recombinant HBc antigen expressed in *Escherichia coli* and *Pichia pastoris*: comparison of size-exclusion chromatography and ultracentrifugation. *Journal of Chromatography B-Analytical Technologies in the Biomedical and Life Sciences*, 753, 51-65.
- SATOH, O., IMAI, H., YONEYAMA, T., MIYAMURA, T., UTSUMI, H., INOUE, K. & UMEDA, M. 2000. Membrane structure of the hepatitis B virus surface antigen particle. *Journal of Biochemistry*, 127, 543-550.
- SCHULTZ, L. D., HOFMANN, K. J., MYLIN, L. M., MONTGOMERY, D. L., ELLIS, R. W. & HOPPER, J. E. 1987. Regulated Overproduction of the Gal4 Gene-Product Greatly Increases Expression from Galactose-Inducible Promoters on Multi-Copy Expression Vectors in Yeast. *Gene*, 61, 123-133.
- SCHUSTER, M., WASSERBAUER, E., NEUBAUER, A. & JUNGBAUER, A. 2001. High speed immuno-affinity chromatography on supports with gigapores and porous glass. *Bioseparation*, 9, 259-268.
- SEDDIGH-TONEKABONI, S., WATERS, J. A., JEFFERS, S., GEHRKE, R., OFENLOCH, B., HORSCH, A., HESS, G., THOMAS, H. C. & KARAYIANNIS, P. 2000. Effect of variation in the common "a" determinant on the antigenicity of hepatitis B surface antigen. *Journal of Medical Virology*, 60, 113-121.
- SEDEREL, W. L. & DEJONG, G. J. 1973. Styrene-Divinylbenzene Copolymers - Construction of Porosity in Styrene Divinylbenzene Matrices. *Journal of Applied Polymer Science*, 17, 2835-2846.

SHAEIWITZ, J. A., BLAIR, J. B. & RUAAN, R. C. 1989. Evidence That Yeast-Cell Wall Debris Can Separate Proteins by Ion-Exchange during Cell-Lysis.

Biotechnology and Bioengineering, 34, 137-140.

SHAMLOU, P. A. 2003. Scaleable processes for the manufacture of therapeutic quantities of plasmid DNA. *Biotechnology and Applied Biochemistry*, 37, 207-18.

SHEPARD, S. R., BRICKMAN-STONE, C., SCHRIMSHER, J. L. & KOCH, G. 2000. Discoloration of ceramic hydroxyapatite used for protein chromatography.

Journal of Chromatography A, 891, 93-98.

SIMON, K., LINGAPPA, V. R. & GANEM, D. 1988. Secreted hepatitis B surface antigen polypeptides are derived from a transmembrane precursor. *Journal of Cell Biology*, 107, 2163-8.

SINGER, T. & MULLER, M. 2007. The many ways to purify plasmid DNA. In: SUBRAMANIAN, G. (ed.) *Bioseparation and Bioprocessing. A Handbook*. Germany: Wiley-VCH.

SIOUFFI, A. M. 2006. About the C term in the van Deemter's equation of plate height in monoliths. *Journal of Chromatography A*, 1126, 86-94.

SIU, S. C., BALDASCINI, H., HEARLE, D. C., HOARE, M. & TITCHENER-HOOKER, N. J. 2006a. Effect of fouling on the capacity and breakthrough characteristics of a packed bed ion exchange chromatography column. *Bioprocess and Biosystems Engineering*, 28, 405-14.

SIU, S. C., BOUSHABA, R., TOPOYASSAKUL, V., GRAHAM, A., CHOUDHURY, S., MOSS, G. & TITCHENER-HOOKER, N. J. 2006b. Visualising fouling of a chromatographic matrix using confocal scanning laser microscopy. *Biotechnology and Bioengineering*, 95, 714-23.

SMITH, M. L., MASON, H. S. & SHULER, M. L. 2002. Hepatitis B surface antigen (HBsAg) expression in plant cell culture: Kinetics of antigen accumulation in batch culture and its intracellular form. *Biotechnology and Bioengineering*, 80, 812-22.

- SMREKAR, F., PODGORNIK, A., CIRINGER, M., KONTREC, S., RASPOR, P., STRANCAR, A. & PETERKA, M. 2010. Preparation of pharmaceutical-grade plasmid DNA using methacrylate monolithic columns. *Vaccine*, 28, 2039-2045.
- SONVEAUX, N., CONRATH, K., CAPIAU, C., BRASSEUR, R., GOORMAGHTIGH, E. & RUYSSCHAERT, J. M. 1994. The topology of the S protein in the yeast-derived hepatitis B surface antigen particles. *Journal of Biological Chemistry*, 269, 25637-45.
- SONVEAUX, N., THINES, D. & RUYSSCHAERT, J. M. 1995. Characterization of the Hbsag Particle Lipid-Membrane. *Research in Virology*, 146, 43-51.
- SORGER, D. & DAUM, G. 2003. Triacylglycerol biosynthesis in yeast. *Applied Microbiology and Biotechnology*, 61, 289-99.
- STABY, A., JOHANSEN, N., WAHLSTROM, H. & MOLLERUP, I. 1998. Comparison of loading capacities of various proteins and peptides in culture medium and in pure state. *Journal of Chromatography A*, 827, 311-8.
- STRYER, L. 1999. *Biochemistry*, W.H. Freeman and Company.
- SUSANTO, A., HERRMANN, T., VON LIERES, E. & HUBBUCH, J. 2007. Investigation of pore diffusion hindrance of monoclonal antibody in hydrophobic interaction chromatography using confocal laser scanning microscopy. *Journal of Chromatography A*, 1149, 178-188.
- SVEC, F. 2010. Porous polymer monoliths: amazingly wide variety of techniques enabling their preparation. *Journal of Chromatography A*, 1217, 902-24.
- SVEC, F. & FRECHET, J. M. J. 1992. Continuous Rods of Macroporous Polymer as High-Performance Liquid-Chromatography Separation Media. *Analytical Chemistry*, 64, 820-822.

SVEC, F. & FRECHET, J. M. J. 1995a. Kinetic Control of Pore Formation in Macroporous Polymers - Formation of Molded Porous Materials with High-Flow Characteristics for Separations or Catalysis. *Chemistry of Materials*, 7, 707-715.

SVEC, F. & FRECHET, J. M. J. 1995b. Modified Poly(Glycidyl Methacrylate-Co-Ethylene Dimethacrylate) Continuous Rod Columns for Preparative-Scale Ion-Exchange Chromatography of Proteins. *Journal of Chromatography A*, 702, 89-95.

SVEC, F. & FRECHET, J. M. J. 1995c. Molded Rods of Macroporous Polymer for Preparative Separations of Biological Products. *Biotechnology and Bioengineering*, 48, 476-480.

SVEC, F. & FRECHET, J. M. J. 1995d. Temperature, a Simple and Efficient Tool for the Control of Pore-Size Distribution in Macroporous Polymers. *Macromolecules*, 28, 7580-7582.

SVEC, F. & FRECHET, J. M. J. 1996. New designs of macroporous polymers and supports: From separation to biocatalysis. *Science*, 273, 205-211.

SVEC, F. & FRECHET, J. M. J. 1999. Molded rigid monolithic porous polymers: An inexpensive, efficient, and versatile alternative to beads for the design of materials for numerous applications. *Industrial & Engineering Chemistry Research*, 38, 34-48.

SVEC, F. & FRECHET, J. M. J. 2003. Rigid Macroporous Organic Polymer Monoliths Prepared by Free Radical Polymerization. In: SVEC, F. & FRECHET, J. M. J. (eds.) *Monolithic Materials*. The Netherlands: Elsevier.

SVEC, F. & TENNIKOVA, T. 2003. Historical Review. In: SVEC, F., TENNIKOVA, T. & DEYL, Z. (eds.) *Monolithic Materials; Preparation, properties and applications*. The Netherlands: Elsevier.

SVEC, F., TENNIKOVA, T. & DEYL, Z. 2003. *Monolithic materials*, The Netherlands, Elsevier.

TEETERS, M. A., CONRARDY, S. E., THOMAS, B. L., ROOT, T. W. & LIGHTFOOT, E. N. 2003. Adsorptive membrane chromatography for purification of plasmid DNA. *Journal of Chromatography A*, 989, 165-173.

TEETERS, M. A., ROOT, T. W. & LIGHTFOOT, E. N. 2002. Performance and scale-up of adsorptive membrane chromatography. *Journal of Chromatography A*, 944, 129-39.

TENNIKOV, M. B., GAZDINA, N. V., TENNIKOVA, T. B. & SVEC, F. 1998. Effect of porous structure of macroporous polymer supports on resolution in high-performance membrane chromatography of proteins. *Journal of Chromatography A*, 798, 55-64.

TENNIKOVA, T. B., BELENKII, B. G. & SVEC, F. 1990. High-Performance Membrane Chromatography - a Novel Method of Protein Separation. *Journal of Liquid Chromatography*, 13, 63-70.

TENNIKOVA, T. B., BLEHA, M., SVEC, F., ALMAZOVA, T. V. & BELENKII, B. G. 1991. High-Performance Membrane Chromatography of Proteins, a Novel Method of Protein Separation. *Journal of Chromatography*, 555, 97-107.

TENNIKOVA, T. B. & FREITAG, R. 2000. An introduction to monolithic disks as stationary phases for high performance biochromatography. *Hrc-Journal of High Resolution Chromatography*, 23, 27-38.

TENNIKOVA, T. B. & SVEC, F. 1993. High-Performance Membrane Chromatography - Highly Efficient Separation Method for Proteins in Ion-Exchange, Hydrophobic Interaction and Reversed-Phase Modes. *Journal of Chromatography*, 646, 279-288.

TESKE, C. A., SCHROEDER, M., SIMON, R. & HUBBUCH, J. 2005. Protein-labeling effects in confocal laser scanning microscopy. *Journal of Physical Chemistry B*, 109, 13811-13817.

THONART, P., CUSTINNE, M. & PAQUOT, M. 1982. Zeta potential of yeast cells: application in cell immobilization. *Enzyme and Microbial Technologies*, 4, 191-194.

TLEUGABULOVA, D., FALCON, V., PENTON, E., SEWER, M. & FLEITAS, Y. 1999. Aggregation of recombinant hepatitis B surface antigen induced in vitro by oxidative stress. *Journal of Chromatography B-Analytical Technologies in the Biomedical and Life Sciences*, 736, 153-66.

TLEUGABULOVA, D., FALCON, V., SEWER, M. & PENTON, E. 1998. Aggregation of recombinant hepatitis B surface antigen in *Pichia pastoris*. *Journal of Chromatography B-Analytical Technologies in the Biomedical and Life Sciences*, 716, 209-19.

TLEUGABULOVA, D., REYES, J., COSTA, L., DIAZ, J. & MADRAZO-PINOL, J. 1997. Size exclusion chromatography of Hepatitis B surface antigen particles. *Chromatographia*, 45, 317-320.

TO, B. C. S. & LENHOFF, A. M. 2011. Hydrophobic interaction chromatography of proteins. IV. Protein adsorption capacity and transport in preparative mode. *Journal of Chromatography A*, 1218, 427-440.

TRILISKY, E. I. & LENHOFF, A. M. 2007. Sorption processes in ion-exchange chromatography of viruses. *Journal of Chromatography A*, 1142, 2-12.

TSENG, W. C., HO, F. L., FANG, T. Y. & SUEN, S. Y. 2004. Effect of alcohol on purification of plasmid DNA using ion-exchange membrane. *Journal of Membrane Science*, 233, 161-167.

TUR, K. M. & CH'NG, H. S. 1998. Evaluation of possible mechanism(s) of bioadhesion. *International Journal of Pharmaceutics*, 160, 61-74.

UEBERBACHER, R., HAIMER, E., HAHN, R. & JUNGBAUER, A. 2008. Hydrophobic interaction chromatography of proteins - V. Quantitative assessment of conformational changes. *Journal of Chromatography A*, 1198, 154-163.

- UEBERBACHER, R., RODLER, A., HAHN, R. & JUNGBAUER, A. 2010. Hydrophobic interaction chromatography of proteins: Thermodynamic analysis of conformational changes. *Journal of Chromatography A*, 1217, 184-190.
- ULMER, J. B., VALLEY, U. & RAPPUOLI, R. 2006. Vaccine manufacturing: challenges and solutions. *Nature Biotechnology*, 24, 1377-83.
- UNGER, K. K., SKUDAS, R. & SCHULTE, M. M. 2008. Particle packed columns and monolithic columns in high-performance liquid chromatography-comparison and critical appraisal. *Journal of Chromatography A*, 1184, 393-415.
- URBAS, L., JARC, B. L., BARUT, M., ZOCHOWSKA, M., CHROBOCZEK, J., PIHLAR, B. & SZOLAJSKA, E. 2011a. Purification of recombinant adenovirus type 3 dodecahedral virus-like particles for biomedical applications using short monolithic columns. *Journal of Chromatography A*, 1218, 2451-9.
- URBAS, L., KOSIR, B., PETERKA, M., PIHLAR, B., STRANCAR, A. & BARUT, M. 2011b. Reversed phase monolithic analytical columns for the determination of HA1 subunit of influenza virus haemagglutinin. *Journal of Chromatography A*, 1218, 2432-2437.
- URTHALER, J., SCHLEGL, R., PODGORNIK, A., STRANCAR, A., JUNGBAUER, A. & NECINA, R. 2005. Application of monoliths for plasmid DNA purification development and transfer to production. *Journal of Chromatography A*, 1065, 93-106.
- VALENZUELA, P., GRAY, P., QUIROGA, M., ZALDIVAR, J., GOODMAN, H. M. & RUTTER, W. J. 1979. Nucleotide sequence of the gene coding for the major protein of hepatitis B virus surface antigen. *Nature*, 280, 815-9.
- VALENZUELA, P., MEDINA, A. & RUTTER, W. J. 1982. Synthesis and Assembly of Hepatitis-B Virus Surface-Antigen Particles in Yeast. *Nature*, 298, 347-350.

- VALLIERE-DOUGLASS, J., WALLACE, A. & BALLAND, A. 2008. Separation of populations of antibody variants by fine tuning of hydrophobic-interaction chromatography operating conditions. *Journal of Chromatography A*, 1214, 81-9.
- VAN DER WAL, A., MINOR, M., NORDE, W. & ZEHNDER, A. J. B. 1997. Electrokinetic Potential of Bacterial Cells. *Langmuir*, 13, 165-171.
- VAN REIS, R. & ZYDNEY, A. 2007. Bioprocess membrane technology. *Journal of Membrane Science*, 297, 16-50.
- VICENTE, T., FABAR, R., ALVES, P. M., CARRONDO, M. J. T. & MOTA, J. P. B. 2011a. Impact of Ligand Density on the Optimization of Ion-Exchange Membrane Chromatography for Viral Vector Purification. *Biotechnology and Bioengineering*, 108, 1347-1359.
- VICENTE, T., ROLDAO, A., PEIXOTO, C., CARRONDO, M. J. & ALVES, P. M. 2011b. Large-scale production and purification of VLP-based vaccines. *Journal of Invertebrate Pathology*, 107 Suppl, S42-8.
- VIKLUND, C., SVEC, F., FRECHET, J. M. J. & IRGUM, K. 1996. Monolithic, "molded", porous materials with high flow characteristics for separations, catalysis, or solid-phase chemistry: Control of porous properties during polymerization. *Chemistry of Materials*, 8, 744-750.
- VOSS, C. 2008. Downstream processing of plasmid DNA for gene therapy and genetic vaccination. *Chemical Engineering & Technology*, 31, 858-863.
- WAMPLER, D. E., LEHMAN, E. D., BOGER, J., MCALEER, W. J. & SCOLNICK, E. M. 1985. Multiple chemical forms of hepatitis B surface antigen produced in yeast. *Proceedings of the National Academy of Sciences of the United States of America*, 82, 6830-4.
- WANG, C., SOICE, N. P., RAMASWAMY, S., GAGNON, B. A., UMANA, J., COTONI, K. A., BIAN, N. & CHENG, K. S. 2007. Cored anion-exchange

- chromatography media for antibody flow-through purification. *Journal of Chromatography A*, 1155, 74-84.
- WANG, J., DISMER, F., HUBBUCH, J. & ULBRICHT, M. 2008. Detailed analysis of membrane adsorber pore structure and protein binding by advanced microscopy. *Journal of Membrane Science*, 320, 456-467.
- WHEELWRIGHT, S. M. 1991. *Protein Purification: design and scale up of downstream processing*, Germany, Hanser.
- WHITFIELD, R. J., BATTOM, S. E., BARUT, M., GILHAM, D. E. & BALL, P. D. 2009. Rapid high-performance liquid chromatographic analysis of adenovirus type 5 particles with a prototype anion-exchange analytical monolith column. *Journal of Chromatography A*, 1216, 2725-9.
- WICKRAMASINGHE, S. R., CARLSON, J. O., TESKE, C., HUBBUCH, J. & ULBRICHT, M. 2006. Characterizing solute binding to macroporous ion exchange membrane adsorbers using confocal laser scanning microscopy. *Journal of Membrane Science*, 281, 609-618.
- WILLEY, J., SHERWOOD, L. & WOOLVERTON, C. 2008. *Precott, Harley & Klein's Microbiology*, McGraw Hill Higher Education (USA).
- WILSON, W. W., WADE, M. M., HOLMAN, S. C. & CHAMPLIN, F. R. 2001. Status of methods for assessing bacterial cell surface charge properties based on zeta potential measurements. *Journal of Microbiological Methods*, 43, 153-64.
- WITHKA, J., MONCUSE, P., BAZIOTIS, A. & MASKIEWICZ, R. 1987. Use of high-performance size-exclusion, ion-exchange, and hydrophobic interaction chromatography for the measurement of protein conformational change and stability. *Journal of Chromatography*, 398, 175-202.
- WOLF, M. W. & REICHL, U. 2011. Downstream processing of cell culture-derived virus particles. *Expert Review of Vaccines*, 10, 1451-75.

WRIGHT, T. L. 2006. Introduction to chronic hepatitis B infection. *American Journal of Gastroenterology*, 101, S1-S6.

WU, S. L., FIGUEROA, A. & KARGER, B. L. 1986. Protein Conformational Effects in Hydrophobic Interaction Chromatography - Retention Characterization and the Role of Mobile Phase Additives and Stationary Phase Hydrophobicity. *Journal of Chromatography*, 371, 3-27.

XIAO, Y., JONES, T. T., LAURENT, A. H., O'CONNELL, J. P., PRZYBYCIEN, T. M. & FERNANDEZ, E. J. 2007a. Protein instability during HIC: hydrogen exchange labeling analysis and a framework for describing mobile and stationary phase effects. *Biotechnology and Bioengineering*, 96, 80-93.

XIAO, Y. Z., RATHORE, A., O'CONNELL, J. P. & FERNANDEZ, E. J. 2007b. Generalizing a two-conformation model for describing salt and temperature effects on protein retention and stability in hydrophobic interaction chromatography. *Journal of Chromatography A*, 1157, 197-206.

XIE, S. F., SVEC, F. & FRECHET, J. M. J. 1997a. Preparation of porous hydrophilic monoliths: Effect of the polymerization conditions on the porous properties of poly(acrylamide-co-N,N'-methylenebisacrylamide) monolithic rods. *Journal of Polymer Science Part a-Polymer Chemistry*, 35, 1013-1021.

XIE, S. F., SVEC, F. & FRECHET, J. M. J. 1997b. Rigid porous polyacrylamide-based monolithic columns containing butyl methacrylate as a separation medium for the rapid hydrophobic interaction chromatography of proteins. *Journal of Chromatography A*, 775, 65-72.

YAMADA, T., IWABUKI, H., KANNO, T., TANAKA, H., KAWAI, T., FUKUDA, H., KONDO, A., SENO, M., TANIZAWA, K. & KURODA, S. 2001. Physicochemical and immunological characterization of hepatitis B virus envelope particles exclusively consisting of the entire L (pre-S1 + pre-S2 + S) protein. *Vaccine*, 19, 3154-63.

YAMAGUCHI, M., SUGAHARA, K., SHIOSAKI, K., MIZOKAMI, H. & TAKEO, K. 1998. Fine structure of hepatitis B virus surface antigen produced by recombinant yeast: comparison with HBsAg of human origin. *FEMS Microbiology Letters*, 165, 363-7.

YANG, H. W., VIERA, C., FISCHER, J. & ETZEL, M. R. 2002. Purification of a large protein using ion-exchange membranes. *Industrial & Engineering Chemistry Research*, 41, 1597-1602.

YAO, K., YUN, J., SHEN, S., WANG, L., HE, X. & YU, X. 2006. Characterization of a novel continuous supermacroporous monolithic cryogel embedded with nanoparticles for protein chromatography. *Journal of Chromatography A*, 1109, 103-10.

YILMAZ, F., BERELI, N., YAVUZ, H. & DENIZLI, A. 2009. Supermacroporous hydrophobic affinity cryogels for protein chromatography. *Biochemical Engineering Journal*, 43, 272-279.

ZENG, C. M., LIAO, J. L., NAKAZATO, K. & HJERTEN, S. 1996. Hydrophobic-interaction chromatography of proteins on continuous beds derivatized with isopropyl groups. *Journal of Chromatography A*, 753, 227-234.

ZHANG, Z. R., BURTON, S., WILLIAMS, S., THWAITES, E. & LYDDIATT, A. 2001. Design and assembly of solid-phases for the effective recovery of nanoparticulate bioproducts in fluidised bed contactors. *Bioseparation*, 10, 113-132.

ZHAO, Q., WANG, Y., FREED, D., FU, T. M., GIMENEZ, J. A., SITRIN, R. D. & WASHABAUGH, M. W. 2006. Maturation of recombinant hepatitis B virus surface antigen particles. *Human Vaccines*, 2, 174-80.

ZHOU, J. X. & TRESSEL, T. 2006. Basic concepts in Q membrane chromatography for large-scale antibody production. *Biotechnology Progress*, 22, 341-349.

ZMAK, P. M., PODGORNIK, H., JANCAR, J., PODGORNIK, A. & STRANCAR, A. 2003. Transfer of gradient chromatographic methods for protein separation to

Convective Interaction Media monolithic columns. *Journal of Chromatography A*, 1006, 195-205.

ZOCHLING, A., HAHN, R., AHRER, K., URTHALER, J. & JUNGBAUER, A.
2004. Mass transfer characteristics of plasmids in monoliths. *Journal of Separation Science*, 27, 819-827.

9 APPENDIX

This section contains graphs which contain VLP values instead of normalised data. These are the same graphs presented in the thesis but have been added to allow the reader to have information on the actual amounts of VLP during chromatographic experiments.

9.1 SECTION 3

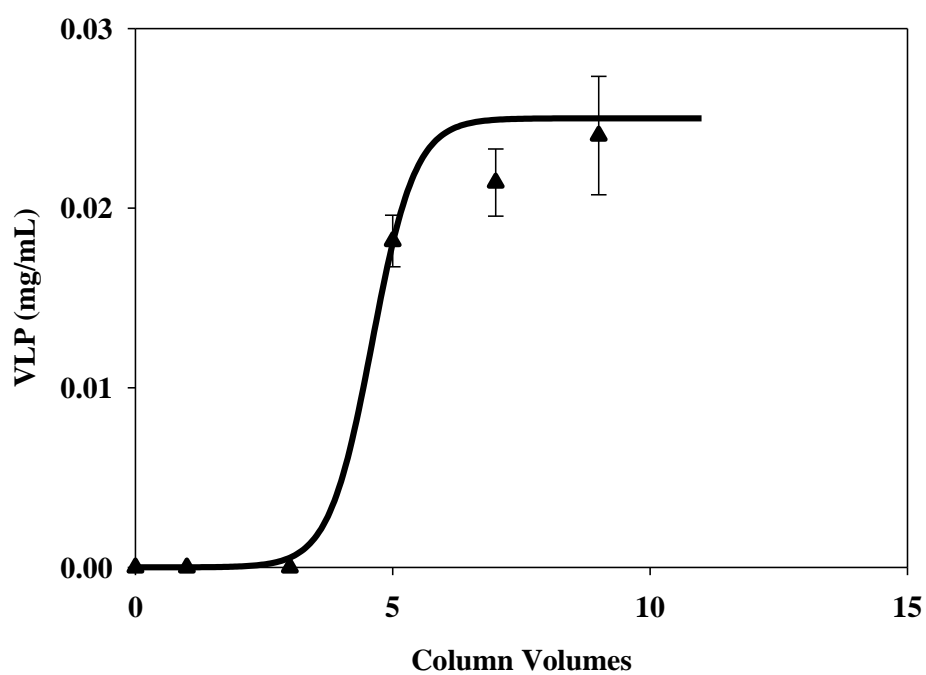


Figure 9-1 Breakthrough curve for crude feed at 1.0M ammonium sulphate on an OH monolith. ($n=3$). (Raw data for Figure 3-12)

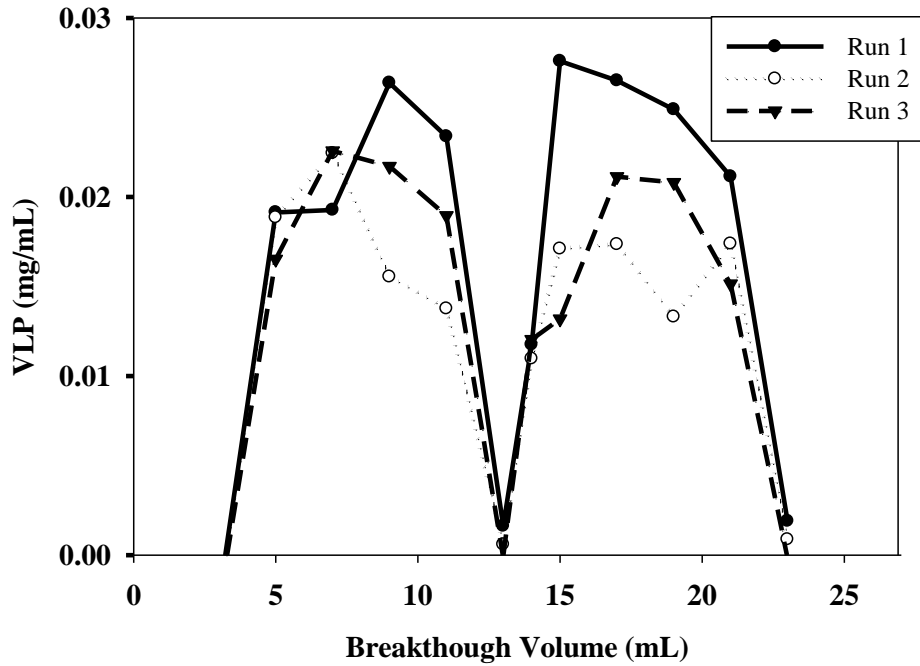


Figure 9-2 Breakthrough curves using 25mL of crude feed material over 3 consecutive run on a new column. The amount of VLP was monitored using ELISA. (Raw data for Figure 3-13)

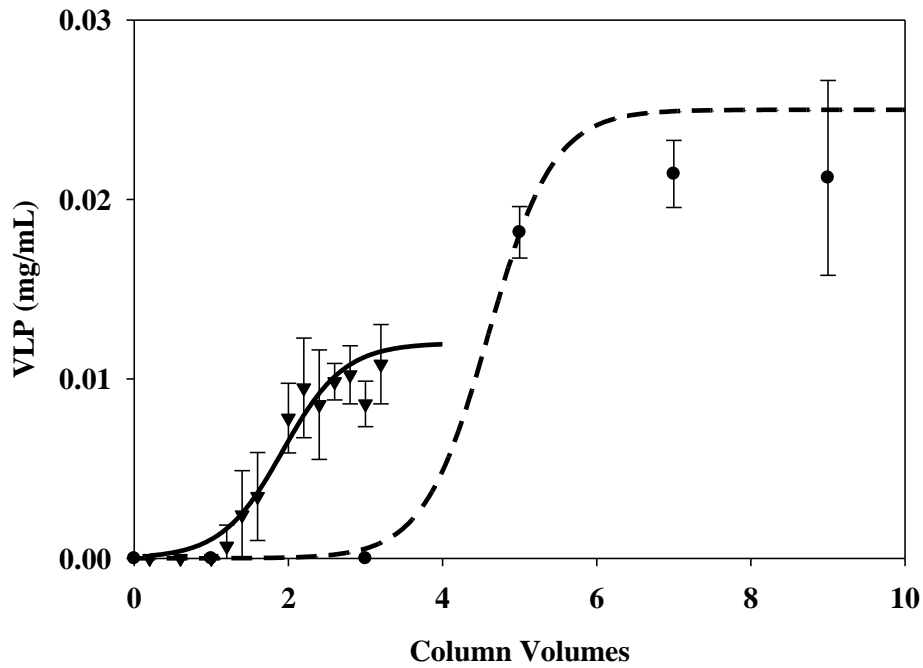


Figure 9-3 Comparison of dynamic binding capacity of butyl-S Sepharose 6 FF 1mL HiTrap column (▲) and a monolith OH 1mL column (●). 10% breakthrough is indicated by the dotted line. The columns were loaded with untreated homogenised

yeast and the VLP breakthrough was monitored using ELISA. ($n=2$ for butyl-S column and $n=3$ for OH monolith. Error bars are 1 S.D.) (Raw data for Figure 3-14)

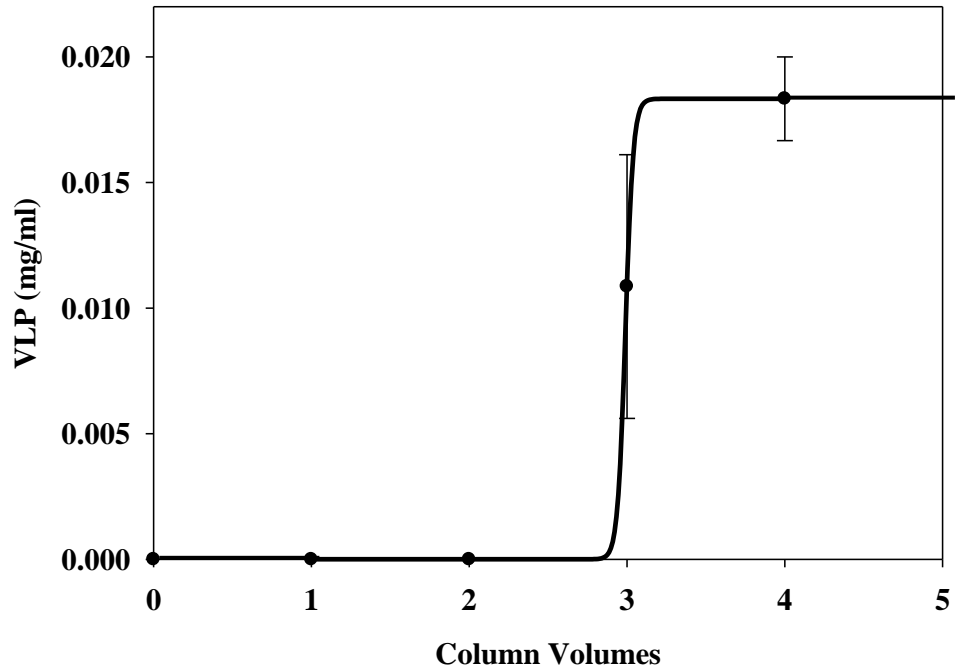


Figure 9-4 Breakthrough curve of VLP on a large pore OH monolith, analysed by ELISA. ($n=3$). (Raw data for Figure 3-15)

9.2 SECTION 4

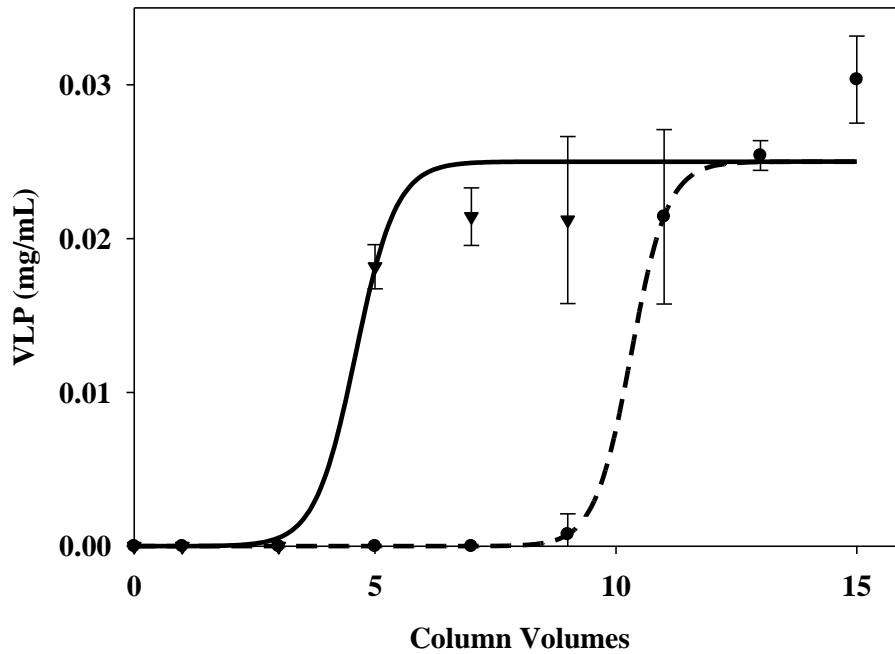


Figure 9-5 Comparison of the dynamic binding capacity of the 1mL OH monolith when a crude feed (▲) and a reduced lipid feed (●) are applied to the column. 10% breakthrough is indicated by the dotted line. (Raw data for Figure 4-8)

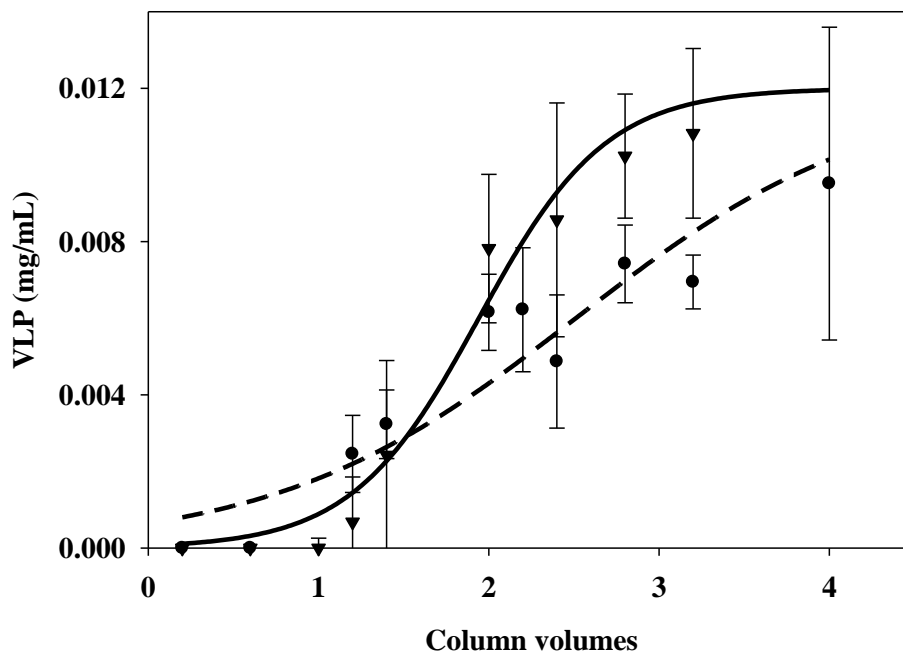


Figure 9-6 Comparison of the dynamic binding capacity on a Butyl-S resin column when a crude feed (solid line ▲) and reduced lipid feed (dotted line ●) are applied to the column. (Raw data for Figure 4-9)